UNIVERSIDADE D
COIMBRA

Bruno Rodrigues Teixeira

ORGANIC MATTER VARIATION DURING THE TOARCIAN OCEANIC ANOXIC EVENT IN THE CENTRAL AND NORTHERN ATLANTIC MARGINS: THE INTERPLAY BETWEEN LOCAL CONSTRAINTS *VS* GLOBAL EVENTS

Tese no âmbito do Doutoramento em Geologia, área de especialização em Processos Geológicos, orientada pelo Professor Doutor Luís Vítor da Fonseca Pinto Duarte, Doutor Ricardo Ferreira Louro Silva, Professor Doutor João Graciano Mendonça Filho e apresentada ao Departamento de Ciências da Terra da Faculdade de Ciências e Tecnologia da Universidade de Coimbra.

Março de 2020

Faculdade de Ciências e Tecnologia
da Universidade de Coimbra

ORGANIC MATTER VARIATION DURING THE TOARCIAN OCEANIC ANOXIC EVENT IN THE CENTRAL AND NORTHERN ATLANTIC MARGINS: THE INTERPLAY BETWEEN LOCAL CONSTRAINTS *VS* GLOBAL EVENTS

Bruno Rodrigues Teixeira

Tese no âmbito do Doutoramento em Geologia, área de especialização em Processos Geológicos, orientada pelo Professor Doutor Luís Vítor da Fonseca Pinto Duarte, Doutor Ricardo Ferreira Louro Silva, Professor Doutor João Graciano Mendonça Filho e apresentada ao Departamento de Ciências da Terra da Faculdade de Ciências e Tecnologia da Universidade de Coimbra.

Março de 2020

1 2 9 0

UNIVERSIDADE D
COIMBRA

This work was supported by the Fundação para a Ciência e Tecnologia through the grant SFRH/BD/115002/2016. This is also a contribution of the Council of the International Geoscience Programme (IGCP) Project 655–Toarcian Oceanic Anoxic Event: Impact on marine carbon cycle and ecosystems (IUGS-UNESCO).

Acknowledgements/Agradecimentos

Gostaria de expressar a minha gratidão a todos aqueles que, de uma forma ou outra, apoiaram, incentivaram e colaboraram na concretização desta tese. Nesta oportunidade, dedico um especial agradecimento:

- ao Prof. Doutor Luís Vítor Duarte, orientador, amigo e o grande responsável por esta jornada. Agradeço a confiança que sempre depositou em mim, o acompanhamento rigoroso, orientação perspicaz, as conversas enriquecedoras e os valiosos ensinamentos que transmitiu não só ao longo destes três anos mas ao longo de todo o meu percurso académico;

- ao Doutor Ricardo Louro Silva, orientador com conhecimentos científicos irrefutáveis, trouxe sempre uma crítica construtiva que muito ajudou o desenvolvimento desta tese. Além disso, sempre foste um grande amigo e fundamental para a conclusão desta fase da minha vida. Levo destes anos a tua amizade, que estimarei para o resto da vida;

- ao Prof. Doutor João Graciano Mendonça Filho, orientador, pelo apoio, aconselhamento, confiança e amizade. Obrigado pela disponibilidade de recursos, pelos 6 meses incríveis no Rio de Janeiro e por me ter permitido trabalhar num dos melhores laboratórios de geoquímica orgânica;

- a toda a equipa do LAFO-UFRJ, pela ajuda na obtenção dos resultados desta tese. Tenho de agradecer em especial à Noélia Franco, Guilherme Santos, Milton, Joalice Mendonça, Thiago, Donizete, Jaqueline e Karen por me terem feito sentir "em casa" (novamente) durante a minha estadia no Rio de Janeiro. Obrigado pela amizade e carinho, pela hospitalidade, simpatia e por todos os momentos divertidos;

- To Dr. Grant Wach for the opportunity to visit and conduct research at the Basin and Reservoir Lab (Dalhousie University, Canada), the strategic project UID/MAR/04292/2020 awarded to the Marine and Environmental Sciences Centre (MARE), and the Irish Centre for Research in Applied Geosciences, iCRAG (Ireland), who partially supports this work, either providing funds for travel, field-work, or supervision;

- ao Departamento de Ciências da Terra da Universidade de Coimbra, ao MARE e respetivos técnicos e colaboradores (em especial à Alexandra Baeta) que proporcionaram o apoio necessário para que esta tese se desenrolasse positivamente;

- a todas as pessoas amigas que conheci e reencontrei nesta jornada do doutoramento, em Marrocos, Espanha, Brasil e Canadá. Um agradecimento especial ao Driss Sadki (merci beaucoup pour tout!), ao Matías Reolid (gracias por la ayuda) e à Bruna Stock (e família) por me terem acolhido tão bem no Brasil. Agradeço especialmente ao Gabriel e à Sílvia por todos os dias durante aqueles três meses intensos. As palavras serão sempre poucas para agradecer a experiência única que me proporcionaram;

- Aos Prof. Doutores María José Comas-Rengifo e Antonio Goy pela colaboração e apoio no trabalho desenvolvido nas Astúrias;

- Aos meus companheiros e amigos do FC São Silvestre agradeço o apoio, paciência, boa disposição, companheirismo e, sobretudo, a vossa amizade. Agradeço em especial ao Tiago Bogalho, Pedro Campos, Bartolomeu Rodrigues, Francisco Cardoso, Diogo Ávila, David Seiça, Xavi Cortesão, Ricardo Carvalho, Pedro Ferreira, Joaquim Gonçalves e Sérgio Bogalho. Todos foram uma enorme ajuda nesta fase da minha vida;

- Aos meus amigos de Viseu. Ao José Fernandes, Eduardo Coelho, Gonçalo Correia, Joana Gomes, Vanessa Salgueiral, Anaísa Machado, Pipa Ferreira, André Borges, Daniel Sousa, Joana Alves, Filipa Ferreira, Jessica Ferreira e Cláudia Costa pelas palavras de encorajamento, pela paciência e apoio sem fim. Obrigada por terem preservado a nossa amizade mesmo quando eu faltei em alguns momentos. Sou uma pessoa melhor graças a vocês;

- À minha equipa da Geonatour que pôde dar-me o equilíbrio de que tanto precisava. Obrigada pela (tanta!) paciência e pelas palavras amigas durante estes anos. Esta iniciativa empreendedora começou ao mesmo tempo que o doutoramento. Multipliquei as vezes que vos disse para confiarem em mim, que ia ter tempo para tudo e hoje reconheço que, sem a vossa ajuda, sem as palavras de força do Fábio Antunes, António Figueiredo, Francisco Veiga Simão, Jorge Carvalho e Ricardo Peixoto, tudo teria desabado…hoje tudo é uma realidade e uma certeza! Obrigado;

- Aos meus colegas e amigos Rui Pires, Rafael Correia, Gustavo Santiago, Ricardo Marques, Marta Reis, João Duarte, Patrícia Rita, Vânia Correia, Filipa Domingos e Carolina Fonseca pelo companheirismo e ajuda na aprendizagem da Geologia. Agradeço-vos todos os momentos durante estes anos;

- À Patrícia Alves, ao Sérgio Sêco e Margarida Porto Gouveia. Obrigada pelo vosso apoio incondicional, paciência e amizade durante todo este percurso. Vocês foram realmente importantes para o desfecho desta tese e espero deixar-vos orgulhosos;

- À minha Carolina Antunes, melhor amiga, meu amor…pelo enorme apoio e suporte que me deste durante esta fase da minha vida. Estas quatro linhas são poucas para te agradecer por todos os momentos (tantos!) e palavras. Sempre carinhosa, animada e com um miminho para me encorajar, foste/és incrível! Uma grande parte desta tese pertence-te e por isso também ta dedico;

- à minha Mãe, Pai e Irmã pelo apoio incondicional e investimento incomensurável. São a minha maior motivação, "porto-seguro" e acreditem que vos devo tudo. Mesmo à distância e com falta de tempo, houve sempre uma palavra de ânimo nos meus momentos de desassossego. Agora que tudo terminou, espero ter mais tempo para partilhar novas conquistas e alegrias. É a vocês que decido esta tese.

A todos, o meu muito obrigado.

Abstract

In many locations of the northwestern Tethyan, Boreal and Panthalassic margins, the uppermost Pliensbachian–Lower Toarcian is characterised by the occurrence of organic-rich sediments. Significant perturbations of the global carbon cycle, related with an excess of ^{12}C in the atmospheric and ocean reservoirs, are recorded as a negative carbon isotope excursions (CIE) in carbonate, bulk organic matter (OM), fossil wood, kerogen and individual organic compounds, linked to the Pliensbachian–Toarcian Event (Pl–Toa Event) and Toarcian Oceanic Anoxic Event (TOAE). Contrariwise, the uppermost Pliensbachian–Lower Toarcian successions in northern Africa and most of Iberian Peninsula basins (Central–Northern Atlantic margin) are poor in OM. It is hypothesized that OM deposition and preservation in northern Africa and most of the Iberian Peninsula basins during the Pl–Toa Event and TOAE was controlled by the interplay of local–regional constraints and global forcings, therefore resulting in unique OM assemblages and differentiated from the organic-rich northern European basins. The main objective of this thesis was the analysis of kerogen assemblages from the uppermost Pliensbachian–Lower Toarcian references sections of the Middle Atlas (northern Africa), Betic Cordillera, Lusitanian and Asturian (Iberian Peninsula) basins based on total organic carbon (TOC), palynofacies, and $\delta^{13}C$ in kerogen ($\delta^{13}C_{Kerogen}$).

The obtained results indicate that the studied sections generally have low TOC contents (below 1 wt.%). The TOAE interval in the Asturian Basin and a discrete level in the Peniche section (Lusitanian Basin) recorded high TOC values, reaching up to 2.9 wt.% at Asturian Basin and likely signalling local episodes of OM preservation promoted by dysoxic conditions. The obtained $\delta^{13}C_{Kerogen}$ profiles in this study presented similarities with previously published high-resolution $\delta^{13}C_{Wood}$ and $\delta^{13}C_{Org}$ records. Even with small differences between the studied sections, the $\delta^{13}C_{Kerogen}$ record presented a positive trend during the Emaciatum/Spinatum and Polymorphum/Tenuiscostatum zones, followed by the negative trend associated with the TOAE. The difference in magnitude between $\delta^{13}C$ records from different locations probably reflects the impact of local and/or regional environmental processes over global forcing. The kerogen assemblages are characterised almost exclusively by terrestrial OM, with a high abundance of opaque phytoclasts, suggesting that the OM was sourced from an area characterised by semi-arid or arid climate. Around the base of Polymorphum/Tenuiscostatum and Levisoni/Serpentinum zones, small increments in terrestrial OM were observed and represented by non-opaque phytoclasts, and terrestrial palynomorphs (sporomorphs, tetrads, and agglomerates). These were interpreted to represent an increase in fluvial runoff associated with the palaeoenvironmental perturbations of the Pl–Toa Event and TOAE.

The subsequent change to higher $\delta^{13}C_{Kerogen}$ values during the TOAE $\delta^{13}C$ positive trend is more abrupt in the Asturian Basin (probably reflecting a low sedimentation rate) and more gradual in the western Iberian sections. During the middle part of the Levisoni/Serpentinum Zone, the $\delta^{13}C$ remains relatively stable with the return to more positive $\delta^{13}C$ values and it was suggested that after

the carbon cycle perturbation the climates gradually cooled, favouring kerogen assemblages similar to the ones observed before the TOAE.

Keywords: Organic matter, Palynofacies, Organic and isotopic geochemistry, Pl–Toa Event, TOAE, Middle Atlas and Iberian basins.

Resumo

Em diversos locais das margens noroeste do Tétis, Boreal e Pantalassa, o topo do Pliensbaquiano Superior–Toarciano Inferior é caracterizado pela ocorrência de sedimentos ricos em matéria orgânica (MO). Perturbações significativas do ciclo global de carbono, relacionadas com excesso de ^{12}C nos reservatórios atmosféricos e oceânicos, são registadas como excursões isotópicas negativas em carbonatos, MO, fragmentos de fósseis vegetais, querogénio e compostos individuais orgânicos, e relacionadas com o Evento do Pliensbaquiano–Toarciano (Evento Pl–Toa) e o Evento Oceânico Anóxico do Toarciano (EOAT). Por outro lado, nas sucessões do norte de África e na maioria das bacias da Península Ibérica (margem Central–Norte do Atlântico), o topo do Pliensbaquiano Superior–Toarciano Inferior é pobre em MO. Supõe-se que a deposição e preservação de MO nas bacias do norte de África e da Península Ibérica durante o Evento Pl–Toa e EOAT foi controlada pela interação de restrições locais–regionais e eventos globais, resultando em associações únicas de MO e diferenciadas das bacias ricas em MO do norte da Europa. O principal objetivo desta tese foi a análise de associações de querogénio de secções de referência do topo do Pliensbaquiano Superior–Toarciano Inferior nas bacias do Médio Atlas (norte de África), Cordilheira Bética, Lusitânica e Astúrias (Península Ibérica), com base no carbono orgânico total (COT), palinofácies e $\delta^{13}C$ em querogénio ($\delta^{13}C_{querogénio}$).

Os resultados obtidos indicam que as secções estudadas apresentam geralmente baixos conteúdos de COT (abaixo de 1%). O intervalo do EOAT na Bacia das Astúrias e um nível discreto na secção de Peniche (Bacia Lusitânica) registam valores elevados de COT, atingindo cerca de 2,9% (na Bacia das Astúrias), provavelmente associados com episódios locais de preservação da MO, promovidos por condições disóxicas. Os perfis de $\delta^{13}C_{querogénio}$ obtidos neste estudo apresentam similaridades com os registos de alta resolução de $\delta^{13}C$ em fragmentos de fósseis vegetais e MO, anteriormente publicados. Mesmo com algumas diferenças entre as secções estudadas, o registo do $\delta^{13}C_{querogénio}$ apresenta uma tendência positiva nas zonas de Emaciatum/Spinatum e Polymorphum/Tenuiscostatum, seguida pela tendência negativa associada ao EOAT. A diferença de magnitude entre os registos de $\delta^{13}C$ em diferentes locais, provavelmente reflete o impacto dos processos ambientais locais e/ou regionais sobrepostos aos eventos globais. As associações de querogénio são caracterizadas quase exclusivamente por MO terrestre, com abundância de fitoclastos opacos, sugerindo que a MO será proveniente de uma área caracterizada por clima semiárido ou árido. Na base das zonas Polymorphum/Tenuiscostatum e Levisoni/Serpentinum, são observados pequenos incrementos de MO terrestre, representados por fitoclastos não opacos e palinomorfos terrestres (esporomorfos, tetrades e aglomerados). Estas alterações são interpretadas como representantes de uma intensificação do escoamento fluvial associado às perturbações paleoambientais do Evento Pl–Toa e EOAT.

A consequente mudança para valores de $\delta^{13}C_{querogénio}$ mais positivos durante a parte superior do EOAT é mais abrupta na Bacia das Astúrias (provavelmente reflexo de uma baixa taxa de sedimentação) e mais gradual nas secções da Ibéria ocidental. Durante a parte média da Zona

Levisoni/Serpentinum, os valores de $\delta^{13}C$ permanecem relativamente estáveis, com o retorno de valores mais positivos de $\delta^{13}C$ e sugere-se que após a perturbação do ciclo do carbono os climas arrefeceram gradualmente, favorecendo as associações de querogénio semelhantes aos observados antes do EOAT.

Palavras-chave: Matéria orgânica, Palinofácies, Geoquímica orgânica e isotópica, Evento Pl–Toa, EOAT, Bacias do Médio Atlas e da Iberia.

Contents

List of Figures

List of Tables

Contribution of the co-authors

Professor Luís Vítor Duarte[1] and Dr Ricardo Ferreira Louro Silva[2], as PhD research supervisors, contributed to (1) the delineation and planning of the PhD research project, (2) data collection, (3) discussion and interpretation of results, and (4) reviewed and edited the final version of all manuscripts submitted in international peer-reviewed journals and thesis chapters.

Professor João Graciano Mendonça Filho[3] as the PhD research supervisor contributed to (1) the preliminary delineation and planning of the PhD research project, (2) allowed for the TOC, palynofacies, and thermal maturation analyses to be acquired at his laboratory (Palynofacies and Organic Facies Laboratory), (3) participated in the discussion and interpretation of results, and (4) reviewed the final version of all manuscripts submitted in international peer-reviewed journals and thesis chapters.

Professor Matías Reolid[4] (1) assisted with sample collection at La Cerradura and Fuente Vidriera, (2) contributed as an expert in stratigraphy and sedimentology in the Betic Cordillera (southern Spain), and (3) contributed to the final version of the manuscript published in Palaeogeography, Palaeoclimatology, Palaeoecology.

Professor Driss Sadki[5] (1) assisted with sample collection at Aït Moussa and Issouka, (2) contributed to ammonite biostratigraphy in the Middle Atlas Basin, and (3) aided with the final version of the manuscript published in International Journal of Coal Geology.

Dr Joalice Oliveira Mendonça[3] (1) provided the thermal maturity analysis when presented and (2) contributed to the discussion concerning palynofacies analysis.

Involved institutions:
[1] Department of Earth Sciences and MARE, Faculty of Sciences and Technology of the University of Coimbra, Portugal.
[2] Department of Geology and iCRAG, Trinity College Dublin, The University of Dublin, Ireland.
[3] Palynofacies and Organic Facies Laboratory, Geosciences Institute, Federal University of Rio de Janeiro, Brazil
[4] Department of Geology, Jaén University, Spain
[5] Department of Geology, Faculty of Science, Moulay Ismaïl University of Meknes, Morocco.

I. Introduction

The Upper Pliensbachian–Lower Toarcian (Lower Jurassic) in the Central (northern Gondwana margin) and part of Northern Atlantic (Iberian Massif) basins is characterised by thick carbonate successions, prominent in many areas around northern Africa [High and Middle Atlas (Morocco; e.g. Wilmsen and Neuweiler, 2008; Bodin et al., 2010, 2016; Ait-Itto et al., 2017)] and Iberian Peninsula [Betic Cordillera (southern Spain; e.g. Jiménez and Rivas, 2007; Rodríguez-Tovar and Reolid, 2013; Reolid et al., 2014, 2018), Lusitanian (western Portugal; e.g. Duarte, 1997; Azerêdo et al., 2003, 2010; Duarte et al., 2007, 2018a, 2018b; Silva et al., 2015), Asturian and Basque-Cantabrian (northern Spain; e.g. Valenzuela, 1988; Quesada et al., 2005; Gómez et al., 2008; Gómez and Arias, 2010; Gómez and Goy, 2011)] basins.

A particular feature of the Late Pliensbachian–Early Toarcian interval is that it coincides with a series of major palaeoenvironmental perturbations (e.g. ocean anoxia, warming, possible ocean acidification) and dramatic changes in the marine biota, expressed as a 2nd-order mass extinction event in benthic and pelagic groups (e.g. Harries and Little, 1999; Mattioli et al., 2009; Gómez and Arias, 2010; Danise et al., 2013; Caruthers et al., 2014). This interval is also a period of enhanced preservation of organic matter (OM), with the widespread occurrence of organic-rich sediments in many locations of the northwestern Tethyan, Boreal and Panthalassic margins (Fig. I.1; e.g. Jenkyns and Clayton, 1986; Fleet et al., 1987; Jenkyns, 1988, 2010; Baudin et al., 1990; Röhl et al., 2001; Suan et al., 2011, 2015; Caruthers et al., 2014; Al-Suwaidi et al., 2016; Them II et al., 2017; Silva et al., 2017; Fantasia et al., 2018a; Ruebsam et al., 2018; Fonseca et al., 2018; Suan et al., 2018). This interval is known as the Toarcian Oceanic Anoxic Event (TOAE; Jenkyns, 1988, 2010) and is associated with a significant perturbation of the global carbon cycle, linked with an excess of ^{12}C in the atmospheric and ocean carbon reservoirs. The carbon cycle perturbation is recorded as $\delta^{13}C$ negative carbon isotope excursion (CIE) occurring at the base of the Levisoni/Serpentinum/Falciferum ammonite Zone in carbonate ($\delta^{13}C_{Carb}$), bulk OM ($\delta^{13}C_{Org}$), fossil wood ($\delta^{13}C_{Wood}$), kerogen ($\delta^{13}C_{Kerogen}$) and individual organic compounds ($\delta^{13}C_{Bio}$) (e.g. Jenkyns and Clayton, 1986; Jenkyns, 1988, 2010; Hesselbo et al., 2000, 2007; Jenkyns et al., 2002; Cohen et al., 2004; Hermoso et al., 2009; Bodin et al., 2010, 2016; Littler et al., 2010; Al-Suwaidi et al., 2010; Suan et al., 2010, 2011, 2015; Reolid et al., 2012; French et al., 2014; Kafousia et al., 2014; Caruthers et al., 2014; Kemp and Izumi, 2014; Neumeister et al., 2015; Pieñkowski et al., 2016; Silva et al., 2017; Them II et al., 2017; Xu et al., 2017; Fantasia et al., 2018a, 2018b, 2019; Ruebsam et al., 2020a; Ruebsam and Al-Husseini, 2020).

Before the TOAE, in several successions of the Western Tethys, the Pliensbachian–Toarcian boundary also archive evidence of another carbon cycle perturbation, i.e. the Pliensbachian–Toarcian Event (Pl–Toa Event; e.g. Littler et al., 2010; Ruebsam et al., 2019). The Pl–Toa Event is characterised by a smaller negative CIE, palaeoenvironmental changes (e.g.

enhanced sea surface temperature and continental weathering) and it is coincidental with an extinction pulse in marine benthos at the base of the Polymorphum Zone (e.g. Little and Benton, 1995; Littler et al., 2010; Caruthers et al., 2013).

The Pl–Toa Event and TOAE record in northern Africa and the Iberian Peninsula basins have been the focus of an intense investigation, focusing mainly on stable carbon isotope and macro- and micro-invertebrate analysis (see references above). Notwithstanding, these studies seldom approach the study of kerogens in a multidisciplinary way, i.e. by incorporating sedimentology, typology (palynofacies), and geochemistry (elemental, isotopic, and organic) analysis. The integration of these methods is a powerful tool for palaeoenvironmental research (e.g. Tyson, 1995; Bombardiere and Gorin, 2000; Mendonça Filho et al., 2012; Gonçalves et al., 2013; Silva et al., 2014; Rodrigues et al., 2016; Mendonça Filho and Gonçalves, 2017; Fonseca et al., 2018). Considering the observed variability of organic facies and lithofacies associated with the Pl–Toa Event and TOAE in the Middle Atlas, Betic Cordillera, Lusitanian and Asturian basins (Fig. I.1; e.g. Valenzuela, 1988; Benshili, 1989; Duarte, 1997; Jiménez and Rivas, 2007; Duarte et al., 2007, 2018a, 2018b; Gómez et al., 2008; Gómez and Goy, 2011; Rodríguez-Tovar and Reolid, 2013; Reolid et al., 2014, 2018; Ait-Itto et al., 2017), the intersection of palynofacies methods with classical sedimentological techniques may provide important insights to (1) better understand the OM inventory of each studied basin and (2) clarify palaeoenvironmental changes associated (driving?) with continental weathering and discharge, OM productivity, preservation, and diagenesis processes, and depositional processes. Also, the study of palynofacies and geochemistry holds the potential to contribute to current investigations of modern climate and planetary-scale changes.

I.1. Objectives

As aforementioned, it can be demonstrated that some of the effects associated with the Pl–Toa Event and TOAE occurred at a planetary scale (e.g. Jenkyns, 2010). The global nature of the Pl–Toa Event and TOAE is expressed mainly by a perturbation of the carbon cycle, increased rate of extinctions and the widespread occurrence of organic-rich sediments in many locations during the TOAE (see references above). The deposition of organic-rich facies during the Pl–Toa Event and TOAE has been widely attributed to time intervals characterized by “extensive” anoxic (and euxinic) oceans (e.g. Schouten et al., 2000; Schmid-Röhl et al., 2002; Schwark and Frimmel, 2004; van Breugel et al., 2006; Pearce et al., 2008; French et al., 2014; Thibault et al., 2018; Ruebsam et al., 2018). However, it is argued that the anoxic conditions were not a widespread phenomenon (e.g. McArthur et al., 2008; McArthur, 2019) nor responsible for the TOAE extinction event (e.g. Gómez et al., 2008), raising some pertinent questions regarding the OM record of these particular time intervals. For example: which were the dominant controls on OM

production and preservation in individual sedimentary basins? At which point, global events offset basin constraints and, conversely, local basinal conditions override global environmental drivers?

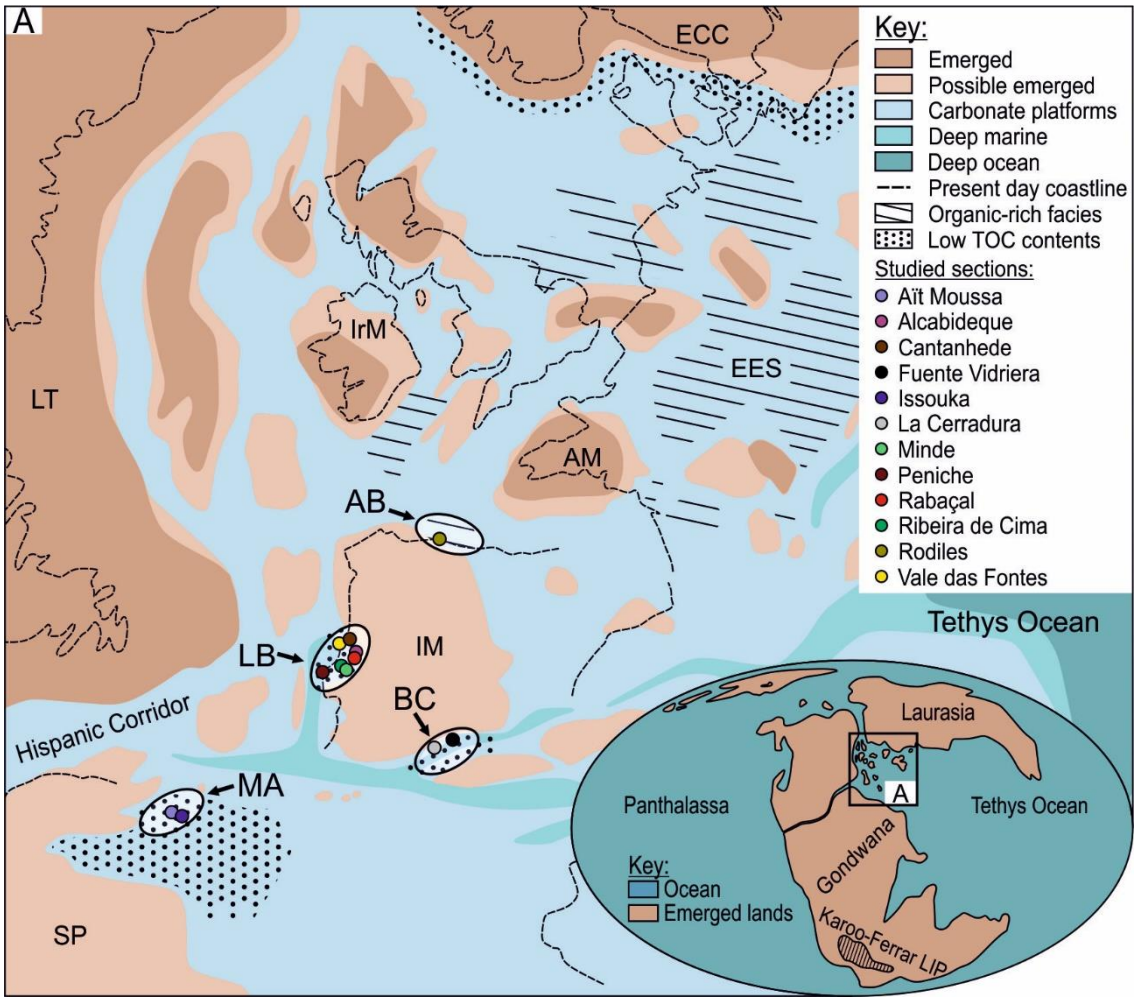

Figure I.1. Global palaeogeography during the Pliensbachian–Toarcian interval (modified from Dera et al., 2009). The black rectangle shows the limit of the map (A). **A**. Palaeogeographic map of the western Tethys during the Early Jurassic (modified from Bassoulet et al., 1993; Thierry and Barrier, 2000) with the general locations of the studied basins and sections. MA – Middle Atlas Basin (Morocco), BC – Betic Cordillera (southern Spain), LB – Lusitanian Basin (western Portugal) and AB – Asturian Basin (northern Spain). SP – Saharan platform; IM – Iberian Massif; AM – Armorican Massif; LT – Laurentia; EES – European Epicontinental sea; IrM – Irish Massif; BM – Bohemian Massif; ECC – East European Craton.

It is hypothesised that OM deposition and preservation in northern Africa and most of the Iberian Peninsula basins during the Pl–Toa Event and TOAE was controlled by the interplay of local–regional constraints and global forcings, therefore resulting in unique OM assemblages and differentiated from northern European locations. This hypothesis will be tested by analysing the variation of the kerogen assemblages during the uppermost Pliensbachian–Lower Toarcian in the

Central and part of Northern Atlantic basins (Middle Atlas, Betic Cordillera, Lusitanian and Asturian; Fig. I.1).

To achieve the proposed objectives, a regional survey focused on the study of sedimentary OM was conducted at the northern Africa sections of Aït Moussa and Issouka (Middle Atlas Basin) and the Iberian Peninsula sections of La Cerradura and Fuente Vidriera (Betic Cordillera), Peniche, Rabaçal, Vale das Fontes, Cantanhede, Alcabideque, Ribeira de Cima, Minde (Lusitanian Basin) and Rodiles (Asturian Basin) (Fig. I.1). This study comprehends a total of one hundred forty-one (141) marly samples and four (4) wood fragments. Ninety-four (94) marly samples were analysed for total organic carbon (TOC), total sulfur (TS), $\delta^{13}C_{Kerogen}$, prepared for palynofacies according to standard techniques and were performed in the Palynofacies and Organic Facies Laboratory (LAFO) of the Rio de Janeiro Federal University (Rio de Janeiro, Brazil) and MAREFOZ (Coimbra University, Portugal). A wood fragment was analysed for the $\delta^{13}C_{Kerogen}$. Furthermore, twenty-nine (29) marly samples and three wood fragments (3) previously collected from Alcabideque and Rodiles sections were analysed for the $\delta^{13}C_{Kerogen}$ dataset. The eighteen marly (18) samples from Peniche have not been subjected to $\delta^{13}C_{Kerogen}$ analysis. To evaluate the thermal maturation, eight (8) samples from the Middle Atlas and Betic Cordillera basins were analysed at the LAFO. Detailed information on laboratory procedures is given in the material and methods section of the four main chapters (II, III, IV and V).

I.2. Thesis structure

The main body of this thesis is presented in an article-based format, composed of four main chapters. The research resulted in twelve (12) scientific publications, from presentations at international meetings to papers published in international peer-reviewed journals.

In addition to the presentation of the thesis structure, several important subjects are described to allow a better comprehension of the studied theme and discussed in this work, such as the main objectives and the motivation that led us to initiate this doctoral project.

The chapters organization follow a northward trend, from the northern Gondwana margin (Middle Atlas Basin; northern Africa) to the northern Iberian Massif (Betic Cordillera, Lusitanian and Asturian basins in the Iberian Peninsula). A brief outline of the main chapters is presented below:

Chapter II is focused on sea-level changes, climate, tectonics, and impact on depositional environments in the Aït Moussa and Issouka sections (Middle Atlas Basin; Morocco) during the Late Pliensbachian–Early Toarcian and the Pl–Toa Event. This chapter was published in the International Journal of Coal Geology.

Chapter III focuses on the link between ^{13}C fractionation during photosynthesis in C3 plants and climate change during the Early Toarcian in the External subbetic, Betic Cordillera (southern Spain). This chapter was published in the journal Palaeogeography, Palaeoclimatology, Palaeoecology.

Chapter IV corresponds to a study focused on the impact and response of Early Toarcian environmental changes (related to the Pl–Toa Event and TOAE) in the land-based ecosystems bordering the marine environments of the Lusitanian Basin. At the date of the submission of this thesis, this chapter was submitted in the journal Palaeogeography, Palaeoclimatology, Palaeoecology.

Chapter V focuses on the deposition and preservation of OM during the latest Pliensbachian–Early Toarcian in the Asturian Basin (northern Spain). The occurrence of OM-rich facies during the TOAE in northern Spain allows investigating the relationship between OM production, depositional conditions, and palaeoceanographic controls and the relationship with the neighbouring counterparts (to be submitted).

A summary of the main conclusions is presented in the final remarks section, along with contributions to the scientific background and geological applications regarding the climatic events during the Early Toarcian in the studied sections. Additionally, considerations regarding future studies are presented.

II. Late Pliensbachian–Early Toarcian palaeoenvironmental dynamics and the Pl–Toa Event in the Middle Atlas Basin (Morocco)

Adapted from:

Rodrigues, B., Silva, R.L., Mendonça Filho, J.G., Driss, S., Mendonça, J.O., Duarte, L.V., 2020. Late Pliensbachian–Early Toarcian palaeoenvironmental dynamics and the Pl–Toa Event in the Middle Atlas Basin (Morocco). International Journal of Coal Geology, 217, 103339. doi.org/10.1016/j.coal.2019.103339.

Accepted: 5 November 2019

Abstract

Geochemical and palynofacies analysis of 38 samples from the Middle Atlas Basin (Aït Moussa and Issouka sections, Morocco) allowed to investigate sea-level changes, climate, and tectonics and impact on depositional environments in the westernmost Tethyan Gondwana-margin during the Late Pliensbachian–Early Toarcian and the Pliensbachian–Toarcian Event (Pl–Toa Event).

The studied sections from the Middle Atlas Basin have low total organic carbon contents. Overall, kerogen assemblages are dominated by the Phytoclast Group, thus showing a strong terrestrial affinity and some degree of proximity to the source. Deposition occurred dominantly in oxic and proximal environments.

Upper Pliensbachian kerogen assemblages from Aït Moussa are dominated by terrestrial particles and agree with the overall regressive character of the sedimentary succession. Uppermost Pliensbachian–lowermost Toarcian kerogen assemblages from Aït Moussa show an increase in marine particles. Considering the overall sedimentological context of the Middle Atlas Basin, these kerogen assemblages are interpreted to reflect local variation in accommodation space (driven by different sedimentation rates or tectonic compartmentalization) or ecological conditions (such as nutrient availability, temperature, turbidity, etc). In the Early Toarcian, above a major regional discontinuity and at the beginning of the Pl–Toa Event, increases in *Botryococcus* sp., amorphous organic matter (AOM), and terrestrial palynomorphs suggest episodes of coastal erosion associated with transgression, likely driven by a combination of eustatic/tectonic changes and warmer and more humid climates leading to an increase in continental weathering and fluvial runoff. On the other hand, increases in sporomorphs and pollen grains occurring in tetrads and agglomerates indicate regressive episodes associated with increased sedimentation rates driven by enhanced continental weathering and fluvial runoff.

This study shows the strong relationship between sea-level and the combined response of litho-, hydro-, and biosphere during the Early Toarcian, with implications to understand organic productivity and organic matter accumulation and preservation in the Tethys Ocean during the Pl–Toa Event.

Keywords: Organic matter; organic geochemistry; palynofacies; transgressive event; Pl–Toa Event; Middle Atlas; Morocco.

II.1. Introduction

Although still poorly constrained and understood, recent studies (e.g. Hesselbo et al., 2007; Littler et al., 2010; Suan et al., 2010; Xu et al., 2018) demonstrated that sedimentary successions spanning the Pliensbachian–Toarcian boundary archive evidence of a significant perturbation of the carbon cycle, i.e. the Pliensbachian–Toarcian Event (Pl–Toa Event; Littler et al., 2010), associated with major sea-level, biological, and environmental changes. This event is characterised by a negative carbon isotopic excursion at the base of the Lower Toarcian (Polymorphum Zone) and is coincidental with an extinction phase in marine benthos at the base of the Toarcian (e.g. Little and Benton, 1995; Littler et al., 2010; Caruthers et al., 2013). Percival et al. (2015, 2016) suggested that this interval may have witnessed significant continental weathering and volcanic activity. The Pl–Toa Event has been documented in Europe (Hesselbo et al., 2007; Littler et al., 2010; Pieñkowski et al., 2016; Xu et al., 2018; Ruebsam et al., 2019; Rodrigues et al., 2019), Japan (Gröcke et al., 2011; Izumi et al., 2018) and South America (Al-Suwaidi et al., 2010; Fantasia et al., 2018b).

In the Middle Atlas Basin, Morocco (Fig. II.1), Upper Pliensbachian–Lower Toarcian sedimentary successions are poor in organic matter (OM) and expanded (~ 80 m of Lower Toarcian sediments) when compared with several European counterparts (see, for example, Hesselbo et al., 2007; Ait-Itto et al., 2017, 2018). The Pliensbachian–Toarcian transition in much of this basin is characterised by a sharp lithological change, from limestone- to shale-dominated. This lithological variation is interpreted to have resulted from a major “deepening” phase (i.e., Wilmsen and Neuweiler, 2008), leading to changes in proximity to the shoreline, terrigenous sediment supply and carbonate factories, water column depth, light availability, among many other parameters (e.g. Wright, 1992; Schlager, 2005; Catuneanu, 2018). Distribution of sedimentary OM along continental margins strongly depends on local to regional biological, hydrological, geological, climatic, and depositional constraints. Investigation of kerogen assemblages from the Middle Atlas Basin may provide important insights to the understanding of Late Pliensbachian–Early Toarcian environmental changes and the Pl–Toa Event (see other

examples, Tyson, 1995; Bombardiere and Gorin, 2000; Silva et al., 2014; Rodrigues et al., 2016; Mendonça Filho and Gonçalves, 2017).

In this study, we analysed 38 marl samples from the Aït Moussa and Issouka sections of the Middle Atlas Basin [total organic carbon (TOC), sulphur (TS), total carbonate content, palynofacies, and thermal maturity analysis]. The main goal was to characterise the Upper Pliensbachian–Lower Toarcian kerogen assemblages (content and type) and investigate sedimentary OM source, sea-level changes, climate, and the record of the Pl–Toa Event in the western Tethyan margin. This study shows the strong relationship between sea-level and the combined response of litho-, hydro-, and biosphere during the Early Toarcian, with implications to understand organic productivity and OM accumulation and preservation in the western Tethyan margin during the Pl–Toa Event.

II.2. Geological background

The Atlas Mountain Range of northern Africa, spanning from the Moroccan Atlantic margin to Tunisia, consists of several Phanerozoic sedimentary basins greatly affected by tectonic processes (e.g. Piqué et al., 2002). The Middle and High Atlas Mountains expose the history of two closely related intracontinental rift basins (Mattauer et al., 1977), encompassing sediments from the Triassic to the Neogene, and deformed and exhumed during the Alpine Orogeny as part of an aulacogen rift system (e.g. Frizon de Lamotte et al., 2008).

The Atlas rift basins recorded two main phases of crustal extension: i) Triassic to Early Jurassic, with fault block mosaics, red beds, evaporites and basalts (e.g. Mattis, 1977); and ii) Early Jurassic, with shallow- and deep-water argillaceous limestones, shallow and deep-water carbonate build-ups, and carbonate platform depositional environments (Warme, 1988).

During the Early Jurassic, the Middle Atlas Basin was open towards the southwestern end of the Tethys Ocean and was separated from the nascent northern Atlantic Ocean by the Moroccan Meseta (Bassoulet et al., 1993). The sedimentary evolution of this basin was mostly controlled by tectonic activity, combined with changes in the sedimentation rates and global eustatic variations (Wilmsen and Neuweiler, 2008).

In the Middle Atlas, extensive shallow-water carbonate production during the Hettangian–Pliensbachian (e.g. Wilmsen and Neuweiler, 2008) was followed by the rapid demise of neritic carbonate production during the Pliensbachian–Toarcian transition. The demise of the neritic carbonate factories resulted in a major lithological break in both shallow- and deep-water settings. Carbonate-rich Pliensbachian rocks (informal unit of “Calcaires de l′Ouarirt”; Benzaquen et al., 1965) are overlain by marls at the base and siliciclastic-rich Toarcian sediments at the top (“Couches d’Issouka”) (Benshili, 1989). This lithological break is associated with a major climatic shift, from arid towards more humid, and global eustatic variations during the earliest Toarcian (e.g. Bodin et al., 2016) which, associated with an increase in accommodation

space, allowed for the deposition of an expanded and continuous sedimentary record spanning the Pliensbachian–Toarcian interval (Piqué et al., 2002). The biostratigraphy in the Middle Atlas has been established with ammonites (zonation based on the Mediterranean zonation; Benshili, 1989; El Hammichi et al., 2008) with further biostratigraphic data provided by benthic foraminifera (Bejjaji et al., 2010).

II.2.1. Description of the studied sections of the Middle Atlas Basin

II.2.1.1. Aït Moussa section

The Aït Moussa section is located SE of the village of Aït Moussa (N33°25'21.92"; W4°20'34.45"), exposed along the left side of the Aït Bazza wadi (Fig. II.1). This outcrop exposes approximately 60 m of a succession of alternating limestones, marly–limestone, and marls, with ammonites, foraminifera, and other fauna. Previous studies and new ammonite data (*unpublished data*) collected from the Aït Moussa section allow to identify the Algovianum, Emaciatum, and Polymorphum zones (see also Benzaquen et al., 1965; Benshili, 1989; El Arabi et al., 2001; El Hammichi, 2002). The lower part of the Upper Pliensbachian (Algovianum Zone) is dominated by limestones with marly interbeds. The Algovianum–Emaciatum zone transition marks a gradual increase in argillaceous sedimentation, characterised by an increase in the thickness of marl beds. In general, limestones consist of fossiliferous biomicrites/wackestones, rich in belemnites and ammonites. The Toarcian sediments (Polymorphum Zone) consist at the base of ~ 1.5 m of thin marl-limestone alternations that become progressively more argillaceous upwards with rare thin (centimetric) limestone beds.

II.2.1.2. Issouka section

The Issouka section is located SW of Immouzer Marmoucha, near the village of Issouka (N33°26’55.56’’; W4°20’33.83’’) (Fig. II.1). The outcrop exposes approximately 136 m of grey and dark marls and limestones (e.g. Bejjaji et al., 2010), locally rich in ammonites. This study analysed about 32m of the Toarcian succession. The topmost part of the Pliensbachian comprises bioclastic limestones enriched in belemnites, bivalves, brachiopods, and siliceous sponges (see also Ait-Itto et al., 2017, 2018). The beginning of the Lower Toarcian succession (Polymorphum Zone) is characterised by marl–limestone alternations with foraminifera, belemnites, echinoids,

and gastropods (Benshili, 1989; Bejjaji et al., 2010). Upwards, marls become dominant and with intercalation of thin limestones beds (see also Ait-Itto et al., 2017, 2018).

II.3. Material and methods

Thirty-eight marly samples were collected from the Upper Pliensbachian–Lower Toarcian interval at the Aït Moussa (24 samples) and Issouka (14 samples from Lower Toarcian) sections (Fig. II.1) and analysed for TOC, TS, carbonate content, palynofacies, and thermal maturity. TOC, TS, carbonate content, palynofacies, and thermal maturity analyses were conducted in the Palynofacies and Organic Facies Laboratory (LAFO) of the Rio de Janeiro Federal University (Rio de Janeiro, Brazil).

II.3.1. Kerogen isolation

Kerogen was isolated from the rock matrix using the standard, non-oxidative procedure described, for example, by Tyson (1995) and Mendonça Filho et al. (2012), among others. First, all samples were mechanically disaggregated to approximately 2 mm rock chips. Afterwards, each sample was sequentially acid-treated to remove carbonates (HCl 37% for 18h), then silicates (HF 40% for 24h), and finally neoformed fluorides (HCl 37% for 3h). Between each step, pH was neutralised with distilled water. The organic and non-organic materials were separated by flotation using $ZnCl_2$ (density between 1.9–2.0 g/cm^3). The organic fraction was recovered, and the heavy liquid was eliminated using drops of HCl (10%) followed by a wash with distilled water. After this procedure, strew slides and plugs of concentrated kerogen were prepared.

II.3.2. Geochemical analysis

After acidification for carbonate content determination, TOC and TS were analysed with LECO SC 144 device, following the ASTM Standard D4239-08 (2008) and NCEA-C-1282 (United States Environmental Protection Agency, U.S.EPA, 2002) methods.

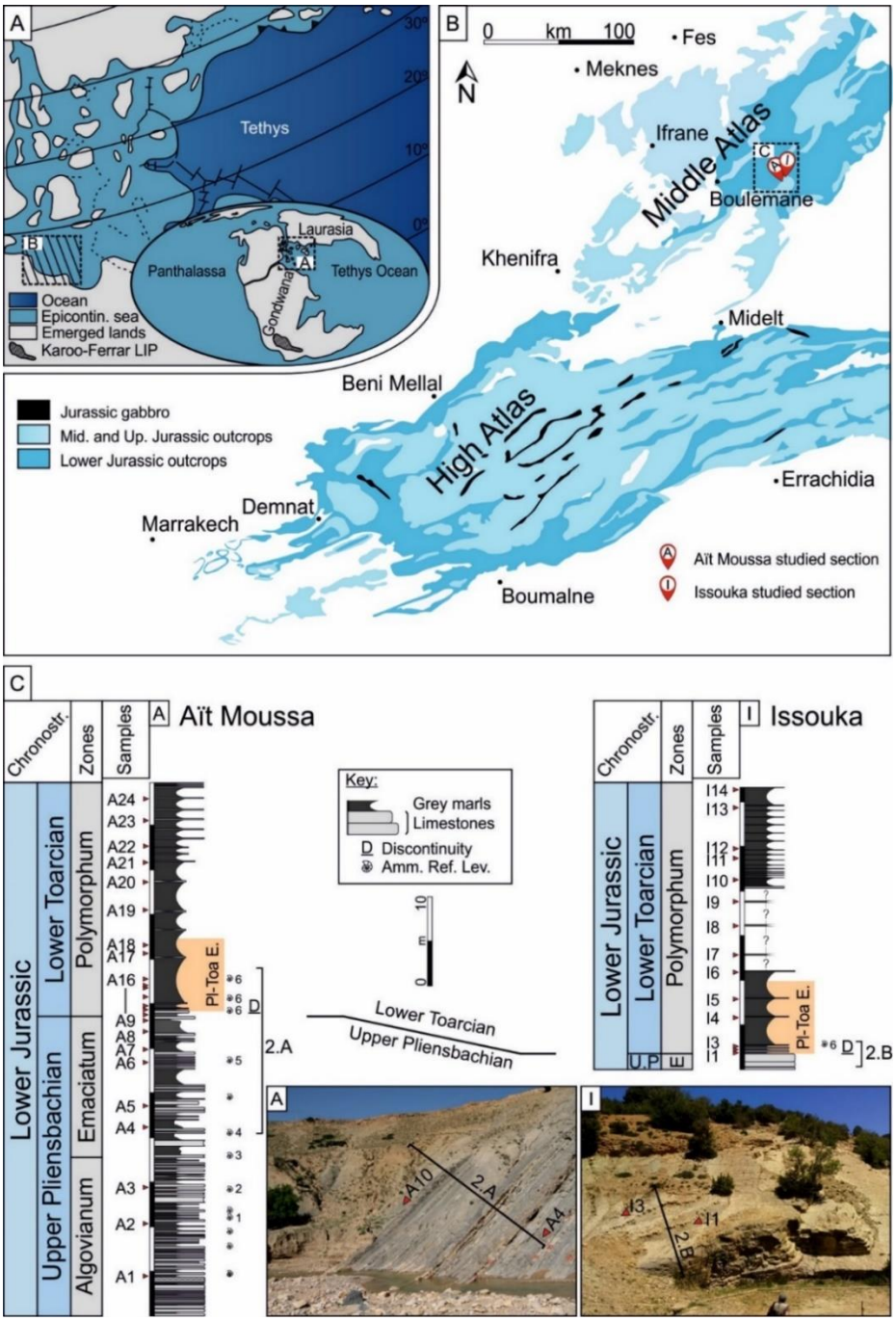

Figure II.1. General geological setting of the Aït Moussa and Issouka sections, Middle Atlas Basin (Morocco). **A**. Palaeogeographic map of the western Tethys during the Early Jurassic (adapted from Bassoulet et al., 1993; Mattioli et al., 2008). The black dash rectangle shows the limit of the map (B). **B**. Geological map of the Jurassic outcrops in the Middle and High Atlas (Morocco; adapted from Hollard et al., 1985). The black dash rectangle shows the limit of the studied outcrops (C). **C**. A - Aït Moussa section; I - Issouka section. The duration of the Pl–Toa Event is based in Ait-Itto et al. (2017, 2018). Ammonite reference levels: 1 – *Pleuroceras solare*, *Leptaleoceras accuratum*, *Leptaleoceras* sp., *Arieticeras algovianum* and *Arieticeras bertrandi*; 2 – *Amaltheus* sp. and *Protogrammoceras meneghinii*; 3 – *Amaltheus* sp. and *Pleuroceras transiens*; 4 – *Pleuroceras spinatum*; 5 – *Amaltheus* sp.; 6 – *Emaciaticeras emaciatum* and *Eodactylites* sp. Mid. and Up. – Middle and Upper; U.P – Upper Pliensbachian; E – Emaciatum Zone; Chronostr. – Chronostratigraphy; Pl–Toa E. – Pliensbachian–Toarcian Event.

II.3.3. Palynofacies

Batches of kerogen isolates were sieved (20 μm), and strew slides were prepared according to the methodological procedure outlined in Tyson (1995) and Mendonça Filho et al. (2012). Additionally, unsieved strew slides were also prepared. Transmitted white light (TWL) and incident blue light (fluorescence mode; FM) microscopic techniques were used for the qualitative and quantitative (at least 300 particles per slide) examinations of the kerogen groups. The main palynofacies kerogen groups, i.e., Phytoclast, Amorphous, and Palynomorph, and an additional group, Zooclast (remains of animal-derived organic particles), were recognised using pre-established descriptive categories (see Tyson, 1995; Mendonça Filho and Gonçalves, 2017), providing a robust and reproducible identification scheme. Strew slides counts were recalculated as a relative percentage (%).

II.3.4. Vitrinite reflectance

Vitrinite reflectance (R_o) was measured in 3 plugs of concentrated kerogen [two samples from Aït Moussa (A10 and A19) and one from Issouka (I1)]. Analysis followed the standard procedures (ISO 7404-2, 2009) and was performed with a Carl Zeiss Axioskop 2-Plus microscope equipped with a spectrophotometer J&M (MSP 200), with 50× objective in immersion oil (ηe=1.518–23 °C), according to ASTM Standard D7708 (2014). The microscope was calibrated with Spinel (0.425 % R_r) standard.

II.4. Results

II.4.1. Aït Moussa section

II.4.1.1. TOC, TS and carbonate content

In the Aït Moussa section, TOC average is 0.39 wt.%, reaching up to 0.64 wt.% in the sample A4 (base of Emaciatum Zone; Fig. II.2 and Table II.1). TS varies between 0.01–0.59 wt.% (average 0.16 wt.%), with the highest TS determined in the sample A7 (Emaciatum Zone; Table

II.1). The carbonate content range between 23–78%, falling below 50% during Polymorphum Zone (between samples A11–A24).

II.4.1.2. Palynofacies

In the Aït Moussa section, kerogen assemblages include the main kerogen groups: Phytoclast, Amorphous, and Palynomorph, although dominated by the phytoclast components (average ~ 60%, reaching up to ~ 82% in sample A11, base of Polymorphum Zone; Fig. II.2 and Table II.1).

II.4.1.2.1. Phytoclast Group

The Phytoclast Group is the most abundant kerogen group (Fig. II.2 and Table II.1), the lowest contents are observed in samples A21 (32%), A24 (38%), A9 (42%) (Fig. II.2 and Table II.1) and are dominated by opaque (OP; Fig. II.3A) and non-opaque particles (NOP; Figs. II.3B and II.3C). NOP average content is ~52% and OP average content is ~48%.

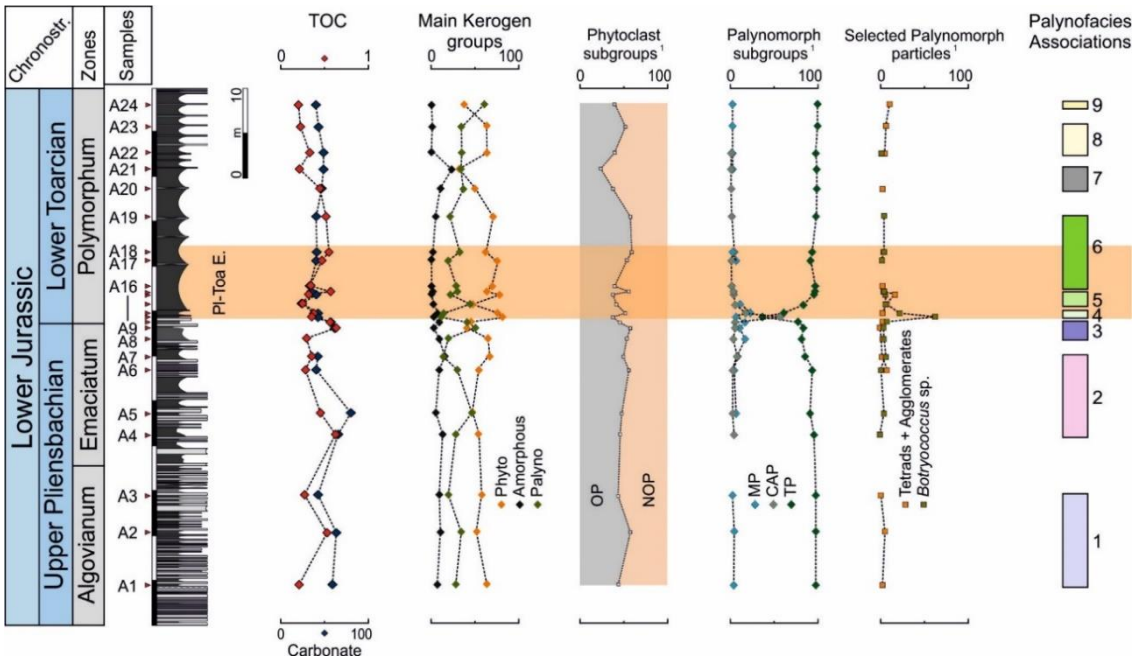

Figure II.2. TOC, carbonate content, palynofacies associations and main intervals (1 – 9) from Aït Moussa section, Middle Atlas (Morocco). Phyto – phytoclasts; Palyno – palynomorphs; OP – opaque; NOP – non-opaque; MP – marine palynomorphs; CAP – continental aquatic palynomorphs; TP – terrestrial palynomorphs; [1] – recalculated to 100%.

II.4.1.2.2. Amorphous Group

These particles present diffuse limits or are unstructured and are classified as amorphous organic matter (AOM). The AOM is rare in all samples (average of ~ 6%; Fig. II.2 and Table II.1). AOM colouration varies between brown to pale brown in TWL (Figs. II.3A and II.3G) and yellow to orange in FM and presents inclusions of palynomorphs (Figs. II.3F and II.3G).

II.4.1.2.3. Palynomorph Group

Particles belonging to the Palynomorph Group occur in moderate amounts in most samples (average of ~ 30%), ranging from 12% (A11) to 60% (A24). Terrestrial palynomorphs are mainly represented by sporomorphs (Figs. II.3B and II.3C), with some pollen grains occurring in tetrads (Figs. II.3C and II.3F) or agglomerates (Fig. II.3C). Pollens grains belonging to the genus *Classopollis* (Fig. II.3B) are present. Continental aquatic palynomorphs are represented by very low amounts of zygospores of *zygnemataceae* and *Botryococcus* sp. (Fig. II.3D and II.3E). The first occurrence of the genus *Botryococcus* sp. occurs in the sample A4, increasing in the base of the Polymorphum Zone (samples A12 and A13; 61% and 21%, respectively). Marine palynomorphs, such as dinoflagellate cysts (*Nannoceratopsis gracilis* (Fig. II.3F), *Luehndea spinosa* (Fig. II.3G), acritarchs (Figs. II.3B and II.3F), and prasinophyte algae occur in low amounts, peaking between samples A8–A13 (average of 13%). The Zoomorph subgroup is mainly represented by foraminiferal test-linings.

II.4.1.3. Vitrinite Reflectance

Vitrinite reflectance values in the Aït Moussa section vary between 0.45% and 0.46% R_o.

II.4.2. Issouka section

II.4.2.1. TOC, TS and carbonate content

TOC contents in the Issouka section average 0.21 wt.%, reaching up to 0.31 wt.% in sample I1 (base of the Polymorphum Zone). TS content is very low, ranging from 0.02 wt.% to <0.01 wt.% (Table II.2). The carbonate content ranges between 26–52%, with an average value of 37% (Fig. II.4 and Table II.2).

II.4.2.2. Palynofacies

In the Issouka section, Phytoclast Group is the most abundant kerogen group (average of ~ 88% and reaching up to ~ 99% in the sample I10; Fig. II.4 and Table II.2).

II.4.2.2.1. Phytoclast Group

Sample I9 records the lowest content of phytoclasts, 58% (Fig. II.4 and Table II.2). The NOP (Fig. II.5A) and OP (Fig. II.5B) present average value of ~51%, and ~49%, respectively.

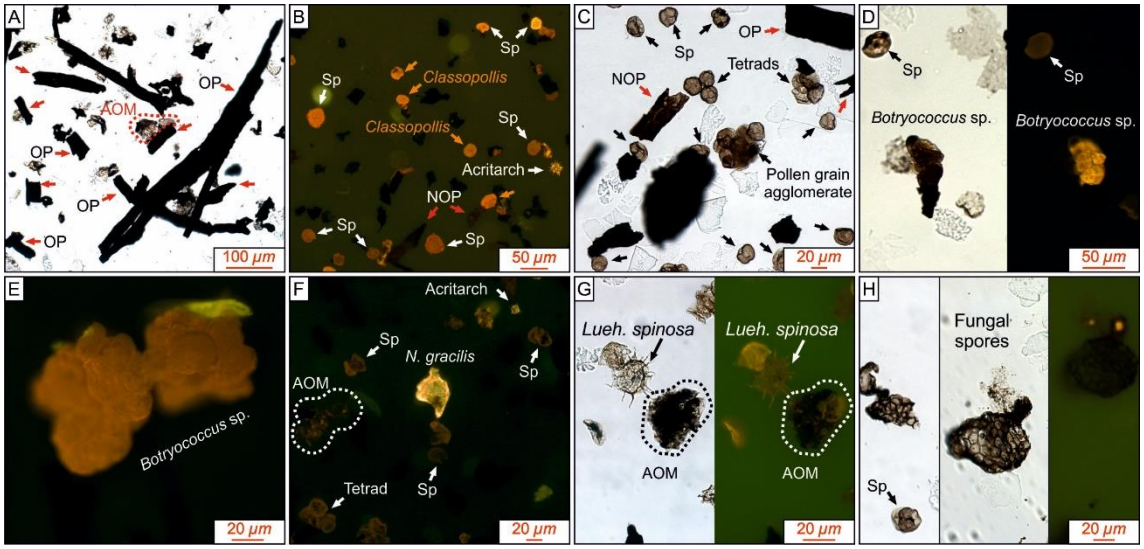

Figure II.3. Transmitted white light (TWL) and Fluorescence Mode (FM) photomicrographs of the studied kerogen assemblages from the Aït Moussa section, Middle Atlas (Morocco). **A**. Sample A6 (Emaciatum Zone) with opaque (OP) and amorphous organic matter (AOM); **B**. Sample from Polymorphum Zone (A20) with non-opaque phytoclasts (NOP), sporomorphs, *Classopollis*-pollens (orange arrow) and acritarch; **C**. Sample A24 (Polymorphum Zone) with OP, NOP, sporomorphs, tetrads and pollen grain agglomerate; **D**. TWL and FM images from sample A12 (base of Polymorphum Zone) with *Botryococcus* sp. and sporomorph; **E**. Example of degraded *Botryococcus* sp. from Polymorphum Zone; **F**. FM image of *Nannoceratopsis gracilis*, AOM, sporomorphs, tetrad and small acritarch from sample A17 (Polymorphum Zone); **G**. TWL and FM images from sample A9 (top of Emaciatum Zone) with *Luehndea spinosa* and sporomorph; **H**. Examples of fungal spores from Polymorphum Zone (sample A20 with fungal spore and sporomorph and sample A21). OP – Opaque phytoclast; NOP – Non-opaque phytoclast; Sp – Sporomorph; AOM – Amorphous organic matter; *N. gracilis* – *Nannoceratopsis gracilis*.

Table II.1. TOC, TS, carbonate content and palynofacies data from Aït Moussa section, Middle Atlas Basin (Morocco).

Sample ID	TOC (wt.%)	TS (wt.%)	Carb (wt.%)	Phytoclast Group (%)	Phytoclast[1]		Amorphous Group (%)	Palynomorph Group (%)	Palynomorph[1]							Zoo. (%)	Palynofacies associations
					OP (%)	NOP (%)			Mar[2] (%)	Contin.[3] (%)	Continental palynomorphs[1](%)						
											Sp .	Tet.	Agg.	*Botryo.*	Zyg.		
A 24	0.20	0.018	40	38	40	60	1	60	1	99	90	7	3	0	0	1	PA9
A 23	0.22	0.013	43	65	52	48	1	34	1	99	93	6	1	0	0	1	PA8
A 22	0.33	0.030	48	64	39	61	2	34	1	99	93*	3	2	1	1	0	
A 21	0.22	0.16	49	32	24	76	24	35	1	99	99*	0	0	0	1	10	PA7
A 20	0.45	0.056	47	51	39	61	10	36	0	100	96*	2	0	0	2	4	
A 19	0.51	0.098	39	71	59	41	5	23	0	100	97	0	0	3	0	1	PA6
A18	0.54	0.23	41	62	59	41	2	33	2	98	98	0	0	2	0	3	
A 17	0.46	0.15	40	76	54	46	2	19	6	94	98	0	0	2	0	3	
A 16	0.33	0.075	33	69	39	61	1	29	0	100	96	2	1	0	1	2	
A15	0.57	0.20	35	64	56	44	2	29	0	100	78	8	9	5	0	5	PA5
A 14	0.32	0.012	39	77	37	63	1	21	0	100	87	5	2	5	2	1	
A 13	0.25	0.012	23	49	41	59	3	45	10	90	74	0	3	21	3	4	
A 12	0.37	0.41	41	76	51	49	6	14	21	79	39	0	0	61	0	4	PA4
A 11	0.35	0.03	42	82	39	61	4	12	5	95	90	2	0	6	2	2	
A 10	0.56	0.31	57	46	46	54	9	40	15	84	93	1	0	2	4	4	PA3
A 9	0.63	0.27	61	42	58	42	4	50	10	90	95	2	0	2	2	4	
A 8	0.29	0.13	--	65	54	46	9	21	15	85	90	3	0	5	3	5	
A 7	0.35	0.59	42	67	51	49	15	14	7	92	91	7	0	1	1	4	PA2
A 6	0.28	0.12	39	55	55	45	9	30	3	97	98	0	0	2	0	6	
A 5	0.45	0.33	78	46	49	51	5	46	5	95	96	0	0	4	0	3	
A 4	0.64	0.28	64	55	47	53	14	27	0	100	98	2	0	0	0	4	
A 3	0.27	0.15	41	58	45	54	8	20	2	98	96	3	1	0	0	13	PA1
A 2	0.53	0.053	63	52	59	41	11	34	3	97	98	2	0	0	0	3	
A 1	0.22	0.12	53	64	44	54	7	29	2	98	90	7	3	0	0	0	

Carb – carbonate content; OP – opaque; NOP – non-opaque; Mar – marine; Contin. – continental; Sp – sporomorph; Tet – tetrad; Agg – agglomerate; *Botryo.* – *Botryococcus* sp; Zig. – Zygospores of *zygnemataceae*; Zoo. – Zooclasts; [1] – recalculated to 100%; [2] – total marine microplankton (dinoflagellate cysts, acritarchs and prasinophyte algae); [3] – total continental palynomorphs (sporomorphs, tetrads, agglomerates, *Botryococcus* sp. and zygospores of *zygnemataceae*); *observation of fungal spores.

II.4.2.2.2. Amorphous Group

Despite the very low abundance of AOM in the Issouka section (average of ~ 1%; Fig. II.4 and Table II.2), AOM particles exhibit the same features as observed in the Aït Moussa section. Colouration ranges between yellow and orange in FM and brown to pale brown in TWL.

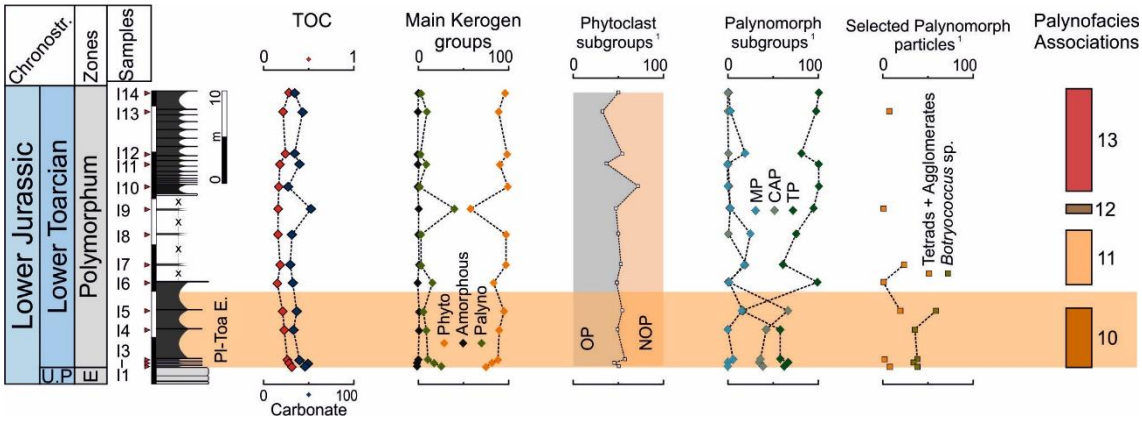

Figure II.4. TOC, carbonate content, palynofacies associations from Issouka section, Middle Atlas (Morocco). Layers with "x" – poorly exposed; Phyto – phytoclasts; Palyno – palynomorphs; OP – opaque; NOP – non-opaque; MP – marine palynomorphs; CAP – continental aquatic palynomorphs; TP – terrestrial palynomorphs; [1] – recalculated to 100%.

II.4.2.2.3. Palynomorph Group

Continental and marine palynomorphs occur in low amounts in most of the samples from the Issouka section (Fig. II.4 and Table II.2), ranging from 1% (sample I10) to 40% (sample I9). The observed palynomorphs consist mostly of sporomorphs (Figs. II.5A–C), with some belonging to the genus *Classopollis*. Tetrads (samples I1, I3, I5 to I7, I9, and I13, reaching up ~ 25% at I7) and agglomerates of pollen grains (samples I1, I5, and I6; Fig. II.5D) are also present. Despite the presence of zygospores of *zygnemataceae*, continental aquatic palynomorphs are mainly composed by *Botryococcus* sp., with an increase during the base of Polymorphum Zone (samples I1 to I5, reaching up 60% at the sample I5; Fig. II.5E). Marine components, such as dinoflagellate cysts (*Luehndea spinosa*), acritarchs (Fig. II.5F), and prasinophyte algae [*Cymatiosphaera* (Fig. II.5G) and *Tasmanites* (Fig. II.5H)] are present.

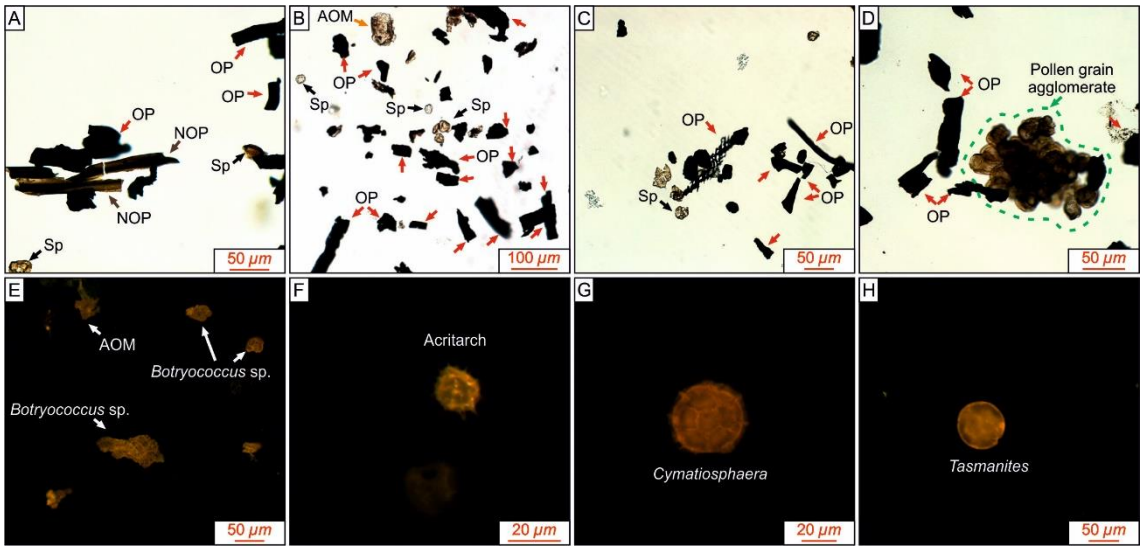

Figure II.5. Transmitted white light (TWL) and Fluorescence Mode (FM) photomicrographs of the studied kerogen assemblages from Issouka section, Middle Atlas (Morocco). **A**. Sample I3 with opaque (OP), non-opaque phytoclasts (NOP) and sporomorphs; **B**. TWL image with several OP, few sporomorphs and amorphous organic matter (AOM); **C**. OP and sporomorphs; **D**. Sample I1 with pollen grain agglomerate of *Classopollis* and OP; **E**. Several examples of *Botryococcus* sp. (sample I1); **F**–**H**. FM marine palynomorphs: acritarch, *Cymatiosphaera*, and *Tasmanites*. OP – Opaque phytoclast; NOP – Non-opaque phytoclast; Sp – Sporomorphs; Amorphous organic matter – AOM.

II.4.2.3. Vitrinite Reflectance

Vitrinite reflectance value in Issouka section is 0.48% R_o.

Table II.2. TOC, TS, carbonate content and palynofacies data from Issouka section, Middle Atlas Basin (Morocco).

Sample ID	TOC (wt.%)	TS (wt.%)	Carb (wt.%)	Phytoclast Group (%)	Phytoclast[1]		Amorphous Group (%)	Palynomorph Group (%)	Palynomorph[1]							Zoo. (%)	Palynofacies associations
					OP (%)	NOP (%)			Mar[2] (%)	Contin.[3] (%)	Continental palynomorphs[1](%)						
											Sp .	Tet.	Agg.	*Botryo*.	Zyg.		
I 14	0.27	0.02	34	96	51	49	1	3	0	100	100	0	0	0	0	0	
I 13	0.21	<0.01	42	90	33	67	0	9	4	96	92	8	0	0	0	1	
I 12	0.24	0.01	34	98	56	44	0	2	20	80	100	0	0	0	0	0	PA13
I 11	0.18	<0.01	40	91	38	62	0	9	0	100	100	0	0	0	0	0	
I 10	0.17	<0.01	26	99	73	27	0	1	0	100	100	0	0	0	0	0	
I 9	0.16	<0.01	52	58	48	52	1	40	3	97	96	2	0	0	2	1	PA12
I 8	0.16	0.02	31	96	51	49	1	3	25	75	100	0	0	0	0	0	
I 7	0.18	0.02	30	96	54	46	1	2	20	80	50	25	0	0	25	1	PA11
I 6	0.15	<0.01	32	83	48	52	0	16	2	98	96	2	2	0	0	1	
I 5	0.21	0.01	37	95	55	45	1	4	17	83	0	10	10	60	20	0	
I 4	0.22	0.02	32	90	50	50	1	9	0	100	57	0	0	36	7	0	
I 3	0.27	0.01	40	88	59	41	1	10	6	94	58	3	0	39	0	1	PA10
I 2	0.28	0.01	48	82	47	53	0	18	0	100	65	0	0	35	0	0	
I 1	0.31	0.01	46	74	51	49	0	26	0	100	52	5	4	39	0	0	

Carb – carbonate content; OP – opaque; NOP – non-opaque; Mar – marine; Contin. – continental; Sp – sporomorph; Tet – tetrad; Agg – agglomerate; *Botryo*. – *Botryococcus sp*; Zig. – Zygospores of *zygnemataceae*; Zoo. – Zooclasts; [1] – recalculated to 100%; [2] – total marine microplankton (dinoflagellate cysts, acritarchs and prasinophyte algae); [3] – total continental palynomorphs (sporomorphs, tetrads, agglomerates, *Botryococcus* sp. and zygospores of *zygnemataceae*).

II.5. Discussion

II.5.1. Thermal maturity

Vitrinite reflectance data from the Upper Pliensbachian–Lower Toarcian interval are within the same range as data obtained for the lower and middle Pliensbachian in Aït Moussa by Sachse et al. (2012), although slightly lower (vitrinite reflectance values between 0.5 and 0.6 % R_o). In this study, vitrinite reflectance indicates that the studied successions are immature (between 0.45 and 0.48 % R_o). However, and at a basin-scale (see Bejjaji et al., 2010), thermal maturity might be higher in regions with a different burial history.

II.5.2. Deposition and environmental conditions during the Late Pliensbachian–Early Toarcian in the Middle Atlas Basin inferred from kerogen assemblages

TOC contents in the Aït Moussa and Issouka sections reach up to 0.64 wt.% (Tables II.1 and II.2). The very low amounts of particles belonging to the Amorphous Group and the high abundance of phytoclasts and terrestrial palynomorphs indicate that kerogen assemblages are mostly of terrestrial affinity, suggesting proximity to the parent flora (Fig. II.6). Marine organic-walled microplankton, such as dinoflagellate cysts (*Luehndea spinosa* and *Nannoceratopsis* sp.), acritarchs, and prasinophyte algae (*Cymatiosphaera* and *Tasmanites*), coupled with the presence of marine macrofauna, such as belemnites and ammonites, show that deposition occurred in a marine depositional environment.

In the ternary kerogen and palynofacies plot for marine series of Tyson (1995), the dominance of the Phytoclast Group with low to moderate amounts of continental palynomorphs indicates deposition in oxic and proximal depositional environments, although with some variation (Fig. II.6). Sample A21 from Aït Moussa falls in field V (near route D, see Figure II.6 caption) and has the highest AOM content, suggesting the punctual occurrence of suboxic-dysoxic conditions. In general, palynofacies data from the Middle Atlas Basin are consistent with the overall palynological context of the neighbouring High Atlas Basin (Fig. II.1), where kerogen assemblages are mostly of terrestrial affinity and with a minor contribution of marine microplankton (Bodin et al., 2016).

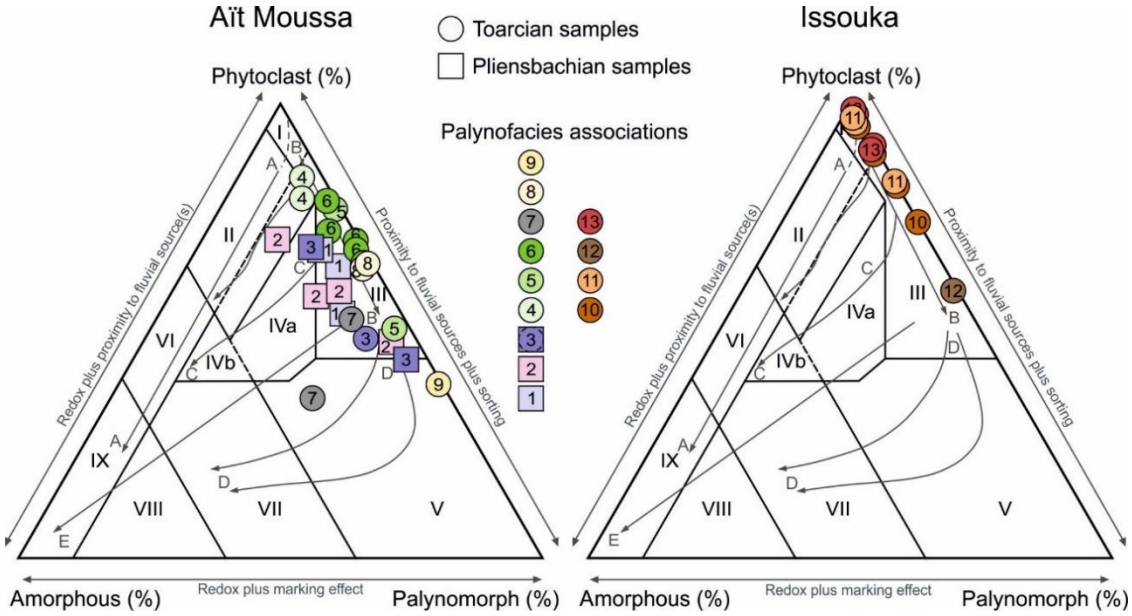

Figure II.6. Ternary kerogen and palynofacies plots for marine series (Tyson, 1995) based on the relative abundance of Phytoclast, Amorphous and Palynomorph Groups in the Aït Moussa and Issouka sections, Middle Atlas (Morocco). Palynofacies and environmental fields: (I) highly proximal shelf or basin, (II) marginal dysoxic-anoxic basin, (III) heterolithic oxic shelf (proximal shelf), (IV) shelf to basin transition, (V) mud-dominated oxic shelf (distal shelf), (VI) proximal suboxic-anoxic shelf, (VII) distal dysoxic-anoxic shelf, (VIII) distal dysoxic-oxic shelf and (IX) distal suboxic-anoxic basin. Transport paths: (A) direct path from source to anoxic basin, (B) Phytoclasts move away from the source out across shallow-marine shelf, (C) redirection of phytoclasts into the basin from route B, (D) continuation of route B with further reduction in phytoplankton organic carbon values and progressive sorting of phytoclasts and palynomorphs and (E) poorly defined shelf to basin pathway.

Based on the relative amount and occurrence of kerogen particles, the studied successions were divided into several Palynofacies associations (PA); nine (1 to 9) in Aït Moussa and four in Issouka (10 to 13). These PAs are interpreted to represent distinct intervals associated with Early Toarcian palaeoenvironmental changes in the Middle Atlas Basin.

II.5.2.1. Aït Moussa section

Palynofacies Association 1

This association corresponds to the lower part of the Aït Moussa section (Algovianum Zone; Fig. II.2 and Table II.1). TOC reaches up 0.53 wt.%, and the carbonate content varies between 41–63 wt.%. PA1 kerogen assemblages are dominated by the Phytoclast Group (varying

between 52–64%; Fig. II.2 and Table II.1). The Palynomorph Group is the second group in dominance (reaching up 34%), mainly composed of terrestrial palynomorphs.

The relatively high amounts of terrestrial sporomorphs (some pollen grains occurring in tetrads and agglomerates), low amounts of marine palynomorphs, and overall sedimentological characteristics (alternation of thin marls and medium-bedded fossiliferous limestones rich in belemnites and ammonites) suggest that deposition occurred in an oxic shallow-marine carbonate depositional environment (Fig. II.6).

Palynofacies Association 2

PA2 is characterised by the occurrence of *Botryococcus* sp. associated with low amounts of marine palynomorphs. TOC contents are similar to PA1, with TOC reaching up 0.64 wt.%. PA2 is dominated by the Phytoclast Group, between 46–67% (Fig. II.2 and Table II.1). The Palynomorph Group is dominated by terrestrial palynomorphs, mainly by the sporomorph subgroup.

Botryococcus sp. commonly thrives in shallow and oxygenated continental freshwater lakes, ponds, or other stagnant water bodies, although it can be found in a variety of depositional environments (mostly due to redeposition and fluvial transport) (Tyson, 1995). PA2 is interpreted to broadly correspond to the same depositional environment as PA1 (most samples fall within field III; Fig. II.6), however representing more proximal deposition.

Palynofacies Association 3

PA3 interval is characterised by an increase in marine palynomorphs (acritarchs and dinoflagellate cysts) when compared with PA2. It corresponds to the Pliensbachian Toarcian transition. TOC average is 0.49 wt.%, reaching up to 0.63 wt.% and carbonate content reach up to 61 wt.%. The Palynomorph Group increases in importance and is dominated by terrestrial palynomorphs (sporomorphs).

PA3 is indicative of deposition in an oxic proximal marine environment (Fig. II.6), as suggested by the increased occurrence of marine palynomorphs, significant amounts of phytoclasts, and the general sedimentological framework of the studied succession, i.e. increase in marly (argillaceous) sedimentation. PA3 is difficult to interpret within the broad context of the Middle Atlas Basin as it is lithologically different from Issouka, where the correlative interval is dominantly calcareous. The sedimentological differences between these two nearby locations likely reflect local variation in accommodation space, either driven by changes in sediment supply and sedimentation rates or tectonic compartmentalization (Fedan, 1978). The increase in marine components (acritarchs and dinoflagellate cysts) may also reflect local ecological conditions associated with the posited Late Pliensbachian cooling (e.g. Price, 1999; Dera et al., 2011; Korte and Hesselbo, 2011; Correia et al., 2017b), corroborated by belemnite $\delta^{18}O$ data from the Issouka section (Ait-Itto et al., 2017), and preceding the palaeoenvironmental changes of the Pl–Toa Event (Littler et al., 2010) (Fig. II.7).

Palynofacies Association 4

PA4 corresponds to the first sediments deposited after the stratigraphic discontinuity observed at the extreme base of the Lower Toarcian (around the Pliensbachian–Toarcian boundary) and is characterised by an accentuated increase in *Botryococcus* sp. and phytoclasts particles (Fig. II.2 and Table II.1). TOC varies between 0.35–0.37 wt.%, and carbonate content reaches up to 42 wt.%.

The peak occurrence in *Botryococcus* sp. (61% in sample A12) and the increase in phytoclasts particles is interpreted to have resulted from a major transgressive pulse, retrogradation of the shoreline and erosion of coastal areas (leading to re-sedimentation of *Botryococcus* sp. and Phytoclast Group particles in offshore areas), and increased riverine OM input. The relatively good preservation of *Botryococcus* sp. particles suggests some degree of environmental (oxygen) restriction. This PA corresponds to the onset of the Pl–Toa Event in the Middle Atlas Basin.

Palynofacies Association 5

PA5 is characterised by a decrease in *Botryococcus* sp. and an increase in sporomorphs and tetrads and agglomerates of pollen grains. TOC reaches up 0.57 wt.%, and carbonate content vary between 23–39 wt.% (Fig. II.2 and Table II.1).

The increase in sporomorphs, tetrads, agglomerates of pollen grains, and NOP are interpreted to represent increased proximity to the shoreline (e.g. Tyson, 1995; Pieñkowski and Waksmundzka, 2009; Mendonça Filho et al., 2012). Progradation of the shoreline (regression) was the result of high sedimentation rates due to intensification of continental weathering and increased fluvial runoff and flux of terrestrial OM into the marine systems, consistent with warming and enhancement of the hydrological cycle during the Pl–Toa Event and the Early Toarcian (e.g. Jenkyns et al., 2002; Cohen et al., 2004; Hesselbo and Pieñkowski, 2011; Kemp et al., 2011; Brazier et al., 2015; Krencker et al., 2015; Percival et al., 2016; Them II et al., 2017; Xu et al., 2017, 2018; Izumi et al., 2018).

Palynofacies Association 6

PA6 is characterised by the sporomorph subgroup dominance (average of 97%). PA6 kerogen assemblages are dominated by the Phytoclast Group, varying between 62–76% (Fig. II.2 and Table II.1). The Palynomorph group reaches up to 33% (Table II.1). TOC average is ~ 0.46 wt.%, reaching up to 0.54 wt.%, and carbonate content varies between 33–41 wt. %.

PA6 is interpreted as representing deposition in proximal and oxic environments, close to the source area (Fig. II.6), and in continuity with PA5. The presence of sporomorphs and phytoclasts after PA5 reflects the adjustment to the depositional conditions to a decrease in accommodation space and an increase of the energy of the depositional environment (regression) (see PA5). The Pl–Toa Event ends within PA6.

Palynofacies Association 7

PA7 corresponds to the most complex kerogen assemblage of the studied samples, with TOC values reaching up 0.45 wt.% and carbonate content averages of 48 wt.% (Fig. II.2 and Table II.1). This PA is characterised by the lowest content of phytoclasts (32% in sample A21) with the highest amounts of AOM and particles of the Zooclast Group (probably remains of foraminiferal test-linings). Fungal spores are observed in the kerogen assemblages (Table II.1).

PA7 is interpreted to be the result of a transgressive episode associated with coastal erosion, offshore sediment transport, and basin restriction (oxygen stressed) (Fig. II.6). In addition to the occurrence of spores and pollen grains, the presence of fungal spores suggests a strong connection with climate-driven processes, i.e. increased warming and humidity in the source area (Tyson, 1995; Pieñkowski et al., 2016). The occurrence of fungal debris in coastal sediments probably represents allochthonous terrestrial material associated with the degradation of wood and leaves (Tyson, 1995 and references therein) in continental/transitional environments.

Palynofacies Association 8

PA8 kerogen assemblages are dominated by phytoclasts, terrestrial palynomorphs, and low AOM contents (Fig. II.2 and Table II.1). TOC reaches up 0.33 wt.%, and the carbonate content vary between 43–48 wt.%.

The change from PA7 to PA8 is here interpreted to represent an initial regressive episode and decreased environmental restriction.

Palynofacies Association 9

PA9 is dominated by palynomorphs, reaching up 60% (highest recorded value; Fig. II.2 and Table II.1), with low TOC values (0.2 wt.%) and low carbonate content (40 wt.%). This interval is characterised by high relative content of sporomorph subgroup, marked by an increase of sporomorphs, tetrads, and agglomerates of pollen grains.

The change from PA8 to PA9 is here interpreted to represent the continuation of the regressive episode initiated in PA8.

II.5.2.2. Issouka section

Palynofacies Association 10

PA10 corresponds to the first sediments deposited after the stratigraphic discontinuity at the base of the Toarcian. Although this discontinuity is more evident at Issouka than in Aït Moussa (Fig. II.1), TOC, carbonate content and the kerogen assemblages are broadly similar to PA4 of Aït Moussa. TOC and carbonate content present average value of 0.26 wt.% and 41 wt.%, respectively. PA10 is essentially characterised by the high amount of *Botryococcus* sp. and phytoclasts (Fig. II.4 and Table II.2). The occurrence of *Botryococcus* sp. in these intervals reflects the same

transgressive tendency observed at Aït Moussa (PA4). The Pl–Toa Event is circumscribed to this interval (see Ait-Itto et al., 2017, 2018).

Palynofacies Association 11

PA11 is characterised by a sharp decrease in *Botryococcus* sp. and is dominated by the phytoclasts with small amounts of terrestrial palynomorphs (sporomorphs, tetrads and agglomerates of pollen grains). TOC values reaching up 0.18 wt.% and carbonate content averages 31 wt.% (Fig. II.4 and Table II.2). The change from PA10 to PA11 is interpreted to be related to aggradation/progradation of the shoreline in a regressive context reflecting the same response to the environmental changes registered at Aït Moussa (PA5 and PA6).

Palynofacies Association 12

PA12 is characterised by the sharp decrease of phytoclast content and the increase in palynomorphs. TOC value in this interval is 0.16 wt.%, and carbonate content reaches up to 52 wt.%. The Palynomorph Group assemblages are enriched in sporomorphs and small amounts of tetrads of pollen grains (Fig. II.4 and Table II.2).

PA12 is interpreted to be the result of the same transgressive episode observed at Aït Moussa (PA7). Although this episode is more intense at Aït Moussa when compared to Issouka, the increase in terrestrial palynomorphs suggests a connection with climate-driven processes, i.e. increased warming and humidity in the source area (Tyson, 1995; Pieñkowski et al., 2016), associated with coastal erosion and offshore sediment transport. The differences observed in kerogen assemblages between these two nearby locations reflect local changes in sediment supply.

Palynofacies Association 13

PA13 kerogen assemblages are dominated by phytoclasts, varying between 90–99%. The Palynomorph Group reaches up 9 %. TOC average is 0.21 wt.%, reaching up to 0.27 wt.%, and carbonate content varies between 26–42 wt. % (Fig. II.4 and Table II.2).

PA13 is interpreted as representing deposition in proximal and oxic environments, close to the source area (Fig. II.6). The presence of phytoclasts and sporomorphs after PA12 reflects the adjustment to the depositional conditions associated with a decrease in accommodation space together with an increase of the energy of the depositional environment (regression).

II.5.3. Changes in relative sea-level during the Late Pliensbachian–Early Toarcian and the Pl–Toa Event in the Middle Atlas Basin

Overall, the Late Pliensbachian Emaciatum (=Spinatum) Zone is regarded as a cool climate interlude, speculatively leading to the development of ice-house conditions (e.g. Price, 1999; van de Schootbrugge et al., 2005; Dera et al., 2011; Korte and Hesselbo, 2011; Suan et al., 2011; Price et al., 2013; Silva and Duarte, 2015; Ruebsam et al., 2019). This cooling event was associated with a significant eustatic sea-level fall and the occurrence of widespread hiatuses and other major erosional surfaces throughout the West Tethys and Arctic shelf seas (e.g. Marjanac and Steel, 1997; Hardenbol et al., 1998; Hallam, 2001; Suan et al., 2011; Barth et al., 2018). The Emaciatum Zone in both studied sections of the Middle Atlas Basin is characterised by the dominantly regressive calcareous "Calcaires de l'Ouarirt" (Figs. II.1, II.2, II.4 and II.7). Similar limestone-dominated units are observed in the High Atlas Basin (Ouchbis Formation; Bodin et al., 2016) and Lusitanian Basin (Lemede Formation; Duarte, 2007). This regressive trend is traceable across several European locations (e.g. Hardenbol et al., 1998; Morard et al., 2003; Quesada et al., 2005; Dera et al., 2010).

The earliest Toarcian is characterised by a major eustatic sea-level rise (locally associated with tectonic activity), which led to a major transgression in many basins worldwide (e.g. Hallam, 2001; Hardenbol et al., 1998; Wilmsen and Neuweiler, 2008; Duarte et al., 2010; Haq, 2018). This transgression was coincidental with a change to warmer and more humid climates and increased continental weathering and fluvial runoff (e.g. Cohen et al., 2004; McArthur et al., 2008; Bodin et al., 2010; Jenkyns, 2010; Korte and Hesselbo, 2011; Percival et al., 2015). In many locations, including the reference section of Peniche (Portugal) where the Toarcian GSSP is defined (see Pittet et al., 2014; Rocha et al., 2016), this time interval is characterised by the rapid transition (transgression) from shallow marine carbonates to hemipelagic marls (e.g. El Arabi et al., 2001; Wilmsen and Neuweiler, 2008; Duarte et al., 2010; Suan et al., 2010). In the Middle Atlas Basin, this transgressive event is materialized by the widespread deposition of marls and shales ("Couches d'Issouka"), owing to the combined action of i) tectonic activity (Benshili, 1989), ii) the onset of the Early Toarcian eustatic sea-level rise (e.g. Hardenbol et al., 1998; Hallam, 2001; Haq, 2018) and iii) the demise in the neritic carbonate factories which resulted in a major lithological break in both shallow- and deep-water settings, as reported in High Atlas Basin (see Wilmsen and Neuweiler, 2008; Bodin et al., 2016) (Fig. II.7). As aforementioned, the extreme base of the Lower Toarcian in the Middle Atlas Basin represents a 2nd-order transgressive–regressive (T–R) cycle boundary (Hardenbol et al., 1998; Jacquin and de Graciansky, 1998). Due to the resolution of this study, 3rd-order depositional sequences are not recognised in the Early Toarcian. The succession from the Late Pliensbachian (Emaciatum Zone) may correspond to the 3rd-order regressive phase in Hardenbol et al. (1998); the low-resolution sampling of the Algovianum Zone (PA1) and transition with Emaciatum Zone does not allow a clear identification of the 3rd-order transgressive phase (Fig. II.7).

Variation of sedimentary OM during the Early Toarcian (Polymorphum Zone) in the Middle Atlas Basin is interpreted to be associated with 4th-order relative sea-level changes driven by a combination of eustatic/tectonic and climatic/environmental forcing (Fig. II.7). Due to the

poor constraint or absence of the top of the Polymorphum Zone and the different hierarchical sequential schemes (3rd-order in Pittet et al. (2014) and 4th-order in this work), it is not possible to establish a sequential correlation with the reference section of Peniche.

Overall, PA2 follow the Late Pliensbachian regressive trend (Figs. II.6 and II.7). Deposition in a proximal shallow-water environment with continental influence is indicated through the high abundance of phytoclasts particles, presence of *Botryococcus* sp., and sporomorphs.

During the Pliensbachian–Toarcian transition, depositional conditions differed between Aït Moussa (PA3) and Issouka. The sedimentological differences between these two nearby locations reflect local changes in accommodation space, likely driven by variation in sediment supply and sedimentation rates, tectonic compartmentalization, or other ecological parameters, such as nutrient availability, water column depth, turbidity, etc. The increase in marine palynomorphs abundance (*Nannoceratopsis gracilis* and *Luehndea spinosa*) at Aït Moussa (PA3) is coincidental with the posited Late Pliensbachian cooling (see references above), which predated the Pl–Toa Event.

Lower Toarcian kerogen assemblages from Aït Moussa and Issouka record two short-term transgressive events (PA4, PA7, PA10 and PA12, respectively), where increases in *Botryococcus* sp., AOM particles and terrestrial palynomorphs indicate probable episodes of coastal erosion associated with transgression (of eustatic/tectonic? origin) concomitant with warmer and more humid climates leading to an increase in continental weathering and fluvial runoff. PA4 and PA10 correspond to the onset of the Pl–Toa Event.

Regressive intervals (PA5, PA6, PA8, PA9, PA11 and PA13) are characterised by phytoclasts particles and increases in sporomorphs, tetrads, and agglomerates of pollen grains. Kerogen assemblages from the Middle Atlas Basin (PA4, PA5, PA6, PA8, PA9, PA10, PA11 and PA13) suggest increased riverine runoff and terrestrial OM flux to the marine environments, indicating that regression occurred when sedimentation rates outpaced the rates of Early Toarcian sea-level rise (Posamentier and Allen, 1999; Catuneanu, 2006, 2017; Haq, 2018). Increased sedimentation rates in the Middle Atlas Basin resulted from the posited warming and intensification of the Lower Toarcian hydrological cycle, leading to enhanced continental weathering and increased fluvial runoff and riverine OM input into marine areas (e.g. Jenkyns et al., 2002; Cohen et al., 2004; McArthur et al., 2008; Bodin et al., 2010; Littler et al., 2010; Hesselbo and Pieñkowski, 2011; Brazier et al., 2015; Krencker et al., 2015; Percival et al., 2016; Them II et al., 2017; Xu et al., 2017, 2018; Izumi et al., 2018). PA5 and PA6 are included in the later stages of the Pl–Toa Event interval (Jenkyns, 1988; Cohen et al., 2004; Percival et al., 2016; Them II et al., 2017; Xu et al., 2017; Izumi et al., 2018).

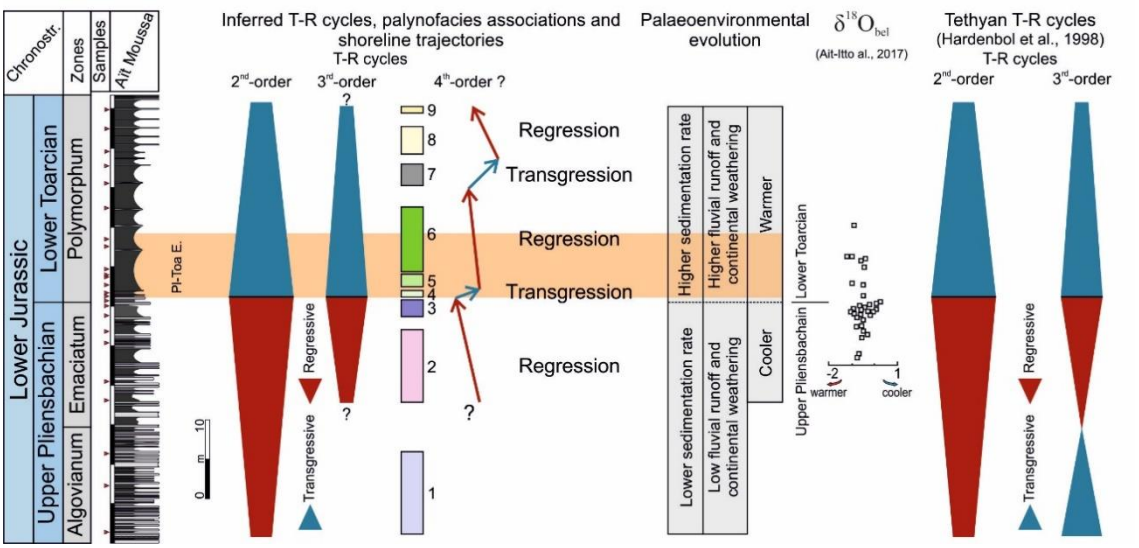

Figure II.7. Inferred Transgressive–Regressive (T–R) cycles, palynofacies associations and shoreline trajectories, main sedimentary events, tentative of palaeoenvironmental evolution, correlation with belemnite $\delta^{18}O$ data (Ait-Itto et al., 2017), and comparison with the T–R cycles in the Tethyan areas for the Upper Pliensbachian (Algovianum Zone)–Lower Toarcian (Polymorphum Zone) at the Aït Moussa section, Middle Atlas (Morocco).

II.6. Conclusions

This study presents new geochemical, palynofacies and thermal maturity data from the Upper Pliensbachian–Lower Toarcian marine successions at Aït Moussa and Issouka (Middle Atlas Basin, Morocco). From these datasets and their interpretation, it is possible to conclude that:

- The studied successions have low TOC contents and kerogen assemblages are dominated by organic particles from the Phytoclast Group. Vertical palynofacies variation was controlled by proximity to the shoreline, water depth, environmental restriction, climate, accommodation space, and tectonism.

- Vitrinite reflectance data show that organic material in the studied successions is immature.

- The studied Middle Atlas sections are some of the best examples of the Early Toarcian sea-level rise and the joint response of litho- and biosphere to sea-level change. Increases in *Botryococcus* sp., AOM, and terrestrial palynomorphs indicate episodes of coastal erosion associated with transgression related with eustatic rises/tectonic pulses? and warmer and more humid climates, whereas heterogeneous phytoclast assemblages with increases in sporomorphs and pollen grains occurring in tetrads and agglomerates indicate regressive episodes associated with increased sedimentation rates. Increased continental weathering, fluvial runoff, and input of riverine OM into marine areas resulted from warming and enhancement of the hydrological cycle during the Early Toarcian and the Pl–Toa Event.

III. Sedimentary organic matter and $\delta^{13}C_{Kerogen}$ variation on the southern Iberian palaeomargin (Betic Cordillera, SE Spain) during the latest Pliensbachian–Early Toarcian

Adapted from:

Rodrigues, B., Silva, R.L., Reolid, M., Mendonça Filho, J.G., Duarte, L.V., 2019. Sedimentary organic matter and $\delta^{13}C_{Kerogen}$ variation on the southern Iberian palaeomargin (Betic Cordillera, SE Spain) during the latest Pliensbachian–Early Toarcian. Palaeogeography, Palaeoclimatology, Palaeoecology, 534, 109342. doi.org/10.1016/j.palaeo.2019.109342.

Accepted: 23 August 2019

Abstract

The Early Toarcian Oceanic Anoxic Event (TOAE) is characterised by major palaeoenvironmental and palaeoceanographical changes (ocean anoxia, global warming, ocean acidification, among others), and a severe perturbation of the global carbon cycle. Although widespread oceanic anoxia was a significant control on the occurrence of organic-rich facies during the TOAE in several locations of the northern Tethyan margin, the effects of anoxia, oceanic productivity, and dilution are poorly understood in other worldwide locations, such as the southern Tethyan and Iberian margins.

In this study, we report new geochemical [total organic carbon (TOC), sulphur (TS), $CaCO_3$, $\delta^{13}C$ from kerogen isolates ($\delta^{13}C_{Kerogen}$)], palynofacies and thermal maturation data from the Upper Pliensbachian–Lower Toarcian successions in La Cerradura and Fuente Vidriera, External Subbetic domain, Betic Cordillera (SE Spain). The obtained results indicate that these successions have low TOC contents (~ 0.3 wt.%), with TOC reaching up to 0.46 wt.% around the Polymorphum–Serpentinum ammonite zone boundary in La Cerradura. $\delta^{13}C_{Kerogen}$ negative carbon isotope excursions are observed at the base of the Polymorphum Zone, the Pliensbachian–Toarcian Event (Pl–Toa Event), and base of the Serpentinum Zone (TOAE). Overall, the low maturity kerogen assemblages are dominated by terrestrial OM and with a minor marine component. Small increments in terrestrial OM, non-opaque phytoclasts, and palynomorphs are observed just before and during the TOAE in the studied area.

During the Early Toarcian, in the External Subbetic domain, accumulation and preservation of OM was low and with a significant terrestrial contribution, similarly to other locations around the southern margins of Iberia and Tethys. The dominance of the opaque phytoclast subgroup, the occurrence of *Classopollis*, and the relatively more positive $\delta^{13}C$ of terrestrial kerogen suggest that OM was mostly sourced from an area characterised by a semi-arid climate (i.e. with pronounced arid periods) during most of the Polymorphum Zone. The TOAE negative carbon isotope excursion

is accompanied by an increase in terrestrial OM, with a slight increase in the non-opaque phytoclast subgroup and terrestrial palynomorph subgroup. The increase of non-opaque phytoclast and terrestrial palynomorphs are in line with the posited enhancements of the hydrological cycle and export of terrestrial OM into marine environments during the TOAE. This study suggests a link between ^{13}C fractionation during photosynthesis in C3 plants and climate during the Early Toarcian. This link suggests coupling of the water and terrestrial carbon cycles before and during the TOAE.

Keywords: Organic geochemistry; Palynofacies; ^{13}C fractionation; Pl–Toa Event; TOAE; Iberian Peninsula.

III.1. Introduction

The Early Toarcian records major environmental changes affecting climate, ecosystems, geochemical cycles, and the widespread occurrence of organic-rich sediments in many locations of the northwestern Tethyan, Boreal and Panthalassic margins (e.g. Jenkyns and Clayton, 1986; Fleet et al., 1987; Jenkyns, 1988, 2010; Baudin et al., 1990; Röhl et al., 2001; Suan et al., 2011, 2015; Caruthers et al., 2014; Al-Suwaidi et al., 2016; Them II et al., 2017; Silva et al., 2017; Fantasia et al., 2018b; Ruebsam et al., 2018). An important perturbation of the global carbon cycle is coeval with the most significant episode of organic matter (OM) deposition and preservation during the Early Toarcian (e.g. Jenkyns, 1988; Hesselbo et al., 2000). This interval corresponds to the Early Toarcian Oceanic Anoxic Event (TOAE) and is characterised worldwide by a negative carbon isotopic excursion (CIE) at the base of the Serpentinum/Falciferum/Levisoni ammonite Zone, superimposed on a broader early Toarcian positive CIE recorded in carbonates, fossil wood and OM (e.g. Jenkyns and Clayton, 1986; Jenkyns, 1988, 2010; Hesselbo et al., 2000, 2007; Jenkyns et al., 2002; Cohen et al., 2004; Hermoso et al., 2009; Bodin et al., 2010, 2016; Littler et al., 2010; Suan et al., 2010, 2011, 2015; Reolid et al., 2012; Kafousia et al., 2014; Caruthers et al., 2014; Kemp and Izumi, 2014; Al-Suwaidi et al., 2016; Pieñkowski et al., 2016; Silva et al., 2017; Them II et al., 2017; Xu et al., 2017; Fantasia et al., 2018b; Ruebsam et al., 2018).

Preservation and accumulation of OM in marine environments depends on the complex interplay between several mechanisms and feedbacks (e.g. productivity, preservation due to anoxia, dilution of OM, and water column stratification; Tyson, 1995; Zonneveld et al., 2010). Although ocean anoxia was a significant control in OM preservation in many locations of the northwestern Tethyan margin (see Jenkyns and Clayton, 1986; Fleet et al., 1987; Jenkyns, 1988, 2010; Baudin et al., 1990; Röhl et al., 2001; Xu et al., 2018; Baroni et al., 2018), the relative contributions of anoxia (or lack thereof), productivity and sedimentary dilution leading to the occurrence of organic-rich facies in the Tethyan and Panthalassic margins during the Early Toarcian are still poorly understood.

There is a marked dichotomy between the northern and southern Tethyan margins regarding the distribution of OM. Lower Toarcian organic-rich facies are restricted to the northwestern Tethyan margin, Boreal area, and several Panthalassic sections (e.g. Jenkyns and Clayton, 1986; Jenkyns, 1988, 2010; Röhl et al., 2001; van de Schootbrugge et al., 2005, 2013; Hesselbo et al., 2007; Suan et al., 2011, 2015; Caruthers et al., 2014; Them II et al., 2017; Baroni et al., 2018; Ruebsam et al., 2018) and contrast with the low organic contents and expanded thickness of contemporaneous successions of the southern Tethyan and Iberian margins, where the Lower Toarcian reaches up to ~150 m such us observed in Morocco (e.g. Bodin et al., 2010, 2016). Contrariwise, the shallow-water Lower Toarcian stratigraphic successions in the Betic Cordillera (southern Spain) are remarkably thin and poor in OM (low in TOC content; Rodríguez-Tovar and Reolid, 2013; Reolid, 2014a, 2014b; Reolid et al., 2014). Based on geochemical detrital proxies (Si/Al, K/Al, Rb/Al, Ti/Al, and Zr/Al), Rodríguez-Tovar and Reolid (2013) and Reolid (2014a, 2014b) suggested that organic input from emerged areas broadly dominated sedimentary OM in the External Subbetic domain (Betic Cordillera) during the Early Toarcian, with subordinated dependence in marine productivity and redox conditions at the seafloor. Lack of persistent anoxia (at least in bottom-waters) was favoured by local physiography and vigorous circulation, leading to the organic-poor sediments of the south Iberian Palaeomargin (Rodríguez-Tovar and Uchman, 2010; Rodríguez-Tovar and Reolid, 2013; Reolid, 2014a, 2014b).

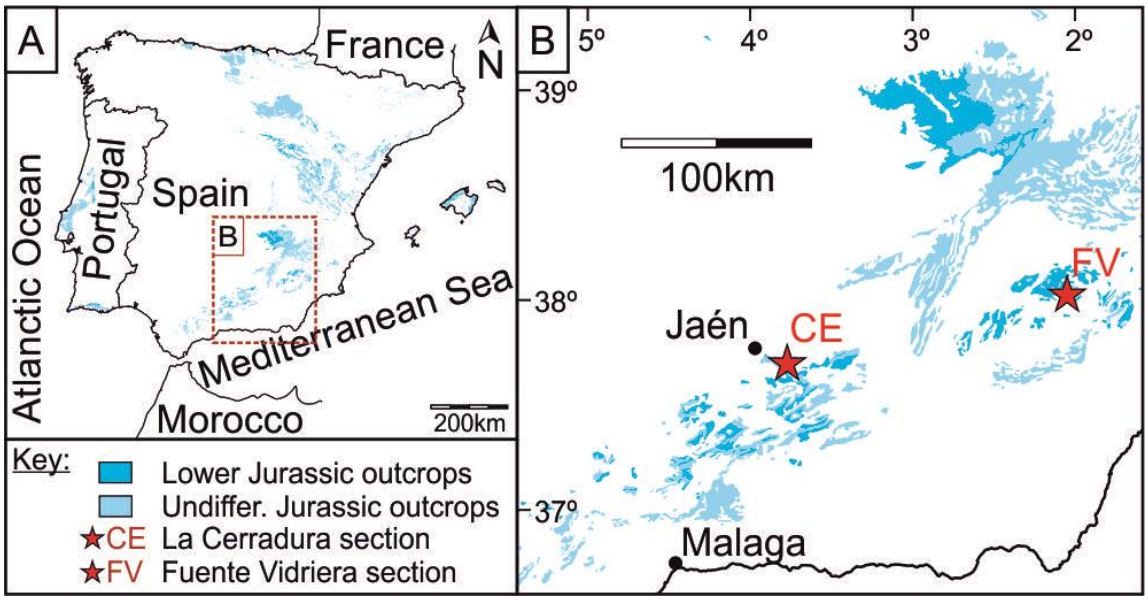

Figure III.1. Geological map of the Jurassic outcrops in the Betic Cordillera and the Tabular Cover (south Iberian Palaeomargin) and location of the La Cerradura section (CE) and Fuente Vidriera section (FV) (adapted from Rodríguez-Fernandez et al., 2016). Note: Undiffer. – Undifferentiated.

This study is focused on the characterisation of sedimentary OM (palynofacies and $\delta^{13}C$ analysis), conducted for the first time in fine-grained marly samples from two key sections in the External Subbetic: La Cerradura and Fuente Vidriera (Figs. III.1 and III.2). The main objective of

this study is to investigate palaeoclimatic, palaeogeographical, and palaeoceanographical controls on the occurrence of organic facies during the Early Toarcian in the south Iberian Palaeomargin and, therefore, elucidate on the observed dichotomy regarding the distribution of organic-rich facies between the northern and southern Tethyan margins.

III.2. Geological background

The External Zones of the Betic Cordillera extends across the south and south-eastern Spain and comprises the Prebetic and Subbetic domains, with a thick Triassic–Miocene sedimentary column (Vera, 2004). The south Iberian successions were deposited in a large shallow carbonate platform developed during the earliest Jurassic (García-Hernández et al., 1989; Vera, 2004). After the Early Pliensbachian, the epeiric platform was fragmented by a rifting episode, and the Prebetic and Subbetic domains were differentiated. After rifting, the distal setting of the south Iberian Palaeomargin, represented by the Subbetic domain, was affected by listric faults and evolved to pelagic swells with low subsidence and central troughs (see Vera, 2004).

The La Cerradura (Jaén; 37º41´47.8´´N; 3º37´57.6´´W) and Fuente Vidriera (Murcia; 38º03´19.8´´N; 2º07´01.7´´E) sections are located in the External Subbetic (Fig. III.1). The studied Lower Jurassic successions in this area consist of hemipelagic facies of marls and marly limestones dated as Upper Pliensbachian–Aalenian (Zegrí Formation; Fig. III.2). Ammonite biostratigraphy is used for correlation and follows Jiménez (1986) and Jiménez and Rivas (2007).

III.2.1. Description of the studied sections

III.2.1.1. La Cerradura section

The La Cerradura section is located in the province of Jaén, ~17 km south of the city of Jaén, and crops out in a road-cut along motorway A44. The section extends from the Algovianum Zone (Pliensbachian) to the Serpentinum Zone (Toarcian) and consists of about 81 m of marl–marly limestone rhythmites belonging to the Zegrí Formation (Reolid et al., 2018, and references therein). The studied interval corresponds to ~ 25 m of the upper part of the sedimentary succession (Fig. III.2). The lower part of the studied interval consists of white–grey marly limestones and grey marls with abundant ammonites and trace fossils, and it is dated from the top of Emaciatum Zone (uppermost Pliensbachian) and Polymorphum Zone (Lower Toarcian) based on foraminiferal assemblages and ammonites (Ruget and Martínez-Gallego, 1979; Jiménez, 1986). The reduced

thickness and the large number of ammonites observed at the top of the Polymorphum Zone suggest the existence of an omission surface at the Polymorphum-Serpentinum boundary.

The Serpentinum Zone is represented by a thick interval of dark grey marls with rare fossils of invertebrates (Sandoval et al., 2012; Reolid et al., 2014; Baeza-Carratalá et al., 2017). The significant colour change observed (Fig. III.2) is related to the decrease of carbonate content and the increase in clay minerals (Reolid et al., 2014, 2019a).

III.2.1.2. Fuente Vidriera section

The Fuente Vidriera section is located in the province of Murcia. This section comprises approximately 50 m of marls with marly–limestone intercalations and the studied interval corresponds to ~ 25 m, belonging to Zegrí Formation (Polymorphum and Serpentinum zones; Jiménez and Rivas, 2007) (Fig. III.2). Chronostratigraphy of Fuente Vidriera section is based on stratigraphic correlation due to the scarcity of index fossils (Jiménez and Rivas, 2007). In addition, foraminiferal studies (Ruget and Martínez-Gallego, 1979) have been also conducted in this section. Despite the chronostratigraphic uncertainty regarding placement of zone boundaries, the Polymorphum and Serpentinum zones are identified in this location (Jiménez, 1986; Jiménez et al., 1996; Jiménez and Rivas, 2007).

III.3. Material and methods

Twenty-eight marly samples were collected from the uppermost Pliensbachian–Lower Toarcian interval at the La Cerradura (18 samples) and Fuente Vidriera (10 samples) sections (Fig. III.2) and analysed for total organic carbon (TOC), total sulphur (TS), total carbonate content ($CaCO_3$), $\delta^{13}C$ in kerogen isolates ($\delta^{13}C_{Kerogen}$), palynofacies and thermal maturation. To avoid contamination and to minimize the impact of weathering related alteration of the sediments, the sampling was performed after removal of about 15 cm of superficial sediments. TOC, TS, $CaCO_3$, $\delta^{13}C_{Kerogen}$, palynofacies and thermal maturation analysis were conducted in the Palynofacies and Organic Facies Laboratory (LAFO) of the Rio de Janeiro Federal University (Rio de Janeiro, Brazil). $\delta^{13}C_{Kerogen}$ was analysed at MAREFOZ Laboratory (University of Coimbra, Portugal).

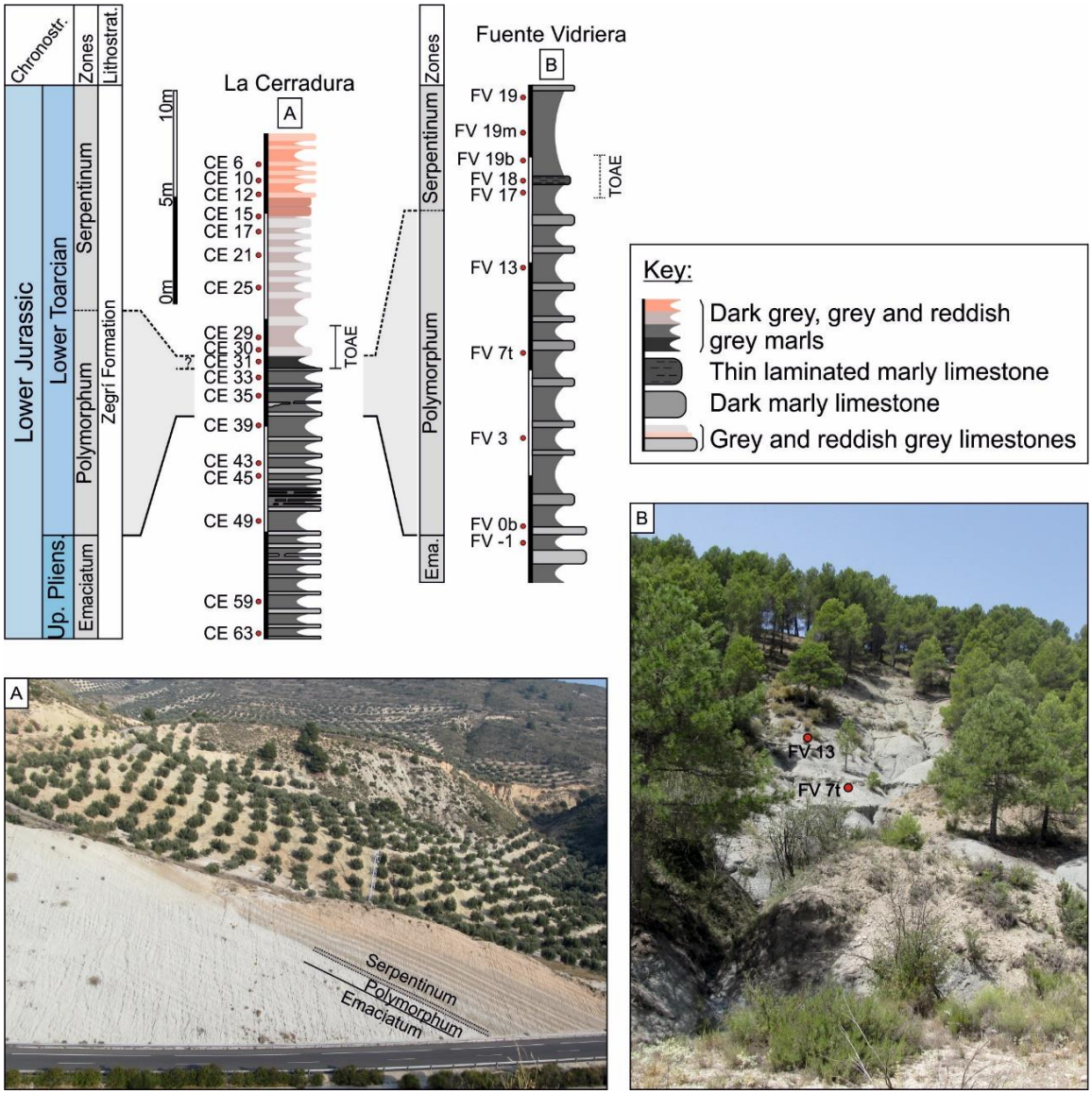

Figure III.2. Simplified stratigraphic logs of the uppermost Pliensbachian–Lower Toarcian interval in the La Cerradura and Fuente Vidriera sections (modified from Reolid et al., 2014; Reolid, 2014a). The duration of the TOAE in La Cerradura section is based in Reolid et al. (2014) and Fuente Vidriera in Reolid (2014a). **A**. Field view of La Cerradura section; **B**. Field view of Fuente Vidriera section. Chronostr. – Chronostratigraphy; Up. Pliens. – uppermost Pliensbachian; Ema. – Emaciatum Zone; Poly – Polymorphum Zone.

III.3.1. Kerogen isolation

Kerogen was isolated from the rock matrix using the standard, non-oxidative procedure described, for example, by Tyson (1995) and Mendonça Filho et al. (2012), among others. First, all samples were mechanically disaggregated to approximately 2 mm rock chips. Afterwards, each sample was sequentially acid-treated to remove carbonates (HCl 37% for 18 h), then silicates (HF

40% for 24 h), and finally neoformed fluorides (HCl 37% for 3 h). Between each step, the pH material was neutralised with distilled water. The organic and non-organic material were separated by flotation using $ZnCl_2$ (density between 1.9–2.0 g/cm^3). The organic fraction was recovered, and the heavy liquid was eliminated using drops of HCl (10%) followed by a wash with distilled water. After the flotation process, the isolated kerogen was sieved at 20 μm.

III.3.2. Geochemical analysis

After acidification for $CaCO_3$ content determination, obtained by difference through the insoluble residue, TOC and TS were determined using a LECO SC 144 device, with an analytical precision of ±0.1% and following the ASTM Standard D4239-08 (2008) and NCEA-C-1282 (United States Environmental Protection Agency, U.S.EPA, 2002) methods.

III.3.3. Palynofacies

Batches of kerogen isolates were sieved (20 μm) and unsieved strew slides were prepared according to the methodological procedure outlined in Tyson (1995) and Mendonça Filho et al. (2012). Transmitted white light (TWL), reflected white light (RWL), and incident blue light (fluorescence mode; FM) microscopic techniques were used for the qualitative and quantitative (at least 300 particles per slide) examinations of the kerogen groups. The main palynofacies kerogen groups, i.e., Phytoclasts, Amorphous, and Palynomorphs, and an additional group, Zooclast, were recognised using pre-established descriptive categories (see Tyson, 1995) and Mendonça Filho et al. (2012), providing a robust and reproducible identification scheme (see Tables III.1 and III.2). The obtained strewn slides counts were recalculated as relative percentage (%).

III.3.4. Vitrinite reflectance

Vitrinite reflectance (R_o) was measured in 5 plugs of concentrated kerogen prepared according to standard procedures (ISO 7404-2, 2009), [2 samples from La Cerradura (CE 15 and CE 39) and 2 from Fuente Vidriera (FV -1 and FV 18)]. The analyses were performed with a Carl Zeiss Axioskop 2-Plus microscope equipped with a spectrophotometer J&M (MSP 200), with 50× objective in immersion oil (ηe=1.518–23°C), according to ASTM Standard D7708 (2014). The microscope was calibrated with Spinel (0.425% Rr) standards.

III.3.5. $\delta^{13}C_{Kerogen}$

Kerogen concentrates (see section III.3.1) were mounted in tin capsules and $\delta^{13}C$ was determined in carbonate-free ($\delta^{13}C_{Kerogen}$) fraction using a Flash EA 1112 Series elemental analyser coupled online via a Finningan Conflo III interface to a Thermo Delta V S mass spectrometer. Internal precision is better than ±0.1‰ for $\delta^{13}C$ (Acetanilide Standard from Thermo Electron Corporation). Gas species of different mass were separated in a magnetic field then simultaneously measured using a Faraday cup collector array to measure the isotopomers of CO_2 at m/z 44, 45, and 46.

III.4. Results

III.4.1. La Cerradura section

III.4.1.1. TOC, TS and carbonate content

TOC average is ~ 0.3 wt.%, reaching up to ~ 0.46 wt.% in sample CE 31 (around the boundary between the Polymorphum–Serpentinum zones; Fig. III.3 and Table III.1). TS vary between 0.01–0.27 wt.% (average value of 0.09 wt.%), with the highest TS contents observed in sample CE 17. The $CaCO_3$ contents range between 32–80%, with a slight decrease between samples CE 35 and CE 15 (Fig. III.3 and Table III.1), especially in the dark grey marls of the Serpentinum Zone.

III.4.1.2. Carbon isotopes

$\delta^{13}C_{Kerogen}$ varies between -23.30 and -20.74‰ (Fig. III.3 and Table III.1). From uppermost Emaciatum Zone until the base of Serpentinum Zone, $\delta^{13}C_{Kerogen}$ are relatively more positive, between -22‰ and -21‰. At the beginning of the Serpentinum Zone (sample CE 30), a slight decrease of about 1.3‰ is observed, reaching the minimum value of -23.30‰. Upwards, $\delta^{13}C_{Kerogen}$ values shift again to more positive values, between -22‰ and -21‰ (Fig. III.3 and Table III.1).

III.4.1.3. Palynofacies

La Cerradura section is thermally immature (vitrinite reflectance values vary between 0.49% R_o and 0.51% R_o) and the kerogen assemblages include the main kerogen groups: Phytoclast, Amorphous, and Palynomorph, dominated by the Phytoclast Group (average ~ 92%, reaching up to ~ 99% in sample CE 6; Figs. III.3 and III.4, Table III.1).

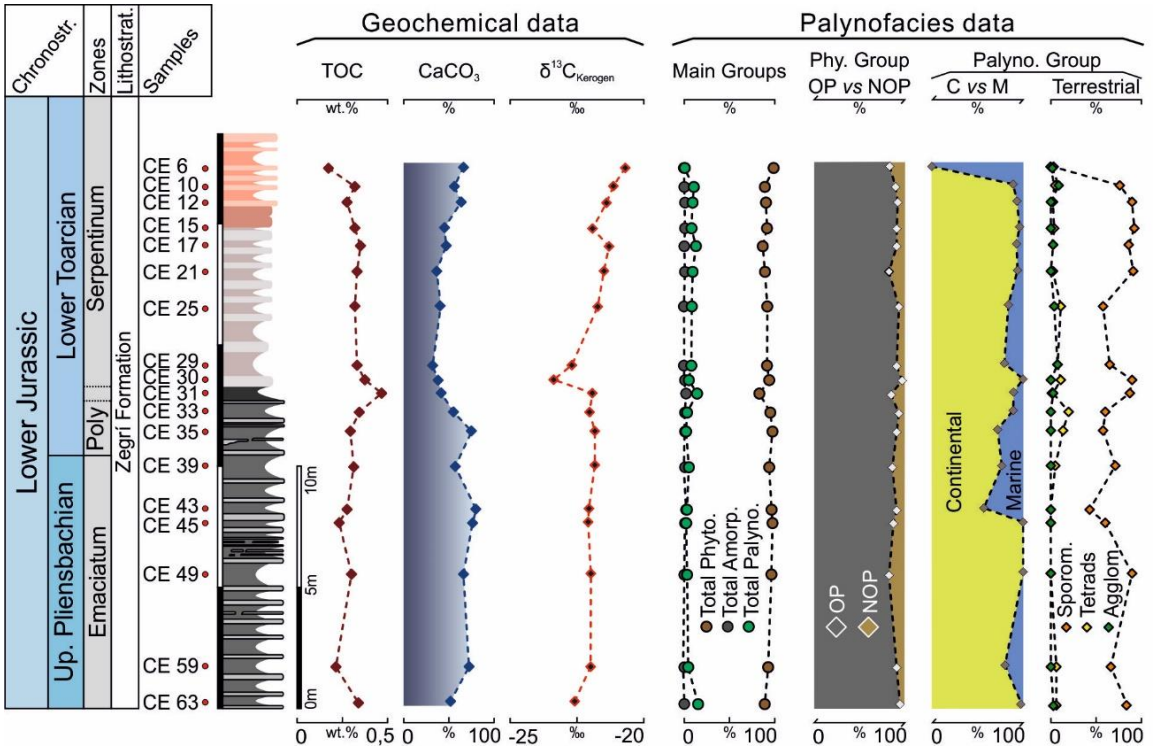

Figure III.3. TOC, $CaCO_3$, $\delta^{13}C_{Kerogen}$ and palynofacies associations from La Cerradura section, External Subbetic (Betic Cordillera, SE Spain). Up. Pliensbachian – Upper Pliensbachian; Poly – Polymorphum Zone; OP – opaque; NOP – non-opaque; C – continental; M – marine; Sporom. – sporomorphs; Agglom. – agglomerates.

The Phytoclast Group is the most abundant kerogen group, with the lowest content is observed in sample CE 31 (83%) (Figs. III.3 and III.4, Table III.1). Opaque phytoclasts are the main subgroup (average value of ~89%; Figs. III.5A and III.5B). The non-opaque phytoclasts subgroup is the second most represented Phytoclast Group, averaging ~11% (Fig. III.5A). Other Phytoclast Group particles, such as cuticles, membranes, and sclereids are extremely rare or absent (Fig. III.5C).

The Amorphous Group is rare in all samples (average of ~ 1%; Figs. III.3 and III.4, Table III.1). Particles present diffuse limits or are unstructured and are classified as amorphous organic matter (AOM). AOM colouration ranges between brown to pale brown in TWL (Fig. III.5D) and yellow and orange in FM, presenting inclusions of palynomorphs and pyrite (Figs. III.5E and III.5F).

Particles belonging to the Palynomorph Group occur in low amounts in most of the samples, ranging from 0% (CE 6) to 15% (CE 63) (Fig. III.3 and Table III.1). Most of the particles have inclusions of pyrite (Fig. III.6A).

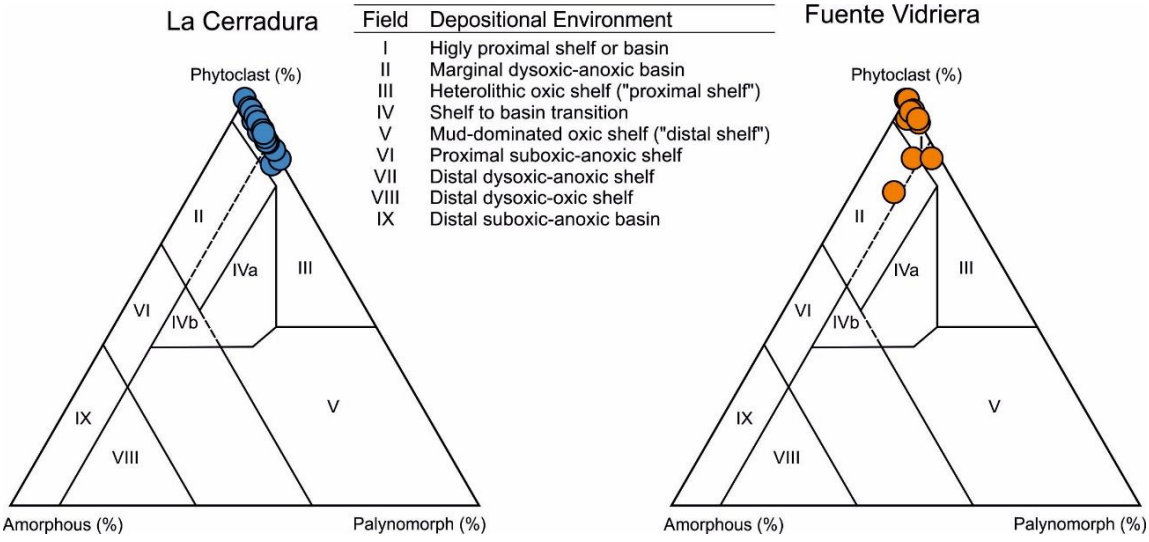

Figure III.4. Ternary kerogen and palynofacies plots for marine series (Tyson, 1995) based on the relative abundance of Phytoclast, Amorphous and Palynomorph Groups in the La Cerradura and Fuente Vidriera sections, External Subbetic (Betic Cordillera, SE Spain). Palynofacies and environmental fields: (I) highly proximal shelf or basin, (II) marginal dysoxic-anoxic basin, (III) heterolithic oxic shelf (proximal shelf), (IV) shelf to basin transition, (V) mud-dominated oxic shelf (distal shelf), (VI) proximal suboxic-anoxic shelf, (VII) distal dysoxic-anoxic shelf, (VIII) distal dysoxic-oxic shelf and (IX) distal suboxic-anoxic basin.

Continental palynomorphs are mainly represented by terrestrial palynomorph subgroup such as sporomorphs, with some pollen occurring in tetrads or agglomerates (Figs. III.6D and III.6E). Pollens belonging to the genus *Classopollis* (Fig. III.6B) are present. Continental aquatic palynomorphs are represented by very low amounts of zygospores of *zygnemataceae* (Fig. III.6F).

Marine palynomorphs, such as dinoflagellate cysts (*Luehndea spinosa* and *Nannoceratopsis gracilis*; Fig. III.6G), acritarchs (Fig. III.6H), and prasinophyte algae (*Tasmanites*) occur in low amounts in sample CE 59 (20%) and in the intervals between samples CE 43–CE 31 (average of 23%) and CE 29–CE 25 (average of 17%). The Zoomorph Group is represented by foraminiferal test-linings (Fig. III.6I).

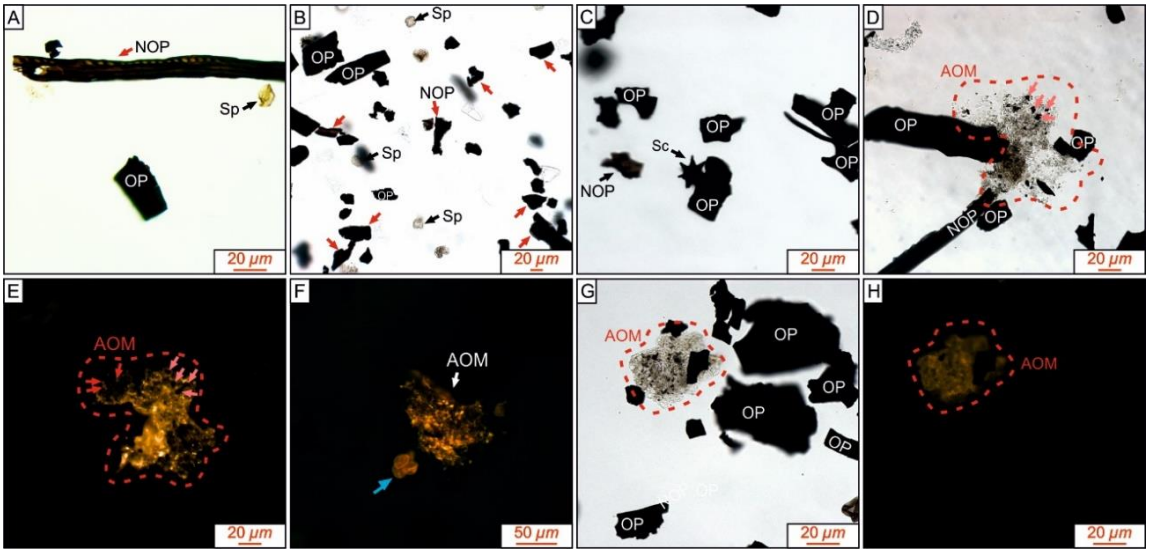

Figure III.5. Transmitted white light (TWL) and Fluorescence Mode (FM) photomicrographs of the studied kerogen assemblages from La Cerradura and Fuente Vidriera sections, External Subbetic (Betic Cordillera, SE Spain). **A**. Sample CE 45 (top of Emaciatum Zone) with opaque (OP), non-opaque phytoclasts (NOP) and sporomorph; **B**. OP assemblage with NOP and few sporomorphs from sample FV 19 (Serpentinum Zone); **C**. Example of sclereid (Sc) and OP from sample CE 6 (Serpentinum Zone); **D** and **E**. TWL and FM images from sample CE 35 (Polymorphum Zone) with AOM with palynomorphs (red arrow) and framboidal pyrite (pink arrow) inclusions, OP, and NOP; **F**. FM image of AOM and tetrads from the genus *Classopollis* (blue arrow) from sample CE 31 (around the Polymorphum–Serpentinum zone boundary); **G** and **H**. TWL and FM images from sample FV 13 (Polymorphum Zone) with AOM with OP. OP – Opaque phytoclast; NOP – Non-opaque phytoclast; Sc – Sclereids; AOM – Amorphous organic matter.

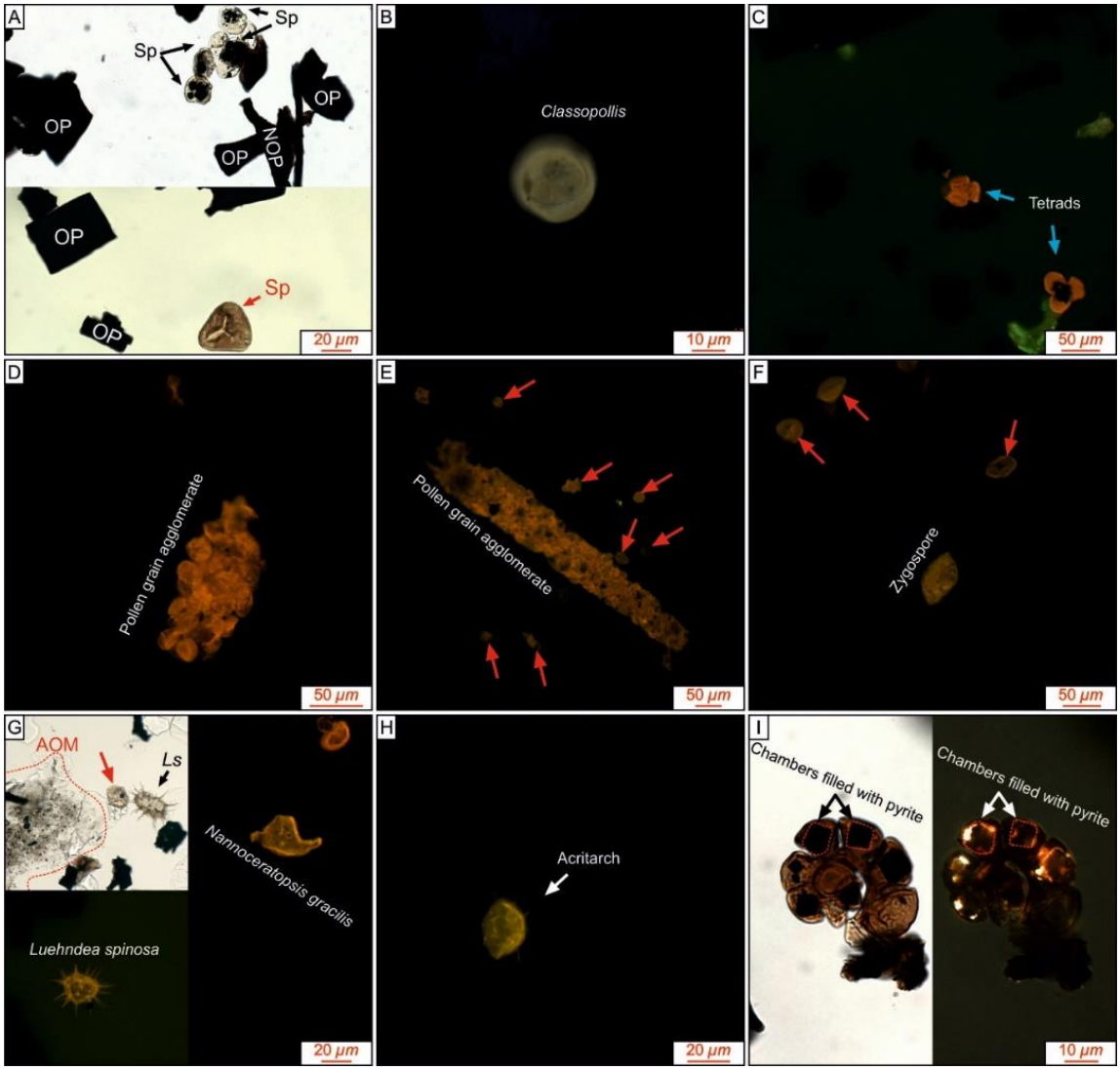

Figure III.6. Transmitted white light (TWL) and Fluorescence Mode (FM) photomicrographs of the studied kerogen assemblages from La Cerradura and Fuente Vidriera sections, External Subbetic (Betic Cordillera, SE Spain). **A**. TWL images with sporomorphs with pyrite inclusions, OP, and NOP (sample CE 15; Serpentinum Zone) and an example of one sporomorph with trilete mark, OP, and NOP (sample FV 13; Polymorphum Zone); **B** and **C**. FM images from sample CE39 (top of Emaciatum Zone) with a *Classopollis* pollen grain and two tetrads from the genus *Classopollis* (blue arrow) and from sample FV 3 (base of Polymorphum Zone); **D** and **E**. FM images from sample CE 25 (Serpentinum Zone) with a pollen grain agglomerate and several sporomorphs (red arrow; sample CE 31); **F**. FM image of zygospore of *zygnemataceae* and sporomorphs (red arrow) from sample CE 17 (Serpentinum Zone); **G**. TWL image from sample FV 13 (Polymorphum Zone), with *Luehndea spinosa*, AOM, sporomorphs (red arrow), FM image from samples CE 39 and CE 10 (top of Emaciatum and Serpentinum zones) with *Luehndea spinosa* and *Nannoceratopsis gracilis*; **H**. FM image of sample CE 29 with acritarch; **I**. TWL image from sample CE 39 (top of Emaciatum Zone) with foraminiferal test-linings with chambers filled with pyrite. OP – Opaque phytoclast; NOP – Non-opaque phytoclast; Sp – Sporomorphs; Ls – *Luehndea spinosa*.

Table III.1. TOC, TS, $CaCO_3$ content, $\delta^{13}C_{Kerogen}$ and palynofacies data from La Cerradura section, External Subbetic domain (Betic Cordillera, SE Spain).

Sample ID	TOC (wt%)	TS (wt%)	$CaCO_3$ (wt%)	$\delta^{13}C_{Kerogen}$ (‰)	Phytoclast Group (%)	Phytoclast[1]		Amorphous Group (%)	Palynomorph Group (%)	Palynomorph[1]		Continental palynomorphs[1]				Zooclasts (%)
						OP (%)	NOP (%)			Mar[2] (%)	Contin[3] (%)	Sp (%)	Tet (%)	Agg (%)	FM (%)	
CE 6	0.17	0.01	66	-20,74	99	86	14	0	0	0	0	0	0	0	0	1
CE 10	0.32	0.16	56	-21.18	89	89	11	0	11	9	91	76	6	9	0	0
CE 12	0.27	0.08	64	-21.40	90	91	9	0	9	7	93	90	3	0	0	0
CE 15	0.31	0.12	46	-21.91	91	90	10	1	8	4	96	92	4	0	0	0
CE 17	0.35	0.27	47	-21.42	87	90	10	0	13	7	93	85	2	2	2	0
CE 21	0.33	0.10	37	-21.53	90	82	18	1	10	6	94	91	3	0	0	0
CE 25	0.32	0.08	41	-21.74	92	93	7	0	8	15	85	58	12	4	12	0
CE 29	0.33	0.15	32	-22.78	92	91	9	0	8	19	81	65	8	8	0	0
CE 30	0.37	0.07	38	-23.30	94	96	4	0	6	0	100	89	11	0	0	0
CE 31	0.46	0.10	42	-21.98	84	85	15	2	14	9	91	86	2	2	0	0
CE 33	0.34	0.10	55	-22.04	96	92	8	0	3	10	90	60	20	0	10	1
CE 35	0.29	0.09	75	-21.84	97	90	10	0	2	29	71	57	14	0	0	0
CE 39	0.31	0.07	57	-21.83	94	86	14	0	5	24	76	71	6	0	0	0
CE 43	0.27	0.05	80	-22.08	96	90	10	2	2	43	57	43	0	0	14	0
CE 45	0.23	0.04	76	-22,07	98	86	14	1	2	0	100	60	0	0	40	0
CE 49	0.30	0.07	66	-22.01	96	82	18	0	3	0	100	89	0	0	11	1
CE 59	0.21	0.05	72	-22.02	93	90	10	0	5	20	80	67	7	0	7	2
CE 63	0.34	0.06	52	-22,59	85	94	6	0	15	2	98	83	4	4	6	0

OP – opaque; NOP – non-opaque; Mar – marine; Contin – continental; Sp – sporomorph; Tet – tetrad; Agg – agglomerate; FM. – freshwater microplankton; [1] – recalculated to 100 %; [2] – total marine microplankton (dinoflagellate cysts, acritarchs and prasinophyte algae); [3] – total continental palynomorphs [sporomorphs, tetrads, agglomerates and freshwater microplankton (i.e., zygospores of *zygnemataceae*)].

III.4.2. Fuente Vidriera section

III.4.2.1. TOC, TS and carbonate content

TOC contents in Fuente Vidriera section average about 0.3 wt.%, reaching up to 0.44 wt.% in sample FV -1 (uppermost Emaciatum Zone) and FV 3 (base of Polymorphum Zone; Fig. III.7 and Table III.2). TS contents are low, ranging from 0.01 to 0.009 wt.%. $CaCO_3$ content ranges between 46–77%, presenting an average value of 52% (Fig. III.7 and Table III.2).

III.4.2.2. Carbon isotopes

$\delta^{13}C_{Kerogen}$ varies between -24.55‰ and -21.89‰ (Fig. III.7 and Table III.2). Between samples FV1 and FV 0b (extreme base of Polymorphum Zone), $\delta^{13}C_{Kerogen}$ decreases from -21.89‰ to -24.55‰, stabilising afterwards and maintain a positive trend between -23‰ and -22‰. In sample FV 19b (Serpentinum Zone), $\delta^{13}C_{Kerogen}$ decreases again, reaching the minimum value of the section (-24.55‰). Upwards, $\delta^{13}C_{Kerogen}$ shifts to more positive values (Fig. III.7 and Table III.2).

III.4.2.3. Palynofacies

Fuente Vidriera section is also thermally immature (vitrinite reflectance values vary between 0.50% R_o and 0.51% R_o) and the Phytoclast Group is the most abundant kerogen group (average of ~ 92% and reaching up to ~ 100% in the first two samples; Figs. III.4 and III.7, Table III.2).

Samples FV 3, FV 7t and FV 19b record the lowest Phytoclast Group contents, 76% and 85%, respectively (Fig. III.7 and Table III.2). Opaque phytoclast subgroup is the main subgroup (average value of ~80%; Figs. III.5B and III.5G); Non-opaque phytoclast subgroup shows average values of ~20% (Fig. III.5B). Other Phytoclast Group particles, such as cuticles, membranes, and sclereids were not observed.

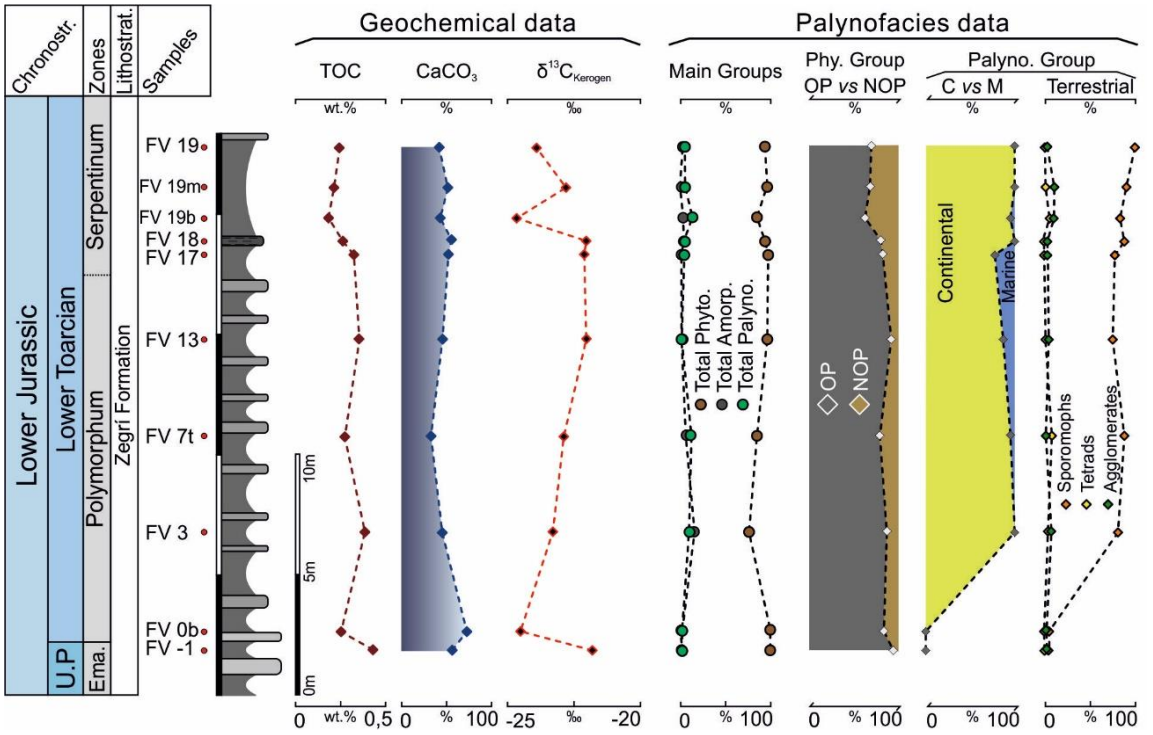

Figure III.7. TOC, $CaCO_3$, $\delta^{13}C_{Kerogen}$ and palynofacies associations from the Fuente Vidriera section, External Subbetic (Betic Cordillera, SE Spain). U.P. – uppermost Pliensbachian; Ema. – Emaciatum Zone; OP – opaque; NOP – non-opaque; C – continental; M – marine.

The particles from the Amorphous Group in Fuente Vidriera exhibits the same features as the particles from the La Cerradura section. Colouration ranges between brown to pale brown in TWL (Fig. III.5G) and yellow and orange in FM (Fig. III.5H). Despite the very low abundance of AOM in the Fuente Vidriera section (average of ~ 3%; Figs. III.4 and III.7, Table III.2), in sample FV 3 (Polymorphum Zone) AOM constitutes 14% of the kerogen assemblage (Fig. III.7 and Table III.2).

Both terrestrial and marine kerogen particles from the Palynomorph Group occur in low amounts in most of the samples from the Fuente Vidriera section (Fig. III.7 and Table III.2), ranging from 0% (FV -1 and FV 0b) to 13% (FV 19b). The observed palynomorphs consist mostly of terrestrial palynomorph subgroup such as sporomorphs (Fig. III.6A), with some belonging to the genus *Classopollis*. Tetrads (samples FV 3, FV 7t and FV 19b; Fig. III.6C) and pollen grain agglomerates (samples FV 3, FV 19b and FV 19m) are also present. In samples FV 3 and FV 18, sporomorphs have pyrite framboid inclusions. Very low percentages of zygospores of *zygnemataceae* represent continental aquatic palynomorphs, however with an increase in samples FV 13 and FV 18. Marine palynomorphs, such as dinoflagellate cysts (*Luehndea spinosa*; Fig. III.6G) and acritarchs are rare.

Table III.2. TOC, TS, $CaCO_3$ content, $\delta^{13}C_{Kerogen}$ and palynofacies data from the Fuente Vidriera section, External Subbetic domain (Betic Cordillera, SE Spain).

Sample ID	TOC (wt%)	TS (wt%)	$CaCO_3$ (wt%)	$\delta^{13}C_{Kerogen}$ (‰)	Phytoclast Group (%)	Phytoclast[1]		Amorphous Group (%)	Palynomorph Group (%)	Palynomorph[1]		Continental palynomorphs[1]				Zooclasts (%)
						OP (%)	NOP (%)			Mar[2] (%)	Contin[3] (%)	Sp (%)	Tet (%)	Agg (%)	FM (%)	
FV 19	0.25	0.013	46	-23.95	93	70	30	1	5	0	100	100	0	0	0	0
FV 19m	0.22	0.013	55	-22,79	96	69	31	1	4	0	100	91	0	9	0	0
FV 19b	0.19	0.013	47	-24.55	85	63	37	2	13	5	95	83	5	7	0	0
FV 18	0.27	0.012	59	-22.08	94	80	20	2	3	0	100	89	0	0	11	1
FV 17	0.33	0.009	56	-22.13	97	83	17	0	3	22	78	78	0	0	0	0
FV 13	0.36	0.013	49	-22.07	96	92	8	1	3	13	87	75	0	0	13	0
FV 7t	0.28	0.01	36	-22.91	85	79	21	6	9	4	96	89	7	0	0	0
FV 3	0.39	0.071	49	-23.34	76	87	13	14	9	0	100	81	4	4	4	0
FV 0b	0.26	0.01	77	-24.55*	100	84	16	0	0	0	0	0	0	0	0	0
FV -1	0.44	0.01	60	-21.89	100	95	5	0	0	0	0	0	0	0	0	0

OP – opaque; NOP – non-opaque; Mar – marine; Contin – continental; Sp – sporomorph; Tet – tetrad; Agg – agglomerate; FM. – freshwater microplankton; [1] – recalculated to 100 %; [2] – total marine microplankton (dinoflagellate cysts, acritarchs and prasinophyte algae); [3] – total continental palynomorphs [sporomorphs, tetrads, agglomerates and freshwater microplankton (i.e., zygospores of *zygnemataceae*)].

III.5. Discussion

III.5.1. $\delta^{13}C_{Kerogen}$ events and chemostratigraphic correlation of the la Cerradura and Fuente Vidriera sections

Stable carbon isotopes are one of the most important and useful tools in sedimentary geology, as they can be used to characterise, reconstruct, and trace past climatic and oceanographic changes. The Upper Pliensbachian–Lower Toarcian interval is characterised by a well-known $\delta^{13}C$ pattern (similar in carbonates, fossil wood and OM). Superimposed on a broader Lower Toarcian positive $\delta^{13}C$ trend, the TOAE is characterised worldwide by a negative CIE at the base of the Serpentinum/Falciferum/Levisoni Zone (e.g. Jenkyns and Clayton, 1986; Jenkyns, 1988, 2010; Hesselbo et al., 2000, 2007; Jenkyns et al., 2002; Cohen et al., 2004; Hermoso et al., 2009; Bodin et al., 2010, 2016; Littler et al., 2010; Suan et al., 2010, 2011, 2015; Reolid et al., 2012; Kafousia et al., 2014; Caruthers et al., 2014; Kemp and Izumi, 2014; Pieñkowski et al., 2016; Silva et al., 2017; Them II et al., 2017; Xu et al., 2017; Fantasia et al., 2018b). In many locations, a TOAE positive CIE follows the TOAE negative CIE (e.g. Jenkyns and Clayton, 1986; Jenkyns, 1988, 2010; Hesselbo et al., 2000, 2007; Jenkyns et al., 2002; Cohen et al., 2004; Duarte et al., 2007; Kafousia et al., 2014; Them II et al., 2017).

Several mechanisms, or combinations thereof, are suggested as the cause for the TOAE negative CIE and carbon cycle perturbation: eruption of the Karoo-Ferrar Large Igneous Province (Pálfy and Smith, 2000), rapid release of methane from gas hydrate contained in marine continental-margin sediments (Hesselbo et al., 2000), thermogenic methane release related to sill emplacement and magmatic intrusions (McElwain et al., 2005; Svensen et al., 2007), increased CO_2 input from terrestrial OM decomposition due to increased fungal activity (Pieñkowski et al., 2016), or increased input of methane from terrestrial environments (Them II et al., 2017). The TOAE is preceded by a smaller scale negative CIE around the base of the Toarcian (Polymorphum Zone; Hesselbo et al., 2007; Ruebsam et al., 2019), the Pl–Toa Event (Littler et al., 2010). Littler et al. (2010) suggested that the Pl–Toa Event resulted from a perturbation (most likely analogous to the one occurring during the TOAE) affecting the entire ocean-atmosphere system and coinciding with an extinction phase in marine benthos at the Toarcian Stage boundary.

$\delta^{13}C_{Carb}$ from different sites in the External Subbetic show a similar pattern from the uppermost Pliensbachian–Lower Toarcian, with the record of the TOAE negative CIE (e.g., Sandoval et al., 2012; Reolid, 2014a; Reolid et al., 2014). The obtained coarse-resolution $\delta^{13}C_{Kerogen}$ record from Fuente Vidriera reveals a short negative CIE of about 3‰ between the Upper Pliensbachian and Lower Toarcian, here interpreted to correspond to the Pl–Toa Event (cf. Hesselbo et al., 2007; Littler et al., 2010) (Fig. III.8). The Pl–Toa Event excursion is not observed in the dataset from the La Cerradura section, likely due to the coarse resolution of this dataset. The

TOAE negative CIE at the base of the Serpentinum Zone is expressed in the $\delta^{13}C_{Kerogen}$ datasets from La Cerradura and Fuente Vidriera (shift of ~1.5‰ in La Cerradura and ~2.5‰ in Fuente Vidriera). Whether these values represent the full expression of the TOAE in the External Subbetic is unknown. Even though these sections have high carbonate contents, a decrease in $CaCO_3$, more expressive in La Cerradura, is also observed in this interval, interpreted to be associated with the biocalcification crisis of the TOAE (Tremolada et al., 2005; Mattioli et al., 2009; Bodin et al., 2010, 2016; Sandoval et al., 2012; Reolid, 2014a; Reolid et al., 2014). After the TOAE negative CIE, $\delta^{13}C_{Kerogen}$ presents a slight enrichment in ^{13}C (interpreted as the recovery interval of the Serpentinum Zone), although without the well define positive CIE that marks the end of the TOAE in several other basins (e.g. Hesselbo et al., 2000; 2007; Röhl et al., 2001; Suan et al., 2015; Silva et al., 2017), probably because only the lower part of the Serpentinum Zone is preserved in both sections (e.g. Sandoval et al., 2012; Fig. III.8).

III.5.2. Sources of organic matter during the Early Toarcian in the External Subbetic sections

TOC contents from La Cerradura and Fuente Vidriera reaches up to 0.46 wt.% (Fig. III.8 and Tables III.1, III.2), indicating that these sections are poor in OM [Rodríguez-Tovar and Reolid (2013) reported a sample at the base of the Serpentinum Zone with a TOC content reaching up to 0.98 wt.%].

The Phytoclast Group dominates the kerogen assemblages from La Cerradura and Fuente Vidriera, clearly indicating sedimentary OM mostly of terrestrial affinity, with a minor expression of marine microplankton, such as dinoflagellate cysts (*Luehndea spinosa* and *Nannoceratopsis gracilis*), acritarchs, and prasinophyte algae.

High relative abundances of particles belonging to the Phytoclast Group in the kerogen assemblages are usually interpreted to reflect high terrestrial supply, preferential preservation of phytoclasts in oxidising conditions, selective sedimentation due to hydrodynamic equivalence, or reworking of coastal sediments during transgressions (see Tyson, 1995 and references therein). In both studied sections, the opaque phytoclast subgroup dominates the Phytoclast Group. Opaque phytoclasts are not usually discussed in terms of palaeoclimate, palaeovegetation, or other environmental scenarios, mainly because refractory OM is usually interpreted as an indication of burial overprint, recycling of older OM, and oxidation either during deposition or weathering (e.g. Tyson, 1995).

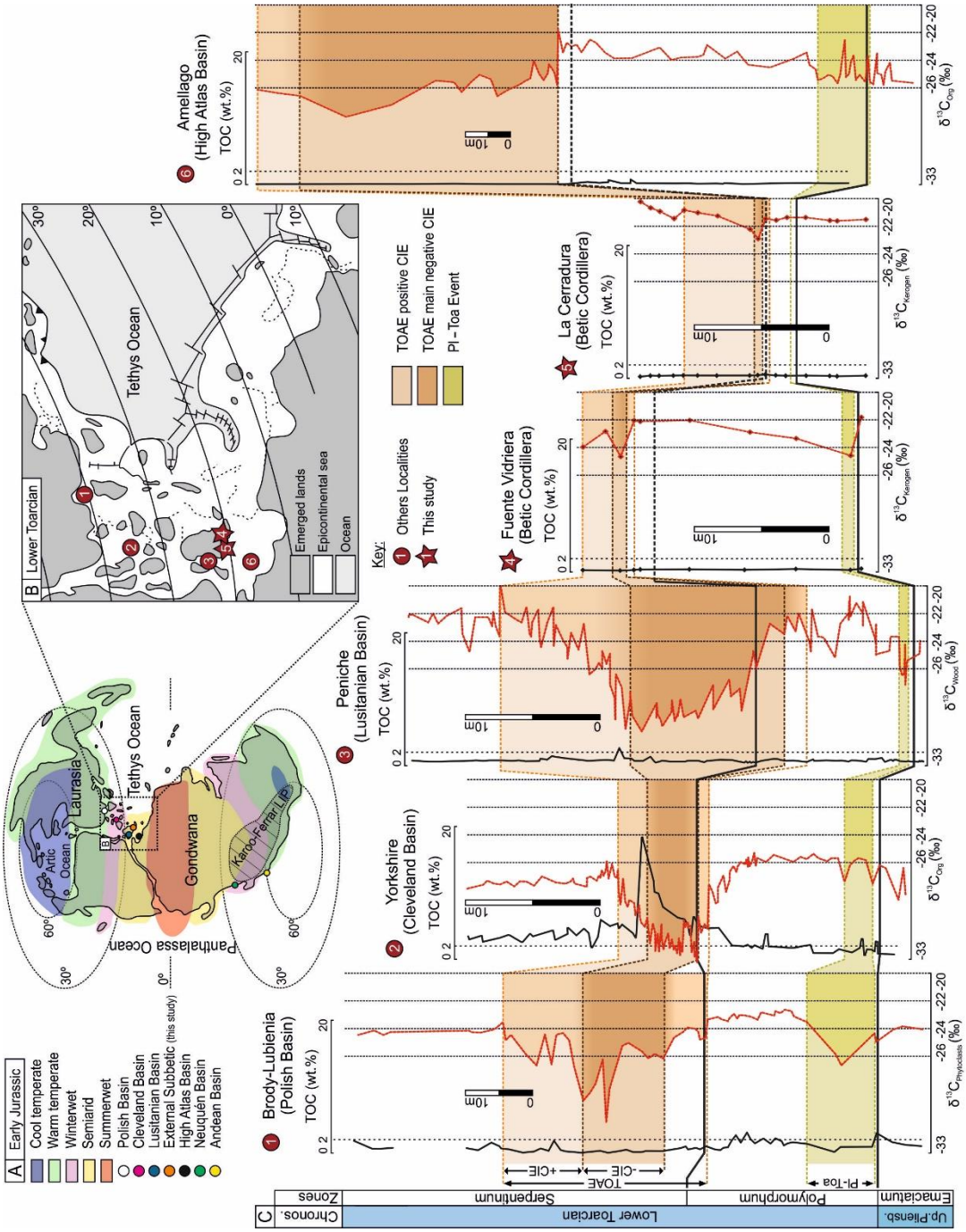

Figure III.8. **A**. Global map, palaeolocation of Polish, Cleveland, Lusitanian, External Subbetic, High Atlas, Neuquén and Andean basins and Early Jurassic palaeoclimatic belts inferred from sedimentological and palaeophytogeographic data (modified from Dera et al. 2009); **B**. Tethyan map modified from Thierry and Barrier (2000) with the location of the La Cerradura and Fuente Vidriera sections (red star with 4 and 5 numbers, respectively) and other areas discussed in the text regarding Lower Toarcian (Early Jurassic) palaeogeography. Localities: 1 - Brody-Lubienia (Polish Basin); 2 - Yorkshire (Cleveland Basin); 3 - Peniche (Lusitanian Basin); 6 - Amellago (High Atlas Basin); **C**. $\delta^{13}C_{Phytoclasts}$, $\delta^{13}C_{Org}$, $\delta^{13}C_{Wood}$, and $\delta^{13}C_{Kerogen}$ records spanning the Pl–Toa Event and TOAE. Geochemical data, Pl–Toa Event and TOAE limits of Brody-Lubienia, Yorkshire, Peniche, and Amellago are from Pieñkowski et al. (2016), Cohen et al. (2004), Hesselbo et al. (2007), Baker et al. (2017) and Bodin et al. (2010, 2016), respectively.

Because these processes would affect the entire kerogen assemblage, the low thermal maturity of the studied sections (R_o between 0.48 and 0.51%), the drastic contrast between opaque (black) and light brown non-opaque phytoclasts, and the high transmittance and bright fluorescence of AOM particles and terrestrial and marine palynomorphs (Figs. III.5 and III.6) rejects maturation or superficial weathering as the main process leading to the relatively high abundance of opaque phytoclasts.

Particles of the opaque phytoclast subgroup mostly correspond to oxidised land plant tissues and charcoal (recycled coalified material may also occur in the opaque phytoclast subgroup) (Tyson, 1995). Opaque (oxidised) phytoclasts are thought to be formed by desiccation, oxidation, fungal mouldering of woody material in aerobic conditions in the upper part of soils and peats (e.g. Styan and Bustin, 1983; Tyson, 1995). Charcoal is the product of the natural pyrolysis of terrestrial macrophyte material in high temperatures and under conditions of oxygen starvation (e.g. Chaloner, 1989). Several studies suggest that the occurrence of opaque phytoclasts is favoured by strongly seasonal climates (with pronounced arid periods) and with significant water table fluctuations (e.g. Tyson, 1995; Lamberson et al., 1996).

It is interpreted here that the dominance of the opaque phytoclast subgroup during the Lower Toarcian interval in La Cerradura and Fuente Vidriera indicates that terrestrial OM was mostly sourced from an area characterised by a semi-arid climate (i.e. with pronounced arid periods). The reworking of phytoclasts in/from neighbouring semi-arid coastal environments during the Early Toarcian transgression (e.g. Gallego-Torres et al., 2015) may have also contributed to the high abundances of the Phytoclast Group and the opaque phytoclast subgroup in the studied sections. The occurrence of pollens *Classopollis* is an important palaeoclimatic indicator (Vakhrameyev, 1982), likely indicating dominant warm and dry climates.

The interpretation of a prevalent semi-arid climate in the source area leading to kerogen assemblages with high abundances of particles belonging to the opaque phytoclast subgroup is consistent with independent sedimentological proxies and inferred global climatic zonation (Fig. III.8A), where the south Iberian Palaeomargin is located in the (hot) semi-arid climatic belt (e.g. Rees et al., 2000; Dera et al., 2009; Palomo et al., 1985). Computer simulations also suggest a decrease in net moisture in this area during the Early Toarcian warming event (Dera and Donnadieu, 2012). In addition, comparison with the more 'humid' northern areas, such as the Polish Basin (Pieñkowski et al., 2016) and the Grands Causses and Quercy basins (Fonseca et al., 2018), demonstrates a regional pattern in opaque phytoclasts distribution, where the northern sections have lower amounts of opaque phytoclasts than sections from the External Subbetic. This observation reinforces the interpretation that climate may have been a first-order control in the OM source area in the south Iberian Palaeomargin.

III.5.2.1. The effect of the TOAE carbon cycle perturbation on OM input and preservation in the Betic Cordillera

The Early Toarcian carbon-cycle perturbation (associated with enhanced greenhouse effect) is interpreted to have promoted wetter climates in mid-latitudes and an accelerated hydrological cycle, thus leading to an intensification of continental weathering, fluvial runoff, and flux of sediments and terrestrial OM to epicontinental areas, continental margins, and deeper marine basins (e.g. Jenkyns et al., 2002; Cohen et al., 2004; Kemp et al., 2011; Dera and Donnadieu, 2012; Brazier et al., 2015; Krencker et al., 2015; Percival et al., 2016; Them II et al., 2017; Xu et al., 2017, 2018; Izumi et al., 2018; Baroni et al., 2018). Ultimately, increased nutrient delivery and stimulated primary productivity may have resulted in marine hypoxia, anoxia, and potentially euxinia in nearshore environments, especially in areas of the northwestern Tethyan margin (e.g. Jenkyns, 2010; Baroni et al., 2018).

The relatively small increase in the non-opaque phytoclast subgroup just before and during the TOAE negative CIE (Figs. III.3, III.7 and Tables III.1, III.2) in Fuente Vidriera fits the overall TOAE model and is interpreted to be the combined result of: a) the decreased contribution of opaque phytoclasts from emerged areas due to generally slightly wetter conditions (decreased potential for oxidation of phytoclasts in soils and peats, e.g. Lamberson et al., 1996) and slightly lower atmospheric oxygen (decreased charcoal contribution by decreasing forest fire frequency; Lamberson et al., 1996; Baker et al., 2017). b) the increased transport of non-opaque phytoclasts (and terrestrial palynomorphs) to the marine environment due to increased fluvial runoff (Tyson, 1995 and references therein);

Despite the abundance of the Phytoclast Group (opaque and non-opaque phytoclasts) in La Cerradura and Fuente Vidriera, it is possible to observe an increase in the Palynomorph Group at specific intervals. In La Cerradura, increases in pollens occurring in tetrads and agglomerates are observed between samples CE 39–25 (topmost Emaciatum–Serpentinum zones), peaking between samples CE 30–25 (topmost Polymorphum/base of Serpentinum zones?) (Fig II.3 and Table III.1). In Fuente Vidriera, increases in tetrads and agglomerates are observed in samples FV 3 and FV 7t (Polymorphum Zone) and FV 19b (base of Serpentinum Zone) (Fig. III.7 and Table III.2). Sample FV 19b corresponds to the TOAE negative CIE and is also concomitant with an increase in non-opaque phytoclasts and decreases in TOC, $CaCO_3$, and total Phytoclast Group contribution. In the La Cerradura section, marine palynomorphs are abundant between samples CE 43–35 (Pliensbachian–Toarcian boundary) and samples CE 29–25 (lower Serpentinum Zone) (Fig. III.3 and Table III.1). In the Fuente Vidriera section, an increase in marine palynomorphs are observed in samples FV 13 (Polymorphum Zone) and FV 17 (Serpentinum Zone) (Fig. III.7 and Table III.2).

The increases in the non-opaque subgroup and Palynomorph Group (mainly sporomorph subgroup) in Fuente Vidriera and the overall increment of terrestrial OM contribution in La

Cerradura and Fuente Vidriera just before and during the TOAE negative CIE is consistent with a slight increase in continental runoff, associated with the Lower Toarcian enhancement of the hydrological cycle (e.g. Jenkyns et al., 2002; Cohen et al., 2004; Hesselbo and Pieñkowski, 2011; Kemp et al., 2011; Brazier et al., 2015; Krencker et al., 2015; Percival et al., 2016; Them II et al., 2017; Xu et al., 2017, 2018; Izumi et al., 2018). Reolid et al. (2019a) reported large wood fragments, mainly in the dark marls of the Serpentinum Zone, suggesting enhanced fluvial and nutrient input. However, the overwhelming abundance of the opaque phytoclast subgroup (~ 90%) suggests that the dominant climate mode in the source area was semi-arid.

Reolid (2014b) suggested that pyritization of spicules of siliceous sponges and radiolarians, and the formation of pyrite framboids (mean size of 6.3–7.1 μm) in Fuente Vidriera took place under a dominantly dysoxic bottom water-column/sediments. Persistent anoxic/euxinic conditions in the studied sections are excluded by the sediment characteristics (partly homogenous and bioturbated), TOC-lean sediments, the almost continuous record of trace fossils and foraminifera (Rodríguez-Tovar and Uchman, 2010; Reolid, 2014a), lack of enrichment in redox-sensitive elements (Rodríguez-Tovar and Reolid, 2013; Reolid et al., 2014) and pyrite framboids size analysis (Gallego-Torres et al., 2015).

Summarising, TOC contents and palynofacies analysis indicates that during the Early Toarcian (possibly also the TOAE) terrestrial OM in the south Iberian Palaeomargin was sourced from a dominantly semi-arid environment (i.e. contrasting seasons with a prolonged dry season). There are indications of a small increment in water availability in the area during the Early Toarcian carbon cycle perturbation, however without a drastic change in climate in the source area. Unlike many Tethyan basins (e.g. Jenkyns, 2010), the small increase in continental runoff during the TOAE carbon cycle perturbation in the south Iberian Palaeomargin apparently did not sustained a significant burst in marine productivity and, consequently, significant export of marine OM into sediments.

III.5.3. $\delta^{13}C$ from C3 plants and climatic regimes in the Polymorphum Zone interval

Several regional studies (e.g. Rees et al., 2000; Dera et al., 2009), clay mineral assemblages dominated by illite (Palomo et al., 1985) and palynofacies analysis of La Cerradura and Fuente Vidriera suggest that during the Polymorphum Zone climatic conditions in the south Iberian Palaeomargin were dominantly semi-arid (see section III.5.2.). Previously, it was considered that mean annual precipitation and altitude are the main controls in ^{13}C fractionation during photosynthesis in C3 plants (e.g. Körner et al., 1991; Hesselbo et al., 2007). More recently, Lomax et al. (2019) experiments show that a wide variation in ^{13}C discrimination as a function of water availability is independent of CO_2 treatment and Cornwell et al. (2018) demonstrated that

fractionation of ^{13}C during photosynthesis in modern C3 plants truly depends on a complex array of climatic and soils parameters that affect the supply of water to the plant (including annual precipitation, frost frequency, soil pH and silt content), strength of atmospheric demand for water (including wind, atmospheric pressure, and potential evapotranspiration), and the balance of CO_2 supply through the stomata and demand at the sites of photosynthesis in leaves. These new observations show that the global pattern in $\delta^{13}C$ discrimination is very different from the previously reported climate–trait relationships, and where it is assumed that the groups of plants fractionate differently, independently of climate or other factors. Overall, Cornwell et al. (2018) model predict lowest fractionation in the major desert areas of the globe (arid and semi-arid climates) and highest fractionation in the wet tropical forests and the silt soils on river floodplains of the northernmost hemisphere. The modelled difference in ^{13}C fractionation during photosynthesis reaches up to ~ 8‰ between these two climatic extremes.

A similar relationship between ^{13}C fractionation in terrestrial environments [$\delta^{13}C_{Kerogen}$ (this study), $\delta^{13}C$ in wood phytoclasts separated manually ($\delta^{13}C_{Phytoclasts}$), $\delta^{13}C$ from fossil wood ($\delta^{13}C_{Wood}$) and $\delta^{13}C$ in the decalcified bulk sample ($\delta^{13}C_{Org}$)] and climate is observed during the Polymorphum Zone interval (i.e. the stratigraphic interval between the Pl–Toa Event and TOAE). Several studies demonstrate that terrestrial kerogen dominates in many sections of the northern Tethyan margin (Fig. III.9). In the External Subbetic of the south Iberian Palaeomargin (kerogen dominated by terrestrial OM), Lusitanian Basin (fossil wood; Hesselbo et al 2007), and High Atlas Basin (kerogen dominated by terrestrial OM, dataset not available; Bodin et al., 2016), $\delta^{13}C$ in terrestrial OM from the mid-Polymorphum/Tenuicostatum Zone average around -23‰ and reaches up to -21‰ in a dominantly semi-arid climate (Dera et al., 2009) (Figs. III.8A and III.9). In the same stratigraphic interval, systematically more negative $\delta^{13}C$ values are observed in wood phytoclasts separated manually from the Polish Basin (averages around -24 to -25‰ and reaching up to ~ -23‰; Hesselbo and Pieñkowski, 2011; Pieñkowski et al., 2016). This basin is in the warm temperate/winter-wet climate belts of Dera et al. (2009) (Figs. III.8A and III.9). Polymorphum Zone interval $\delta^{13}C$ values in Type III kerogen from the Andean Basin average around -24.5‰ and reach up to ~ -24‰ in a warm-temperate environment (Fantasia et al., 2018b). Pre-TOAE fossil wood data from the Neuquén Basin (Arroyo Lapa north, Argentina) is more negative than the former examples, ranging between ~ -28 to -30‰ (Al-Suwaidi et al., 2016). This basin is located in the winter-wet climatic belt of Dera et al. (2009) (Figs. III.8A and III.9).

Despite the uncertainty associated with possible analytical, taxonomic, diagenetic, and maturity bias when comparing terrestrial $\delta^{13}C_{Kerogen}$ absolute values from different locations, Polymorphum Zone datasets generally fit the association between ^{13}C fractionation during photosynthesis in C3 plants and climate *sensu* Cornwell et al. (2018) (Fig. III.9). Within the context of the broad Lower Toarcian positive excursion (see Jenkyns, 2010), the northern Tethyan margin (Polish Basin) and southwestern Gondwana margin are constrained to winter-wet/warm temperate climates (Dera et al., 2009) and have more negative $\delta^{13}C$ values (higher fractionation). The southern Iberian and Tethyan margins (Lusitanian Basin, Betic Cordillera, and High Atlas Basin) fall within

the semi-arid climate belt (Dera et al., 2009) and have relatively more positive $\delta^{13}C$ values (lower fractionation) (Fig. III.9). Carbon-isotope data from fossil wood through the upper Bagå Formation in southwestern Bornholm reaches up to ~ -21‰ (Hesselbo et al., 2000), suggesting that, and as posited by Cornwell et al. (2018), factors other than climate may also influence local carbon isotopic trends of terrestrial OM.

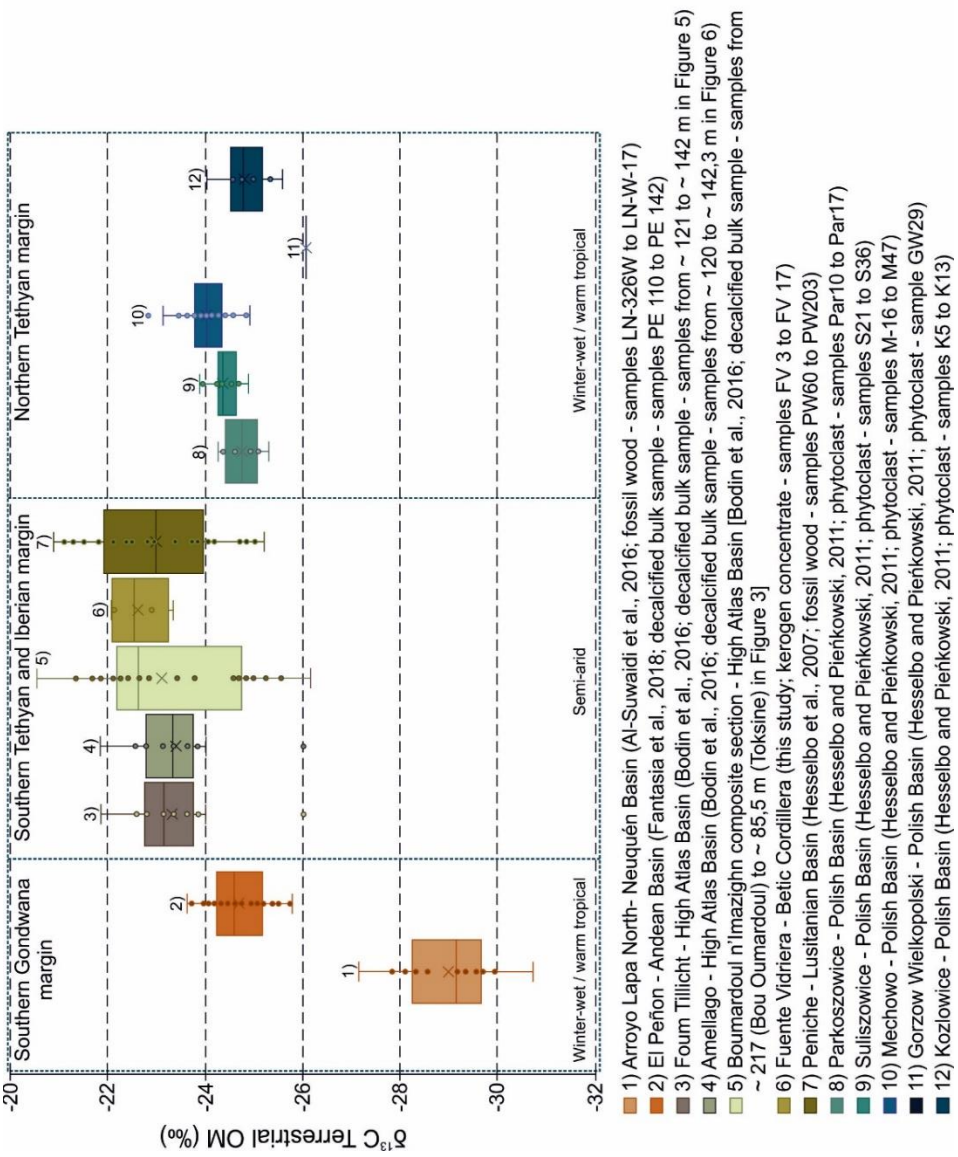

Figure III.9. Polymorphum Zone (excluding the Pl–Toa Event and TOAE) $\delta^{13}C$ record in terrestrial OM from Neuquén Basin (Al-Suwaidi et al., 2016), Andean Basin (Fantasia et al., 2018b), High Atlas Basin (Bodin et al., 2016), External Subbetic domain, Betic Cordillera (this study), Lusitanian Basin (Hesselbo et al., 2007) and Polish Basin (Hesselbo and Pieñkowski, 2011) and general climatic context (Dera et al., 2009).

Summating, this study suggests a coupling between the water and terrestrial carbon cycles during the Early Toarcian and the impact of local and global climatic variability in the $\delta^{13}C$ record in terrestrial OM. Furthering our understanding of the coupled terrestrial carbon and water cycle

during the Early Toarcian is of paramount importance to investigate the role of terrestrial ecosystems in global climate change (see Hesselbo et al., 2007; Pieńkowski et al., 2016; Them II et al., 2017).

III.6. Conclusions

New geochemical and palynofacies analysis from the uppermost Pliensbachian–Lower Toarcian marine successions of La Cerradura and Fuente Vidriera (External Subbetic domain, Betic Cordillera, southern Spain) allow for the following conclusions:

- The studied successions are immature, have low TOC and with kerogen assemblages dominated by the terrestrial OM (dominance of opaque phytoclast subgroup). The intersection of the obtained OM geochemistry data and palynofacies analysis with independent sedimentary proxies suggest a dominantly semi-arid climate in the south Iberian Palaeomargin during the Early Toarcian.

- An increase in terrestrially derived kerogen components (i.e., non-opaque phytoclasts and pollens occurring in tetrads and agglomerates) at the base of Serpentinum Zone is interpreted to represent a slight increase in fluvial runoff associated with the carbon cycle perturbation of the TOAE, apparently with OM still sourced from an area within a semi-arid environment.

- This work suggests that the relatively more positive $\delta^{13}C_{Kerogen}$ record in the studied sections during the Polymorphum Zone interval has probably resulted from a decreased ^{13}C fractionation during photosynthesis in C3 plants in “arid” environments when compared with more northern “humid” environments.

- This study suggests that the water and terrestrial carbon cycles were coupled during the Late Pliensbachian and Early Toarcian.

IV. Sedimentary organic matter and Early Toarcian environmental changes in the Lusitanian Basin (Portugal)

Adapted from:

Rodrigues, B., Duarte, L.V., Silva, R.L., Mendonça Filho, J.G., (submitted). Sedimentary organic matter and Early Toarcian environmental changes in the Lusitanian Basin (Portugal). Palaeogeography, Palaeoclimatology, Palaeoecology

Submitted: 4 March 2020

Abstract

The objective of this study is to investigate the relationship between Early Toarcian climatic events and the composition of kerogen assemblages in the Lusitanian Basin (Portugal). In particular, we aim to understand how the Pliensbachian–Toarcian Event (Pl–Toa Event) and Toarcian Oceanic Anoxic Event (TOAE) affected the continental areas of the Iberian Massif and how possible variations in continental sources of organic matter (OM) were expressed in marginal-marine and hemipelagic depositional environments during the Early Toarcian.

We present here a characterisation [total organic carbon (TOC), total sulphur (TS), $\delta^{13}C$ in kerogen isolates ($\delta^{13}C_{Kerogen}$), and palynofacies] of kerogen assemblages from several uppermost Pliensbachian (Emaciatum Zone)–Lower Toarcian sections in the Lusitanian Basin and including the Peniche section, which contains the Toarcian GSSP. Overall, TOC is low (average 0.4 wt.%), with the highest values reaching up 2.08 wt.% in a discrete level located approximately 10.5 m above the base of the Levisoni Zone at Peniche. The TOAE negative carbon isotope excursion is observed in kerogen isolates at the base of the Levisoni Zone throughout the basin. Palynofacies analysis demonstrates that the kerogen assemblages are mostly of terrestrial affinity, with the dominance of the Phytoclast Group and terrestrial palynomorphs, and with punctual increases in amorphous organic matter, freshwater (e.g. *Botryococcus* sp.) and marine microplankton (dinoflagellate cysts, acritarchs, and prasinophyte algae) in specific stratigraphic locations.

A change in palynofacies assemblages associated with the TOAE is observed around the base of Levisoni Zone. Although with slight differences between sections, the TOAE interval records an increase in non-opaque phytoclasts (NOP) and cuticle fragments, also associated with an increased contribution of terrestrial palynomorphs (increase in sporomorphs and *Classopollis* in tetrads and agglomerates) and decrease in marine palynomorphs. The increases in NOP and terrestrial palynomorphs support the postulated enhancement of the hydrological cycle and increased export of terrestrial OM into marine environments during the Early Toarcian, especially during the TOAE.

Understanding the impact of the Early Toarcian climatic events on land-based ecosystems may provide important insights into current climate change.

Keywords: Organic geochemistry, Palynofacies, Pliensbachian–Toarcian Event, Toarcian Oceanic Anoxic Event, Portugal.

IV.1. Introduction

During the Early Toarcian, two major environmental events are globally recognised; the Pliensbachian–Toarcian Event (Pl–Toa Event; Littler et al., 2010) and Early Toarcian Oceanic Anoxic Event (TOAE; Jenkyns, 2010). These events are associated with global warming (e.g. Suan et al., 2010; Gómez et al., 2016), perturbations of the carbon cycle (e.g. Hesselbo et al., 2000, 2007; Littler et al., 2010; Pieñkowski et al., 2016; Fantasia et al., 2018b; Ruebsam et al., 2019), marine anoxia with the widespread deposition of organic matter (OM)-rich sediments in many locations of the northwestern Tethyan, Boreal and Panthalassic margins (e.g. Jenkyns, 2010), and marine mass extinctions (e.g. Little and Benton, 1995; Caswell et al., 2009; Danise et al., 2013). A link between the TOAE and the emplacement of the Karoo-Ferrar Large Igneous Province has been proposed (Duncan et al., 1997; McElwain et al., 2005; Svensen et al., 2007; Suan et al., 2008b; Percival et al., 2015; Xu et al., 2018). Release of methane (CH_4) from gas hydrates (Hesselbo et al., 2000), increased outgassing of CH_4 and carbon dioxide (CO_2) from terrestrial environments (Pieñkowski et al., 2016; Them II et al., 2017), or the release of CH_4 and CO_2 from the cryosphere (Silva and Duarte, 2015; Ruebsam et al., 2019) might also have contributed to global climate instability in the Late Pliensbachian–Early Toarcian. The main feature of these two events is the negative carbon isotopic excursions (CIE) observed at the base of the Polymorphum/Tenuicostatum (Pl–Toa Event) and Levisoni/Falciferum/Serpentinum (TOAE) ammonite zones, recorded in carbonates, fossil wood, bulk OM, kerogen and individual organic compounds (e.g. Hesselbo et al., 2000, 2007; Littler et al., 2010; Jenkyns, 2010; Pieñkowski et al., 2016; Xu et al., 2018; Fantasia et al., 2019; Rodrigues et al., 2019; Ruebsam et al., 2020a; Storm et al., 2020). Although many studies have been focused on the impact of Early Toarcian environmental changes in the marine realm, there is a growing number of studies highlighting the response of land-based ecosystems to these changes (e.g. Hesselbo and Pieñkowski, 2011; Baranyi et al., 2016; Pieñkowski et al., 2016; Rodrigues et al., 2016, 2019, 2020; Baker et al., 2017; Kemp et al., 2019; Slater et al., 2019).

Mathematical models suggest that enhanced organic carbon burial during an OAE increases atmospheric oxygen and that the rising oxygen concentration leads to termination of the TOAE (Handoh and Lenton, 2003). To test this model, Baker et al. (2017) used fossil charcoal abundance from the Lower Toarcian successions of the Peniche section [Lusitanian Basin (LB), Portugal] and the Mochras borehole (Cardigan Bay Basin, Wales) and hypothesised that the decrease of charcoal contents to background levels following the TOAE indicated that increasing

wildfire activity eventually suppressed oxygen-producing photosynthesis by terrestrial vegetation enough that atmospheric oxygen levels decreased back to pre-TOAE levels. Though, and as noted by Baker et al. (2017), temporal variation of charcoal content in these sections may have been controlled by local biological and hydrological factors and depositional conditions.

The objective of this paper is to investigate the distribution of sedimentary OM during the latest Pliensbachian–Early Toarcian (including the Pl–Toa Event and the TOAE) in several locations of the LB and relationship with major Early Toarcian palaeoenvironmental and palaeoclimatic trends. This study is based on organic geochemistry and palynofacies analysis of the reference sections of Peniche and Rabaçal, complemented by the auxiliary sections of Vale das Fontes, Cantanhede, Alcabideque, Ribeira de Cima and Minde (Fig. IV.1). Understanding the impact of the Early Toarcian climatic changes on land-based ecosystems may provide important insights into current climate change.

IV.2. Geological background and lithostratigraphy

The LB is a small Atlantic margin rift basin, located on the western side of the Iberian Massif (Fig. IV.1). Its Mesozoic sedimentary infill, a continuous sedimentary record dated from the Upper Triassic to the top of the Lower Cretaceous (e.g. Wilson et al., 1989; Rasmussen et al., 1998), resulted from Triassic extension and the subsequent opening of the North Atlantic Ocean. The LB is limited to the east by Hesperian Massif and the west by the igneous Berlenga Horst (e.g. Wilson et al., 1989; Rasmussen et al., 1998; Alves et al., 2002). Several infilling phases have been identified in the LB, limited by regional discontinuities (e.g. Wilson et al., 1989; Kullberg et al., 2013). The studied stratigraphic interval is included in the Triassic–top of the Callovian 1st-order sedimentary cycle (Soares et al., 1993; Azerêdo et al., 2003, 2014). The main features of the analysed intervals from the reference sections of Peniche and Rabaçal (and other auxiliary sections) (Fig. IV.2) are summarised below; a detailed account can be found in Duarte (1997), Duarte and Soares (2002) and Pittet et al. (2014).

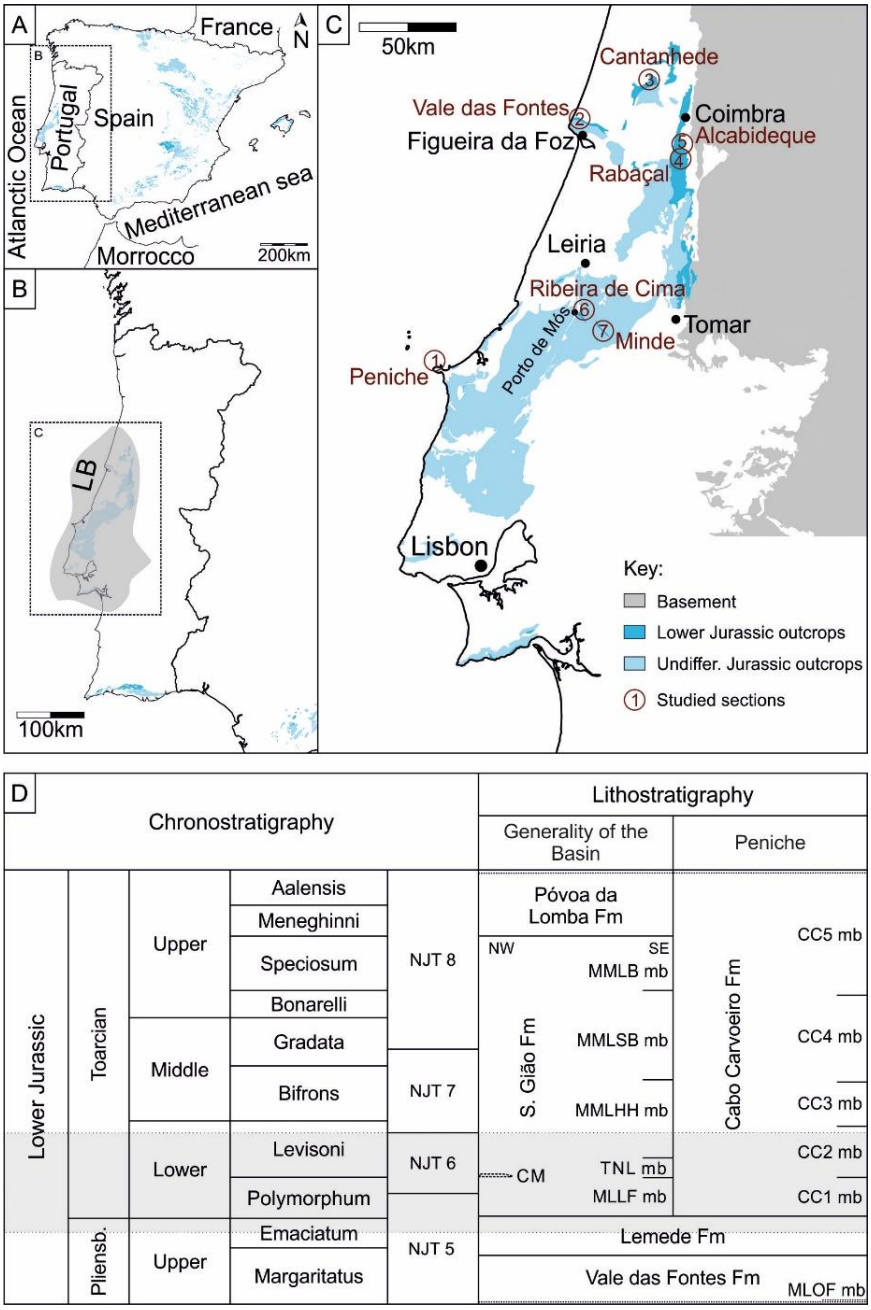

Figure IV.1. Geological context of the studied stratigraphic interval. **A** and **B**. Simplified geological map of Jurassic outcrops in the Iberian Peninsula and location of the Lusitanian Basin (Portugal); **C**. Lower Jurassic outcrops and location of the studied sections in the Lusitanian Basin; **D**. Lithostratigraphic chart for Upper Pliensbachian–Upper Toarcian in the Lusitanian Basin (modified from Duarte and Soares, 2002; Duarte et al., 2004, 2007). Calcareous nannofossil biostratigraphy from Ferreira et al. (2019). Light grey corresponds to the studied interval. LB – Lusitanian Basin; Undiffer. – Undifferentiated; MLOF mb – Marl-Limestone with Organic-Rich Facies member; MLLF mb – Marly limestones with *Leptaena* fauna member; TNL mb – Thin nodular limestones member; CM – Chocolate Marls; MMLHH – Marls and marly limestones with *Hildaites* and *Hildoceras* member; MMLSB mb – Marls and marly limestones with sponge bioconstructions member; MMLB mb – Marls and marly limestones with brachiopods member; CC1 mb – Cabo Carvoeiro 1 member; CC2 mb – Cabo Carvoeiro 2 member; CC3 mb – Cabo Carvoeiro 3 member; CC4 mb – Cabo Carvoeiro 4 member; CC5 mb – Cabo Carvoeiro 5 member.

IV.2.1. Peniche section

The Peniche section (Figs. IV.2A and IV.3; 39°22'12.29"N, 9°23'6.82"W) includes the Global boundary Stratotype Section and Point for the Toarcian Stage (Rocha et al., 2016; Duarte et al., 2017). The studied interval (~ 47 m thick; Fig. IV.3) includes the top of the Lemede Formation (Fm), Emaciatum Zone, represented by alternations of thick limestones with thin marls with abundant ammonites and belemnites. The Toarcian is represented by the Cabo Carvoeiro Fm, which is subdivided into five informal members (Duarte and Soares, 2002). The first member (mb) of the Cabo Carvoeiro Fm, the Cabo Carvoeiro (CC) 1 mb, Polymorphum Zone, consists of bioturbated marls, sometimes micaceous, alternating with highly fossiliferous marly limestones, bearing belemnites, pyritised ammonites, tiny brachiopods and bivalves (Comas-Rengifo et al., 2015; Rita et al., 2019). The CC2 mb (Levisoni Zone) consists of siliciclastic-rich marls (mainly quartz and phyllosilicates), interbedded with sandy marly limestones, rare carbonate sandstones, and microconglomerates (quartz and feldspar) (Fig. IV.3; see Wright and Wilson, 1984; Duarte, 1997; Fantasia et al., 2019). Ammonites are recorded in this mb and benthic macrofauna is rare (Duarte et al., 2018a). Marly limestones and greyish marls with rare brachiopods dominate the base of CC3 mb (e.g. Duarte and Soares, 2002).

IV.2.2. Rabaçal and other auxiliary sections

The Upper Pliensbachian–Lower Toarcian in the North and Central areas of the LB, including the reference stratigraphic section of Rabaçal (Fig. IV.3) [composite section with samples collected at Fonte Coberta (Fig. IV.2B; 40°03′36.5″N, 8°27′33.4″W) and Maria Pares (Fig. IV.2C; 40°03′08.0″N, 8°27′30.5″W), ~ 40.5 m thick in both sections] and the auxiliary sections [Vale das Fontes (Figs. IV.2D and IV.3; 40°12′10.00″N, 8°51′31.00″W, ~ 12.5 m thick), Cantanhede (Figs. IV.2E and IV.3; 40°20'0.82"N, 8°35'50.66"W, ~ 10 m thick), Alcabideque (40°06′46.00″N, 8°27′49.00″W; ~ 20 m thick), Ribeira de Cima (39°34′55.00″N, 8°49′07.00″W, ~ 9 m thick) and Minde (Figs. IV.2F and IV.3; 39°30'21.54"N, 8°41'8.84"W, ~ 8m thick)], are dominated by alternating limestone, marly limestone, and marl successions with ammonites and other macro and microfauna (Fig. IV.3).

The uppermost Pliensbachian (Lemede Fm, Emaciatum Zone) is dominated by bioturbated alternations of centimetric limestones with abundant belemnites, ammonites, bivalves, and brachiopods, with thin marls (e.g. Duarte, 2007; Paredes et al., 2018). The lowermost Toarcian is more argillaceous and is dominated by decimetric greyish marls and strongly bioturbated centimetric marly limestones, very rich in benthic and nektonic macrofauna, such as small brachiopods, belemnites, pyritised ammonites, bivalves, and *Zoophycos* (Duarte, 1997; Piazza et al., 2019). This interval corresponds to the Marly limestones with *Leptaena* fauna (MLLF) mb and is dated from the Polymorphum Zone (e.g. Duarte and Soares, 2002; Duarte et al., 2018b). Around

the boundary between the Polymorphum–Levisoni zones and as recorded in many locations of the LB, a significant sedimentary change is observed, marked by the deposition of thin grey to brownish limestones and marlstones of the Thin Nodular Limestones (TNL) mb. The limestone facies include calcilutites to fine calcarenites with irregular bounding surfaces (amalgamated structures, usually strongly bioturbated with very common *Thalassinoides*) and rare ammonites (*Hildaites* sp.) (e.g. Duarte et al., 2004; Pittet et al., 2014; Miguez-Salas et al. 2017; Rodríguez-Tovar et al., 2017). Laterally, in some sections of the basin, the thin limestones exhibit turbidite-tempestite features, such as plane-parallel lamination, hummocky cross-stratification, symmetrical ripples, and rare current ripples (e.g. Duarte, 1997; Duarte et al., 2004; Pittet et al., 2014). The base of TNL mb in some sections of the northern part of the LB exhibits a singular facies characterised by brownish marls and mudstones with very low carbonate contents and scarce macro and microfauna ("Chocolate Marls" in Vale das Fontes and Alcabideque sections; Duarte, 1997; Pittet et al., 2014; Rodrigues et al., 2016) (Figs. IV.1 and IV.3). The TNL mb is overlain by a thick marly succession dated from the middle-upper part of the Levisoni Zone [Marls and marly limestones with *Hildaites* and *Hildoceras* (MMLHH) mb], associated with the maximum flooding interval of the Toarcian 2nd-order sequence (Duarte et al., 2004, 2007).

IV.3. Material and methods

Forty-six (46) marly samples were collected from the studied sections (twenty-three from Peniche, eleven from Rabaçal, three from Vale das Fontes, three from Cantanhede, five from Ribeira de Cima, and one from Minde) and analysed for total organic carbon (TOC), total sulphur (TS) and palynofacies (Fig. IV.3 and Tables IV.1, IV.2). Thirty-eight (38) marly samples and one wood fragment were analysed for $\delta^{13}C$ in kerogen isolates ($\delta^{13}C_{Kerogen}$), including samples previously collected for geochemical, palynofacies and biomarkers analysis (see Rodrigues et al., 2016) (Tables IV.1 and IV.2).

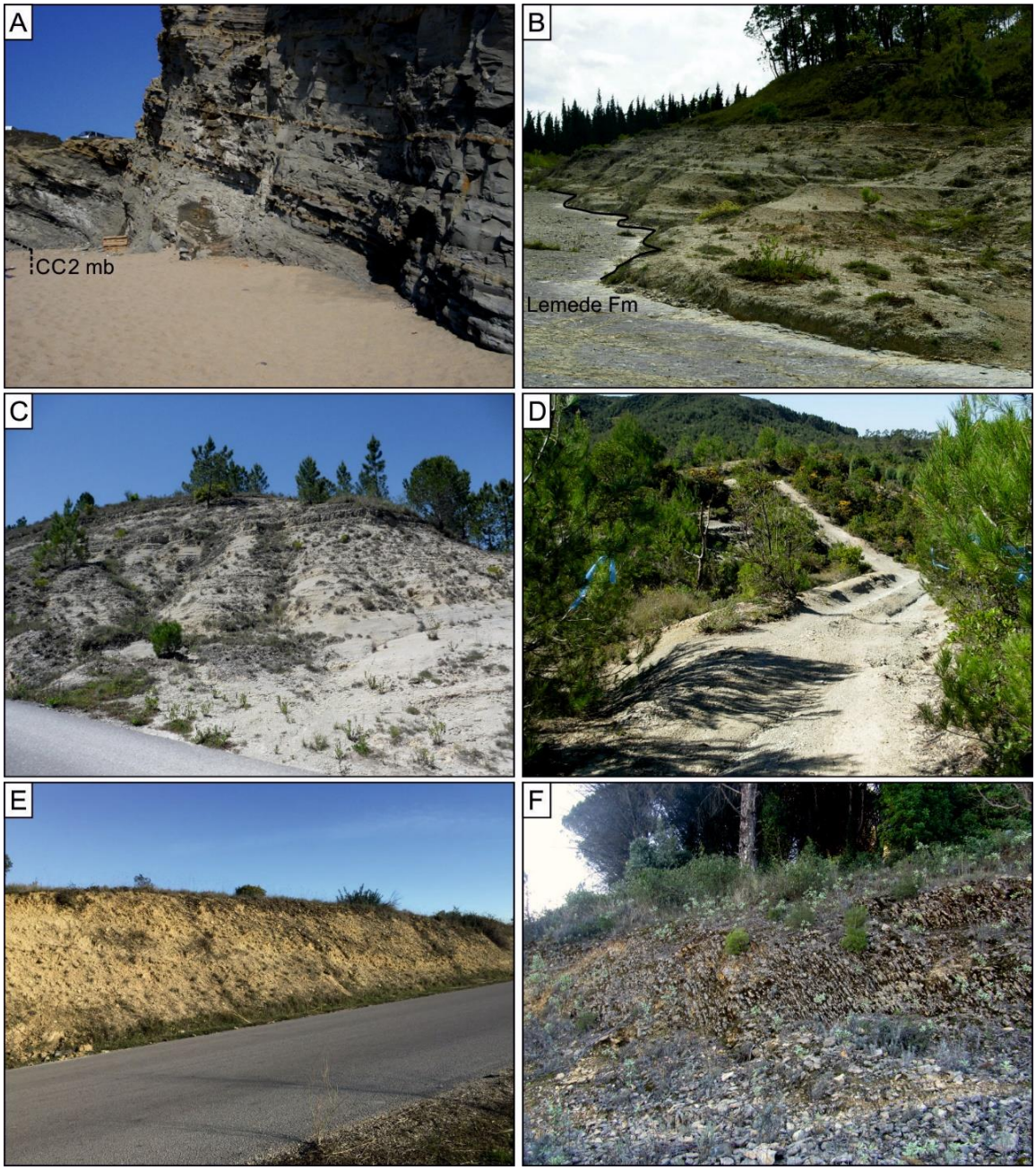

Figure IV.2. General field view of the studied sections. **A**. Base of the Levisoni Zone (Cabo Carvoeiro 2 member) at Praia do Abalo beach (Peniche section); **B**. Lowermost Polymorphum Zone (which includes the Lemede–S. Gião formations boundary) at Fonte Coberta (Rabaçal composite section); **C** – Upper part of the Levisoni Zone (Marls and marly limestones with *Hildaites* and *Hildoceras* member) at Maria Pares (Rabaçal composite section); **D**. Polymorphum Zone (Marly limestones with *Leptaena* fauna member) at Vale das Fontes; **E**. Levisoni Zone (Thin nodular limestones member) at Cantanhede; **F**. Levisoni Zone (Thin nodular limestones member) at Minde.

Sampling was performed after removal of about 15 cm of superficial sediments. TOC, TS, carbonate content and palynofacies analysis were conducted at the Palynofacies and Organic Facies Laboratory (LAFO) of the Rio de Janeiro Federal University (Rio de Janeiro, Brazil) and $\delta^{13}C_{Kerogen}$ analysis were conducted at the MAREFOZ (Coimbra University, Portugal).

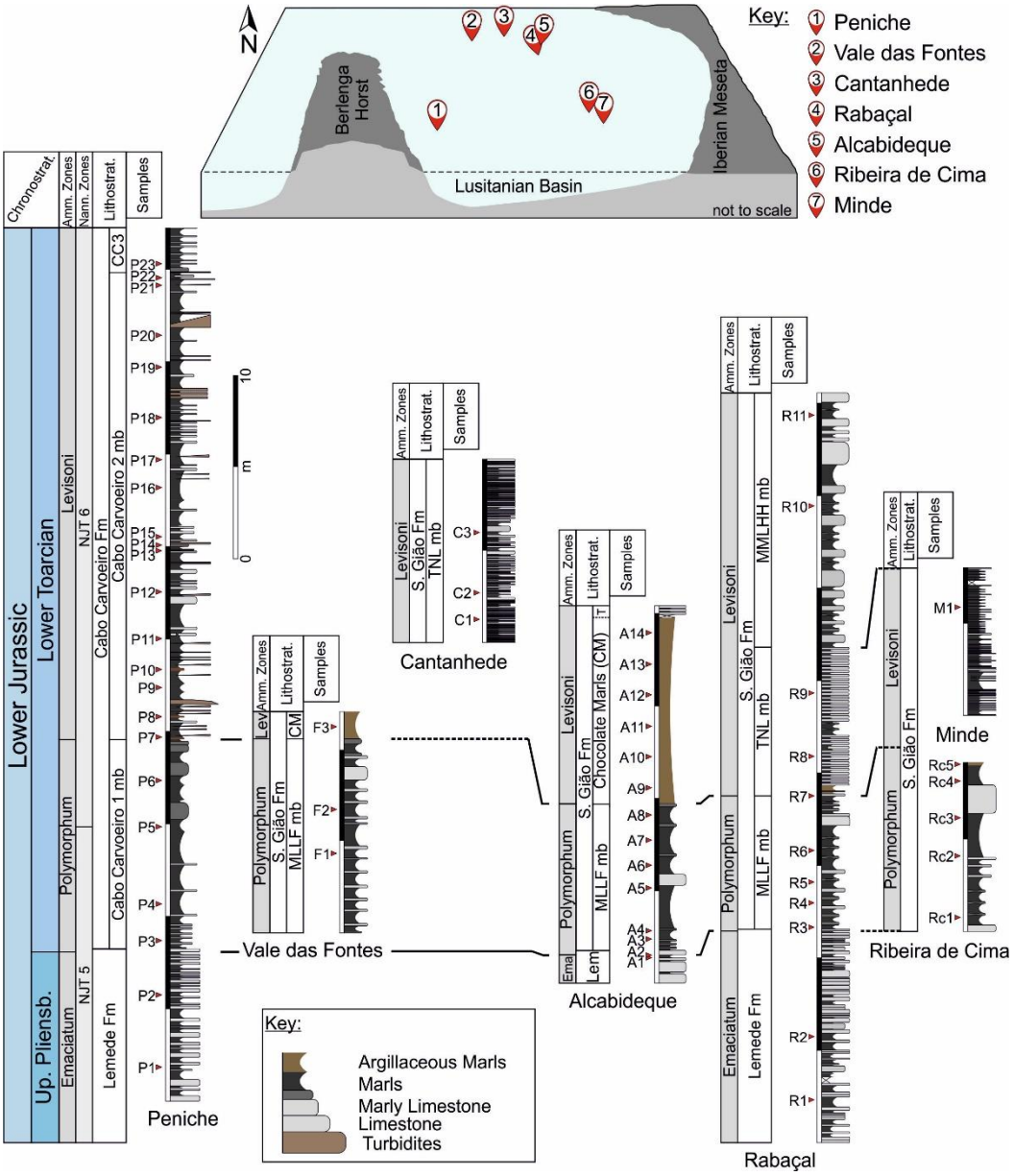

Figure IV.3. Palaeogeographic location of studied sections and stratigraphic logs of the uppermost Pliensbachian–Lower Toarcian interval at Peniche, Vale das Fontes, Cantanhede, Alcabideque, Rabaçal, Ribeira de Cima, and Minde sections, Lusitanian Basin (Portugal) (modified from Duarte, 1995, 1997; Alcabideque section from Rodrigues et al., 2016). Up. Pliensb. – Upper Pliensbachian; Amm. Zones – Ammonite zones; Nann. Zones – Calcareous nannofossils zones; CC3 – Cabo Carvoeiro 3 member; Ema. – Emaciatum Zone; Lev. – Levisoni Zone; MLLF mb – Marly limestones with *Leptaena* fauna member; CM – Chocolate marls; TNL mb – Thin Nodular Limestones member; Lem. – Lemede Formation; MMLHH mb – Marls and marly limestones with *Hildaites* and *Hildoceras* member.

TOC and TS were determined using a LECO SC 144 device, with an analytical precision of ±0.1 wt.% following the ASTM Standard D4239-08 (2008) and NCEA-C-1282 (United States Environmental Protection Agency, U.S.EPA, 2002) methods. Carbonate content was obtained by difference through the insoluble residue after acidification for the removal of carbonates. Kerogen was isolated from the rock matrix isolated using the standard, non-oxidative procedure described, for example, by Tyson (1995) and Mendonça Filho et al. (2012), among others.

The palynofacies analysis was performed using transmitted white light (TWL) and incident blue light (fluorescence mode; FM) techniques through optic microscopy, following the methodology and classification scheme for the OM groups and subgroups of Tyson (1995) and Mendonça Filho and Gonçalves (2017). The main palynofacies kerogen groups [i.e., Phytoclasts, Amorphous, and Palynomorphs, and an additional group, Zooclast (remains of animal-derived organic particles)] provided a robust and reproducible identification scheme. The obtained strew slides counts were recalculated as a relative percentage, and additionally, unsieved strew slides were also prepared.

$\delta^{13}C$ was determined in carbonate-free fraction with the kerogen concentrates prepared according to standard methodology (see explanation above; Mendonça Filho et al., 2012), using a Flash EA 1112 Series elemental analyser coupled online via a Finningan Conflo III interface to a Thermo Delta V S mass spectrometer. Internal precision is better than ±0.1‰ for $\delta^{13}C$ (Acetanilide Standard from Thermo Electron Corporation). Gas species of different mass were separated in a magnetic field then simultaneously measured using a Faraday cup collector array to measure the isotopomers of CO_2 at m/z 44, 45, and 46.

IV.4. Results

IV.4.1. Peniche

TOC content in the Peniche section average 0.6 wt.%, reaching up to 2.08 wt.% in sample P13 (~10.5 m above the base of Levisoni Zone; Fig. IV.4 and Table IV.1). Average TS is 0.5 wt.%, reaching up to 3.08 wt.% in the sample with the highest TOC content. Carbonate contents range between 18–57%, with a slight decrease in the Levisoni Zone (Fig. IV.4 and Table IV.1).

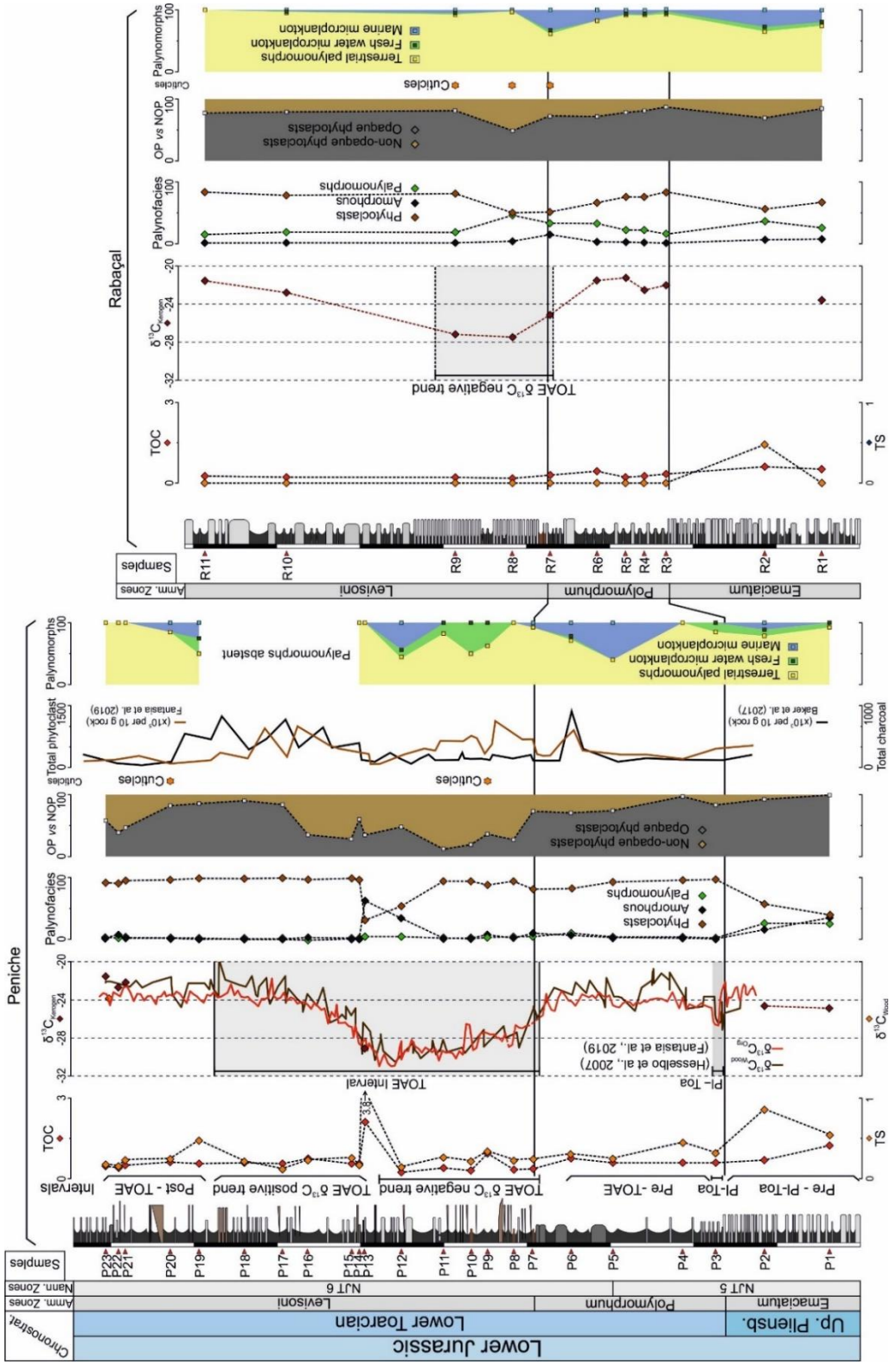

Figure IV.4. TOC, TS, $\delta^{13}C_{Kerogen}$, $\delta^{13}C_{Org}$, $\delta^{13}C_{Wood}$, palynofacies associations and main intervals from Peniche and Rabaçal key sections, Lusitanian Basin (Portugal). $\delta^{13}C_{Wood}$ and $\delta^{13}C_{Org}$ data from the supplementary information of Hesselbo et al. (2007) and Fantasia et al. (2019), respectively. Total charcoal and phytoclast abundance from Baker et al. (2017) and Fantasia et al. (2019), respectively. The record of the Pl–Toa Event and TOAE interval in the Peniche section is based on Hesselbo et al. (2007) and Fantasia et al. (2019). Up. Pliensb. – Upper Pliensbachian.

Palynofacies analysis indicates that the kerogen assemblages include the main kerogen groups (Phytoclast, Amorphous, and Palynomorph, and Zooclast; Fig. IV.4 and Table IV.1). The Peniche succession is dominated by phytoclasts (average 86%), with a slight dominance of opaque phytoclasts (OP) (average 60%; Figs. IV.4, IV.5A and IV.5D). Non-opaque phytoclasts (NOP) are more abundant at the base of the Levisoni Zone (between samples P8 and P16; an average of 67%), concomitantly to an apparent increase in the size of phytoclasts particles (Fig. IV.5G).

The Amorphous Group is rare (average 9%), with a increase in the middle part of Levisoni Zone (samples P12 and P13; Fig. IV.4 and Table IV.1). These particles present diffuse or unstructured limits and are classified as amorphous organic matter (AOM). AOM shows a colouration between brown to pale brown in TWL (Fig. IV.5A) and yellow to orange with inclusions of palynomorphs in FM (Figs. IV.5C and IV.5H). This AOM corresponds to the marine OM.

The Palynomorph Group is observed in most samples (average of 4%; Fig. IV.4 and Table IV.1), ranging from 0% to 23%. Terrestrial palynomorphs are the most abundant subgroup, mainly represented by sporomorphs, including pollen grains belonging to the genus *Classopollis* (Figs. IV.5B, IV.5C and IV.5F) and some pollen grains occurring in tetrads or agglomerates (Figs. IV.5F and IV.5I). Continental aquatic palynomorphs are represented by zygospores of *zygnemataceae* and *Botryococcus* sp. (mainly in the Emaciatum Zone) (Fig. IV.5C). Marine palynomorphs, such as dinoflagellate cysts (*Nannoceratopsis gracilis*, *Luehndea spinosa*), acritarchs (Fig. IV.5E) and prasinophyte algae occur in low amounts in the Levisoni Zone (samples P13, P18 and P19). The Zoomorph subgroup is mainly represented by foraminiferal test-linings.

$\delta^{13}C_{kerogen}$ obtained from seven samples varies between -21.62‰ and -29.15‰. The more negative value was determined in sample P13; the top of the section shows more positive values (average of -22.57‰; Fig. IV.4 and Table IV.1).

IV.4.2. Rabaçal

TOC and TS values varies between 0.16 to 0.61 wt.% and <0.01 to 0.46 wt.%, respectively. The highest TOC and TS are observed in the uppermost Emaciatum Zone (sample R2; Fig. IV.4 and Table IV.2). Carbonate content ranges between 54 and 76%, presenting an average value of 55% (Fig. IV.4 and Table IV.2).

Palynofacies analysis indicated the same general trend from the Peniche section, with kerogen assemblages being dominated by phytoclasts, however, with a slightly lower average, 71% (Fig. IV.4 and Table IV.2). The Phytoclast Group is dominated by OP (average of 76%; Figs. IV.4, IV.6A and IV.6D), with a decrease at the base of Levisoni Zone (sample R8; NOP value of 51%) (Figs. IV.4, IV.6G and Table IV.2). Cuticle fragments are observed at the base of Levisoni Zone (Figs. IV.6E, IV.6H and Table IV.2). Despite the low contents of AOM (~ 3%), it increases to about

14% at the top of the Polymorphum Zone (Fig. IV.4 and Table IV.2). The AOM particles in Rabaçal present the same characteristics as in the Peniche section (Fig. IV.6F).

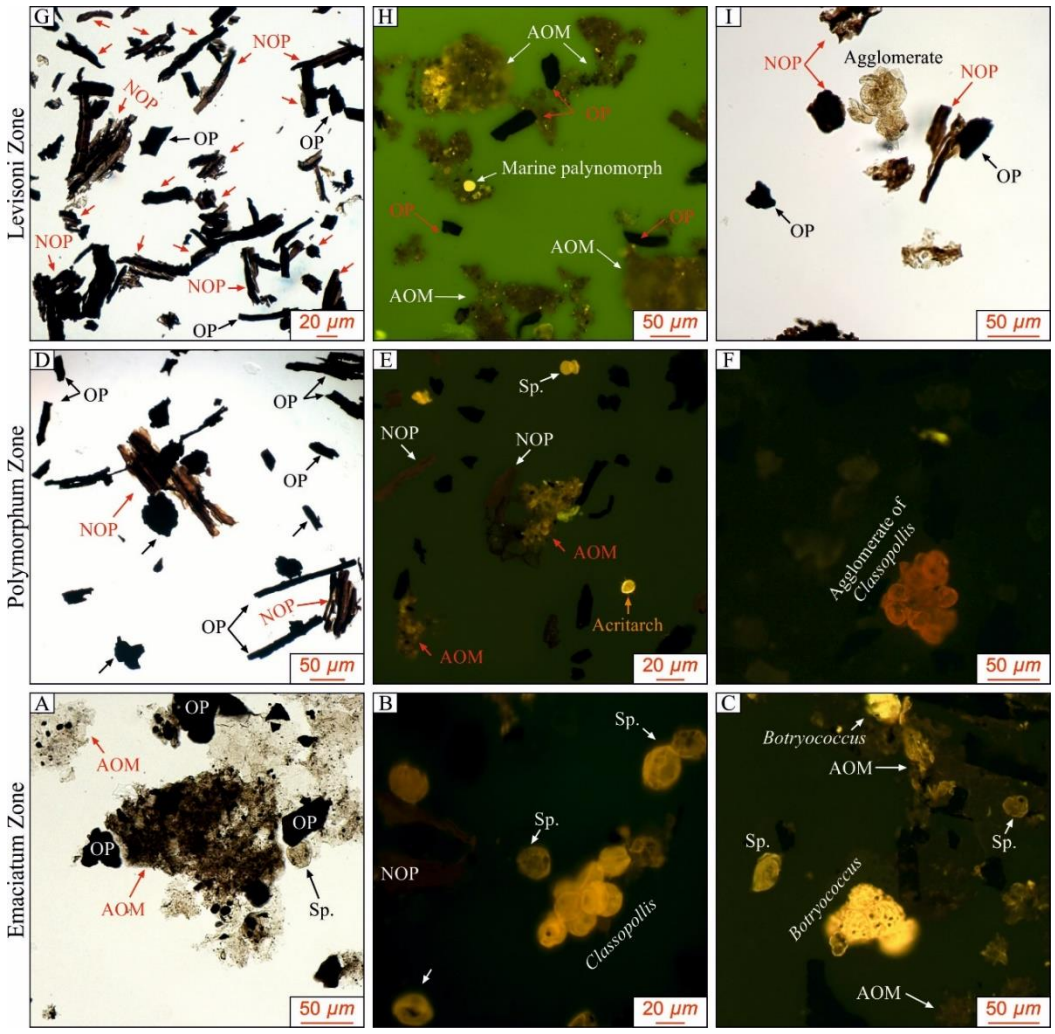

Figure IV.5. Photomicrographs of the studied kerogen assemblages from the Peniche section, Lusitanian Basin (Portugal). **A**. Sample P1 with amorphous organic matter (AOM), opaque phytoclasts (OP) and sporomorphs; **B**. Sample P2 with non-opaque phytoclasts (NOP), sporomorphs and *Classopollis*; **C**. Sample P1 with *Botryococcus* sp., sporomorphs, and AOM; **D**. Sample P4 (base of Polymorphum Zone) with OP and NOP; **E**. Sample P5 with NOP, sporomorphs, AOM and an acritarch; **F**. Sample P7, example of *Classopollis* agglomerate; **G**. Sample P11, dominance of NOP with some OP; **H**. Sample P13, dominance of AOM with a marine palynomorph and OP; **I**. Sample P14, OP, NOP and agglomerate. Transmitted white light (TWL): A, D, G and I; Fluorescence Mode (FM): B, C, E, F and H. OP – Opaque phytoclast; NOP – Non-opaque phytoclast; Sp – Sporomorphs; Amorphous organic matter – AOM.

Table IV.1. TOC, TS, carbonate content, $\delta^{13}C_{Kerogen}$ and palynofacies data from the central sectors of Lusitanian Basin (Portugal).

Sample ID	TOC (wt%)	TS (wt%)	Carb (wt%)	$\delta^{13}C_{Kerogen}$ (‰)	Phytoclast Group (%)	Phytoclast[1]		Amorphous Group (%)	Palynomorph Group (%)	Palynomorph[1]			Terrestrial palynomorphs[1]			Zoo (%)
						OP (%)	NOP (%)			Mar[2] (%)	FM [3] (%)	Terrest[4] (%)	Sp (%)	Tet (%)	Agg (%)	
Peniche section																
P23	0.44	0.19	46	-21.62	92	58	42	2	3	0	0	100	100	0	0	3
Pwf	----	----	----	-23.82	----	----	----	----	----	----	----	----	----	----	----	----
P22	0.4	0.18	42	-22.68	90	39	61	8	2	0	0	100	83	17	0	0
P21	0.49	0.25	37	-22.17	96	47	53	1	3	0	0	100	100	0	0	1
P20	0.63	0.27	41	----	96*	82	18	1	2	14	0	86	100	0	0	0
P19	0.55	0.5	40	----	99	86	14	0	1	25	25	50	100	0	0	0
P18	0.6	0.22	43	----	99	91	9	1	0	0	0	0	0	0	0	0
P17	0.56	0.14	38	----	100	84	16	0	0	0	0	0	0	0	0	0
P16	0.76	0.26	33	----	97	35	65	3	0	0	0	0	0	0	0	0
P15	0.55	0.28	35	----	98	29	71	1	0	0	0	0	0	0	0	0
P14	0.56	0.2	37	----	96	61	39	2	2	0	0	100	100	0	0	0
P13	2.08	3.8	53	-29.15	32	35	65	62	6	0	0	100	100	0	0	0
P12	0.23	0.17	28	----	55	47	53	34	4	43	14	43	100	0	0	8
P11	0.4	0.28	35	----	94	12	88	1	2	0	17	83	100	0	0	3
P10	0.31	0.24	21	----	94	19	81	2	1	0	50	50	0	0	100	2
P9	0.95	0.34	20	----	88*	36	64	7	3	0	38	63	100	0	0	2
P8	0.33	0.23	18	----	95	27	73	1	4	0	0	100	100	0	0	1
P7	0.35	0.24	22	----	82	73	27	10	4	7	0	93	77	15	8	4
P6	0.74	0.3	38	----	82	71	29	6	9	23	3	73	95	0	5	3
P5	0.57	0.24	56	----	93	75	25	3	3	60	0	40	100	0	0	1
P4	0.59	0.44	46	----	96	98	2	1	3	0	0	100	100	0	0	0
P3	0.58	0.32	40	----	97	80	20	0	2	0	14	86	67	17	17	1
P2	0.68	0.85	56	-24.72	57	85	15	18	23	10	10	80	98	0	2	2
P1	1.23	0.54	57	-24.92	40	99	1	38	23	1	6	93	100	0	0	1
Minde section																
M1	0.33	0.015	25	-28.56	16*	10	90	78	5	20	7	73	100	0	0	1
Ribeira de Cima section																
Rc5	0.29	0.015	73	-23.76	76*	49	51	4	20	10	3	87	79	3	17	1
Rc4	0.33	0.02	74	-26.19	49*	39	61	12	37	13	2	86	95	1	4	2
Rc3	0.26	0.015	68	-22.02	71*	50	50	4	24	1	3	96	91	3	6	0
Rc2	0.34	0.016	63	-22.86	71	39	61	2	26	6	6	88	88	7	6	1
Rc1	0.44	0.017	72	-23.08	58	35	65	1	40	1	3	96	100	0	0	1

Carb – carbonate contet; * – presence of cuticles; OP – opaque; NOP – non-opaque; Mar – marine; Terrest – terrestrial; Sp – sporomorph; Tet – tetrad; Agg – agglomerate; [1] – recalculated to 100 %; [2] – total marine microplankton; [3] FM – freshwater microplankton (zygospores of *zygnemataceae* and *Botryococcus* sp.); [4] – total terrestrial palynomorphs (sporomorphs, tetrads and agglomerates).

The Palynomorph Group occurs in moderate amounts in all samples, ranging from 14% to 46% in the Levisoni Zone (samples R11 and R8, respectively; Fig. IV.4 and Table IV.2). This group is dominated by terrestrial palynomorphs, mainly represented by sporomorphs, with some pollen grains occurring in tetrads and agglomerates (Figs. IV.6C and IV.6I). Pollen grains belonging to the genus *Classopollis* are also present. Continental aquatic palynomorphs show the same trend of Peniche and are also observed *Botryococcus* sp. in the Emaciatum Zone (Fig. IV.6B). Marine palynomorphs, such as dinoflagellate cysts [*Nannoceratopsis gracilis* and *senex* (Figs. IV.6E and IV.6F), *Luehndea spinosa* (Fig. IV.6C)] and acritarchs are abundant, particularly at the top of Emaciatum and Polymorphum zones, and prasinophyte algae (*Tasmanites*; Fig. IV.6I) occur in low amounts at the topmost Emaciatum and Polymorphum zones, and base of Levisoni Zone (samples R2, R7 and R9, respectively). Foraminiferal test-linings mainly represent the Zoomorph subgroup.

The $\delta^{13}C_{Kerogen}$ varies between -21.33‰ and -27.5‰. From the top of Emaciatum Zone until the top of Polymorphum Zone, $\delta^{13}C_{Kerogen}$ is relatively more positive, between -23‰ and -21‰. At the Polymorphum-Levisoni zone boundary, a negative shift is observed, reaching up to -27.5‰ at the base of Levisoni Zone (sample R8). Upwards, $\delta^{13}C_{Kerogen}$ values shift again to more positive values at sample R10 ranging from -22.78‰ to -21.51‰ (Fig. IV.4 and Table IV.2).

IV.4.3. Ribeira de Cima and Minde auxiliary sections

TOC varies between 0.10 to 0.44 wt.%, with the highest TOC value recorded at Ribeira de Cima (Sample Rc1). TS values are low and average 0.02 wt.%. The carbonate content presents an average value of 60% and the lowest values are observed in the Levisoni Zone (average of 36%; Table IV.1).

The Phytoclast Group dominates the kerogen assemblage (Fig. IV.7A; an average of 57%). A decrease in this group is observed, during the Levisoni Zone, in the Minde section (sample M1; with 16%). The NOP particles dominate the Phytoclast Group with an average value of 63%, reaching up 65% during the Polymorphum Zone at Ribeira de Cima section (sample Rc1; Fig. IV.7A) and 90% during the Levisoni Zone at Minde section. Despite the low AOM content in these sections, is emphasised the presence of AOM particles in Polymorphum Zone of Ribeira de Cima (Fig. IV.7B) and Levisoni Zone (sample M1, reaching up 79%; Table IV.1).

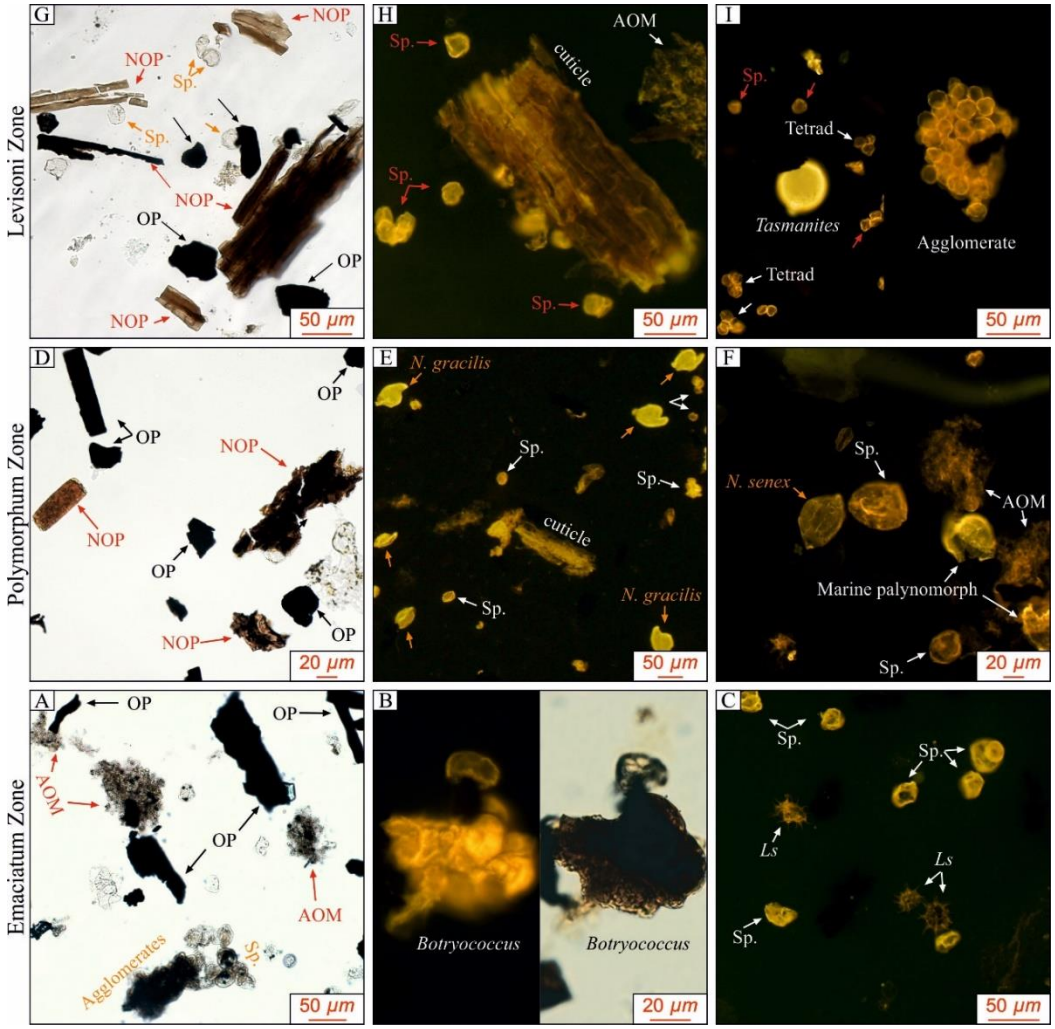

Figure IV.6. Photomicrographs of the studied kerogen assemblages from the Rabaçal section, Lusitanian Basin (Portugal). **A**. Sample R1 with amorphous organic matter (AOM), opaque phytoclasts (OP) and sporomorphs and agglomerate; **B**. *Botryococcus* sp. (sample R2); **C**. Sample R2, several examples of *Luehndea spinosa* and sporomorphs; **D**. Sample R5 with OP and NOP; **E** and **F**. Sample R7 with *Nannoceratopsis gracilis* and *senex*, unidentified marine palynomorphs, AOM, sporomorphs and cuticle; **G**. Sample R8 with several NOP particles, sporomorphs and some OP; **H**. Sample R8, example of a large cuticle with sporomorphs and AOM; **I**. Sample R9 with several tetrads, sporomorphs, agglomerate and *Tasmanites*. Transmitted white light (TWL): A, B, D and G; Fluorescence Mode (FM): B, C, E, F, H and I. OP – Opaque phytoclast; NOP – Non-opaque phytoclast; Sp – Sporomorphs; Amorphous organic matter – AOM; Ls – *Luehndea spinosa*; N. – *Nannoceratopsis*.

The Palynomorph Group occurs in moderate content in the Polymorphum Zone (average of 29% in Ribeira de Cima). This group is dominated by terrestrial palynomorphs (an average of 88%), mainly represented by sporomorphs (Fig. IV.7B), with some pollen grains occurring in tetrads and agglomerates, particularly in the top of Polymorphum Zone. Continental aquatic palynomorphs, such as zygospores of *zygnemataceae* are observed in Ribeira de Cima. Marine palynomorphs (*Nannoceratopsis gracilis* (Fig. IV.7B), *Luehndea spinosa*, acritarchs and

prasinophyte algae) are present, particularly in the top of Polymorphum Zone at Ribeira de Cima section. The Zooclast Group is mainly represented by fragments of foraminiferal test-linings.

The $\delta^{13}C_{Kerogen}$ in the Ribeira de Cima section presented relatively more positive values (average of -23.58‰) and the Minde section (Levisoni Zone) recorded the lowest value (-28.56‰; Table IV.1).

IV.4.4. Vale das Fontes, Cantanhede and Alcabideque auxiliary sections

TOC values average 0.19 wt.%, with the highest value recorded in Polymorphum Zone at Vale das Fontes section (sample F2 with 0.31 wt.%; Table IV.2). TS is insignificant, reaching up 0.02%. The carbonate contents range between 25–57% in the Vale das Fontes section and between 47–56% in Cantanhede section.

Palynofacies analysis indicated the dominance of the Phytoclast Group, with a slight increase of OP during the Polymorphum Zone (observed in Vale das Fontes; an average of 56%; Fig. IV.7C). The Levisoni Zone presented several cuticle fragments and an increase of NOP (Figs. IV.7E and IV.7F).

The AOM content in Vale das Fontes fits in the others studied sections, however, the Levisoni Zone of Cantanhede section presented an increase in AOM (sample C3), reaching up 70% (Table IV.2).

The Palynomorph Group varies between 12–73%, with the highest values recorded in the Cantanhede section. This group is dominated by terrestrial palynomorphs, mainly represented by sporomorphs, with some pollen grains occurring in tetrads (Fig. IV.7C) and agglomerates (Fig. IV.7G and III.7H). Pollens grains belonging to the genus *Classopollis* (Fig. IV.7C) are also present. Continental aquatic and marine palynomorphs are rare, with few zygospores of *zygnemataceae*. The exception is recorded in the Levisoni Zone at the Cantanhede section (sample C3), with some examples of marine palynomorphs such as *Nannoceratopsis gracilis* and *Nannoceratopsis senex* (Fig. IV.7D), *Luehndea spinosa* and acritarchs.

Table IV.2. TOC, TS, carbonate content, $\delta^{13}C_{Kerogen}$ and palynofacies data from the northern sectors of Lusitanian Basin (Portugal).

Sample ID	TOC (wt%)	TS (wt%)	Carb (wt%)	$\delta^{13}C_{Kerogen}$ (‰)	Phytoclast Group (%)	Phytoclast[1]		Amorphous Group (%)	Palynomorph Group (%)	Palynomorph[1]			Terrestrial palynomorphs[1]			Zoo (%)
						OP (%)	NOP (%)			Mar[2] (%)	FM [3] (%)	Terrest [4] (%)	Sp (%)	Tet (%)	Agg (%)	
Vale das Fontes section																
F3	0.10	<0.01	25	----	52*	60	40	1	21	1	1	98	90	2	8	0
F2	0.31	0.018	51	-21.35	79	60	40	2	16	3	3	93	95	4	2	0
F1	0.30	0.015	57	-21.69	83	52	48	1	13	4	0	96	94	2	4	1
Cantanhede section																
C3	0.16	0.013	47	----	18*	54	46	70	12	66	2	32	100	0	0	0
C2	0.11	0.022	55	-27.40	24	49	51	3	73	1	0	99	95	1	4	0
C1	0.16	0.020	56	-24.96	29*	34	66	10	61	0	0	100	95	1	4	0
Alcabideque section [TOC, TS, carbonate content and palynofacies data from Rodrigues et al. (2016)]																
A14	0.13	0.01	25	-26.00	33	45	55	0	67	1	0	99	73	7	20	0
A13	0.17	0.01	43	-27.48	67	49	51	0	33	2	0	98	57	2	41	0
A12	0.15	0.01	43	-25.01	52	51	49	2	46	0	1	99	64	9	27	0
A11	0.19	0.02	36	-26.79	61	49	51	2	37	1	1	98	70	10	20	0
A10	0.15	0.01	28	-26.83	40	57	43	1	59	1	1	98	73	12	15	0
A9	0.23	0.01	30	-25.46	68	86	14	3	29	3	0	97	80	16	3	0
A8	0.41	0.36	68	-23.74	31	52	48	15	54	24	2	74	98	1	1	0
A7	0.27	0.01	62	-22.70	83	54	46	1	16	4	0	96	92	0	8	0
A6	0.15	0.01	72	-21.59	100	65	35	0	0	0	0	0	0	0	0	0
A5	0.16	0.01	62	----	83	67	33	2	15	2	0	98	71	8	21	0
A4	0.17	0.01	63	-21.33	71	65	35	0	29	0	0	100	86	4	10	0
A3	0.15	0.01	59	----	99	50	50	1	0	0	0	100	100	0	0	0
A2	0.17	0.01	67	-21.93	47	49	51	0	51	4	0	96	93	1	6	0
A1	0.13	0.01	59	-21.81	82	47	53	0	18	5	5	89	76	0	24	0
Rabaçal section																
R11	0.24	0.018	65	-21.51	84	78	22	1	14	0	0	100	82	12	6	0
R10	0.22	<0.01	72	-22.78	79	80	20	2	19	1	1	98	91	3	6	0
R9	0.18	0.025	54	-27.23	82*	81	19	1	18	5	2	93	92	4	4	1
R8	0.16	0.013	69	-27.50	50*	49	51	4	46	1	0	99	90	1	9	0
R7	0.30	0.017	64	-25.10	52*	73	27	14	33	35	4	61	92	1	7	1
R6	0.42	0.02	59	-21.64	67	73	27	1	32	17	0	83	98	1	1	1
R5	0.21	0.01	61	-21.33	77	79	21	1	21	5	3	92	96	1	3	0
R4	0.24	0.01	63	-22.49	78	82	18	1	21	6	3	91	86	7	7	0
R3	0.31	0.04	55	-22.08	84	88	12	0	16	2	4	94	76	12	12	0
R2	0.61	0.46	75	----	58	70	30	6	36	28	7	65	100	0	0	0
R1	0.50	0.05	76	-23.63	68	85	15	6	25	20	6	74	93	5	2	0

Carb – carbonate contet; * – presence of cuticles; OP – opaque; NOP – non-opaque; Mar – marine; Terrest – terrestrial; Sp – sporomorph; Tet – tetrad; Agg – agglomerate; [1] – recalculated to 100 %; [2] – total marine microplankton; [3] FM – freshwater microplankton (zygospores of *zygnemataceae* and *Botryococcus* sp.); [4] – total terrestrial palynomorphs (sporomorphs, tetrads and agglomerates).

The $\delta^{13}C_{Kerogen}$ varies between -21.35‰ and -27.4‰. Vale das Fontes section presented the relatively more positive values (reaching up -21.69‰ in Polymorphum Zone) and Cantanhede recorded more negative $\delta^{13}C_{Kerogen}$ values, reaching up -27.4‰ at sample C2 (Levisoni Zone; Table IV.2). The Alcabideque section reveals the same trend in Emaciatum and Polymorphum zones, with more positive values (average of 22.18‰). During the Levisoni Zone is observed a notorious decrease, reaching the minimum value of -27.48‰ (Table IV.2).

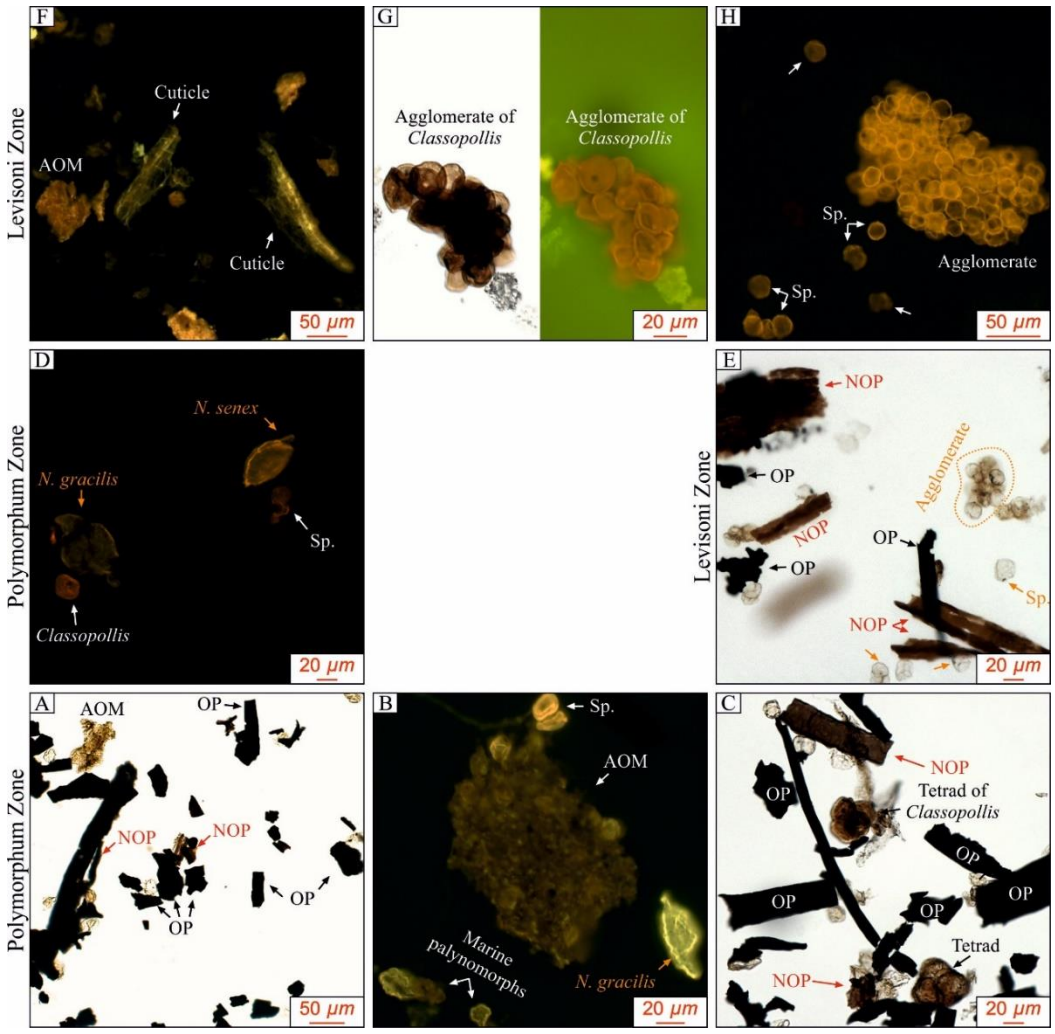

Figure IV.7. Photomicrographs of the studied kerogen assemblages from the central and northern sections, Lusitanian Basin (Portugal). **A**. Sample Rc1 with opaque phytoclasts (OP), non-opaque phytoclasts (NOP) and amorphous organic matter (AOM); **B**. Sample Rc4 with AOM, unidentified marine palynomorphs, *Nannoceratopsis gracilis*, and sporomorphs; **C**. Sample F1 with OP, NOP and two tetrads (one with *Classopollis* sp.); **D**. Sample F2 with sporomorph, *Classopollis* sp., *Nannoceratopsis gracilis* and *Nannoceratopsis senex*; **E**. Sample C1 with OP, NOP, sporomorphs and agglomerate; **F**. Sample M1 showing several examples of AOM and two cuticles; **G**. Sample F3 with *Classopollis* agglomerate; **H**. Sample C1 with agglomerate and several sporomorphs. Transmitted white light (TWL): A, C, E and G; Fluorescence Mode (FM): B, D, F, G and H. OP – Opaque phytoclast; NOP – Non-opaque phytoclast; Sp – Sporomorphs; Amorphous organic matter – AOM.

IV.5. Discussion

IV.5.1. Organic matter preservation across the Pliensbachian–Early Toarcian in the Lusitanian Basin

Similarly to other southern Tethyan locations, such as the External Subbetic domain, Betic Cordillera (e.g. Reolid et al., 2018; Rodrigues et al., 2019) and the Middle and High Atlas Basin (e.g. Bodin et al., 2010; Ait-Itto et al., 2017; Rodrigues et al., 2020), the uppermost Pliensbachian–Lower Toarcian successions of the LB are poor in OM (TOC average of 0.4 wt.%). In our study, the Peniche section records the highest TOC values of the basin (average ~ 0.6 wt.%) reaching up 2.47 wt.% in a discrete level located ~10.5 m above the base of Levisoni Zone. Hesselbo et al. (2007) and Fantasia et al. (2019) reported similar elevated TOC contents from the same level. The overall low organic contents of the LB contrast with the contemporaneous organic-rich deposition of several northwestern Tethyan and Panthalassic margins (e.g. Baudin et al., 1990; Röhl et al., 2001; Suan et al., 2011; Them II et al., 2017; Fantasia et al., 2018b; Fonseca et al., 2018) and with preceding Lower Jurassic successions in the LB (see Duarte et al., 2010; 2012; Silva et al., 2011, 2015; Poças Ribeiro et al., 2013). The occurrence of OM-rich sediments in the LB is particularly expressive in the mid-Upper Pliensbachian (Marly-Limestones with organic-rich facies (MLOF) mb from the Vale das Fontes Fm (Fig. IV.1D); Davoei-Margaritatus zones), with TOC reaching up to 26 wt.% (Silva et al., 2015). This TOC-richer unit is correlated with a phase of restriction that favoured OM deposition and preservation, associated with maximum flooding intervals, related with 2nd-order transgressive phases at the basinal scale (see Silva et al., 2011, 2012).

IV.5.2. Climatic and environmental control on the variation of kerogen assemblages in the uppermost Pliensbachian–Lower Toarcian in the Lusitanian Basin

As aforementioned, the kerogen assemblages of the uppermost Pliensbachian–Lower Toarcian in the LB are mostly of terrestrial affinity, mainly composed of phytoclasts and continental palynomorphs. Nonetheless, the Peniche section is punctuated by increases in AOM; in other studied sections, an increase in marine microplankton and AOM in some levels is observed.

To evaluate the variation of kerogen assemblages and $\delta^{13}C$ in the LB and possible association with previously recorded Early Toarcian palaeoenvironmental changes (sea-level changes, temperature, etc), the studied interval was divided into six intervals: i) pre-Pl–Toa Event (corresponding to shallowing and overall cooling phase of the Emaciatum Zone); ii) Pl–Toa Event

(coincidental with the negative CIE at the base of Polymorphum Zone); iii) Pre-TOAE (Polymorphum Zone); iv) TOAE $\delta^{13}C$ negative trend [between the beginning of TOAE interval and the minimum in the $\delta^{13}C_{Org}$ curve from Fantasia et al. (2019)]; v) TOAE $\delta^{13}C$ positive trend [between the highest TOC value and the end of TOAE interval from Fantasia et al. (2019)]; vi) Post-TOAE.

IV.5.2.1. Pre-Pl–Toa Event

The Emaciatum Zone in LB is characterised by the dominantly regressive limestones of the Lemede Fm (Duarte, 2007; Duarte et al., 2010), associated with a significant eustatic sea-level fall and overall cooler environments (e.g. Price, 1999; Suan et al., 2008a, 2010; Korte and Hesselbo, 2011; Silva and Duarte, 2015; Ruebsam et al., 2019; Rodrigues et al., 2020). The studied kerogen assemblages agree with the regressive character of this interval, comprising abundant phytoclast particles, subordinated amounts of terrestrial palynomorphs and continental aquatic palynomorphs (*Botryococcus* sp.), and rare AOM particles (Figs. IV.4, IV.8, IV.9, and Tables IV.1, IV.2). The kerogen assemblages of the Lemede Fm are typical of oxygenated proximal shallow-water marine environments with a substantial continental influence (e.g. Tyson, 1995) and contrasts with preceding MLOF mb (Silva and Duarte, 2015),

Average $\delta^{13}C_{Kerogen}$ from the Rabaçal and Alcabideque sections is -22.4‰. Although limited by the low resolution of the studied sections in the LB, the more positive $\delta^{13}C_{Kerogen}$ in the LB are similar to those recorded in Betic Cordillera, where average $\delta^{13}C_{Kerogen}$ is -22.1‰ (Rodrigues et al., 2019) and average $\delta^{13}C_{Org}$ is -23.1‰ (Ruebsam et al., 2020a).

Some argillaceous levels from the top of the Lemede Fm at Peniche have slight higher TOC (an increase of ~ 0.6 wt.%) and AOM (average around 28%) contents and more negative $\delta^{13}C_{Kerogen}$ values (average -24.8‰). These features suggest increased environmental restriction when compared to the other LB sections (Figs. IV.4, IV.8 and IV.9). The Rabaçal section registers an increase of ~ 18% in marine palynomorphs, mostly dinoflagellates cysts such as *Luehndea spinosa* (Fig. IV.6C). The increase in marine palynomorphs is compatible with Rodrigues et al. (2016), which observed an increase in the relative abundance of *Nannoceratopsis senex* in the Alcabideque section (near Rabaçal) in the same time interval. Correia et al. (2017a, 2018) observed an increase in the abundance of *Luehndea spinosa* and *Nannoceratopsis* spp. at the top of Emaciatum Zone and before the Pl–Toa Event in the Peniche and Rabaçal sections. These dinoflagellate cysts are probably linked to increased nutrient levels (see Fantasia et al., 2019), favoured by local ecological conditions (see Baranyi et al., 2016 and references therein). The relationship between increased marine components and nutrient levels in this time interval was also noted in La Cerradura section, Betic Cordillera (see Rodrigues et al., 2019).

The generalised increase in marine components in the LB and others southern Tethyan and northern of Gondwana successions is likely associated with the Late Pliensbachian cooling (e.g.

Correia et al., 2017a), preceding the palaeoenvironmental changes of the Pl–Toa Event (see below). Recently, van de Schootbrugge et al. (2019) proposed that the increase in dinoflagellate cysts during the Late Pliensbachian in the southern Tethyan successions was the result of an important connection between the Arctic Sea and the Tethys Ocean through the Viking Corridor.

IV.5.2.2. Pl–Toa Event

As in many other basins worldwide (e.g. Hallam, 2001; Hardenbol et al., 1998; Haq, 2018), a rapid transition (transgression) from shallow marine carbonates to hemipelagic marls (MLLF and CC1 members) is registered just above the Pliensbachian–Toarcian transition in the LB (e.g. Duarte, 1997; Duarte et al., 2010; Rocha et al., 2016). Concomitantly, a minor negative CIE linked to Pl–Toa Event is expressed in the $\delta^{13}C$ records from different substrates in the Peniche and Rabaçal sections (see Hesselbo et al., 2007; Suan et al., 2008a; Pittet et al., 2014; Ferreira et al., 2015; Fantasia et al., 2019). The Pl–Toa Event is associated with slightly warmer and humid climates which induced an increase in continental weathering and fluvial runoff (e.g. Hesselbo et al., 2007; Littler et al., 2010; Pieñkowski et al., 2016; Xu et al., 2018; Ruebsam et al., 2019; Fantasia et al., 2019; Rodrigues et al., 2020).

A slight increase of NOP particles characterises the kerogen assemblage of the sample collected from this interval at Peniche (Fig. IV.4). The same feature is observed in the Ribeira de Cima section at the base of Polymorphum Zone, accompanied by an increase in terrestrial palynomorphs (sporomorphs; Table IV.1). The increase in NOP and terrestrial palynomorphs could be the result of increased delivery of these particles from rivers (Tyson, 1995 and references therein) and are consistent with a slight increase in fluvial runoff, associated with the Pl–Toa Event.

IV.5.2.3. Pre-TOAE

The $\delta^{13}C_{Kerogen}$ values (around -23‰) from the pre-TOAE interval show remarkable similarities with $\delta^{13}C_{Wood}$, $\delta^{13}C_{Org}$, and $\delta^{13}C_{Kerogen}$ from other locations in the southern Tethyan and Iberian margins [LB (Hesselbo et al., 2007; Fantasia et al., 2019) and Betic Cordillera (Rodrigues et al., 2019; Ruebsam et al., 2020a)] and northern of Gondwana [Middle Atlas (*unpublished data*) and High Atlas Basin (Bodin et al., 2016)]. The OP subgroup (mostly oxidised land plant tissues and charcoal particles; see Tyson, 1995) dominates the kerogen assemblages in the studied sections during the pre-TOAE (Polymorphum Zone) interval (including during the Pl–Toa Event; Figs. IV.4, IV.8, IV.9 and Tables IV.1, IV.2). The occurrence of OP particles is favoured by strongly seasonal climates (with pronounced arid periods) and with significant water table fluctuations (e.g. Tyson, 1995; Lamberson et al., 1996). The kerogen assemblages and the more positive $\delta^{13}C$ in the

Polymorphum Zone fit with the palaeolatitude proposed for LB and other southern Tethyan, Iberian and northern of Gondwana basins. During the earliest Toarcian, the LB was situated in the semi-arid climate belt (Rees et al., 2000), with low precipitation as expressed by the clay mineral assemblages (Dera et al., 2009), dominated by xerophytic flora (see Diéguez et al., 2010; Philippe et al., 2017) and more positive $\delta^{13}C$ patterns (decreased ^{13}C fractionation during photosynthesis in C3 plants; see Rodrigues et al., 2019; Ruebsam et al., 2020a).

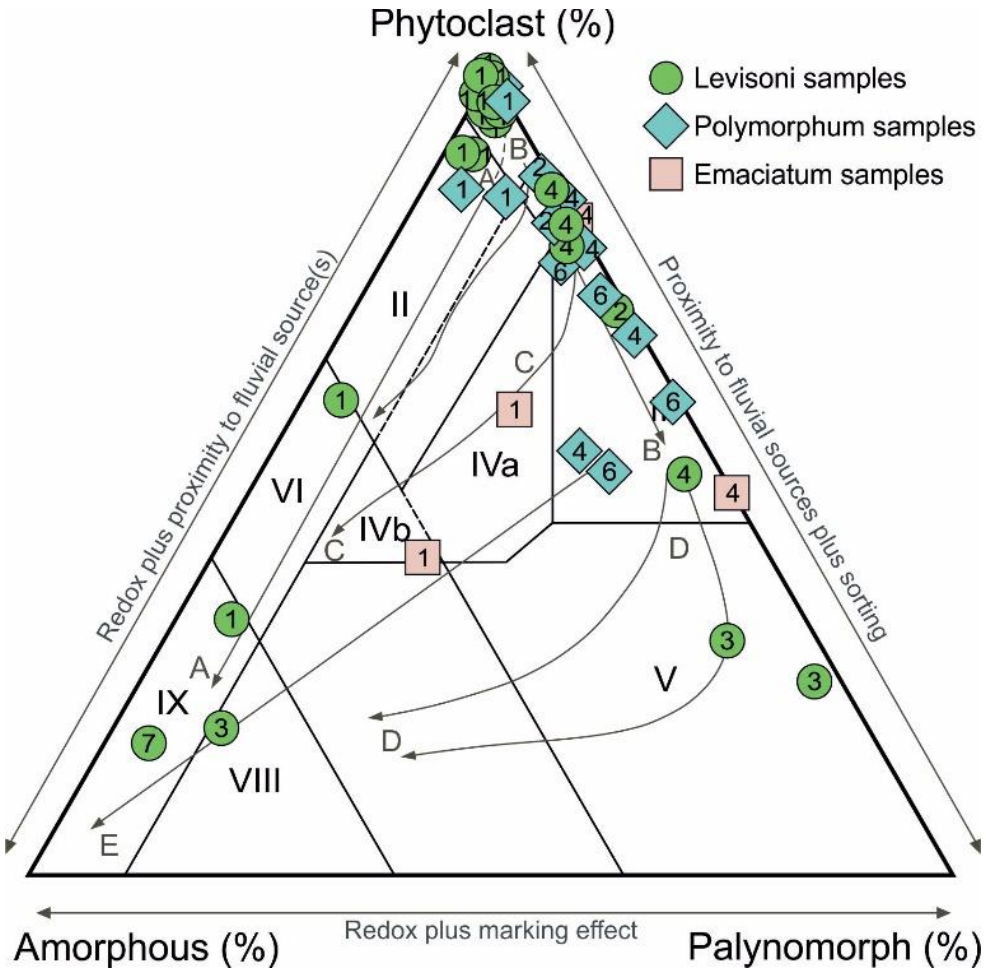

Figure IV.8. Ternary kerogen and palynofacies plots for marine series (Tyson, 1995) based on the relative abundance of Phytoclast, Amorphous, and Palynomorph Groups of the studied stratigraphic interval in the Lusitanian Basin (Portugal). The numbers in the samples correspond to the number of the studied sections presents in Fig. IV.1. Palynofacies and environmental fields: (I) highly proximal shelf or basin, (II) marginal dysoxic-anoxic basin, (III) heterolithic oxic shelf (proximal shelf), (IV) shelf to basin transition, (V) mud-dominated oxic shelf (distal shelf), (VI) proximal suboxic-anoxic shelf, (VII) distal dysoxic-anoxic shelf, (VIII) distal dysoxic-oxic shelf and (IX) distal suboxic-anoxic basin. Transport paths: (A) direct path from source to anoxic basin, (B) Phytoclasts move away from the source out across shallow-marine shelf, (C) redirection of phytoclasts into the basin from route B, (D) continuation of route B with further reduction in phytoplankton organic carbon values and progressive sorting of phytoclasts and palynomorphs and (E) poorly defined shelf to basin pathway.

There is a progressive increase in NOP upwards (particularly observed in Peniche and Rabaçal), interpreted to reflect an increase in the riverine supply of NOP particles (Tyson, 1995; Figs. IV.4 and IV.9) within the context of ongoing global warming and intensification of humid conditions culminating during the TOAE (e.g. Cohen et al., 2004; McArthur et al., 2008; Jenkyns, 2010; Korte and Hesselbo, 2011; Percival et al., 2015). The climatic trend is also supported by the increase in K/(I+C) ratios at Peniche (Fantasia et al., 2019) and $\delta^{18}O_{Brach}$ data from the Peniche and Rabaçal sections (Suan et al., 2008a; Ferreira et al., 2015).

At the top of Polymorphum Zone, probably coincidental with the first negative $\delta^{13}C$ shift associated with the TOAE, a decrease in $\delta^{13}C_{Kerogen}$ values is observed (~ 3‰ in Rabaçal and ~ 4‰ in Ribeira de Cima; Figs. IV.4, IV.9 and Table IV.2). The kerogen assemblages present an increase in terrestrial palynomorphs and relative abundances of *Nannoceratopsis gracilis* (Fig. IV.6E) in the more proximal sections (Rabaçal, Ribeira de Cima, and Alcabideque sections) (see also Rodrigues et al., 2016). Correia et al. (2017a, 2017b) also reported an increase in this dinoflagellate cysts in the Peniche and Vale das Fontes sections. As said before, probably there is a connection between dinoflagellate cysts and increased nutrient levels. Baker et al. (2017) reveal a brief enhancement of fire activity associated with the deposition of charcoal particles around this interval in Peniche section. These features suggest that nearby-emerged areas of LB were affected by wildfires and probably induced an increase in the surface runoff accompanied by the export of nutrient into marine environments, favouring the presence of dinoflagellate cysts.

IV.5.2.4. TOAE $\delta^{13}C$ negative trend

The TOAE $\delta^{13}C$ negative trend is well documented in $\delta^{13}C_{Carb}$, $\delta^{13}C_{Wood}$, $\delta^{13}C_{Org}$ datasets from the Peniche section (Hesselbo et al., 2007; Fantasia et al., 2019). The $\delta^{13}C_{Kerogen}$ record from Rabaçal, Alcabideque, Cantanhede, and Minde present a negative shift of ~ -5‰. The 2‰ difference in magnitude of the TOAE negative CIE between Peniche and the remaining sections probably reflects the coarse resolution of these datasets.

The kerogen assemblages in the generality of LB follow the sedimentary and ^{13}C signal disturbance. At Peniche, an abrupt increase in NOP particles is observed (Figs. IV.4, IV.5G and Table IV.1). In the Rabaçal and more northern sections, is observed an increase in NOP, cuticle fragments, terrestrial palynomorphs (sporomorphs and *Classopollis* in tetrads and agglomerates) and a decrease in marine palynomorphs (Figs. IV.8 and IV.9). It was suggested that the decrease in charcoal contents (included in the OP subgroup in palynofacies studies; Tyson, 1995) associated with the TOAE resulted from the suppression of fire activity due to an increase in humidity. Besides, higher precipitation rates are proposed to have enhanced continental weathering and fluvial runoff (e.g. Cohen et al., 2004; Percival et al., 2016; Them II et al., 2017).

The presence of AOM probable flora origin in Cantanhede and Minde sections (70 and 78%, respectively) is not associated to elevated TOC and TS values and suggest deposition in a typical oxygenated marine environment (e.g. Tyson, 1995). Amorphization of these particles likely occurred in continental or transitional setting (Silva et al., 2013).

The observed changes in the kerogen assemblages are interpreted to be the combined result of increased fluvial runoff, wetter conditions, and slightly lower atmospheric oxygen concentrations during the TOAE $\delta^{13}C$ negative trend, favouring the export of NOP and other terrestrial particles into the marine environment. In the LB sections, the TOAE interval corresponds to a disturbance of the marl–limestone background sedimentary infill that includes turbidites (CC2 mb in Peniche section) and tempestites (TNL mb in the generality of the basin) (see Wright and Wilson, 1984; Duarte, 1997; Duarte et al., 2004, 2007; Pittet et al., 2014), accompanied with a biotic crisis (e.g. Cabral et al., 2013; Comas-Rengifo et al. 2015; Ferreira et al., 2015; Rita et al., 2016; Miguez-Salas et al., 2017; Rodríguez-Tovar et al., 2017; Piazza et al., 2019; Reolid et al., 2019b), indicating that both the continental and marginal-marine environments were affected by the TOAE. Moreover, this interval in the LB was also been associated to an important tectonic phase, such as confirmed by the occurrence of palaeoseismites in the southernmost part of the basin (Fig. IV.8; see Duarte, 1997; Kullberg et al., 2001).

IV.5.2.5. TOAE $\delta^{13}C$ positive trend

The TOAE positive $\delta^{13}C$ trend at Peniche is well represented in $\delta^{13}C_{Carb}$, $\delta^{13}C_{Wood}$, $\delta^{13}C_{Org}$ (Hesselbo et al., 2007; Fantasia et al., 2019) and allows to establish a correspondence with the $\delta^{13}C_{Kerogen}$ values obtained in the Rabaçal section (average ~ -22.2‰).

The initial stages of the TOAE $\delta^{13}C$ positive trend are associated with the highest TOC contents and an increase in AOM in the Peniche section (Figs. IV.4 and IV.5H). The reason for the occurrence of this elevated TOC level is unclear, but it is speculated that the influx of freshwater and nutrients from the continents likely promoted dysoxic conditions and promoted the preservation of OM (e.g. McArthur et al., 2008; Röhl et al., 2001; van de Schootbrugge et al., 2005).

In the Peniche section, NOP abundances remain relatively elevated for the first half of the TOAE $\delta^{13}C$ positive trend, decreasing to pre-TOAE values ~15 m above the base of Levisoni Zone and well before the termination of the TOAE (Fig. IV.4). The decrease in NOP particles is roughly coincidental with an increase in charcoal abundance (Figs. IV.4 and IV.9; Baker et al., 2017). It was suggested that after the carbon cycle perturbation associated with the TOAE $\delta^{13}C$ negative trend, climates gradually cooled and became dried (e.g. Suan et al., 2008a; Dera et al., 2009; Ferreira et al., 2015; Korte et al., 2015), thus reactivating fire-activity and favouring the transport of OP into the marginal marine environments of the LB.

IV.5.2.6. Post-TOAE

After the TOAE interval, the $\delta^{13}C$ remains relatively stable during the middle part of the Levisoni Zone. The obtained $\delta^{13}C_{Kerogen}$ and $\delta^{13}C_{Wood}$ in Peniche section (sample Pwf) values fit quite well with the $\delta^{13}C_{Wood}$ and $\delta^{13}C_{Org}$ record (Fig. IV.4; see Hesselbo et al., 2007; Fantasia et al., 2019). The gradual return of the hemipelagic marls (see also Duarte et al., 2004, 2007) and biotic recovery (see references above) is conveyed with the gradual re-establishment of the depositional conditions observed before the TOAE. The kerogen assemblages in the Peniche section presented a slight increase in continental palynomorphs (sporomorphs) and NOP particles (see Figs. IV.4 and IV.9). This change can be linked to the small shift to more humid conditions and an increase in fluvial runoff. After the end of the TOAE, a shift to warmer and humid climate conditions is inferred from the Peniche section by an increase in the K/(I+C) (Fantasia et al., 2019). Rare dinoflagellate cysts and the absence of AOM suggest an oxygenated water column towards the maximum peak transgression of the Toarcian 2nd-order sequence (Fig. IV.9; see Duarte et al., 2004, 2007).

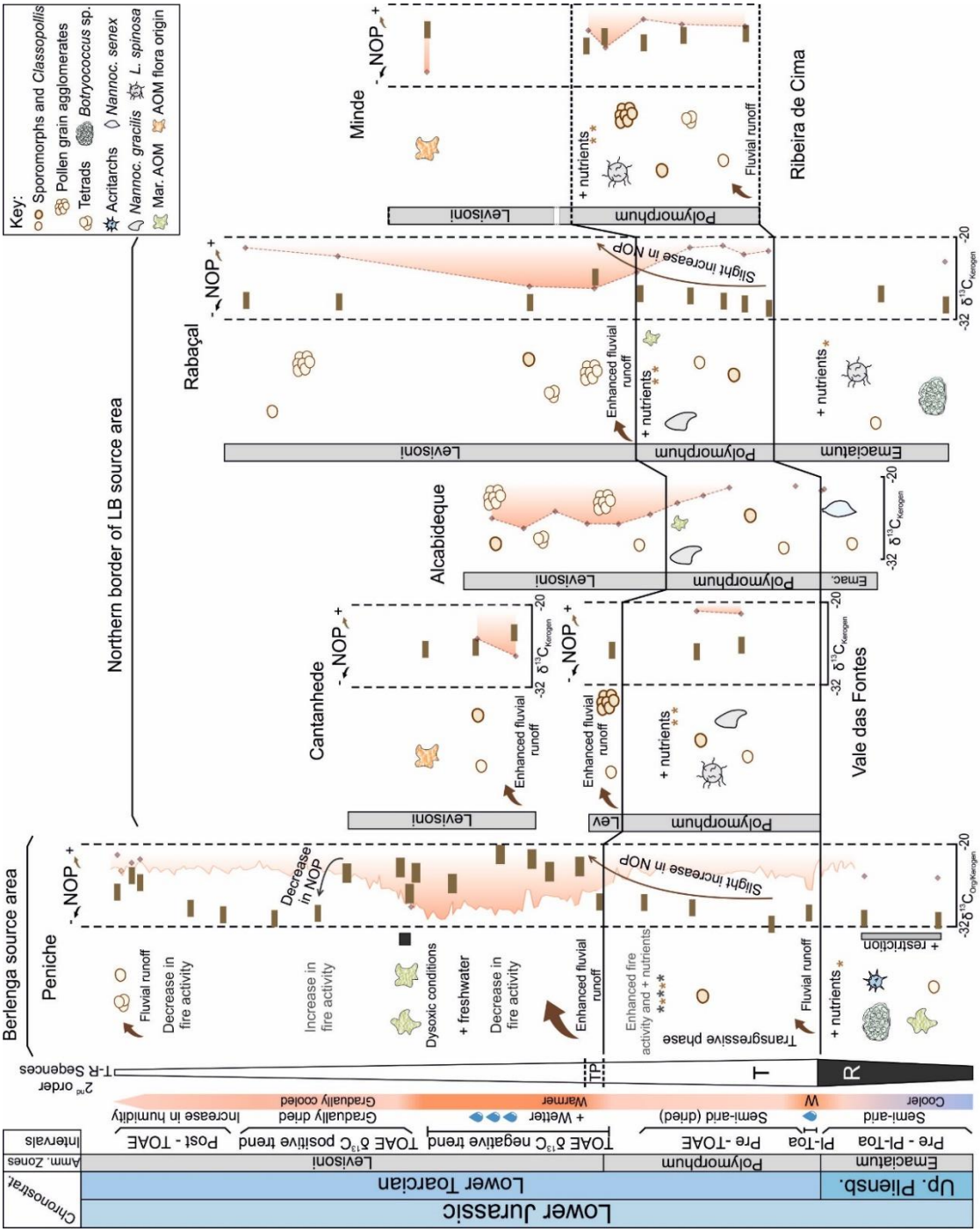

Figure IV.9. Schematic palaeoenvironmental evolution from latest Pliensbachian – Early Toarcian with the main intervals, palynofacies evidences and the relationship with palaeoenvironmental parameters occurring in the studied sections at Lusitanian Basin (Portugal). The palaeogeographic location of studied sections and stratigraphic samples positions are based in Fig. IV.3. $\delta^{13}C_{Org}$ data in Peniche from the supplementary information of Fantasia et al. (2019) and the palynofacies evidence in Alcabideque from Rodrigues et al. (2016). The transgressive (T)–regressive (R) 2nd order sequences are from Duarte (2007). W – warmer; R – Regressive; T – Transgressive; TP – Tectonic phase (e.g. Duarte. 1997; Kullberg et al., 2001); NOP – non-opaque phytoclasts; OM – organic matter; Mar. AOM – marine amorphous organic matter; *Nannoc*. – *Nannoceratopsis*; *L.spinosa* – *Luehndea spinosa*.

IV.6. Conclusion

The latest Pliensbachian–Early Toarcian successions in the LB are dominated by hemipelagic carbonate deposits, showing stark lateral facies differentiation during the Levisoni Zone in the several sectors of the basin. Mainly developed in the reference sections of Peniche and Rabaçal, the following findings are derived from new organic geochemistry, palynofacies, and $\delta^{13}C_{Kerogen}$ analysis:

- Contrasting with the contemporaneous northwestern Tethyan and Panthalassic margins and with preceding Lower Jurassic successions in the LB, the studied sedimentary sections have, in general, low TOC and the kerogen assemblages are mostly of terrestrial affinity, with a dominance of Phytoclast Group and terrestrial palynomorphs. However, punctuated by an increase in Amorphous Group, freshwater, and marine microplankton.

- Before the Pl–Toa Event (latest Emaciatum Zone; latest Pliensbachian) is recorded an increase in marine palynomorphs (mainly *Luehndea spinosa*) interpreted to have resulted from an increment in nutrient availability, likely associated with the Late Pliensbachian cooling.

- The more positive $\delta^{13}C_{Kerogen}$ values and abundance in OP recorded during the Polymorphum Zone (Pre-TOAE interval), supported a semi-arid climate. The gradual increase in NOP reflects an increase in riverine supply within the context of ongoing global warming and intensification of humid conditions. At the top of Polymorphum Zone, the presence of marine palynomorphs (mainly *Nannoceratopsis gracilis*) is consistent with the export of nutrient into marine environments, during increased large fire events in LB.

- During the TOAE $\delta^{13}C$ negative trend, the Peniche section presented an abrupt increase in NOP particles. At Rabaçal and other auxiliary sections is observed a slight increase in NOP, cuticle fragments, terrestrial palynomorphs (sporomorphs and *Classopollis* in tetrads and agglomerates) and a decrease in marine palynomorphs. The slightly lower atmospheric oxygen and wetter conditions observed during the TOAE $\delta^{13}C$ negative trend in LB are consistent with an enhanced continental weathering and fluvial runoff.

- During the initial phase of TOAE $\delta^{13}C$ positive trend in Peniche, is recorded the highest TOC and AOM content in the LB associated with dysoxic conditions. Upwards, the NOP abundances decrease to pre-TOAE values and roughly agree with the reactivating fire-activity in the LB, suggesting that the climates gradually cooled and became dried (with sparse shifts to humid climate) conveyed with the gradual re-establishment of the depositional conditions observed before the TOAE.

V. Variation of kerogen assemblages and $\delta^{13}C_{Kerogen}$ in the uppermost Pliensbachian–Lower Toarcian succession of Asturian Basin (northern Spain)

V.1. Introduction

During the Early Toarcian, the Earth systems experienced severe episodes of environmental perturbation, the largest one recognised as the Toarcian Oceanic Anoxic Event (TOAE) and characterised by profound disturbances in geochemical, sedimentary, and biological cycles (e.g. Jenkyns and Clayton, 1986; Hesselbo et al., 2000, 2007; Mattioli et al., 2009; Kemp and Izumi, 2014; Brazier et al., 2015; Percival et al., 2016; Them II et al., 2017; Xu et al., 2017; 2018; Izumi et al., 2018; Fantasia et al., 2019).

One of the most researched features of the TOAE is the associated large disruption of the carbon cycle, expressed by a negative carbon isotopic excursion (CIE) at the base of the Serpentinum/Levisoni/Falciferum ammonite Zone (e.g. Hesselbo et al., 2000, 2007; Kemp et al., 2005; Al-Suwaidi et al., 2010; French et al., 2014; Pieñkowski et al., 2016; Them II et al., 2017; Fantasia et al., 2019; Rodrigues et al., 2019; Ruebsam et al., 2020a), and contemporaneous with widespread deposition of organic matter (OM). OM-rich sediments are particularly noticeable around the northwestern Tethyan margin in the central and northern European epicontinental basins (e.g. Baudin et al., 1990; Jenkyns, 2010). In these areas, deposition took place in warm and humid conditions, associated with intensification of the hydrological cycle and subsequent enhanced fluvial and nutrient input into the basins (e.g. Cohen et al., 2004; Dera et al., 2009; Brazier et al., 2015; Fantasia et al., 2018a).

In contrast to the OM-rich facies of the northern European epicontinental basins, in the southern Tethyan, western and southern Iberian, and northern Gondwana margins, the TOC-rich intervals are spatially and temporally restricted (e.g. Hesselbo et al., 2007; Bodin et al., 2010, 2016; Gómez and Goy, 2011; Reolid et al., 2012, 2014; Rodrigues et al., 2016, 2019, 2020; Ait-Itto et al., 2017; Fantasia et al., 2019; Ruebsam et al., 2020b and Chapter IV). The lack of OM enrichment is attributed to generally oxic conditions and low productivity associated, semi-arid climate, and general circulation patterns (e.g. van de Schootbrugge et al., 2005; Baroni et al., 2018; Rodrigues et al., 2019).

An emerging research topic regarding the TOAE is devoted to understanding how local processes modulated the potential to develop marine anoxia (e.g. Wignall et al., 2005; McArthur et al., 2008; Fantasia et al., 2018a, 2019). The Rodiles section from the Asturian Basin (northern Spain) presents an important enrichment in OM record across the Tenuicostatum–Serpentinum zones. Gómez et al. (2008) reported an interval with total organic carbon (TOC) reaching up 3.2 wt.% and Rodrigues et al. (2015) presented a sample with 2.9 wt.% from the base of Serpentinum

Zone, dominated by amorphous organic matter (AOM). The good biostratigraphical control (see Valenzuela, 1988; Gómez et al., 2008) and the previous studies focusing on the TOAE (see Gómez et al., 2008, 2016) highlights the importance of this section to investigate palaeoclimatic and palaeoenvironmental changes occurring before and during the TOAE.

In this study, we re-evaluate and expand on the geochemical and palynofacies preliminary data previously published by Rodrigues et al. (2015) from the Rodiles section (Fig. V.1). The samples were also analysed for carbon-isotope in kerogen isolates ($\delta^{13}C_{Kerogen}$). The main objectives of this study were to (1) complement the existing dataset for the Rodiles section, to (2) investigate the relationship between OM production, depositional conditions, and palaeoceanographic controls on the occurrence of OM-rich facies during the Early Toarcian in the Asturian Basin, and (3) investigate the relationship with the neighbouring counterparts.

V.2. Geological background

The Asturian Basin is a small sedimentary basin, located on the northern part of the Iberian Massif (Figs. V.1A and V.1B). This basin is one of the several rift-related Peri-Tethyan Mesozoic basins whose origin is related to the opening of the Atlantic Ocean (e.g. Hiscott et al., 1990). The sedimentary infill is of Mesozoic age, unconformably deposited in a Paleozoic basement and covered by Cenozoic deposits. The basement and the Mesozoic infill suffered several tectonic episodes related to the Permian–Triassic extensional continental rifting process (e.g. Quesada and Robles, 1995) and the Upper Jurassic–Cretaceous opening of the Bay of Biscay (e.g. Quesada and Robles, 1995; Hernández, 2000; Aurell et al., 2002).

The Jurassic succession of the Asturian Basin is divided into two depositional stratigraphic units, separated by a disconformity related to a rifting episode (see Suárez Vega, 1974). The studied stratigraphic interval (latest Pliensbachian – Early Toarcian) is included in the lower unit (Villaviciosa Group; Hettangian to Lower Bajocian) and is characterised by the deposition of thick rhythmic alternations of micritic/marly limestones and marls comprising the Santa Mera Member from Rodiles Formation (e.g. Valenzuela et al., 1986). The Rodiles section is located about ~8 km northeast of the Villaviciosa village (43º32'22"N; 5º22'22"W; Fig. V.1B), in the eastern part of the Asturias regional autonomy (northern Spain) and crops out near the Rodiles beach. It corresponds to ~20 m of the Rodiles Formation (Fig. V.1C) and initiates with white–grey marly limestones and grey marls with abundant ammonites dated from the Spinatum (Fig. V.2A; Upper Pliensbachian) and Tenuicostatum (Lower Toarcian) zones. At the top of Tenuicostatum–base of Serpentinum Zones is observed a laminated dark grey marls interval, enriched in OM (see Gómez et al., 2008; Rodrigues et al., 2015). The remaining Serpentinum Zone is composed of alternations of white–grey marly limestones bioturbated and grey marls (Fig. V.2B).

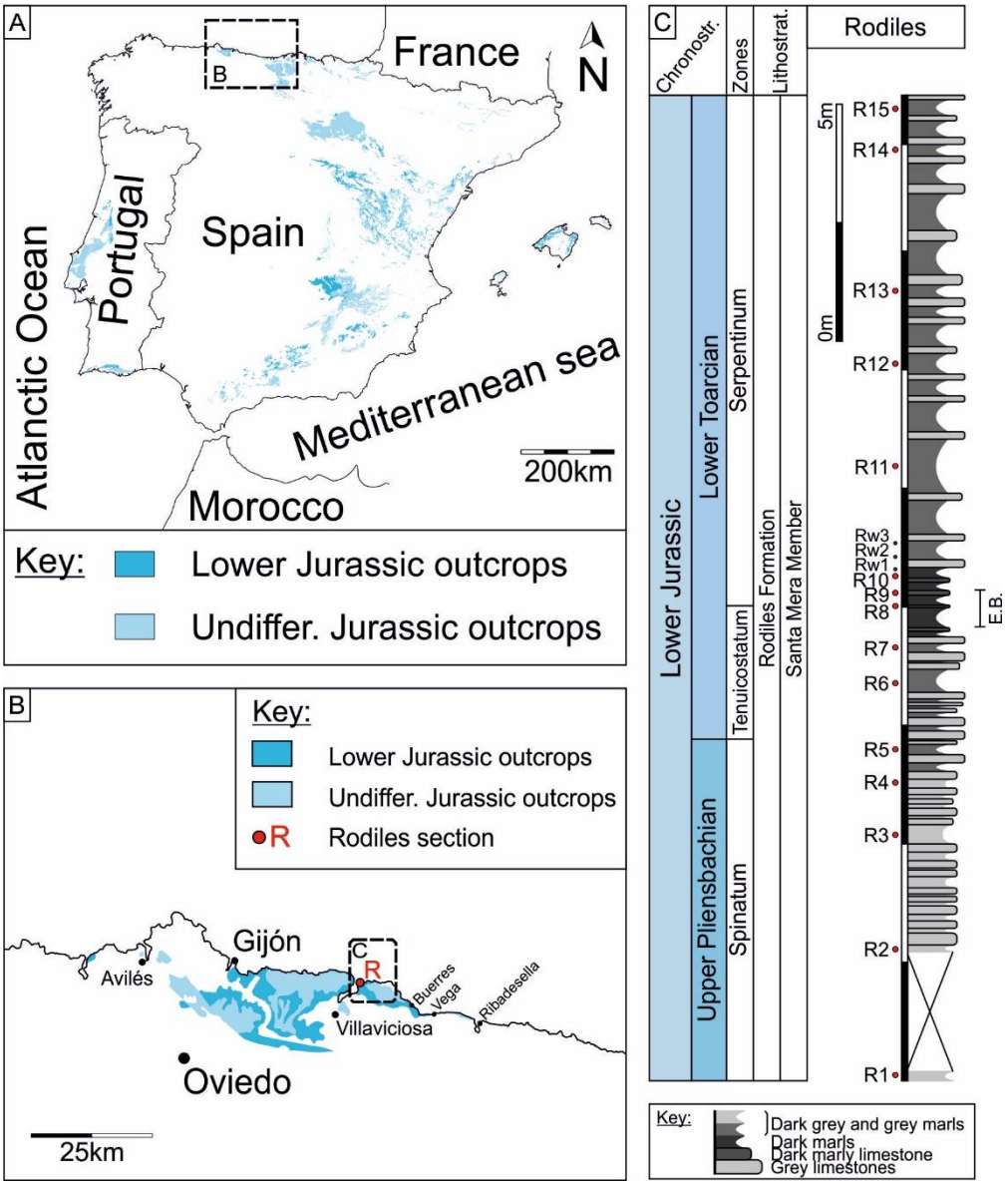

Figure V.1. Geological setting and studied section. **A**. Geological map of the Jurassic outcrops in the Iberian Peninsula; **B**. Geological map of the Jurassic outcrops in the Asturian Basin and location of the Rodiles section (R) (adapted from Rodríguez-Fernandez et al., 2016); **C**. Simplified stratigraphic log of the Upper Pliensbachian–Lower Toarcian interval in the Rodiles section (modified from Gómez and Goy, 2011). The duration of the extinction boundary (E.B.) based in Gómez and Goy (2011). Undiffer. – Undifferentiated.

V.3. Material and methods

Previously obtained TOC and TS contents are summarized below and listed in Table V.1. The re-evaluation of the palynofacies data was performed at the Palynofacies and Organic Facies Laboratory (LAFO) of the Rio de Janeiro Federal University (Rio de Janeiro, Brazil), following the classification scheme for the OM groups [i.e., Phytoclasts, Amorphous, and Palynomorphs, and an additional group, Zooclast (remains of animal-derived organic particles)] and subgroups

of Mendonça Filho and Gonçalves (2017). Additionally, using kerogen concentrates of marly and wood samples (carbonate-free fraction previously obtained according to the standard, non-oxidative procedure; see, for example, Tyson, 1995; Mendonça Filho et al., 2012), $\delta^{13}C$ ($\delta^{13}C_{Kerogen}$) was determined at MAREFOZ (Coimbra University, Portugal). The $\delta^{13}C_{Kerogen}$ was obtained using a Flash EA 1112 Series elemental analyser coupled online via a Finningan Conflo III interface to a Thermo Delta V S mass spectrometer. Internal precision is better than ±0.1‰ for $\delta^{13}C$ (Acetanilide Standard from Thermo Electron Corporation). Gas species of different mass were separated in a magnetic field then simultaneously measured using a Faraday cup collector array to measure the isotopomers of CO_2 at m/z 44, 45, and 46.

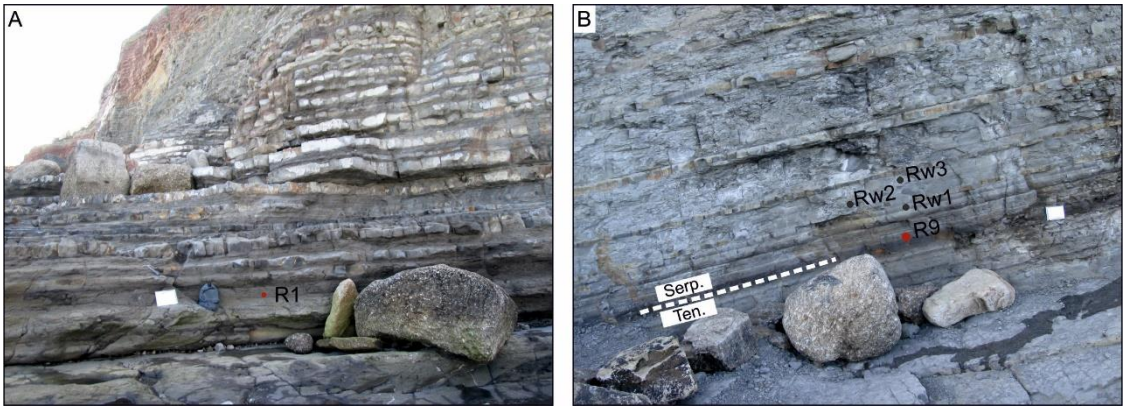

Figure V.2. Field view of the Rodiles studied section. **A**. The rhythmic white–grey marly limestones and grey marls from Spinatum Zone and the position of sample R1; **B**. General view of the laminated dark grey marls interval, with the position of samples R9 and Rw1–3 (wood fragments). The white dashed line corresponds to the limit between the Tenuicostatum and Serpentinum zones (see Gómez et al., 2008).

V.4. Results

V.4.1. TOC and TS content

TOC average is 0.8 wt.%, reaching up to 2.9 wt.% at the base of Serpentinum Zone (sample R9; Fig. V.3 and Table V.1). TS average is 1.1 wt.%, with the highest TS contents observed in the topmost of Spinatum Zone (sample R5; 2.5 wt.%) and at the topmost of Tenuicostatum–base of Serpentinum zones (between samples R8 and R9; ~ 3.5 wt.%). Carbonate contents range between 20–57%, with the lowest value recorded in the topmost of Spinatum Zone (sample R5). Between the topmost of Tenuicostatum–base of Serpentinum zones is observed a decrease in carbonate (samples R8 and R9; Fig. V.3 and Table V.1).

V.4.2. Carbon isotopes

$\delta^{13}C_{Kerogen}$ varies between -31.47 and -23.73‰ (Fig. V.3 and Table V.1). From Spinatum Zone to the base of Serpentinum Zone, $\delta^{13}C_{Kerogen}$ presents relatively more positive values, between -23‰ and -25‰. At the topmost of Tenuicostatum–base of Serpentinum zones is observed a distinct negative CIE (about 6‰), reaching the minimum value of -31.47‰ at the base of Serpentinum Zone (sample R9). Upwards, $\delta^{13}C_{Kerogen}$ recorded a positive trend, with mean values of -25‰ (Fig. V.3 and Table V.1). $\delta^{13}C_{Kerogen}$ of fossil wood varies from -27.54 to -25.07‰, which is in good agreement with the $\delta^{13}C_{Kerogen}$ record (Fig. V.3 and Table V.1).

V.4.3. Palynofacies

Kerogen assemblages include the main kerogen groups; Phytoclast, Amorphous, Palynomorph, and Zooclast (Fig. V.3 and Table V.1). The Phytocast Group dominates the kerogen assemblages (average 62%; Fig. V.3 and Table V.1), with the dominance of the non-opaque phytoclasts (NOP; Figs. V.3, V.4A, V.4B, and Table V.1). Opaque particles (OP) are present in smaller amounts (average 35%); however, increasing slightly at the top of the succession (Figs. V.3 and V.4A). Membranes are mainly observed in the Spinatum Zone (reaching up 45% at the sample R5) and there is a slight increase in cuticles (Fig. V.4C) at the topmost of Tenuicostatum–base of Serpentinum zones (Table V.1).

The Amorphous Group presented a large variation, between 5–83% (average of 26%; Fig. V.3 and Table V.1), with an increase at the topmost of Tenuicostatum–base of Serpentinum zones (between samples R8–R10). These particles present diffuse or unstructured limits and are classified as amorphous organic matter (AOM). AOM particles are brown to pale brown in TWL (Fig. V.4D) and yellow to orange in FM, and present inclusions of palynomorphs (Figs. V.4E and V.4F) suggesting a marine origin. Particles belonging to the Palynomorph Group occur in low amounts, ranging from 3% in the Spinatum Zone (samples R1 and R2) to 13% in the Serpentinum Zone (sample R12). Terrestrial palynomorphs are mainly represented by the sporomorph subgroup, with sporomorphs (Fig. V.4G) and *Classopollis* (Fig. V.4H).

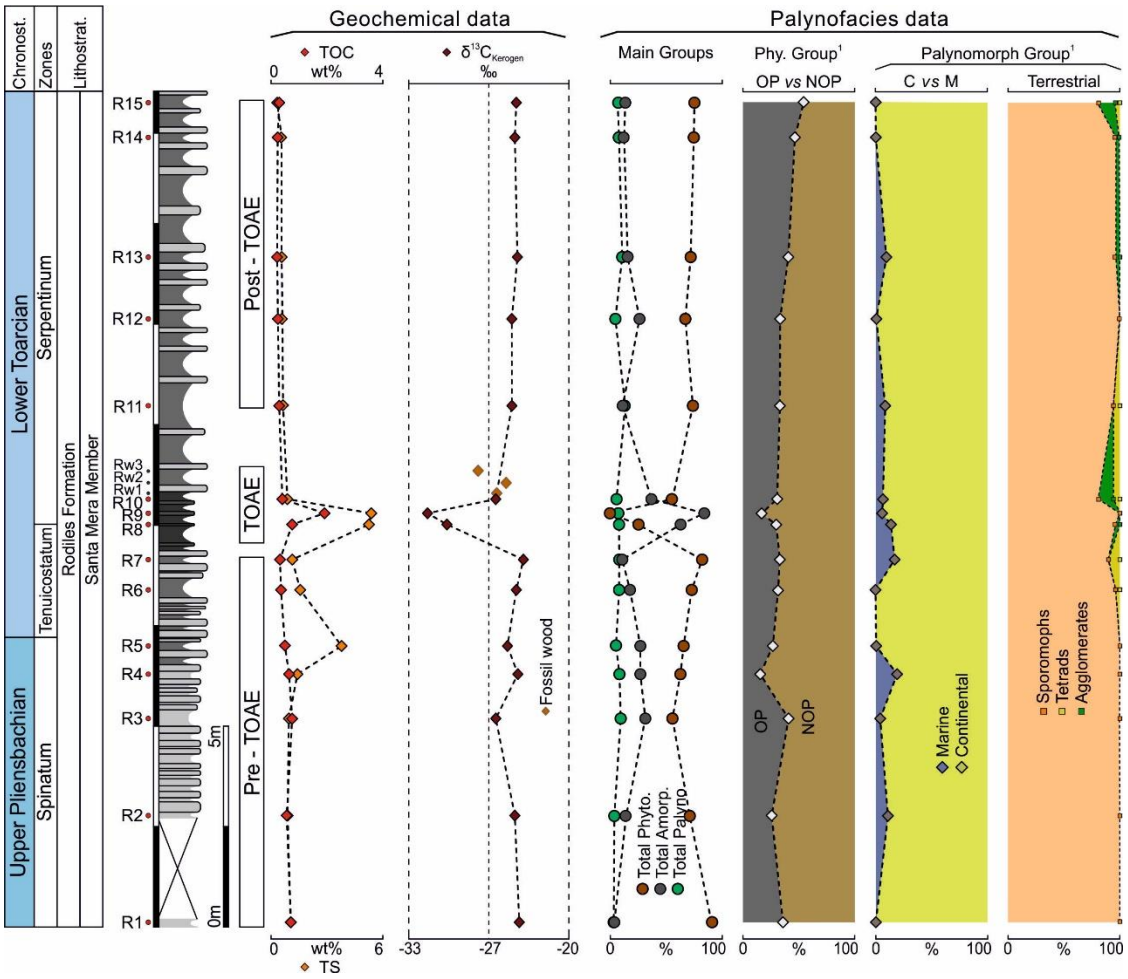

Figure V.3. TOC, TS, $\delta^{13}C_{Kerogen}$, palynofacies associations and main intervals from Rodiles section, Asturian Basin (northern Spain). Phyto. – phytoclasts; Amorp. – amorphous; Palyno. – palynomorphs; OP – opaque phytoclasts; NOP – non-opaque phytoclasts.

Some pollen occurring in tetrads or agglomerates (Figs. V.4H and V.4I) are also present. Freshwater microplankton is rare and is represented by zygospores of *zygnemataceae*. Marine palynomorphs, such as dinoflagellate cysts (*Luehndea spinosa*; Fig. V.4J), acritarchs, and prasinophyte algae (*Tasmanites* genus*;* Fig. V.4K) occur in low amounts, reaching up to 18% in Spinatum Zone (Fig. V.3 and Table V.1). The Zoomorph Group is represented by foraminiferal test-linings (Fig. V.4L).

Figure V.4. Photomicrographs of the studied kerogen assemblages from the Rodiles section, Asturian Basin (northern Spain). **A**. Opaque (OP) and non-opaque phytoclasts (NOP) from Spinatum Zone (sample R3); **B**. Sample from the topmost of Tenuicostatum Zone with NOP (sample R9); **C**. Example of cuticle with OP from Serpentinum Zone (sample R14); **D**–**E**. AOM, OP, and NOP from Spinatum Zone (sample R3); **F**. Image from the topmost of Tenuicostatum Zone with AOM and OP (sample R9); **G**. Sample from Spinatum Zone with sporomorphs, AOM, OP and NOP (sample R4); **H**. Sporomorph, *Classopollis* and tetrad of *Classopollis* from the topmost of Tenuicostatum Zone (sample R9); **I**. Example of pollen grain agglomerate from Serpentinum Zone (sample R12); **J**. *Luehndea spinosa*, AOM, and OP observed at Tenuicostatum Zone (sample R7); **K**. Sample from the base of Serpentinum Zone with *Tasmanites*, AOM and OP (sample R10); **L**. Foraminiferal test-linings, OP, NOP and sporomorph from Serpentinum Zone (sample R12). Transmitted white light (TWL): A, B, C, D, G, H, and L; Fluorescence Mode (FM): E, F, H, I, J, and K. OP – Opaque phytoclast; NOP – Non-opaque phytoclast; Sp – Sporomorphs.

Table V.1. TOC, TS, carbonate content, $\delta^{13}C_{Kerogen}$ and palynofacies data from Rodiles section (northern Spain).

Sample ID	*TOC (wt.%)	*TS (wt.%)	*Carb (wt.%)	$\delta^{13}C_{Kerogen}$ (‰)	Phytoclast Group (%)	Phytoclast[1]				Amorphous Group (%)	Palynom. Group (%)	Palynomorphs[1]						Zoo. (%)
						OP (%)	NOP (%)	Cut (%)	Memb (%)			Mar[2] (%)	Cont.[3] (%)	Continental palynomorphs[1](%)				
														Sp .	Tet.	Agg.	FM	
R15	0.4	0.3	43	-24.22	74	55	44	0	1	13	7	0	100	81	5	14	0	6
R14	0.3	0.2	40	-24.29	74	47	52	0	1	12	7	0	100	88	0	4	8	7
R13	0.3	0.3	46	-24.04	71	41	47	6	6	15	10	9	91	94	0	3	0	4
R12	0.3	0.3	45	-24.63	67	34	57	7	3	26	3	0	100	100	0	0	0	4
R11	0.4	0.4	39	-24.65	73	33	62	1	4	12	13	8	92	89	5	0	0	2
Rv 3	---	---	---	-27.54	---	---	---	---	---	---	---	---	---	---	---	---	---	---
Rv 2	---	---	---	-25.07	---	---	---	---	---	---	---	---	---	---	---	---	---	---
Rv 1	---	---	---	-25.91	---	---	---	---	---	---	---	---	---	---	---	---	---	---
R10	0.6	0.6	42	-26.02	54	31	63	4	1	36	6	6	94	71	6	12	6	4
R9	2.9	3.6	27	-31.47	2	20	80	0	0	83	6	5	95	95	0	0	0	9
R8	1.1	3.5	23	-29.88	24	30	58	10	1	62	7	13	87	95	0	5	0	7
R7	0.4	0.7	41	-23.73	80	33	64	2	1	10	8	16	84	68	8	0	8	2
R6	0.5	1.1	43	-24.21	72	31	66	0	2	17	7	0	100	91	4	0	4	4
R5	0.7	2.5	20	-24.97	65	27	63	0	10	27	5	0	100	100	0	0	0	3
R4	0.9	0.9	50	-24.07	62	14	41	0	45	27	7	18	82	90	0	0	0	4
R3	1.1	0.6	57	-25.95	55	43	32	0	25	31	9	4	96	96	0	0	0	5
R2	0.8	0.6	56	-24.36	70	26	36	0	38	13	3	10	90	100	0	0	0	14
R1	1.0	0.7	47	-23.99	91	36	61	0	3	5	3	0	100	100	0	0	0	1

* Data published by Rodrigues et al. (2015); Carb – carbonate content; OP – opaque; NOP – non-opaque; Cut – cuticle; Memb – membrane; Palynom. – Palynomorphs; Mar – marine; Terrest – terrestrial; Sp – sporomorph; Tet – tetrad; Agg – agglomerate; Botryo. – *Botryococcus* sp ; Zig. – Zygospores of *zygnemataceae*; Zoo. – Zooclasts; [1]– recalculated to 100%; [2] – total marine microplankton (dinoflagellate cysts, acritarchs and prasinophyte algae) and zoomorphs (foraminiferal test-linings); [3] – total terrestrial palynomorphs (sporomorphs, tetrads, agglomerates, b*otryococcus* sp. and zygospores of *zygnemataceae*); Zoo – zooclasts (remains of animal-derived organic particles).

V.5. Discussion

V.5.1. The organic matter preservation during the Pliensbachian–Early Toarcian in northern Spain

As aforementioned, the succession of the Asturian Basin has an average TOC of 0.8 wt.%, reaching up to 2.9 wt.% at the topmost of Tenuicostatum–base of Serpentinum zones (Fig. V.3 and Table V.1) (see Rodrigues et al., 2015). This is compatible with the observed in the Basque-Cantabrian Basin, considered as one of the most prospective sedimentary basins in Spain. Here, organic-rich intervals are located in the Pliensbachian–Early Toarcian interval (see Quesada et al., 1997, 2005; Rosales et al., 2006; Beroiz and Permanyer, 2011). Although this discussion is not the goal of this work, during the Pliensbachian, differential subsidence generated swells and intra-platform troughs, restricting circulation resulted in OM-rich deposition in northern Spain (see Valenzuela et al., 1989; Quesada et al., 1997, 2005; Rosales et al., 2006; García-Ramos and Piñuela, 2010). The occurrence of OM-rich units in the Asturian and Basque-Cantabrian basins is confirmed by several authors (maximum TOC values of 8 and 8.7 wt.%, respectively; e.g. Borrego et al., 1996; Herrero, 1998; Quesada et al., 1997, 2005; Perilli and Comas-Rengifo, 2002; Rosales et al. 2006; Bádenas et al., 2009; Comas-Rengifo and Goy, 2010), and also observed in the Lusitanian Basin (reaching up to 26 %; see Duarte et al., 2010, 2012; Silva et al., 2011, 2015).

Regarding the Early Toarcian interval, the TOC data obtained in this study, intercepted with TOC published data allows to construct a detailed view of Iberian and northern African TOC distribution for the latest Pliensbachian–Early Toarcian time interval, divided into the following intervals: i) Pre-TOAE [uppermost Spinatum (Fig. V.5A) and Tenuicostatum (Fig. IV.5B) zones with the relatively low TOC content, until the last sample before the increase in TOC values), ii) TOAE [between the extinction boundary from Gómez and Goy (2011) and base of Serpentinum Zone (until the last wood sample), matching with the samples with relatively high TOC content] and iii) Post-TOAE.

Overall, it is notorious the contrast between the OM deposition occurred during the latest Pliensbachian–Early Toarcian in the northern Spain (Asturian and Basque–Cantabrian basins), other Iberian (Iberian range, Lusitanian and Betic Cordillera) and northern African (High, Middle and the Saharan Atlas) locations (Fig. V.5; e.g. Hesselbo et al., 2007; Bodin et al., 2010, Gómez and Goy, 2011; Reolid et al., 2012; Rodríguez-Tovar and Reolid, 2013; Rodrigues et al., 2016, 2019, 2020; Danise et al., 2019; Fantasia et al., 2019; Ruebsam et al., 2020b and Chapter IV).

During the Pre-TOAE interval, the Rodiles (Asturian Basin), Tudanca, San Andres (Basque–Cantabrian Basin), and La Almunia (northern Iberian Range) sections recorded several stratigraphic levels with newsworthy TOC content, reaching up ~1.5 wt.% (Figs. V.5A, V.5B). The

Sierra Palomera section, contrasting with previous work (see Gómez and Arias, 2010), presented enrichment in OM, where TOC contents reach up 4.4 wt.% in the Tenuicostatum Zone (IV5B; see Danise et al., 2019). Most of the uppermost Pliensbachian–lowermost Toarcian deposits in the Iberian Range, western and southern Iberian, and northern African sections presented bioturbated facies, with generally well-diversified benthic fauna and TOC values below 1 wt.% (Figs. V.5A, V.5B; see also Gómez and Goy, 2011; Reolid et al., 2018; Duarte et al., 2018a, 2018b), supporting the presence of oxygenated depositional environments.

During the TOAE, TOC values recorded in Rodiles are concordant with the contemporaneous series from the Basque–Cantabrian (Tudanca and San Andrés sections; Fig. V.5C) and others southern Europe sections such in the Valdorbia (Italy) and Monte Mangart (Italian–Slovenian border), with TOC typically between 1–3 wt.% (Jenkyns, 1988; Quesada et al., 1997; Jenkyns et al., 2002; Sabatino et al., 2009; Gómez and Goy, 2011; García-Joral et al., 2011). In the Castrovido section (northern Iberian Range), an increase in TOC is observed at the base of Serpentinum Zone, reaching up ~2.6 wt.% and the Sierra Palomera section recorded TOC values (reaching up ~3.7 wt.%; see Danise et al., 2019). Castrovido is located relatively near to northern Spain and the TOC values fit into the enrichment in OM general pattern. However, the TOC values obtained by Danise et al. (2019) for Sierra Palomera are completely different from previously reported by Gómez and Arias (2010). Gómez and Goy (2011) compared TOC data between northern and central Spanish sections and the highest TOC value recorded in central Spain (Iberian Range) was in the La Almunia section (~0.7 wt.%; Fig. V.5C). Therefore and given the low resolution presented in Gómez and Goy (2011), there is no certainty about the TOC values of Sierra Palomera.

Another interesting observation in this interval is related to the high TOC values recorded in a discrete level of Peniche (Lusitanian Basin; see also Hesselbo et al., 2007; Fantasia et al., 2019 and Chapter IV) and in one sample of the Amellago section (High Atlas Basin; see Bodin et al., 2010) (Fig. V.5C). These elevated TOC values contrast with the general trend TOAE trend in the Lusitanian, Betic Cordillera, High and Saharan Atlas basins (Fig. V.5C), where TOC is generally below 1 wt.% (e.g., Hesselbo et al., 2007; Bodin et al., 2010; Rodrigues et al. 2016, 2019; Fantasia et al., 2019; Ruebsam et al., 2020b and Chapter IV), likely signalling a brief episode of OM preservation promoted by dysoxic conditions.

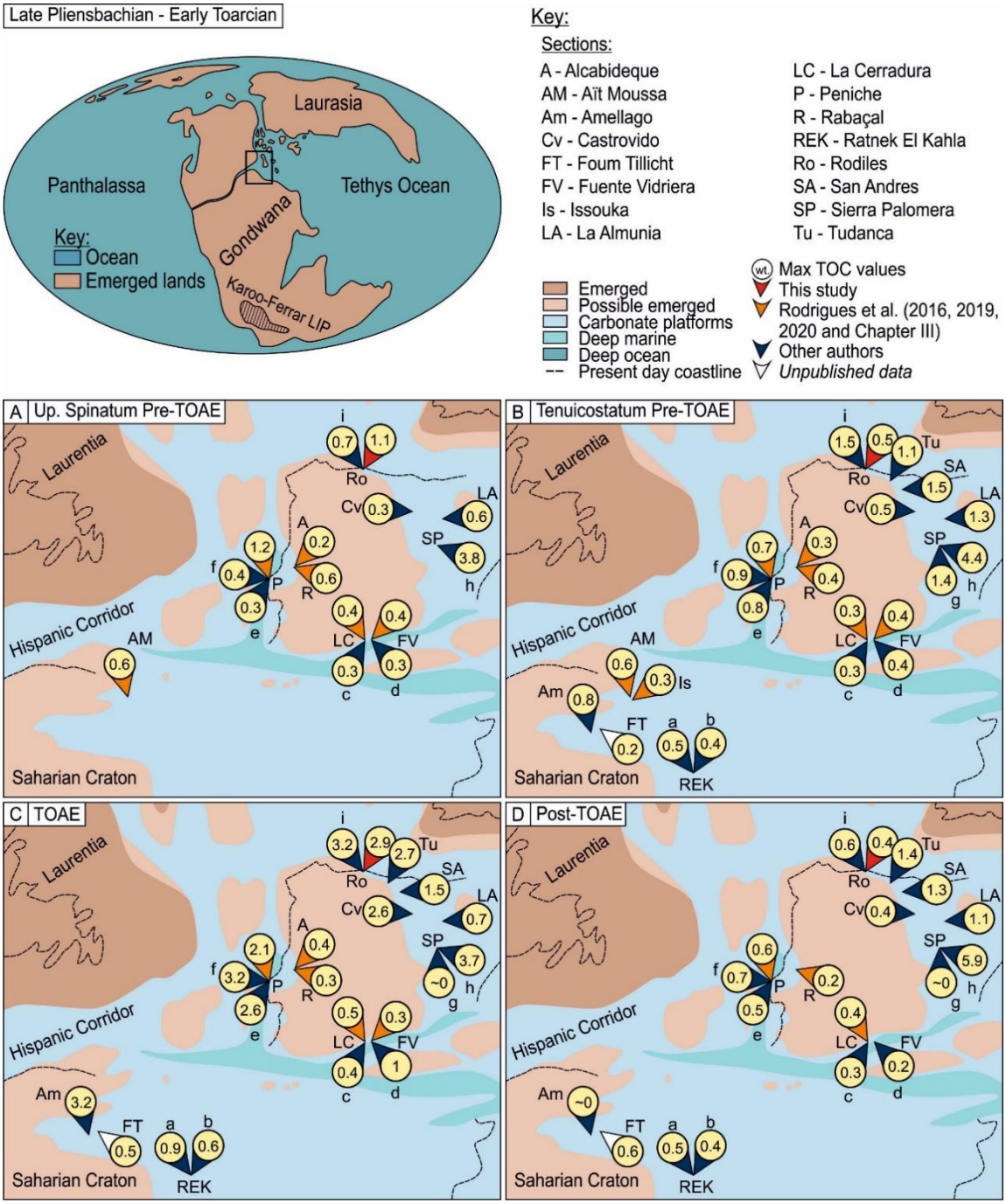

Figure V.5. Palaeogeographic map of the western Tethys during the Late Pliensbachian – Early Toarcian interval (Bassoulet et al., 1993; Thierry and Barrier, 2000) and palaeolocation of the sections in Asturian, Basque–Cantabrian, Lusitanian, Betic Cordillera, Middle, High, and Saharan Atlas basins. The black rectangle shows the limit of the detailed view of Iberian and northern Africa TOC distribution for the uppermost Pliensbachian–Lower Toarcian time interval. **A**. Uppermost Spinatum Pre-TOAE; **B**. Tenuicostatum Pre-TOAE; **C**. TOAE and **D**. Post-TOAE. Highest TOC values from Hesselbo et al. (2007) (e), Gómez et al. (2008) (i), Gómez and Arias (2010) (g), Gómez and Goy (2011), Reolid et al. [2012 (a), 2014 (c)], Rodríguez-Tovar and Reolid (2013) (d), Rodrigues et al. (2016, 2019, 2020), Danise et al. (2019) (h), Fantasia et al. (2019) (f), Ruebsam et al. (2020b) (b) and Chapter IV.

Even so, the TOC values recorded in northern Iberia during the TOAE are relatively low when compared with those recorded in several central and northern Europe basins, with TOC ranging between 5 and 15 wt.% (e.g. Baudin et al., 1990; Röhl et al., 2001; Suan et al., 2011; 2015, 2018; Ruebsam et al., 2018; Fantasia et al., 2018a; Fonseca et al., 2018). OM-rich sediments are particularly expressive across the central and northern Europe areas, probably associated with prolonged anoxic (and euxinic) conditions (e.g. Schouten et al., 2000; Schmid-Röhl et al., 2002; Schwark and Frimmel, 2004; van Breugel et al., 2006; French et al., 2014; Ruebsam et al., 2018).

After the TOAE, TOC contents in Iberian and northern African sections return to the Pre-TOAE pattern (with sparse TOC peaks observed in the Sierra Palomera section; see Danise et al., 2019) (Fig. V.5D). The decrease in TOC values and documented biotic recovery (Gómez et al., 2008; Gómez and Goy, 2011; Reolid et al., 2012; Rodríguez-Tovar and Reolid, 2013; Danise et al., 2019; Ruebsam et al., 2020b) are associated with the re-establishment of depositional conditions observed before the TOAE.

V.5.2. $\delta^{13}C_{Kerogen}$ record and the kerogen assemblages evolution

The Phytoclast Group mostly dominates the Rodiles section with several levels showing an increase in AOM and the marginal occurrence of terrestrial and marine palynomorphs (Fig. V.6). The dominance of phytoclasts is comparable to those reported in western and southern Iberian (Rodrigues et al., 2016, 2019; Baker et al., 2017; Fantasia et al., 2019 and Chapter IV), and Morocco basins (e.g. Bodin et al., 2016; Rodrigues et al., 2020). The mature nature of the studied section (vitrinite reflectance values of 1.1% R_o and Tmax values between 444 and 454°C; see Rodrigues et al., 2015; Deconinck et al., 2020) is attested by the corroded nature of many phytoclasts (Fig. V.4B). Despite the relatively elevated thermal maturity of the studied section, the NOP particles present a slight dominance in the Phytoclast Group (average of ~55%) instead of the OP dominance observed in the other western and southern Iberian basins (see Rodrigues et al., 2016, 2019 and Chapter IV). The higher abundances in NOP in the Asturian Basin likely reflects increased delivery of NOP from rivers (Tyson, 1995 and references therein) and/or decreased contribution of OP from emerged areas due to generally slightly wetter conditions (e.g. Lamberson et al., 1996; Baker et al., 2017; Rodrigues et al., 2019). During the studied interval, the Asturian Basin was in the winter-wet climatic belt (Fig. V.7; see Rees et al., 2000; Dera et al., 2009), supporting increased rainfall and availability of NOP to be exported into the marine system.

Compared with the Lusitanian Basin, the Rodiles section presented a fewer kerogen assemblage variation (see Chapter IV). Even so, the presence of certain organic particles and the variation $\delta^{13}C_{Kerogen}$ values allows an approximation to the previously defined intervals (see section V.5.1).

V.5.2.1. Pre-TOAE

The Early Toarcian negative CIEs correspond to the Pliensbachian–Toarcian Event (Pl–Toa Event; e.g. Littler et al., 2010) and TOAE (Hesselbo et al., 2007; Jenkyns, 2010). Between the negative CIEs, several positive tendencies are observed and appearing to be quite consistent across the Tethyan, Boreal and Pantalassic basins (see, for example, Jenkyns et al., 2002; Hermoso et al., 2013; Ruebsam and Al-Husseini, 2020).

The obtained $\delta^{13}C_{Kerogen}$ data show a positive $\delta^{13}C$ trend in the Spinatum Zone (average of -24.6‰) which can be correlated the Middle Atlas (average -24.3‰; see Chapter VI), Betic Cordillera (average -22.1‰; Rodrigues et al., 2019) and Lusitanian (-22.8‰; see Chapter IV) basins. The presence of small amounts of marine AOM in the Asturias and Middle Atlas basins can partially explain the decrease in $\delta^{13}C_{Kerogen}$ values, corroborating Suan et al. (2015), suggesting that the $\delta^{13}C$ signal is the reflection of the proportions of terrestrial and marine OM.

The increase in marine microplankton such acritarchs and dinoflagellate cysts observed in the uppermost Spinatum Zone (between samples R3-R4) fits with previous observations from the Middle Atlas (Rodrigues et al., 2020), Betic Cordillera (Rodrigues et al., 2019) and Lusitanian (Rodrigues et al., 2016; Correia et al., 2017a, 2017b and Chapter IV) basins. The Spinatum Zone is widely regarded as a dinoflagellate radiation interval (e.g. Slater et al., 2019; van de Schootbrugge et al., 2019), probably triggered by cooling and incursion of more saline waters during the Late Pliensbachian (e.g. van de Schootbrugge et al., 2005, 2019). Cooling conditions during the Spinatum Zone is supported by oxygen isotopic data from bulk carbonate ($\delta^{18}O_{Carb}$) and belemnite ($\delta^{18}O_{Bel}$) in the Asturian Basin (e.g. Gómez et al., 2008, 2016; Gómez and Goy, 2011).

Despite the low resolution of our study (probably cause for non-identification of the Pl–Toa Event), the $\delta^{13}C_{Kerogen}$ data presented a more positive trend (average of ~ -24‰) during the Tenuicostatum Zone and fits with $\delta^{13}C_{Bel}$ and $\delta^{13}C_{Carb}$ data from Rodiles. Comparing with $\delta^{13}C_{Wood}$, $\delta^{13}C_{Org}$, and $\delta^{13}C_{Kerogen}$ records from the western and southern Iberian (see Hesselbo et al., 2007; Fantasia et al., 2019; Rodrigues et al. 2019; Ruebsam et al., 2020a and Chapter IV) and northern African basins [Middle Atlas average ~ -22.8‰ (see Chapter VI), High and Saharan Atlas basins (see Bodin et al., 2016; Ruebsam et al., 2020b)], the Asturias basin presented a slightly more negative $\delta^{13}C_{Kerogen}$ values. The more negative $\delta^{13}C_{Kerogen}$ values from this study are interpreted to reflect increased ^{13}C fractionation during photosynthesis in C3 plants related to higher water availability (see also Rodrigues et al., 2019; Ruebsam et al., 2020a) in the winter-wet climatic conditions observed in Asturian Basin (Fig. V.7; see Rees et al., 2000; Dera et al., 2009).

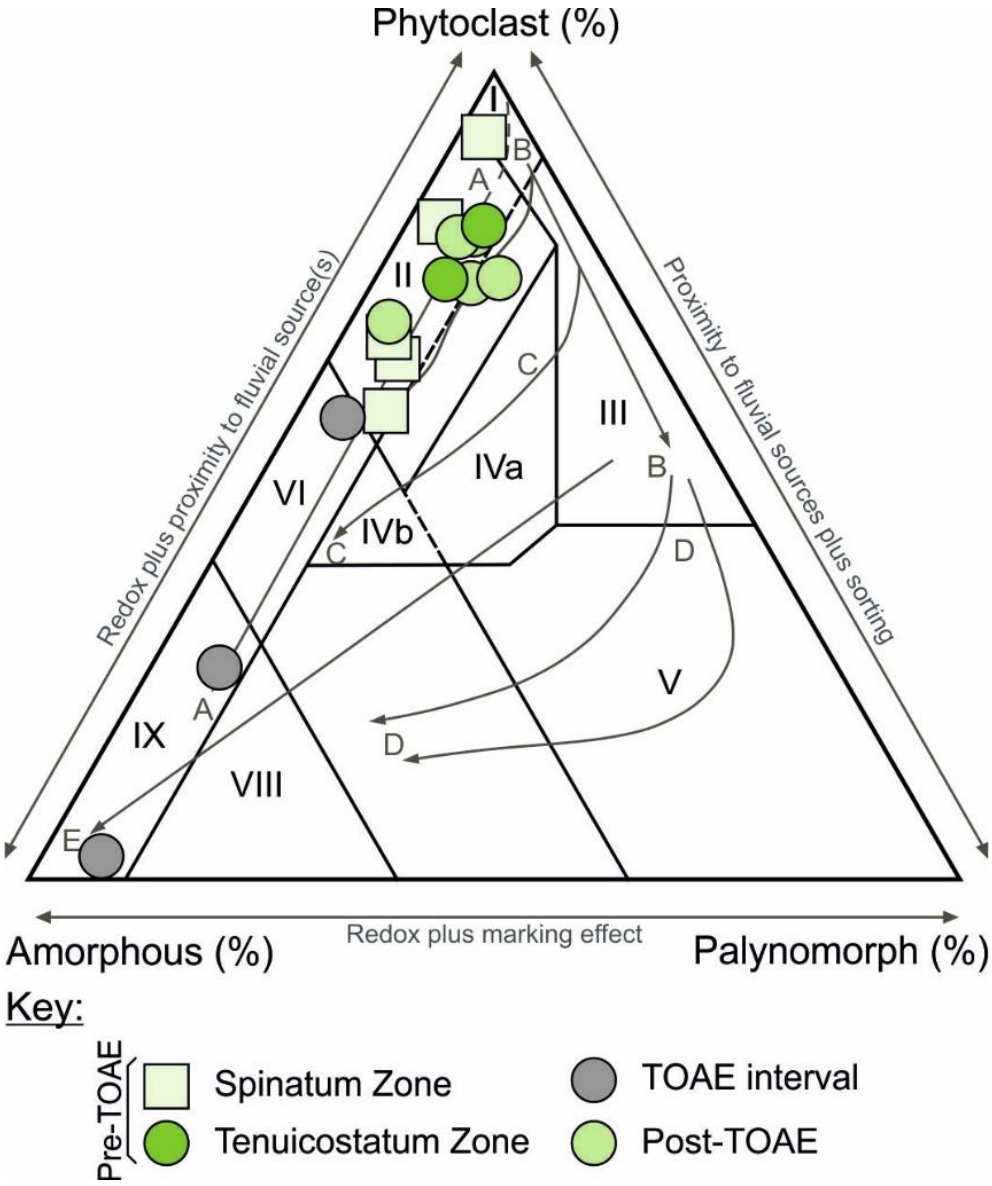

Figure V.6. Ternary kerogen and palynofacies plots for marine series (Tyson, 1995) based on the relative abundance of Phytoclast, Amorphous, and Palynomorph Groups according to the main intervals from Rodiles section, Asturian Basin (northern Spain). Palynofacies and environmental fields: (I) highly proximal shelf or basin, (II) marginal dysoxic-anoxic basin, (III) heterolithic oxic shelf (proximal shelf), (IV) shelf to basin transition, (V) mud-dominated oxic shelf (distal shelf), (VI) proximal suboxic-anoxic shelf, (VII) distal dysoxic-anoxic shelf, (VIII) distal dysoxic-oxic shelf and (IX) distal suboxic-anoxic basin. Transport paths: (A) direct path from source to anoxic basin, (B) Phytoclasts move away from the source out across shallow-marine shelf, (C) redirection of phytoclasts into the basin from route B, (D) continuation of route B with further reduction in phytoplankton organic carbon values and progressive sorting of phytoclasts and palynomorphs and (E) poorly defined shelf to basin pathway.

V.5.2.2. TOAE

The positive trend is interrupted by an abrupt negative CIE of ~ 6‰ in $\delta^{13}C_{Kerogen}$, recorded around the topmost of Tenuicostatum Zone, reaching up ~ 8‰ at the base of Serpentinum Zone. Furthermore, the change to higher $\delta^{13}C_{Kerogen}$ values recorded in the marly and wood samples after the negative CIE is also abrupt (shift of ~5.3‰; Fig. V.3) and probably reflects the return to heavier $\delta^{13}C$ values above the negative CIE. Despite the coarse resolution, the obtained negative CIE is shorter (~ 1m) than the observed in other TOAE sites (e.g. Cohen et al., 2004; Kemp et al., 2005; Hesselbo et al., 2007; Sabatino et al., 2009, Suan et al., 2018; Ruebsam and Al-Husseini, 2020), and the abrupt negative CIE and subsequent change to higher $\delta^{13}C$ values are similar to that reported in Valdorbia, Monte Mangart (Italy and Italian–Slovenian border; Sabatino et al., 2009), Yakoun River and Bighorn Creek (Canadá; Caruthers et al., 2011; Them II et al., 2017), Bächental (Austria; Neumeister et al., 2015), Zázrivá (Slovakia; Suan et al., 2018) and sediment core FR-210-078 (southern Luxembourg; Ruebsam et al., 2019). Nevertheless, these shifts appear far more gradual in other TOAE sites (see also Fig. V.7; e.g. Cohen et al., 2004; Kemp et al., 2005; Hesselbo et al., 2007; Suan et al., 2015; Ruebsam and Al-Husseini, 2020). The negative CIE features recorded in Rodiles, probably reflect a low sedimentation rate instead of rapid changes in the carbon cycle.

The negative CIE is also recorded in $\delta^{13}C_{Carb}$ (shift of 1.5‰; see Gómez et al., 2008) and is coeval with an extinction interval [extinction boundary from Gómez and Goy (2011) corresponding to the disappearance of brachiopods; see García Joral et al., 2011] and enrichment of AOM (Figs. V.3 and V.7). The elevated marine AOM proportions are comparable to those reported from coeval TOAE black shale levels in the UK (Slater et al., 2019), SW Germany (Mädler, 1968), SW France (Fonseca et al., 2018), Switzerland (Gorin and Feist-Burkhardt, 1990), central Italy (Palliani et al., 1998), Hungary (Baranyi et al., 2016) and Slovakia (Suan et al., 2018). Alternatively, the Lusitanian Basin (excluding a discrete level of Serpentinum Zone in Peniche section) and Betic Cordillera are dominated by phytoclasts and terrestrial palynomorphs (terrestrial OM; see Rodrigues et al., 2016, 2019 and Chapter IV) (see Fig. V.7).

The increase in TOC, TS and marine AOM content in the Asturian Basin suggests oxygen deficiency conditions (e.g. Emeis et al., 1991; Tyson and Pearson, 1991; Tyson, 1995), further substantiated by the occurrence of prasinophytes algae (Fig. V.4K) (generally regarded as an indicator of anoxia/suboxic conditions in AOM-rich intervals; see Tyson, 1995 and references therein) and the presence of foraminiferal test-linings in the sample R9 (Fig. V.4L), suggests that the conditions were probably suboxic (see Tyson, 1995).

Two main hypotheses are proposed to explain the geochemical and biological changes associated with the TOAE, (1) increased greenhouse effect (slightly lower atmospheric oxygen; e.g. Hesselbo et al., 2000; Jenkyns, 2003) and (2) increase in marine productivity typically associated with restricted basins (e.g. Küspert, 1982; Röhl et al., 2001; Schmid-Röhl et al., 2002; Frimmel et al., 2004; van de Schootbrugge et al., 2005; McArthur et al., 2008). McArthur et al. (2008) proposed that the development of organic-rich facies in several restricted shallow basins in

the northwestern Tethyan margin, during the TOAE, is related to the warmer and wetter climate. This climatic feature led to an intensification of the hydrological cycle, enhanced continental weathering and increased fluvial runoff and riverine OM and nutrient input into marine areas. This would lead to an increase in primary productivity, and the influx of freshwater probably induced a water column stratification promoting anoxia and preservation of the OM (Röhl et al., 2001; Röhl and Schmid-Röhl, 2005; van de Schootbrugge et al., 2005; McArthur et al., 2008). The presence of abundant particles belonging to the NOP subgroup and Palynomorph Group (mainly pollen grains occurring in tetrads and agglomerates) in Rodiles section at the topmost of Tenuicostatum–base of Serpentinum zones (between samples R8 – R10; Fig. V.3 and Table V.1) are consistent with a slight increase in continental weathering and fluvial runoff and fits the overall TOAE model that favours the deposition and preservation of marine AOM.

V.5.2.3. Post-TOAE

Above the TOAE interval, during the Serpentinum Zone, the $\delta^{13}C_{Kerogen}$ record returns to more positive values (similar to the $\delta^{13}C_{Kerogen}$ recorded during the pre-TOAE interval). These preferentially heavy $\delta^{13}C$ values are also expressed in the $\delta^{13}C_{Wood}$, $\delta^{13}C_{Org}$, and $\delta^{13}C_{Kerogen}$ records from Cleveland, southern German, Iberian, and northern African basins (e.g. Cohen et al., 2004; Kemp et al., 2005; Hesselbo et al., 2007; Suan et al., 2015; Bodin et al., 2016; Fantasia et al., 2019; Rodrigues et al. 2019; Ruebsam et al., 2020a, 2020b; Ruebsam and Al-Husseini, 2020). Concomitantly, it is observed as a drastic drop in TOC, TS and AOM content (Figs. V.3 and V.7). These features and the presence of NOP particles suggested the maintenance of similar climatic patterns as the pre-TOAE interval (Figs. V.3) with the improvement of bottom-water oxygenation. The $\delta^{18}O_{Bel}$ record supported this theory suggesting that the warming episode remained after the TOAE (see also Gómez et al., 2008, 2016).

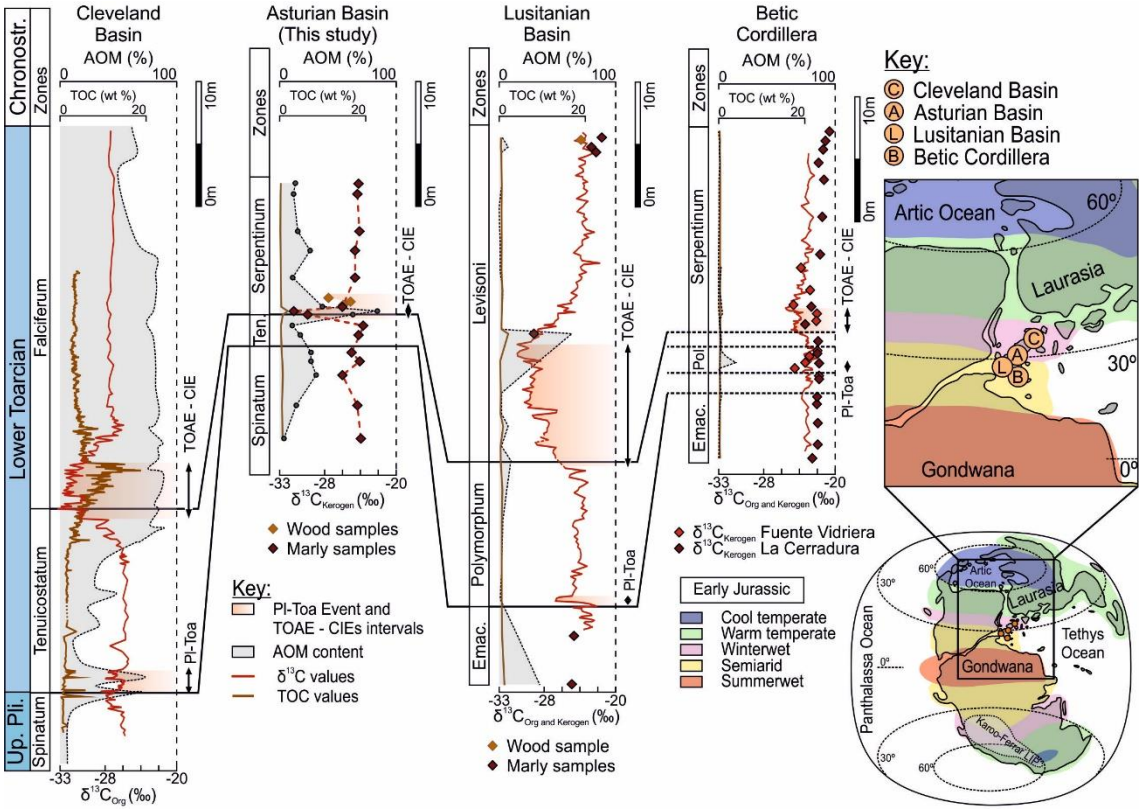

Figure V.7. Correlation between TOC, AOM content and $\delta^{13}C$ records of the uppermost Pliensbachian – Lower Toarcian from Cleveland, Asturian, Lusitanian, and Betic Cordillera Basins. TOC, AOM content, $\delta^{13}C_{Org,}$ and $\delta^{13}C_{Kerogen}$ records, Pl–Toa Event and TOAE negative CIE limits of Cleveland, Lusitanian, and Betic Cordillera basins are from Cohen et al. (2004), Kemp et al. (2005), Hesselbo et al. (2007), Rodrigues et al. (2019), Slater et al. (2019), Ruebsam et al. (2020a) and Chapter IV. Global map with palaeolocation of Cleveland, Asturian, Lusitanian, Betic Cordillera basins and Early Jurassic palaeoclimatic belts modified from Rees et al. (2000) and Dera et al. (2009); Localities: C – Yorkshire (Cleveland Basin); A – Rodiles (Asturian Basin; this study); L – Peniche (Lusitanian Basin); B – La Cerradura and Fuente Vidriera (Betic Cordillera). Up. Pli. – Upper Pliensbachian; Ten. – Tenuicostatum; Emac. – Emaciatum; Poly. – Polymorphum.

V.6. Conclusions

The re-evaluation and expansion of the palynofacies data with the integration of geochemical analysis from the uppermost Pliensbachian–Lower Toarcian marine successions of Rodiles (Asturian Basin, northern Spain) allow for the following conclusions:

- The studied succession is mature and has relatively high TOC values, reaching up to 2.9 wt.%. Phytoclast Group dominates the kerogen assemblages with a drastic change at the topmost of Tenuicostatum–base of Serpentinum zones with the increase in AOM content.

- The relative dominance in NOP particles and relatively more negative $\delta^{13}C_{Kerogen}$ values during the studied interval, suggests a dominantly winter-wet climate in the northern Iberian margin.

- The TOAE interval is marked by a short and abrupt negative CIE in $\delta^{13}C_{Kerogen}$, associated with the highest TOC, TS and AOM contents at the base of Serpentinum Zone. These features suggest a low sedimentation rate, with the deposition and preservation of OM occurring probably under suboxic conditions. The occurrence of NOP and terrestrial palynomorphs in this interval is interpreted to represent a slight increase in continental weathering and fluvial runoff associated with slightly lower atmospheric oxygen and wetter conditions.

- Above the TOAE interval, the $\delta^{13}C_{Kerogen}$ record and the drastic drop in TOC and AOM content indicate that bottom water oxygenation improved after the TOAE, however with the maintenance of the warming episode.

VI. Final remarks

This doctoral thesis is a contribution to the knowledge of the uppermost Pliensbachian–Lower Toarcian TOC, palynofacies, and $\delta^{13}C_{Kerogen}$ record from the Central (northern Gondwana margin) and part of Northern Atlantic (Iberian Massif) basins. In this study, selected samples from several reference sections from the Middle Atlas (Morocco), Betic Cordillera (southern Spain), Lusitanian (western Portugal) and Asturian (northern Spain) basins, were studied in detail and discussed in the four main chapters of this thesis; two of which are published in international peer-reviewed journals (chapters II and III) and, at the date of submission of this thesis, chapter IV was submitted. From these four main chapters (see also their partial conclusions), general conclusions and considerations regarding future studies are presented below:

VI.1. General conclusions

From the obtained TOC data, gathered with previously published TOC datasets, it is notorious that deposition and preservation of OM in northern Africa, western and southern Iberian sections are spatially and temporally restricted, with low TOC content (generally below 1 wt.%; Fig. VI.1A) and suggesting the lack of persistent anoxia, probably favoured by local physiography and vigorous circulation. In the northern Iberian Rodiles section, the TOAE organic-rich interval reaches up 2.9 wt.%. Even so, the TOC values recorded in the Asturian Basin are relatively low when compared with those recorded during the Early Toarcian in the central and northern European epicontinental basins, with TOC generally between 5 and 15 wt%.

Although the $\delta^{13}C_{Kerogen}$ depends on the composition of the individual components of kerogen assemblages, the obtained $\delta^{13}C_{Kerogen}$ profiles in this study present similarities with the high-resolution $\delta^{13}C_{Wood}$ and $\delta^{13}C_{Org}$ records previously published from the western and southern Iberian sections (Fig. VI.2) and allows to establish a correspondence with the $\delta^{13}C_{Kerogen}$ values obtained in the Middle Atlas and Asturian basins. Even with small differences between the studied sections, the $\delta^{13}C_{Kerogen}$ record presents a positive trend during the Emaciatum/Spinatum Zone and the coarse-resolution around the base of Polymorphum/Tenuiscostatum Zone does not allow the full recognition of the Pl–Toa Event small negative CIE observed in more complete and detailed $\delta^{13}C$ data. A positive trend is observed across the Polymorphum/Tenuicostatum Zone, followed by the negative trend associated with the TOAE. The $\delta^{13}C_{Kerogen}$ negative trend presents an amplitude offset between the studied sections, suggesting that superimposed local and/or regional environmental processes may also have influenced the $\delta^{13}C_{Kerogen}$ record. The return to heavier $\delta^{13}C_{Kerogen}$ values above the negative trend seems more abrupt in the Rodiles and appears far more gradual in other studied sections (Fig. VI.2).

The $\delta^{13}C_{Kerogen}$ data combined with palynofacies analysis is a powerful tool for palaeoenvironmental research, with implications to the understanding of oceanic productivity and OM accumulation and preservation. The Phytoclast Group dominates the kerogen assemblages from the studied sections (Fig. VI.1B), indicating that sedimentary OM is mostly of terrestrial affinity. Nonetheless, several levels are punctuated by increases in marine (dinoflagellate cysts, acritarchs, and prasinophyte algae) and freshwater (mainly *Botryococcus* sp.) microplankton and AOM particles (Fig. VI.1B).

The increase in acritarchs and dinoflagellate cysts (*Nannoceratopsis* sp. and *Luehndea spinosa*) in the uppermost Emaciatum/Spinatum Zone in the studied basins fits with a previously observed dinoflagellate radiation interval, probably linked to increased nutrient levels and triggered by cooling and incursion of more saline waters during the Late Pliensbachian. The obtained $\delta^{13}C_{Kerogen}$ data presented a positive trend, however, with a slight decrease in $\delta^{13}C_{Kerogen}$ values in Asturian and Middle Atlas basins. This difference can partially be explained by the presence of small amounts of marine AOM (Figs. VI.1B and VI.2).

At the base of Polymorphum/Tenuicostatum Zone, and connected with the Pl–Toa Event, warmer and more humid climates results in increased delivery of non-opaque phytoclasts (NOP) and terrestrial palynomorphs in the Middle Atlas, Betic Cordillera, and Lusitanian Basin. In the Middle Atlas is also observed an increase in *Botryococcus* sp. particles during the earliest Polymorphum/Tenuicostatum Zone. This evidence is consistent with a slight increase in continental weathering and fluvial runoff.

Phytoclast particles are not usually used for palaeoclimate interpretations. However, it is suggested here that the higher NOP abundances at the base of the Polymorphum/Tenuicostatum Zone likely reflect increased delivery of NOP from rivers and/or decreased contribution of opaque phytoclasts (OP) from emerged areas due to generally slightly wetter conditions. The higher abundances of NOP recorded in the Middle Atlas probably reflected the increase in the delivery of NOP from rivers, while the NOP recorded in Asturian Basin is probably the combination of the effect of increased delivery from rivers associated with the slightly wetter conditions experienced in the winter-wet climatic belt.

The major occurrence of OP particles and the more positive $\delta^{13}C_{Kerogen}$ values in the western and southern Iberian basins suggested that the OM was mostly sourced from an area characterised by a semi-arid or arid climate (Figs. VI.1 and VI.2) with low precipitation rates, resulting in the decreased ^{13}C fractionation during photosynthesis in C3 plants, particularly evident during the Polymorphum/Tenuicostatum Zone.

At the topmost of Polymorphum/Tenuicostatum Zone, a decrease in $\delta^{13}C_{Kerogen}$ values is observed in the Lusitanian and Asturian basins (Fig. VI.2). The kerogen assemblages present an increase in terrestrial palynomorphs and relative abundances of marine microplankton

(*Nannoceratopsis* spp.) in the Lusitanian Basin and are observed an increase in TOC and AOM in the Asturian Basin. Concomitantly, a slight increase in TOC and AOM content is recorded in the Betic Cordillera. It is proposed that the connection between the increase in marine microplankton and AOM particles with increased nutrient levels. Therefore, the kerogen assemblage in the Iberian margin suggests increased surface runoff accompanied by the export of nutrients into marine environments at the beginning of TOAE.

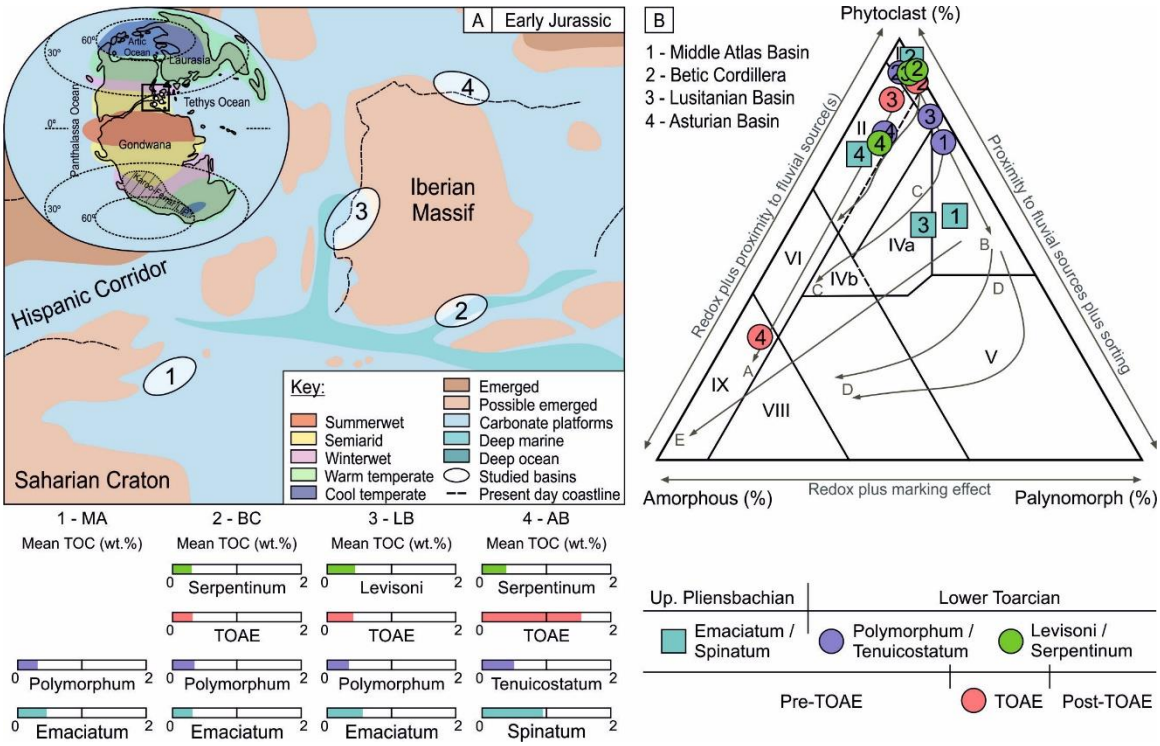

Figure VI.1. TOC and palynofacies variations across the studied interval in the Middle Atlas (1), Betic Cordillera (2), Lusitanian Basin (3); Asturian Basin (4). **A**. Palaeogeographic map of the western Tethys during the Early Jurassic (Bassoulet et al., 1993; Mattioli et al., 2008) with the mean TOC record; **B**. Ternary kerogen and palynofacies plots for marine series (Tyson, 1995) based on the average relative abundance of Phytoclast, Amorphous and Palynomorph Groups. (For interpretation of the palynofacies and environmental fields see figure caption of the ternary kerogen and palynofacies plots presented in chapters II, III, IV and V.

At the base of Levisoni/Serpentinum Zone, the Betic Cordillera, Lusitanian and Asturian basins recorded the TOAE $\delta^{13}C_{Kerogen}$ negative trend (Fig. VI.2) and the kerogen assemblages in the studied basins follow the carbon cycle disturbance. The Betic Cordillera and Lusitanian basins record an increase in NOP and cuticle fragments (particularly evident in the Peniche section), intercepted with the increase of terrestrial palynomorphs (sporomorphs, *Classopollis* sp., tetrads, and agglomerates) and decrease in marine palynomorphs. The Asturian Basin records an enrichment in AOM (with high TOC and TS content), an increase in NOP and terrestrial palynomorphs (mainly tetrads, and agglomerates). These features are interpreted to be the combined result of wetter conditions and slightly lower atmospheric oxygen concentrations leading

to an intensification of the hydrological cycle, enhanced continental weathering and increased fluvial runoff and riverine OM from emerged landmasses into marine areas.

However, and despite the similar terrestrial response of terrestrial components during the TOAE, it is confirmed that the oceanic areas including the western and southern Iberian basins were affected by vigorous circulation and, because of the position of these basins within the semi-arid to arid climate belt, acceleration of the hydrological cycle was less intense and with lower nutrient input when compared with northern Spain. Here, the enrichment in AOM probably reflected an increase in primary productivity caused by the increased continental weathering, fluvial runoff and riverine OM and nutrient input into marine areas. The influx of freshwater probably induced water column stratification promoting suboxic conditions and preservation of OM.

Therefore, the difference in magnitude of the TOAE $\delta^{13}C_{Kerogen}$ negative trend between the studied sections (Fig. VI.2) is probably the reflection of the presence of marine AOM and/or the relationship between the ^{13}C fractionation and water availability during photosynthesis in C3 plants.

The subsequent change to higher $\delta^{13}C$ values, the TOAE positive $\delta^{13}C$ trend, is more abrupt in the Asturian Basin (probably reflecting a low sedimentation rate) and more gradual in the western and southern Iberian sections (Fig. VI.2). Despite the initial stages of the TOAE $\delta^{13}C$ positive trend are associated with the highest TOC contents and an increase in AOM in the Lusitanian Basin (Peniche section), likely signalling a brief episode of OM preservation promoted by dysoxic conditions, it is suggested that after the carbon cycle perturbation the climates gradually cooled, favouring the return of the kerogen assemblage similar to the ones observed before the TOAE. The drastic drop in TOC, TS and AOM content in Asturian Basin and the return of the kerogen assemblage and $\delta^{13}C_{Kerogen}$ values in the other studied sections suggest the improvement of bottom-water oxygenation, conveyed with the gradual re-establishment of the depositional conditions.

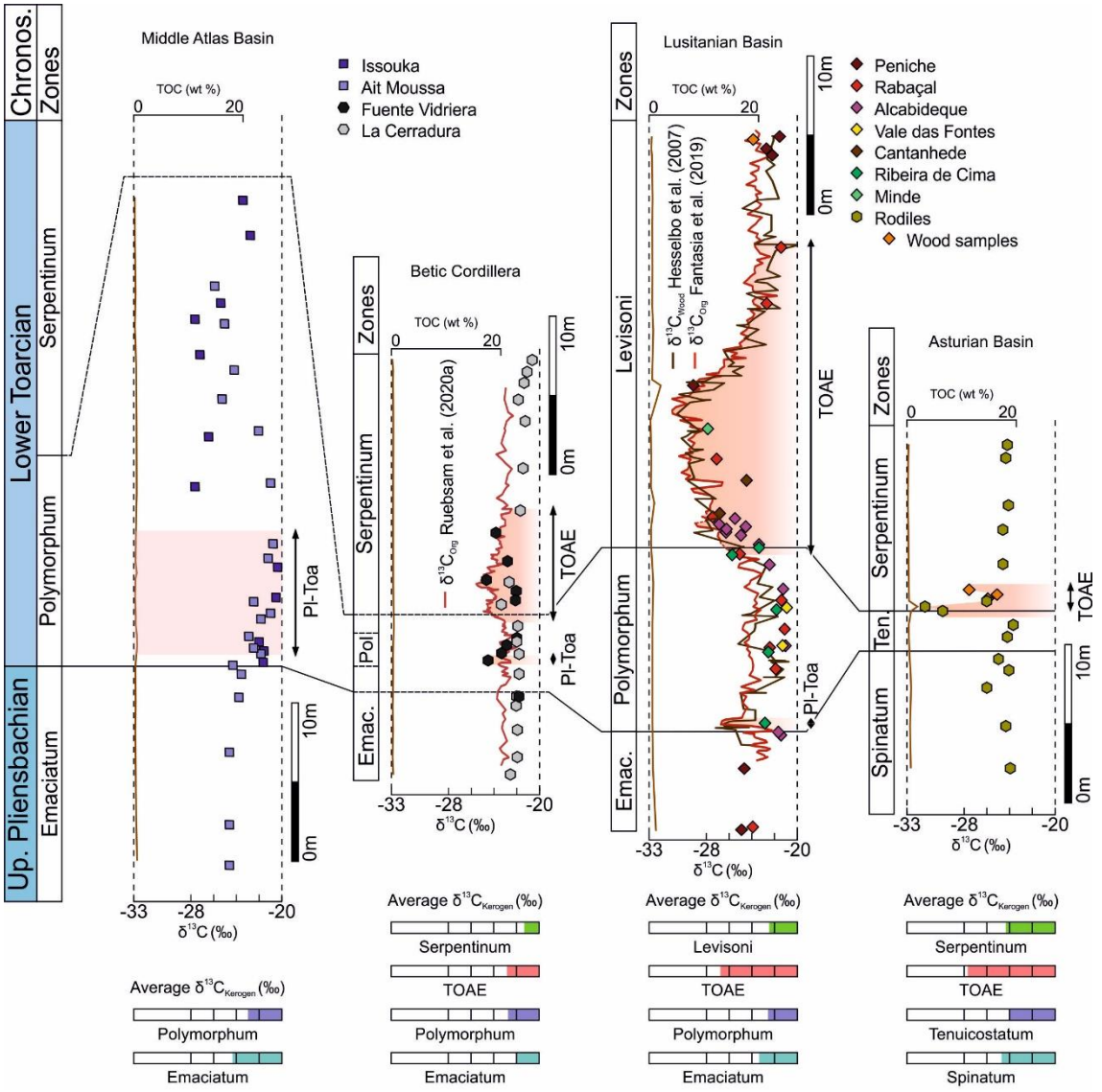

Figure VI.2. The average $\delta^{13}C_{Kerogen}$ data obtained in the studied basins and the comparison between $\delta^{13}C_{Org}$ and $\delta^{13}C_{Wood}$ curves from Betic Cordillera and Lusitanian basins and the $\delta^{13}C_{Kerogen}$ data. The $\delta^{13}C_{Org}$ and $\delta^{13}C_{Wood}$ curves, the Pl–Toa Event and TOAE intervals from Middle Atlas, Betic Cordillera, Lusitanian and Asturian basins are from Hesselbo et al. (2007), Ait-Itto et al. (2017), Fantasia et al. (2019) and Ruebsam et al. (2020a).

VI.2. Future perspectives

This doctoral work presents new evidences to better understand the OM inventory of each studied basin, suggesting that OM deposition and preservation were controlled by the interplay of local-regional constraints and global events. Nonetheless, further studies are needed to improve the knowledge and discussion of these subjects. Therefore is necessary:

- Perform a more detailed sampling campaign (about 1 sample per 5cm) from the uppermost Pliensbachian–Middle Toarcian in the Middle Atlas and Asturian sections, and determine the $\delta^{13}C_{Org}$;

- Perform a high-resolution $\delta^{13}C_{Kerogen}$ and $\delta^{13}C_{Org}$ study from a section with OM derived exclusively from terrestrial sources (preferentially in another climate belt) to observe the amplitude, "shape" differences and discrepancies between these two organic records;

- Reduce the distance between samples around the Pl–Toa Event and TOAE in the studied sections, allowing a better assessment of the vertical variation pattern in OM;

- Expand these findings to other northern Africa and Central Iberian sections.

References

AIT-ITTO, F., PRICE, G.D., AIT ADDI, A., CHAFIKI, D. and MANNANI, I. (2017). Bulk-carbonate and belemnite carbon-isotope records across the Pliensbachian–Toarcian boundary on the northern margin of Gondwana (Issouka, Middle Atlas, Morocco). *Palaeogeography, Palaeoclimatology, Palaeoecology* 466: 128-136. doi.org/10.1016/j.epsl.2018.04.007.

AIT-ITTO, F., MARTINEZ, M., PRICE, G.D. and AIT ADDI, A. (2018). Synchronization of the astronomical time scales in the Early Toarcian: a link between anoxia, carbon-cycle perturbation, mass extinction and volcanism. *Earth and Planetary Science Letters* 493: 1-11. doi.org/10.1016/j.epsl.2018.04.007.

AL-SUWAIDI, A.H., ANGELOZZI, G.N., BAUDIN, F., DAMBORENEA, S.E., HESSELBO, S.P., JENKYNS, H.C., MANCEÑIDO, M.O. and RICCARDI, A.C. (2010). First record of the Early Toarcian Oceanic Anoxic Event from the Southern Hemisphere, Neuquén Basin, Argentina. *Journal of the Geological Society* 167: 633-636. doi.org/10.1144/0016-76492010-025.

AL-SUWAIDI, A.H., HESSELBO, S.P., DAMBORENEA, S.E., MANCEÑIDO, M.O., JENKYNS, H.C., RICCARDI, A.C., ANGELOZZI, G.N. and BAUDIN, F. (2016). The Toarcian Oceanic Anoxic Event (Early Jurassic) in the Neuquén Basin, Argentina: A reassessment of age and carbon isotope stratigraphy. *The Journal of Geology* 124: 171-193. doi.org/10.1086/684831.

ALVES, T.M., GAWTHORPE, R.L., HUNT, D.W. and MONTEIRO, J.H. (2002). Jurassic tectono-sedimentary evolution of the northern Lusitanian Basin (offshore Portugal). *Marine and Petroleum Geology* 19: 727-754. doi.org/10.1016/S0264-8172(02)00036-3.

ASTM Standard D4239-08 (2008). Standard Test Methods for Sulfur in the Analysis Sample of Coal and Coke Using High-temperature Tube Furnace Combustion Methods. ASTM International, West Conshohocken, PA. doi.org/10.1520/D4239-12.

ASTM Standard D7708 (2014). Standard Test Method for Microscopical Determination of Reflectance of Vitrinite Dispersed in Sedimentary Rocks. ASTM International, West Conshohocken, PA. doi.org/10.1520/D7708-14.

AURELL, M., MELÉNDEZ, G. and BÁDENAS, B. (2002). East Iberian basins. In: Gibbons, W., Moreno, T. (Eds.), The Geology of Spain. Geological Society, pp. 223-229.

AZERÊDO, A.C., DUARTE, L.V., HENRIQUES, M.H. and MANUPPELLA, G. (2003). Da dinâmica continental no Triásico aos mares do Jurássico Inferior e Medio. Cadernos da Geologia de Portugal. Instituto Geologico e Mineiro, 43 pp..

AZERÊDO, A.C., SILVA, R.L., DUARTE L.V. and CABRAL, M.C. (2010). Subtidal stromatolites from the Sinemurian of the Lusitanian Basin (Portugal). *Facies* 56: 211-230.

AZERÊDO, A.C., DUARTE, L.V. and SILVA, R.L. (2014). Configuração sequencial em ciclos (2ª ordem) de facies transgressivas-regressivas do Jurássico Inferior e Médio da Bacia Lusitânica (Portugal). *Comunicações Geológicas* 101: 383-386.

BÁDENAS, B., AURELL, M., GARCÍA-RAMOS, J.C., GONZÁLEZ, B. and PIÑUELA, L. (2009). Sedimentary vs. diagenetic control on rhythmic calcareous successions (Pliensbachian of Asturias, Spain). *Terra Nova* 21: 162-170. doi.org/10.1111/j.1365-3121.2009.00869.x.

BAEZA-CARRATALÁ, F.J., REOLID, M. and GARCÍA JORAL, F. (2017). New Deep-water brachiopod resilient assemblage from the South-Iberian Palaeomargin (Western Tethys) and its significance for the brachiopod adaptative strategies around the Early Toarcian Mass Extinction Event. *Bulletin of Geosciences* 92: 233-256. doi.org/10.3140/bull.geosci.1631.

BAKER, S.J., HESSELBO, S.P., LENTON, T.M., DUARTE L.V. and BELCHER C.M. (2017). Charcoal evidence that rising atmospheric oxygen terminated Early Jurassic ocean anoxia. *Nature Communications* 8: 15018. doi:10.1038/ncomms15018.

BARANYI, V., PÁLFY, J., GÖRÖG, A., RIDING, J.B. and RAUCSIK, B. (2016). Multiphase response of palynomorphs to the Toarcian Oceanic Anoxic Event (Early Jurassic) in the Réka Valley section, Hungary. *Review of Palaeobotany and Palynology* 235: 51-70. doi.org/10.1016/j.revpalbo.2016.09.011.

BARONI, I.R., POHL, A., VAN HELMOND, N.G., PAPADOMANOLAKI, N.M., COE, A.L., COHEN, A.S., VAN DE SCHOOTBRUGGE, B., DONNADIEU, Y. and SLOMP, C.P. (2018). Ocean Circulation in the Toarcian (Early Jurassic): A Key Control on Deoxygenation and Carbon Burial on the European Shelf. *Paleoceanography and Paleoclimatology* 33: 994-1012. doi.org/10.1029/2018PA003394

BARTH, G., PIEÑKOWSKI, G., ZIMMERMANN, J., FRANZ, M. and KUHLMANN, G. (2018). Palaeogeographical evolution of the Lower Jurassic: high-resolution biostratigraphy and sequence stratigraphy in the Central European Basin. In: Kilhams, B., Kulka, P.A., Mazur, S., Mc Kie, T., Mijnlieff, H.F., van Ojik, K. (Eds.), Mesozoic Resource Potential in the Southern Permian Basin. Geological Society, London. Special Publications 469, pp. 341-369. doi.org/10.1144/SP469.8.

BASSOULET, J., ELMI, S., POISSON, F., CECCA, F., BELION, Y., GUIRAUD, R. and BAUDIN, F. (1993). Mid Toarcian. In: Dercourt, J., Ricou, L.E., Vrielynck, B. (Eds.), Atlas Tethys, Paleoenvironmental Maps. Becip–Franlab, Rueil–Malmaison, pp. 63-80.

BAUDIN, F., HERBIN, J.-P. and VANDENBROUCKE, M. (1990). Mapping and geochemical characterization of the Toarcian organic matter in the Mediterranean Tethys and Middle East. *Organic Geochemistry* 16: 677-687. doi.org/10.1016/0146-6380(90)90109-D.

BEJJAJI, Z., CHAKIRI, S., REOLID, M. and BOUTAKIOUT, M. (2010). Foraminiferal biostratigraphy of the Toarcian deposits (Lower Jurassic) from the Middle Atlas (Morocco). Comparison with western Tethyan areas. *Journal of African Earth Sciences* 57: 154-162. doi.org/10.1016/j.jafrearsci.2009.08.002.

BENSHILI K. (1989). Lias-Dogger du Moyen Atlas plissé (Maroc): sédimentologie, biostratigraphie et évolution paléogéographique. Documents des Laboratoires de Géologie Lyon 106, 1-285.

BENZAQUEN, M., HAMEL, C. and MEDIONI, R. (1965). Étude stratigraphique préliminaire des formations du bassin de Guercif. Rapport interne. Direction des Mines et de la Géologie, Service de la carte géologique, Bureau d'études des bassins sédimentaires, internal report Nº 30853, 74 pp..

BEROIZ, C. and PERMANYER, A. (2011). Hydrocarbon habitat of the Sedano Trough, Basque-Cantabrian Basin, *Spain. Journal of Petroleum Geology* 34: 387-410. doi.org/10.1111/j.1747-5457.2011.00511.x.

BODIN, S., MATTIOLI, E., FRÖHLICH, S., MARSHALL, J.D., BOUTIB, L., LAHSINI, S. and REDFERN, J. (2010). Toarcian carbon isotope shifts and nutrient changes from the Northern margin of Gondwana (High Atlas, Morocco, Jurassic): palaeoenvironmental implications. *Palaeogeography, Palaeoclimatology, Palaeoecology* 297: 377-390. doi.org/10.1016/j.palaeo.2010.08.018.

BODIN, S., KRENCKER, F.N., KOTHE, T., HOFFMANN, R., MATTIOLI, E., HEIMHOFER, U. and KABIRI, L. (2016). Perturbation of the carbon cycle during the Late Pliensbachian – Early Toarcian: new insight from high-resolution carbon isotope records in Morocco. *Journal of African Earth Sciences* 116: 89-104. doi.org/10.1016/j.jafrearsci.2015.12.018.

BOMBARDIERE, L. and GORIN, G.E. (2000). Stratigraphical and lateral distribution of sedimentary organic matter in Upper Jurassic carbonates of SE France. *Sedimentary Geology* 132: 177-203. doi.org/10.1016/S0037-0738(00)00006-3.

BORREGO, A.G., HAGEMANN, H.W., BLANCO, C.G., VALENZUELA, M. and SUARÉZ DE CENTI, C. (1996). The Pliensbachian (Early Jurassic) "anoxic" event in Asturias, northern Spain: Santa Mera Member, Rodiles Formation. *Organic Geochemistry* 25: 295-309. doi.org/10.1016/S0146-6380(96)00121-0.

BRAZIER, J.M., SUAN, G., TACAIL, T., SIMON, L., MARTIN, J. E., MATTIOLI, E. and BALTER, V. (2015). Calcium isotope evidence for dramatic increase of continental weathering during the Toarcian oceanic anoxic event (Early Jurassic). *Earth and Planetary Science Letters* 411: 164-176. doi.org/10.1016/j.epsl.2014.11.028.

CABRAL, M.C., COLIN, J.P., AZERÊDO, A.C., SILVA, R.L. and DUARTE, L.V. (2013). Registo da extinção dos Metacopina (Ostracoda, Crustacea) no Toarciano de Rabaçal, região de Coimbra. *Comunicações Geológicas* 100: 63-68.

CARUTHERS, A.H., GRÖCKE, D.R. and SMITH, P.L. (2011). The significance of an Early Jurassic (Toarcian) carbon-isotope excursion in Haida Gwaii (Queen Charlotte Islands), British Columbia, Canada. *Earth and Planetary Science Letters* 307: 19-26. doi:10.1016/j.epsl.2011.04.013.

CARUTHERS, A.H., SMITH, P.L. and GRÖCKE, D.R. (2013). The Pliensbachian–Toarcian (Early Jurassic) extinction, a global multi-phased event. *Palaeogeography, Palaeoclimatology, Palaeoecology* 386: 104-118. doi.org/10.1016/j.palaeo.2013.05.010.

CARUTHERS, A.H., SMITH, P.L. and GRÖCKE, D.R. (2014). The Pliensbachian-Toarcian (Early Jurassic) extinction: A North American perspective. In: Keller, G., Kerr, A.C. (Eds.),

Volcanism, Impacts, and Mass Extinctions: Causes and Effects. Geological Society of America Special Paper, 505. Geological Society of America, Boulder, pp. 225-243.

CASWELL B.A., COE A.L. and COHEN A.S. (2009). New range data for marine invertebrate species across the early Toarcian (Early Jurassic) mass extinction. *Journal of the Geological Society* 166: 859-872. doi: 10.1144/0016-76492008-0831.

CATUNEANU, O. (2006). Principles of Sequence Stratigraphy. Elsevier, Amsterdam, 375 pp..

CATUNEANU, O. (2017). Sequence stratigraphy: guidelines for a standard methodology. In: Montenari, M. (Ed.), Stratigraphy and Timescales. Academic Press 2, pp. 1-57.

CATUNEANU, O. (2018). First-order foreland cycles: Interplay of flexural tectonics, dynamic loading, and sedimentation. *Journal of Geodynamics*. doi.org/10.1016/j.jog.2018.03.001.

CHALONER, W.G. (1989). Fossil charcoal as an indicator of palaeoatmospheric oxygen level. *Journal of the Geological Society of London* 146: 171-174.

COHEN, A.S., COE, A.L., HARDING, S.M. and SCHWARK, L. (2004). Osmium isotope evidence for the regulation of atmospheric CO_2 by continental weathering. *Geology* 32: 157-160. doi.org/10.1130/G20158.1.

COMAS-RENGIFO, M.J. and GOY, A. (2010). Caracterización biocronoestratigráfica del Sinemuriense Superior y el Pliensbachiense entre los afloramientos de la Playa Vega y Lastres (Asturias). In: García-Ramos, J.C. (Coord.), Las sucesionesmargo-calcáreasmarinas del Jurásico Inferior y las series fluviales del Jurásico Superior. Acantilados de la playa de Vega (Ribadesella). Guía de campo (excursión A). V Congreso del Jurásico de España, Servitec, Oviedo, pp. 10-18.

COMAS-RENGIFO, M.J., DUARTE, L.V., FÉLIX, F., GARCÍA JORAL, F., GOY, A., and ROCHA, R.B. (2015). Latest Pliensbachian- Early Toarcian brachiopod assemblages from the Peniche section (Portugal) and its correlation. *Episodes* 38: 2-7.

CORNWELL, W.K., WRIGHT, I., TURNER, J., MAIRE, V., BARBOUR, M., CERNUSAK, L., DAWSON, T., ELLSWORTH, D., FARQUHAR, G., GRIFFITHS, H., KEITEL, C., KNOHL, A., REICH, P.B., WILLIAMS, D.G., BHASKAR, R., CORNELISSEN, J.C., RICHARDS, A., SCHMIDT, S., VALLADARES, F., KÖRNER, C., SCHULZE, E., BUCHMANN, N. and SANTIAGO, L.S. (2018). Climate and soils together regulate photosynthetic carbon isotope discrimination within C3 plants worldwide. *Global Ecology & Biogeography* 27: 1056-1067. doi.org/10.1111/geb.12764.

CORREIA, V.F., RIDING, J.B., FERNANDES, P., DUARTE, L.V. and PEREIRA, Z. (2017a). The palynology of the lower and middle Toarcian (Lower Jurassic) in the northern Lusitanian Basin, western Portugal. *Review of Palaeobotany and Palynology* 237, 75-95. dx.doi.org/10.1016/j.revpalbo.2016.11.008.

CORREIA, V.F., RIDING, J., DUARTE, L.V., FERNANDES, P. and PEREIRA, Z. (2017b). The palynological response to the Toarcian Oceanic Anoxic Event (Early Jurassic) at Peniche, Lusitanian Basin, western Portugal. *Marine Micropaleontology* 137: 46-63. doi.org/10.1016/j.marmicro.2017.10.004.

CORREIA, V.F., RIDING, J., DUARTE, L.V., FERNANDES, P. and PEREIRA, Z. (2018). The Early Jurassic palynostratigraphy of the Lusitanian Basin, western Portugal.. *Geobios* 51:537-557. doi.org/10.1016/j.geobios.2018.03.001.

DANISE, S., TWITCHETT, R.J., LITTLE, T.S. and CLÉMANCE, M-E. (2013). The impact of global warming and anoxia on marine benthic community dynamics: an example from the Toarcian (Early Jurassic). *PLoS One* 8: e56255. doi.org/10.1371/journal.pone.0056255.

DANISE, S., CLÉMANCE, M-E., PRICE, G.D., MURPHY, D.P., GÓMEZ, J.J. and TWITCHETT, R.J. (2019). Stratigraphic and environmental control on marine benthic community change through the early Toarcian extinction event (Iberian Range, Spain). *Palaeogeography, Palaeoclimatology, Palaeoecology* 524: 183-200. doi.org/10.1016/j.palaeo.2019.03.039.

DECONINCK, J-F., GÓMEZ, J.J., BAUDIN, F., BISCAY, H., BRUNEAU, L., COCQUEREZ, T., MATHIEU, O., PELLENARD, P. and SANTONI, A-L. (2020). Diagenetic and environmental control of the clay mineralogy, organic matter and stable isotopes (C, O) of Jurassic (Pliensbachian-lowermost Toarcian) sediments of the Rodiles section (Asturian Basin, Northern Spain). *Marine and Petroleum Geology* 115: 104286. doi.org/10.1016/j.marpetgeo.2020.104286.

DERA, G., PELLENARD, P., NEIGE, P., DECONINCK, J.F., PUCEAT, E. and DOMMERGUES, J.L. (2009). Distribution of clay minerals in Early Jurassic Peritethyan seas: palaeoclimatic significance inferred from multiproxy comparisons. *Palaeogeography, Palaeoclimatology, Palaeoecology* 271: 39-51. https://doi.org/10.1016/j.palaeo.2008.09.010.

DERA, G., NEIGE, P., DOMMERGUES, J., FARA, E., LAFFONT, R. and PELLENARD, P. (2010). High-resolution dynamics of Early Jurassic marine extinctions: the case of Pliensbachian–Toarcian ammonites (Cephalopoda). *Journal of the Geological Society of London* 167: 21-33. doi.org/10.1144/0016-76492009-068.

DERA, G., NEIGE, P., DOMMERGUES, J.L. and BRAYARD, A. (2011). Ammonite paleobiogeography during the Pliensbachian–Toarcian crisis (Early Jurassic) reflecting paleoclimate, eustasy, and extinctions. *Global and Planetary Change* 78: 92-105. doi.org/10.1016/j.gloplacha.2011.05.009.

DERA, G. and DONNADIEU, Y. (2012). Modeling evidences for global warming, Arctic seawater freshening, and sluggish oceanic circulation during the Early Toarcian anoxic event. *Paleoceanography* 27, PA2211. doi.org/10.1029/2012PA002283.

DIÉGUEZ, C., PEYROT, D. and BARRÓN, E. (2010). Floristic and vegetational changes in the Iberian Peninsula during Jurassic and Cretaceous. *Review of Palaeobotany and Palynology* 162: 325-340.

DUARTE, L.V. (1995). *O Toarciano da Bacia Lusitaniana. Estratigrafia e evolução sedimentogenética*. Ph.D. Thesis. Centro de Geociências da Universidade de Coimbra. 342 pp..

DUARTE, L.V. (1997). Facies analysis and sequential evolution of the Toarcian-lower Aalenian series in the Lusitanian Basin (Portugal). *Comunicações do Instituto Geológico e Mineiro* 83: 65-94.

DUARTE, L.V. (2007). Lithostratigraphy, sequence stratigraphy and depositional setting of the Pliensbachian and Toarcian series in the Lusitanian Basin, Portugal. In: Rocha, R.B. (Ed.), The Peniche Section (Portugal). Contributions to the Definition of the Toarcian GSSP. International Subcommission on Jurassic Stratigraphy, pp. 17-23.

DUARTE, L.V. and SOARES, A.F. (2002). Litostratigrafia das series margo-calcárias do Jurássico inferior da Bacia Lusitânica (Portugal). *Comunicações do Instituto Geológico e Mineiro* 89: 135-154.

DUARTE, L.V., PERILLI, N., DINO, R., RODRIGUES, R. and PAREDES, R. (2004) - Lower to Middle Toarcian from the Coimbra region (Lusitanian Basin, Portugal): sequence stratigraphy, calcareous nannofossils and stable-isotope evolution. *Rivista Italiana di Paleontologia e Stratigrafia* 110: 115-127. doi: 10.13130/2039-4942/6276.

DUARTE, L.V., OLIVEIRA, L.C. and RODRIGUES, R. (2007). Carbon isotopes as a sequence stratigraphic tool: examples from the Lower and Middle Toarcian marly limestones of Portugal. *Boletín Geológico y Minero* 118: 3-17.

DUARTE, L.V., SILVA, R.L., OLIVEIRA, L.V., COMAS-RENGIFO, M.J. and SILVA, F. (2010). Organic-rich facies in the Sinemurian and Pliensbachian of the Lusitanian Basin, Portugal: Total Organic Carbon distribution and relation to transgressive-regressive facies cycles. *Geologica Acta* 8: 325-340. doi.org/10.1344/105.000001536.

DUARTE, L.V., SILVA, R.L., MENDONÇA FILHO, J.G., POÇAS RIBEIRO, N. and CHAGAS, R.A. (2012). High-resolution stratigraphy, Palynofacies and source rock potential of the Água de Madeiros Formation (Upper Sinemurian) of the Lusitanian Basin, Portugal. *Journal of Petroleum Geology* 35 2: 105-126. doi.org/10.1111/j.1747-5457.2012.00522.x.

DUARTE, L.V., SILVA, R.L., MENDONÇA FILHO, J.G., AZERÊDO, A.C. and PAREDES, R., (2017). Total organic carbon content and carbon stable Isotopes in the Sinemurian shallow-water carbonates (Coimbra Formation) of the Lusitanian Basin. In: 33rd International Meeting of Sedimentology, Book of Abstracts, pp. 255.

DUARTE, L.V., COMAS-RENGIFO, M.J., HESSELBO, S., MATTIOLI, E., SUAN, G., BAKER, S., CABRAL, M.C., CORREIA, V., GARCÍA JORAL, F., GOY, A., REOLID, M., RITA, P., FÉLIX, F., PAREDES, R., PITTET, B. and ROCHA, R.B. (2018a). The Toarcian Oceanic Anoxic Event at Peniche. An exercise in integrated stratigraphy – Stop 1.3. In: Duarte, L.V. and Silva, R.L. (Eds), II International Workshop on the Toarcian Oceanic Anoxic Event: Field Trip Guidebook: IGCP-655- The Toarcian Oceanic Anoxic Event in the Western Iberian Margin and its context within the Lower Jurassic evolution in the Lusitanian Basin. University of Coimbra, Coimbra, Portugal, pp. 33-54. ISBN 978-989-98914-4-9.

DUARTE, L.V., COMAS-RENGIFO, M.J., GARCÍA JORAL, F., GOY, A., MIGUEZ-SALAS, O. and RODRÍGUEZ-TOVAR, F.J. (2018b). Sedimentological and macroinvertebrate record

across the Lower Toarcian in the Rabaçal area - Stop 2.2. In: Duarte, L.V. and Silva, R.L. (Eds), II International Workshop on the Toarcian Oceanic Anoxic Event: Field Trip Guidebook: IGCP-655- The Toarcian Oceanic Anoxic Event in the Western Iberian Margin and its context within the Lower Jurassic evolution in the Lusitanian Basin. University of Coimbra, Coimbra, Portugal, pp. 71-82. ISBN 978-989-98914-4-9.

DUNCAN, R.A., HOOPER, P.R., RAHACEK, J., MARSH, J.S. and DUNCAN, A.R. (1997). The timing and duration of the Karoo igneous event, southern Gondwana. *Journal of Geophysical Research* 102: 18127-18138. doi.org/10.1029/97JB00972.

EL ARABI, H., OUAHHABI, B. and CHARRIÈRE, A. (2001). Les séries du Toarcien–Aalénien du SW du Moyen–Atlas (Maroc): précisions stratigraphiques et signification paléogéographique. *Bulletin de la Société Géologique de France* 172: 723-736. doi.org/10.2113/172.6.723.

EL HAMMICHI, F., ELMI, S., FAURE-MURET, A. and BENSHILI, K. (2002). Une plate-forme en distension, témoin de phases pré-accrétion téthysienne en Afrique du Nord pendant le Toarcien–Aalénien (synclinal Iguer Awragh–Afennourir, Moyen Atlas occidental, Maroc). *Comptes Rendus Geosciences* 334: 1003-1010. doi.org/10.1016/S1631-0713(02)01841-2.

EL HAMMICHI, F., BENSHILI, K. and ELMI, S. (2008). Les faunes d'Ammonites du Toarcien-Aalénien du Moyen Atlas sud-occidental (Maroc). *Revue de Paleobiologie* 27: 429-447.

EMEIS, K.-C., WHELAN, J.K. and TARAFA, M. (1991). Sedimentary and geochemical expressions of oxic and anoxic conditions on the Peru Shelf. *Geological Society, London, Special* Publications 58: 155-170. doi.org/10.1144/GSL.SP.1991.058.01.11.

FANTASIA, A., FÖLLMI, K.B., ADATTE, T., SPANGENBERG, J.E. and MONTERO-SERRANO, J.C. (2018a). The Early Toarcian oceanic anoxic event: Paleoenvironmental and paleoclimatic change across the Alpine Tethys (Switzerland). *Global and Planetary Change* 162: 53-68. doi.org/10.1016/j.gloplacha.2018.01.008.

FANTASIA, A., FÖLLMI, K.B., ADETTE, T., BERNÁRDEZ, E., SPANGENBERG, J.E. and MATTIOLI, E. (2018b). The Toarcian Oceanic Anoxic Event in southwestern Gondwana: An example from the Andean Basin, northern Chile. *Journal of the Geological Society* 175: 883-902. doi.org/10.1144/jgs2018-008.

FANTASIA, A., ADATTE, T., SPANGENBERG, J.E., FONT, E., DUARTE, L.V. and FÖLLMI, K.B. (2019). Global versus local processes during the Pliensbachian–Toarcian transition at the Peniche GSSP, Portugal: A multi-proxy record. *Earth-Science Reviews* 198: 102932. doi.org/10.1016/j.earscirev.2019.102932.

FEDAN, B. (1978). Etude structurale de l'accident sud moyen-atlasique entre Enjil des Ikhatarn et Imouzzer des Marmoucha (Moyen Atlas, Maroc). *Bulletin de l'Institut Scientifique* 3: 169-184.

FERREIRA, J., MATTIOLI, E., PITTET, B., CACHÃO, M. and SPANBENBERG, J.E. (2015). Palaeoecological insights on Toarcian and lower Aalenian calcareous nannofossils from the

Lusitanian Basin (Portugal). *Palaeogeography, Palaeoclimatology, Palaeoecology* 436: 246-262. doi.org/10.1016/j.palaeo.2015.07.012.

FERREIRA, J., MATTIOLI, E., SUCHERÁS-MARX, B., GIRAUD, F., DUARTE, L.V., PITTET, B., SUAN, G., HASSLER, A. and SPANBENBERG, J.E. (2019). Western Tethys Early and Middle Jurassic calcareous nannofossil biostratigraphy. *Earth-Science Reviews* 197: 102908. doi.org/10.1016/j.earscirev.2019.102908.

FLEET, A.J., CLAYTON, C.J., JENKYNS, H.C. and PARKINSON, D.N. (1987). Liassic source rock deposition in western Europe. In: Brooks, J., Glennie, K. (Eds.), Petroleum Geology of North West Europe. Graham and Trotman 1, pp. 59-70.

FONSECA, C., MENDONÇA FILHO, J.G., LÉZIN, C., DUARTE, L.V. and FAURÉ, P. (2018). Organic facies variability during the Toarcian Oceanic Anoxic Event record of the grands Causses and Quercy basins (southern France). *International Journal of Coal Geology* 190: 218-235. doi.org/10.1016/j.coal.2017.10.006.

FRENCH, K.L., SEPULVEDA, J., TRABUCHO-ALEXANDRE, J., GRÖCKE, D.R. and SUMMONS, R.E. (2014). Organic geochemistry of the early Toarcian oceanic anoxic event in Hawsker Bottoms, Yorkshire, England. *Earth and Planetary Science Letters* 390: 116-127. doi.org/10.1016/j.epsl.2013.12.033.

FRIMMEL, A., OSCHMANN, W. and SCHWARK, L. (2004). Chemostratigraphy of the Posidonia Black Shale, SW Germany I. Influence of sea-level variation on organic facies evolution. *Chemical Geology* 206: 199-230. doi.org/10.1016/j.chemgeo.2003.12.007.

FRIZON DE LAMOTTE, D., ZIZI, M., MISSENARD, Y., HAFID, M., EL AZZOUZI, M., MAURY, R.C., CHARRIÈRE, A., TAKI, Z., BENAMMI, M. and MICHARD, A. (2008). The Atlas system. In: Michard, A., Saddiqi, O., Chalouan, A., Frizon de Lamotte, D. (Eds.), Continental Evolution: The Geology of Morocco. *Lecture Notes in Earth Sciences* 116, pp. 133-202.

GALLEGO-TORRES, D., REOLID, M., NIETO-MORENO, V. and MARTÍNEZ-CASADO, F.J. (2015). Pyrite framboid size distribution as a record for relative variations in sedimentation rate: An example on the Toarcian Oceanic Anoxic Event in Southiberian Palaeomargin. *Sedimentary Geology* 330: 59-73. doi.org/10.1016/j.sedgeo.2015.09.013.

GARCÍA-HERNÁNDEZ, M., LÓPEZ-GARRIDO, A.C., MARTÍN-ALGARRA, A., MOLINA, J.M., RUIZ-ORTIZ, P.A. and VERA, J.A. (1989). Las descontinuidades mayores del Jurásico de las Zonas Externas de las Cordilleras Béticas: análisis e interpretación de los ciclos sedimentarios. *Cuadernos de Geologia Iberica* 13: 35-52.

GARCÍA JORAL, F., GÓMEZ, J.J. and GOY, A. (2011). Mass extinction and recovery of the Early Toarcian (Early Jurassic) brachiopods linked to climate change in Northern and Central Spain. *Palaeogeography, Palaeoclimatology, Palaeoecology* 302, 367-380. doi.org/10.1016/j.palaeo.2011.01.023.

GARCÍA-RAMOS, J.C. and PIÑUELA, L. (2010). La ritmita de calizas y margas del Pliensbachiense. In: García-Ramos, J.C. (Coord.), V Congreso del Jurásico de España,Guía de

la excursión A: Las sucesiones margo-calcáreas marinas del Jurásico Inferior y las series fluviales del Jurásico Superior. Acantilados de la playa de Vega (Ribadesella), pp. 21-40.

GÓMEZ, J.J., GOY, A. and CANALES, M.L. (2008). Seawater temperature and carbon isotope variations in belemnites linked to mass extinction during the Toarcian (Early Jurassic) in Central and Northern Spain. Comparison with other European sections. *Palaeogeography, Palaeoclimatology, Palaeoecology* 258: 28-58. doi:10.1016/j.palaeo.2007.11.005.

GÓMEZ, J.J. and ARIAS, C. (2010). Rapid warming and ostracods mass extinction at the Lower Toarcian (Jurassic) of central Spain. *Marine Micropaleontology* 74: 119-135. doi.org/10.1016/j.marmicro.2010.02.001.

GÓMEZ, J.J. and GOY, A. (2011). Warming-driven mass extinction in the early Toarcian (Early Jurassic) of northern and central Spain. Correlation with other time-equivalent European sections. *Palaeogeography, Palaeoclimatology, Palaeoecology* 306: 176-195. doi:10.1016/j.palaeo.2011.04.018.

GÓMEZ, J.J., COMAS-RENGIFO, M.J. and GOY, A. (2016). Palaeoclimatic oscillations in the Pliensbachian (Early Jurassic) of the Asturian Basin (Northern Spain). *Climate of the Past* 12: 1199-1214. doi.org/10.5194/cp-12-1199-2016.

GONÇALVES, P.A., MENDONÇA FILHO, J.G., MENDONÇA, J.O., SILVA, T.F. and FLORES, D. (2013). Paleoenvironmental characterization of a Jurassic sequence on the Bombarral sub-basin (Lusitanian basin, Portugal): insights from palynofacies and organic geochemistry. *International Journal of Coal Geology* 113: 27-40. dx.doi.org/10.1016/j.coal.2013.03.009.

GORIN, G.E. and FEIST-BURKHARDT, S. (1990). Organic facies of lower to middle Jurassic sediments in the Jura Mountains, Switzerland. *Review of Palaeobotany and Palynology* 65: 349-355. doi.org/10.1016/0034-6667(90)90085-W.

GRÖCKE D., HORI R.S., TRABUCHO-ALEXANDRE J. and KEMP, D.B. (2011). An open ocean record of the Toarcian oceanic anoxic event. *Solid Earth* 2: 247-257. doi:10.5194/se-2-245-2011.

HALLAM, A. (2001). A review of the broad pattern of Jurassic sea-level changes and their possible causes in the light of current knowledge. *Palaeogeography, Palaeoclimatology, Palaeoecology* 167: 23-37. doi.org/10.1016/S0031-0182(00)00229-7.

HANDOH, I.C. and LENTON, T.M. (2003). Periodic-Mid Cretaceous Oceanic anoxic events linked by oscillations of the phosphorous and oxygen biogeochemical cycles. *Global Biogeochemical Cycles* 17: 1-11.

HAQ, B.U., 2018. Jurassic sea-level variations: a reappraisal. *The Geological Society of America* 28: 4-10. doi: 10.1130/GSATG359A.1.

HARDENBOL, J., THIERRY, J., FARLEY, M.B., JACQUIN, T., DE GRACIANSKY, P.C. and VAIL, P.R. (1998). Mesozoic and Cenozoic sequence chronostratigraphic framework of European basins. *Society of Economic Paleontologists and Mineralogists* Special Publication 60: 3-13. https://doi.org/10.2110/pec.98.02.0003.

HARRIES, P.J. and LITTLE, C.S. (1999). The early Toarcian (Early Jurassic) and the Cenomanian–Turonian (Late Cretaceous) mass extinctions: similarities and contrasts. *Palaeogeography, Palaeoclimatology, Palaeoecology* 154: 39-66. doi.org/10.1016/S0031-0182(99)00086-3.

HERMOSO, M., CALLONNEC, L.L., MINOLETTI, F., RENARD, M. and HESSELBO, S.P. (2009). Expression of the Early Toarcian negative carbon-isotope excursion in separated carbonate microfractions (Jurassic, Paris Basin). *Earth and Planetary Science Letters* 277: 194-203. doi.org/10.1016/j.epsl.2008.10.013.

HERMOSO, M., MINOLETTI, F. and PELLENARD, P. (2013). Black shale deposition during Toarcian super-greenhouse driven by sea level. *Climate Past* 9: 2703-2712. doi.org/10.5194/cp-9-2703-2013.

HERNÁNDEZ, J. M. (2000). *Sedimentología, Paleogeografía y relación tectónica/sedimentación de los sistemas fluviales, aluviales y palustres de la cuenca rift de Aguilar (Grupo Campóo, Jurásico superior-Cretácico inferior de Palencia, Burgos, Cantabria*). Ph.D. Thesis. Universidad del País Vasco-Euskal Herriko Unibertsitatea.

HERRERO, C. (1998). Foraminíferos del Pliensbachiense en la sección de Camino (Cuenca Vasco-Cantábrica, España). *Cuadernos de Geología Ibérica* 24: 121-139.

HESSELBO, S.P., GRÖCKE, D.R., JENKYNS, H.C., BJERRUM, C.J., FARRIMOND, P., MORGANS BELL, H.S. and GREEN, O.R. (2000). Massive dissociation of gas hydrate during a Jurassic oceanic anoxic event. *Nature* 406: 392-395. doi.org/10.1038/35019044.

HESSELBO, S.P., JENKYNS, H.C., DUARTE, L.V. and OLIVEIRA, L.V. (2007). Carbon-isotope record of the Early Jurassic (Toarcian) Oceanic Anoxic Event from fossil wood and marine carbonate (Lusitanian Basin, Portugal). *Earth and Planetary Science Letters* 253: 455-470. doi.org/10.1016/j.epsl.2006.11.009.

HESSELBO, S.P. and PIEÑKOWSKI, G. (2011). Stepwise atmospheric carbon-isotope excursion during the Toarcian Oceanic Anoxic Event (Early Jurassic, Polish Basin). *Earth and Planetary Science Letters* 301: 365-372. doi.org/10.1016/j.epsl.2010.11.021.

HISCOTT, R.N., WILSON, R..L., GRADSTEIN, F.M., PUJALTE, V., GARCÍA-MONDÉJAR, J., BOUDREAU, R.R. and WISHART, H.A. (1990). Comparative stratigraphy and subsidence history of Mesozoic rift basins of the North Atlantic. *American Association of Petroleum Geologists, Bulletin* 74: 60-76.

HOLLARD H., CHOUBERT G., BRONNER G., MARCHAND J. and SOUGY J. (1985). Carte géologique du Maroc, scale 1:1,000,000. Notes et Mémoires du Service géologique du Maroc, 260 (2 sheets).

ISO 7404-2 (2009). Methods for the petrographic analysis of coals – Part 2: methods of preparing coal samples. International Organization for Standardization 12.

IZUMI, K., KEMP, D.B., ITAMIYA, S. and INUI, M. (2018). Sedimentary evidence for enhanced hydrological cycling in response to rapid carbon release during the early Toarcian

oceanic anoxic event. *Earth and Planetary Science Letters* 481: 162-170. doi.org/10.1016/j.epsl.2017.10.030.

JACQUIN, T. and DE GRACIANSKY, P.C. (1998). Transgressive-regressive (second order) facies cycles: the effects of tectonoeustacy. In: de Graciansky, P.C., Hardenbol, J., Jacquin, T., Vail, P. (Eds.), Mesozoic and Cenozoic Sequence Stratigraphy of European Basins. SEPM Special Publication, 60, pp. 445-466.

JENKYNS, H.C. (1988). The Early Toarcian (Jurassic) oceanic anoxic event: stratigraphic, sedimentary, and geochemical evidence. *American Journal of Science* 288: 101-151. doi:10.2475/ajs.288.2.101.

JENKYNS, H.C. (2003). Evidence for rapid climate change in the Mesozoic–Palaeogene greenhouse world. *Philosophical Transactions of the Royal Society A* 361: 1885-1916. 10.1098/rsta.2003.1240.

JENKYNS, H.C. (2010). Geochemistry of oceanic anoxic events. *Geochemistry Geophyics Geosystems* 11: 1-30. doi.org/10.1029/2009GC002788.

JENKYNS, H.C. and CLAYTON, C.J. (1986). Black shales and carbon isotopes in pelagic sediments from the Tethyan Lower Jurassic. *Sedimentology* 33: 87-106. doi.org/10.1111/j.1365-3091.1986.tb00746.x.

JENKYNS, H.C., JONES, C.E., GRÖCKE, D.R., HESSELBO, S.P. and PARKINSON, D.N. (2002). Chemostratigraphy of the Jurassic System: applications, limitations and implications for palaeoceanography. *Journal of the Geological Society* 159: 351-378. doi.org/10.1144/0016-764901-130.

JIMÉNEZ, A.P. (1986). *Estudio paleontológico de los ammonites del Toarciense inferior y medio de las Cordilleras Béticas (Dactylioceratidae e Hildoceratidae)*. Ph.D. Thesis. Universidad de Granada. 252 pp..

JIMÉNEZ, A.P., JIMÉNEZ DE CISNEROS, C., RIVAS, P. and VERA, J.A. (1996). The Early Toarcian anoxic event in the westernmost Tethys (Subbetic). Paleogeographic and paleobiogeographic significance. *Journal of Geology* 104: 399-416.

JIMÉNEZ, A.P. and RIVAS, P. (2007). El OAE toarciense en la secuencia de la Fuente de la Vidriera, Zona Subbética, región de Caravaca (Murcia). In: Aguirre, J., Company, M., Rodríguez- Tovar, F.J. (Eds.), XXIII Jornadas de la Sociedad Española de Paleontología, Caravaca. Field Trip Guidebook, pp. 3-16.

KAFOUSIA, N., KARAKITSIOS, V., MATTIOLI, E., KENJO, S. and JENKYNS, H.C. (2014). The Toarcian Oceanic Anoxic Event in the Ionian Zone, Greece. *Palaeogeography, Palaeoclimatology, Palaeoecology* 393: 135-145. doi.org/10.1016/j.palaeo.2013.11.013.

KEMP, D.B., COE, A.L., COHEN, A.S. and SCHWARK, L. (2005). Astronomical pacing of methane release in the Early Jurassic period. *Nature* 437: 396–400. doi:10.1038/nature04037.

KEMP, D.B., COE, A.L., COHEN, A.S. and WEEDON, G.P. (2011). Astronomical forcing and chronology of the early Toarcian (Early Jurassic) oceanic anoxic event in Yorkshire, UK. *Paleoceanography* 26, PA4210. doi.org/10.1029/2011PA002122.

KEMP, D.B. and IZUMI, K. (2014). Multiproxy geochemical analysis of a Panthalassic mar-gin record of the early Toarcian oceanic anoxic event (Toyora area, Japan). *Palaeogeography, Palaeoclimatology, Palaeoecology* 414: 332-341. doi.org/10.1016/j.palaeo.2014.09.019.

KEMP, D.B. BARANYI, V., IZUMI, K. and BURGESS, R.D. (2019). Organic matter variations and links to climate across the early Toarcian oceanic anoxic event (T-OAE) in Toyora area, southwest Japan. *Palaeogeography, Palaeoclimatology, Palaeoecology* 530: 90-102. doi.org/10.1016/j.palaeo.2019.05.040.

KÖRNER, CH., FARQUHAR, G.D. and WONG, S.C. (1991). Carbon isotope discrimination by plants follows latitudinal and altitudinal trends. *Oecologia* 88: 30-40. doi.org/10.1007/BF00328400.

KORTE, C. and HESSELBO, S.P. (2011). Shallow marine carbon and oxygen isotope and elemental records indicate icehouse-greenhouse cycles during the Early Jurassic. *Paleoceanography* 26, PA4219. doi.org/10.1029/2011PA002160.

KORTE, C., HESSELBO, S.P., ULLMANN, C.V., DIETL, G., RUHL, M., SCHWEIGERT, G. and THIBAULT, N. (2015). Jurassic climate mode governed by ocean gateway. *Nature Communication* 6: 10015. doi.org/10.1038/ncomms10015.

KRENCKER, F.N., BODIN, S., SUAN, G., HEIMHOFER, U., KABIRI, L. and IMMENHAUSER, A. (2015). Toarcian extreme warmth led to tropical cyclone intensification. *Earth and Planetary Science Letters* 425: 120-130. doi.org/10.1016/j.epsl.2015.06.003.

KULLBERG, J.C., OLÓRIZ, F., MARQUES, B., CAETANO, P. and ROCHA, R.B. (2001). Flat pebble conglomerates: a local marker for Early Jurassic seismicity related to syn-rift tectonics in the Sesimbra area (Lusitanian Basin, Portugal). *Sedimentary Geology* 139: 49-70. doi.org/10.1016/S0037-0738(00)00160-3.

KULLBERG, J.C., ROCHA, R.B., SOARES, A.F., REY, J., TERRINHA, P., AZERÊDO, A.C., CALLAPEZ, P., DUARTE, L.V., KULLBERG, M. C., MARTINS, L., MIRANDA, J. R., ALVES, C., MATA, J., MADEIRA, J., MATEUS, O., and MOREIRA, M. (2013). A Bacia Lusitaniana: Estratigrafia, Paleogeografia e Tectónica. In: Dias, R., Araújo, A., Terrinha, P., Kullberg, J.C. (Eds), Geologia de Portugal: Geologia Meso-cenozóica de Portugal. Livraria Escolar Editora 2, pp. 317-368.

KÜSPERT, W. (1982). Environmental changes during oil shale deposition as deduced from stable isotope ratios. In: Einsele, G., Seilacher, A. (Eds.), Cyclic and Event Stratification. Springer, Berlin, pp. 482-501.

LAMBERSON, M.N., BUSTIN, R.M., KALKREUTH, W.D. and PRATT, K.C. (1996). The formation of inertinite-rich peats in the mid-Cretaceous Gates Formation: implications of the interpretation of mid-Albian history of paleowildfire. *Palaeogeography, Palaeoclimatology, Palaeoecology* 120: 235-260. doi.org/10.1016/0031-0182(95)00043-7.

LITTLE, C.T. and BENTON, M.J. (1995). Early Jurassic mass extinction: a global long term event. *Geology* 23: 495-498. doi.org/10.1130/0091-7613(1995)023<0495:EJMEAG>2.3.CO;2.

LITTLER, K., HESSELBO, S.P. and JENKYNS, H.C. (2010). A carbon-isotope perturbation at the Pliensbachian–Toarcian boundary: evidence from the Lias Group, NE England. *Geological Magazine* 147: 181-192. doi.org/10.1017/S0016756809990458.

LOMAX, B.H., LAKE, J.A., LENG, M.J. and JARDINE P.E. (2019). An experimental evaluation of the use of $\delta^{13}C$ as a proxy for palaeoatmospheric CO^2. *Geochimica et Cosmochimica Acta* 247: 162-174. doi.org/10.1016/j.gca.2018.12.026.

MÄDLER, K. (1968). Die figurierten organischen Bestandteile der Posidonienschiefer. *Beihefte zum Geologischen Jahrbuch* 58, 287-406.

MARJANAC, T. and STEEL, R.J. (1997). Dunlin Group sequence stratigraphy in the Northern North Sea: a model for cook sandstone deposition. *AAPG Bulletin* 81: 276-292.

MATTAUER, M., TAPPONNIER, P. and PROUST, F. (1977). Sur les mécanismes de formation des chaînes intracontinentales. L'exemple des chaînes atlasiques du Maroc. *Bulletin de la Société Géologique de France* 3: 521-526. doi.org/10.2113/gssgfbull.S7-XIX.3.521.

MATTIOLI, E., PITTET, B., SUAN, G. and MAILLIOT, S. (2008). Calcareous nannoplankton changes across the early Toarcian oceanic anoxic event in the western Tethys. *Paleoceanography* 23, PA3208. doi:10.1029/2007PA001435.

MATTIOLI, E., PITTET, B., PETITPIERRE, L. and MAILLIOT, S. (2009). Dramatic decrease of pelagic carbonate production by nannoplankton across the Early Toarcian anoxic event (T-OAE). *Global and Planetary Change* 65: 134-145. doi.org/10.1016/j.gloplacha.2008.10.018.

MATTIS, A.F. (1977). Nonmarine Triassic sedimentation, central High Atlas Mountains, Morocco. *Journal of Sedimentary Research* 47: 107-119. doi.org/10.1306/212F7108-2B24-11D7-8648000102C1865D.

MCARTHUR, J.M., ALGEO, T.J., VAN DE SCHOOTBRUGGE, B., LI, Q. and HOWARTH, R.J. (2008). Basinal restriction, black shales, Re-Os dating, and the early Toarcian (Jurassic) oceanic anoxic event. *Paleoceanography* 23, PA4217. doi.org/10.1029/2008PA001607.

MCARTHUR, J.M. (2019). Early Toarcian black shales: A response to an oceanic anoxic event or anoxia in marginal basins?. *Chemical Geology* 522: 71–83. doi.org/10.1016/j.chemgeo.2019.05.028.

MCELWAIN, J.C., WADE-MURPHY, J. and HESSELBO, S.P. (2005). Changes in carbon dioxide during an anoxic event linked to intrusion of Gondwana coals. *Nature* 435: 479-482. doi.org/10.1038/nature03618.

MENDONÇA FILHO, J.G., MENEZES, T.R., MENDONÇA, J.O., OLIVEIRA, A.D., SILVA, T.F., RONDON, N.F. and SILVA, F.S. (2012). Organic facies: palynofacies and organic geochemistry approaches. In: Panagiotaras, D. (Ed.), Geochemistry Earth's System Processes. InTech, Rijeka, pp. 211-248.

MENDONÇA FILHO, J.G. and GONÇALVES, P.A. (2017). Organic matter: concepts and definitions, Chapter 1. In: Suárez-Ruiz, I., Mendonça Filho, J.G. (Eds.), Geology: Current and Future Developments. The Role of Organic Petrology in the Exploration of Conventional and Unconventional Hydrocarbon Systems. 1. Bentham Science Publishers, United Arab Emirates, pp. 1-33.

MIGUEZ-SALAS, O., RODRÍGUEZ-TOVAR, F.J. and DUARTE, L.V. (2017). Selective incidence of the toarcian oceanic anoxic event on macroinvertebrate marine communities: a case from the Lusitanian basin, Portugal. *Lethaia* 50: 548-560.

MORARD, A., GUEX, J., BARTOLINI, A., MORETTINI, E. and DE WEVER, P. (2003). A new scenario for the Domerian – Toarcian transition. *Bulletin de la Société Géologique de France* 174: 351-356. doi.org/10.2113/174.4.351.

NEUMEISTER, S., GRATZER, R., ALGEO, T.J., BECHTEL, A., GAWLICK, H.J., NEWTON, R.J. and SACHSENHOFER, R.F. (2015). Oceanic response to Pliensbachian and Toarcian magmatic events: implications from an organic-rich basinal succession in the NWTethys. *Global and Planetary Change* 126: 62-83. dx.doi.org/10.1016/j.gloplacha.2015.01.007.

PÁLFY, J. and SMITH, P.L. (2000). Synchrony between Early Jurassic extinction, oceanic anoxic event, and the Karoo-Ferrar flood basalt volcanism. *Geology* 28: 747-750. doi.org/10.1130/0091-7613(2000)28<747:SBEJEO>2.0.CO;2.

PALLIANI, R.B., CIRILLI, S. and MATTIOLI, E. (1998). Phytoplankton response and geochemical evidence of the lower Toarcian relative sea level rise in the Umbria-Marche basin (Central Italy). *Palaeogeography, Palaeoclimatology, Palaeoecology* 142; 33-50. doi.org/10.1016/S0031-0182(97)00152-1.

PALOMO, I.D., HUERTAS, M.O. and HACH-ALI, P.F. (1985). The significance of clay minerals in studies of the evolution of the Jurassic deposits of the Betic Cordillera, SE Spain. *Clay Minerals* 20: 39-52. doi.org/10.1180/claymin.1985.020.1.04.

PAREDES, R., COMAS-RENGIFO, M.J., DUARTE, L.V. and GOY, A. (2018). Upper Pliensbachian–lowermost Toarcian macroinvertebrates (Ammonites, Bivalves) succession prior to the TOAE extinction interval. The example of Fonte Coberta section - Stop 2.1. In: Duarte, L.V. and Silva, R.L. (Eds), II International Workshop on the Toarcian Oceanic Anoxic Event: Field Trip Guidebook: IGCP-655- The Toarcian Oceanic Anoxic Event in the Western Iberian Margin and its context within the Lower Jurassic evolution in the Lusitanian Basin. University of Coimbra, Coimbra, Portugal, pp. 63-70. ISBN 978-989-98914-4-9.

PEARCE, C.R., COHEN, A.S., COE, A.L. and BURTON, K.W. (2008). Molybdenum isotope evidence for global ocean anoxia coupled with perturbations to the carbon cycle during the Early Jurassic. *Geology* 36: 231-234. doi: 10.1130/G24446A.1.

PERCIVAL, L.E., WITT, M.I., MATHER, T.A., HERMOSO, M., JENKYNS, H.C., HESSELBO, S.P., AL-SUWAIDI, A.H., STORM, M.S., XU, W. and RUHL, M. (2015). Globally enhanced mercury deposition during the end-Pliensbachian extinction and Toarcian

OAE: a link to the Karoo-Ferrar Large Igneous Province. *Earth and Planetary Science Letters* 428: 267-280. dx.doi.org/10.1016/j.epsl.2015.06.064.

PERCIVAL, L.E., COHEN, A.S., DAVIES, M.K., DICKSON, A.J., HESSELBO, S.P., JENKYNS, H.C., LENG, M.J., MATHER, T.A., STORM, M.S. and XU, W. (2016). Osmium isotope evidence for two pulses of increased continental weathering linked to Early Jurassic volcanism and climate change. *Geology* 44: 759-762. doi.org/10.1130/G37997.1.

PHILIPPE, M., PUIJALON, S., SUAN, G., MOUSSET, S., THÉVENARD, F. and MATTIOLI, E. (2017). The palaeolatitudinal distribution of fossil wood genera as a proxy for European Jurassic terrestrial climate. *Palaeogeography, Palaeoclimatology, Palaeoecology* 466: 373-381. dx.doi.org/10.1016/j.palaeo.2016.11.029.

PIAZZA, V., DUARTE, L.V., RENAUDIE, J. and ABERHAN, M. (2019). Reductions in body size of benthic macroinvertebrates as a precursor of the early Toarcian (Early Jurassic) extinction event in the Lusitanian Basin, Portugal. *Paleobiology* 45: 296-316.

PIEÑKOWSKI, G. and WAKSMUNDZKA, M. (2009). Palynofacies in Lower Jurassic epicontinental deposits of Poland: tool to interpret sedimentary environments. *Episodes* 32: 21-32.

PIEÑKOWSKI, G., HODBOD, M. and ULLMANN, C.V. (2016). Fungal decomposition of terrestrial organic matter accelerated Early Jurassic climate warming. *Nature Scientific Reports* 6: 31930. doi.org/10.1038/srep31930.

PIQUÉ, A., TRICART, P., GUIRAUD, R., LAVILLE, E., BOUAZIZ, S., AMRHAR, M. and AIT OUALI, R. (2002). The Mesozoic-Cenozoic Atlas belt (North Africa): an overview. *Geodinamica Acta* 15: 185-208. doi.org/10.1016/S0985-3111(02)01088-4.

PERILLI, N. and COMAS-RENGIFO, M.J. (2002). Calibration of Pliensbachian calcareous nannofossils events in two ammonite-controled sections from Northern Spain. *Rivista Italiana di Paleontologia e Stratigrafia* 108: 133-152.

PITTET, B., SUAN, G., LENOIR, F., DUARTE, L.V. and MATTIOLI, E. (2014). Carbon isotope evidence for sedimentary discontinuities in the lower Toarcian of the Lusitanian Basin (Portugal): sea level change at the onset of the Oceanic Anoxic Event. *Sedimentary Geology* 303: 1-14. doi.org/10.1016/j.sedgeo.2014.01.001.

POÇAS RIBEIRO, N., MENDONÇA FILHO, J.G., DUARTE, L.V., SILVA, R.L., MENDONÇA, J.O. and SILVA, T.F. (2013). Palynofacies and organic geochemistry of the Sinemurian carbonate deposits in the western Lusitanian Basin (Portugal): Coimbra and Água de Madeiros formations. *International Journal of Coal Geology* 111: 37-52. http://dx.doi.org/10.1016/j.coal.2012.12.006.

POSAMENTIER, H.W. and ALLEN, G.P. (1999). Siliciclastic sequence stratigraphy: concepts and applications. Concepts in Sedimentology and Paleontology. *Society of Economic Paleontologists and Mineralogists (SEPM)*. 7, 210 pp.. doi.org/10.2110/csp.99.07.

PRICE, G.D. (1999). The evidence and implications of polar ice during the Mesozoic, Earth. Earth-Science Reviews 48: 183-210. doi.org/10.1016/S0012-8252(99)00048-3.

PRICE, G.D., TWITCHETT, R.J., WHEELEY, J.R. and BUONO, G. (2013). Isotopic evidence for long term warmth in the Mesozoic. *Scientific Reports* 3, 1438. doi: 10.1038/srep01438.

QUESADA, S. and ROBLES, S. (1995). Distribution of organic facies in the Liassic carbonate ramps of the Western Basque–Cantabrian (Northern Spain). Field Trip Guide of the 17th International Meeting on Organic Geochemistry.

QUESADA, S., DORRONSORO, C., ROBLES, S., CHALER, R. and GRIMALT, J.O. (1997). Geochemical correlation of oil from the Ayoluengo field to Liassic black shale units in the southwestern Basque-Cantabrian Basin (northern Spain). *Organic Geochemistry* 27: 25-40.

QUESADA, S., ROBLES, S. and ROSALES, I. (2005). Depositional architecture and transgressive–regressive cycles within Liassic backstepping carbonate ramps in the Basque–Cantabrian basin, northern Spain. *Journal of the Geological Society* 162: 531-548. doi.org/10.1144/0016-764903-041.

RASMUSSEN, E.S., LOMHOLT, S., ANDERSEN, C. and VEJBAK, O.V. (1998). Aspects of the structural evolution of the Lusitanian Basin in Portugal and the shelf and slope area offshore Portugal. *Tectonophysics* 300: 199-225. doi.org/10.1016/S0040-1951(98)00241-8.

REES, P.M., ZIEGLER, A.M. and VALDES, P.J. (2000). Jurassic phytogeography and climates: new data and model comparisons. In: Huber, B.T., Macleod, K.G., Wing, S.L. (Eds.), Warm climates in Earth history. Cambridge University Press, pp. 297-318.

REOLID, M. (2014a). Stable isotopes on foraminifera and ostracods for interpreting incidence of the Toarcian Oceanic Anoxic Event in Westernmost Tethys: role of water stagnation and productivity. *Palaeogeography, Palaeoclimatology, Palaeoecology* 395: 77-91. doi.org/10.1016/j.palaeo.2013.12.012.

REOLID, M. (2014b). Pyritized radiolarians and siliceous sponges from oxygen restricted deposits (Lower Toarcian, Jurassic). *Facies* 60: 789-799. doi.org/10.1007/s10347-014-0404-6.

REOLID, M., RODRÍGUEZ-TOVAR, F.J., MAROK, A. and SEBANE, A. (2012). The Toarcian oceanic anoxic event in the Western Saharan Atlas, Algeria (North African Paleomargin): role of anoxia and productivity. *Geological Society of America Bulletin* 124: 1646-1664. doi.org/10.1130/B30585.1

REOLID, M., EMANUELA, M., NIETO, L.M. and RODRÍGUEZ-TOVAR, F.J. (2014). The Early Toarcian Oceanic Anoxic Event in the External Subbetic (South Iberian Palaeomargin, Westernmost Tethys): Geochemistry, nannofossils and ichnology. *Palaeogeography, Palaeoclimatology, Palaeoecology* 411: 79-94. doi.org/10.1016/j.palaeo.2014.06.023.

REOLID, M., MOLINA, J.M., NIETO, L.M. and RODRÍGUEZ-TOVAR, F.J. (2018). External Subbetic Outcrops. In: Toarcian Oceanic Anoxic Event in the South Iberian Palaeomargin. SpringerBrief in Earth Sciences, pp. 23-83.

REOLID, M., ABAD, I. and BENITO, M.I. (2019a). Upper Pliensbachian-Lower Toarcian methane cold seeps interpreted from geochemical and mineralogical characteristics of

celestine concretions (South Iberian palaeo-margin). *Palaeogeography, Palaeoclimatology, Palaeoecology* 530: 15-31. doi.org/10.1016/j.palaeo.2019.05.033.

REOLID M., DUARTE, L.V. and RITA P. (2019b). Changes in foraminiferal assemblages and environmental conditions during the T-OAE (Early Jurassic) in the northern Lusitanian Basin, Portugal. *Palaeogeography, Palaeoclimatology, Palaeoecology* 520: 30-43. doi.org/10.1016/j.palaeo.2019.01.022.

RITA, P., REOLID, M. and DUARTE, L.V. (2016). Benthic foraminiferal assemblages record major environmental perturbations during the Late Pliensbachian–Early Toarcian interval in the Peniche GSSP, Portugal. *Palaeogeography, Palaeoclimatology, Palaeoecology* 454: 267-281. dx.doi.org/10.1016/j.palaeo.2016.04.039.

RITA P., NÄTSCHER P., DUARTE L.V., WEIS R. and DE BAETS K. (2019). Mechanisms and drivers of belemnite body-size dynamics across the Pliensbachian–Toarcian crisis. *Royal Society Open Science* 6: 190494. dx.doi.org/10.1098/rsos.190494.

ROCHA, R.B., MATTIOLI, E., DUARTE, L.V., PITTET, B., ELMI, S., MOUTERDE, R., CABRAL, M.C., COMAS-RENGIFO, M.J., GÓMEZ, J.J., GOY, A., HESSELBO, S.P., JENKYNS, H.C., LITTLER, K., MAILLIOT, S., DE OLIVEIRA, C.V., OSETE, M.L., PERILLI, N., PINTO, S., RUGET, C. and SUAN, G. (2016). Base of the Toarcian Stage of the Lower Jurassic defined by the Global Boundary Stratotype Section and Point (GSSP) at the Peniche Section (Portugal). *Episodes* 39: 460-481. doi:10.18814/epiiugs/2016/v39i3/99741.

RODRIGUES, B., MENDONÇA FILHO, J.G., DUARTE, L.V., MENDONÇA, J.O., COMAS-RENGIFO, M.J. and GOY, A. (2015). Estudo organofaciológico do Pliensbaquiano terminal – Toarciano inferior do perfil de Rodiles (Astúrias, Espanha). *Comunicações Geológicas* 102: 45-48.

RODRIGUES, B., DUARTE, L.V., MENDONÇA FILHO, J.G., SANTOS, L.G. and DONIZETI DE OLIVEIRA, A. (2016). Evidence of terrestrial organic matter deposition across the early Toarcian recorded in the northern Lusitanian Basin, Portugal. *International Journal of Coal Geology* 168: 35-45. doi.org/10.1016/j.coal.2016.06.016.

RODRIGUES, B., SILVA, R.L., REOLID, M., MENDONÇA FILHO, J.G. and DUARTE, L.V. (2019). Sedimentary organic matter and $\delta^{13}C_{Kerogen}$ variation on the southern Iberian palaeomargin (Betic Cordillera, SE Spain) during the latest Pliensbachian–Early Toarcian. *Palaeogeography, Palaeoclimatology, Palaeoecology* 534: 109342. doi.org/10.1016/j.palaeo.2019.109342.

RODRIGUES, B., SILVA, R.L., MENDONÇA FILHO, J.G., SADKI, D., MENDONÇA, J.O. and DUARTE, L.V. (2020). Late Pliensbachian–Early Toarcian palaeoenvironmental dynamics and the Pliensbachian–Toarcian Event in the Middle Atlas Basin (Morocco). *International Journal of Coal Geology* 217: 103339. doi.org/10.1016/j.coal.2019.103339.

RODRÍGUEZ-FERNANDEZ, L.R., LÓPEZ OLMEDO, F., OLIVEIRA, J.T., MEDIALDEA, T., TERRINHA, P., MATAS, J., MARTÍN-SERRANO, A., MARTÍN PARRA, L.M., RUBIO,

F., MARÍN, C., MONTES, M. and NOZAL, F. (2016). Mapa Geológico de la Península Ibérica, Baleares y Canarias a escala 1:1.000.000, edición 2015. Instituto geológico y minero de España (IGME) & Laboratorio Nacional de Energía y Geología de Portugal (LNEG), Madrid.

RODRÍGUEZ-TOVAR, F.J. and UCHMAN, A. (2010). Ichnofabric evidence for the lack of bottom anoxia during the Lower Toarcian Oceanic Anoxic Event (T-OAE) in the Fuente de la Vidriera section, Betic Cordillera, Spain. *Palaios* 25: 576-587.

RODRÍGUEZ-TOVAR, F.J. and REOLID, M. (2013). Environmental conditions during the Toarcian Oceanic Anoxic Event (T-OAE) in the westernmost Tethys: influence of the regional context on a global phenomenon. *Bulletin of Geosciences* 88: 697-712.

RODRÍGUEZ-TOVAR, F.J. MIGUEZ-SALAS, O., and DUARTE, L.V. (2017). Toarcian Oceanic Anoxic Event induced unusual behaviour and palaeobiological changes in Thalassinoides tracemakers. *Palaeogeography, Palaeoclimatology, Palaeoec*ology 485: 46-56. doi.org/10.1016/j.palaeo.2017.06.002.

RÖHL, H., SCHMID-RÖHL, A., OSCHMANN, W., FRIMMEL, A. and SCHWARK, L. (2001). The Posidonia Shale (Lower Toarcian) of SW-Germany: an oxygen-depleted ecosystem controlled by sea level and palaeoclimate. *Palaeogeography, Palaeoclimatology, Palaeoecology* 169: 273-299. doi.org/10.1016/S0031-0182(00)00152-8.

ROSALES, I., QUESADA, S. and ROBLES, S. (2006). Geochemical arguments for identifying second-order sea level changes in hemipelagic carbonate ramp deposits. *Terra Nova* 18: 233-240. https://doi.org/10.1111/j.1365-3121.2006.00684.x.

RUEBSAM, W., MÜLLER, T., KOVÁCS, J., PÁLFY, J. and SCHWARK, L. (2018). Environmental response to the early Toarcian carbon cycle and climate perturbations in the northeastern part of the West Tethys shelf. *Gondwana Research* 59: 144-158. doi.org/10.1016/j.gr.2018.03.013.

RUEBSAM, W., MAYER, B. and SCHWARK, L. (2019). Cryosphere carbon dynamics control Early Toarcian global warming and sea level evolution. *Global and Planetary Change* 172: 440-453. doi.org/10.1016/j.gloplacha.2018.11.003.

RUEBSAM, W., REOLID, M. and SCHWARK, L. (2020a). $\delta^{13}C$ of terrestrial vegetation records Toarcian CO_2 and climate gradientes. *Nature Scientific Reports* 10: 117. doi.org/10.1038/s41598-019-56710-6.

RUEBSAM, W., REOLID, M., MAROK, A. and SCHWARK, L. (2020b). Drivers of benthic extinction during the early Toarcian (Early Jurassic) at the northern Gondwana paleomargin: Implications for paleoceanographic conditions. *Earth-Science Reviews* 203: 103117. https://doi.org/10.1016/j.earscirev.2020.103117.

RUEBSAM, W. and AL-HUSSEINI, M. (2020). Calibrating the Early Toarcian (Early Jurassic) with stratigraphic black holes (SBH). Gondwana Research 82: 317-336. doi.org/10.1016/j.gr.2020.01.011.

RUGET, C. and MARTÍNEZ-GALLEGO, J. (1979). Foraminifères du Liasmoyen et supérieur. Cuadernos de Geología. Universidad de Granada 10: 311-316.

SABATINO, N., NERI, R., BELLANCA, A., JENKYNS, H.C., BAUDIN, F., PARISI, G. and MASETTI, D. (2009). Carbon-isotope records of the Early Jurassic (Toarcian) Oceanic Anoxic Event from the Valdorbia (Umbria–Marche Apennines) and Monte Mangart (Julian Alps) sections: palaeoceanographic and stratigraphic implications. *Sedimentology* 56: 1307-1328. doi.org/10.1111/j.1365-3091.2008.01035.x.

SACHSE, V.F., LEYTHAEUSER, D., GROBE, A., RACHIDI, M. and LITTKE, R. (2012). Organic geochemistry and petrology of a Lower Jurassic (Pliensbachian) petroleum source rock from Aït Moussa, Middle atlas. Moroc. *Journal of Petroleum Geology* 35: 5-24. doi.org/10.1111/j.1747-5457.2012.00516.x.

SANDOVAL, J., BILL, M., AGUADO, R., O'DOGHERTY, L., RIVAS, P., MORARD, A. and GUEX, J. (2012). The Toarcian in the Subbetic basin (southern Spain): bio-events (ammonite and calcareous nannofossils) and carbon-isotope stratigraphy. *Palaeogeography, Palaeoclimatology, Palaeoecology* 342–343: 40-63. doi.org/10.1016/j.palaeo.2012.04.028.

SCHLAGER, W. (2005). Carbonate Sedimentology and Sequence Stratigraphy. SEPM, Concepts in Sedimentology and Paleontology 8, 200 pp..

SCHMID-RÖHL, A., RÖHL, H.J., OSCHMANN, W., FRIMMEL, A. and SCHWARK, L. (2002). Palaeoenvironmental reconstruction of Lower Toarcian epicontinental black shales (Posidonia Shale, SW Germany): global versus regional control. *Geobios* 35: 13-20.

SCHOUTEN, S., VAN KAAM-PETERS, H.M., RIJPSTRA, W.C., SCHOELL, M., SINNINGHE DAMSTÉ, J.S. (2000). Effects of an oceanic anoxic event on the stable carbon isotopic composition of early Toarcian carbon. *American Journal of Science* 300: 1-22. doi: 10.2475/ajs.300.1.1.

SCHWARK, L. and FRIMMEL, A. (2004). Chemostratigraphy of the Posidonia black shale, SW Germany II. Assessment of extent and persistence of photic-zone anoxia using aryl isoprenoid distributions. *Chemical Geology* 206: 231-248. doi.org/10.1016/j.chemgeo.2003.12.008.

SILVA, R.L., DUARTE, L.V., COMAS-RENGIFO, M.J., MENDONÇA FILHO, J.G. and AZERÊDO, A.C. (2011). Update of the carbon and oxygen isotopic records of the Early–Late Pliensbachian (Early Jurassic, 187 Ma): insights from the organic-rich hemipelagic series of the Lusitanian Basin (Portugal). *Chemical Geology* 283: 177-184. doi.org/10.1016/j.chemgeo.2011.01.010.

SILVA, R.L., MENDONÇA FILHO, J.G., DA SILVA, F.S., DUARTE, L.V., SILVA, T.F., FERREIRA, R., and AZERÊDO, A.C. (2012). Can biogeochemistry aid in the palaeoenvironmental/early diagenesis reconstruction of the ~187 Ma (Pliensbachian) organic-rich hemipelagic series of the Lusitanian Basin (Portugal)?. *Bulletin of Geosciences* 87: 373-382. doi.org/10.3140/bull.geosci.1315.

SILVA, R.L., DUARTE, L.V. and MENDONÇA FILHO, J.G. (2013). Optical and geochemical characterization of Upper Sinemurian (Lower Jurassic) fossil wood from the Lusitanian Basin (Portugal). *Geochemical Journal* 47: 489-498. doi:10.2343/geochemj.2.0270.

SILVA, R.L., MENDONÇA FILHO, J.G., AZERÊDO, A.C., SILVA, T.F. and DUARTE, L.V. (2014). Palynofacies and TOC analysis of marine and non-marine sediments across the Middle-Upper Jurassic boundary in the Central-Northern Lusitanian Basin (Portugal), *Facies* 60: 255-276. doi.org/10.1007/s10347-013-0369-x.

SILVA, R.L. and DUARTE, L.V. (2015). Organic matter production and preservation in the Lusitanian Basin and Late Pliensbachian climatic hot snaps. *Global and Planetary Change* 131: 24-34. doi.org/10.1016/j.gloplacha.2015.05.002.

SILVA, R.L., DUARTE, L.V. and COMAS-RENGIFO, M. (2015). Facies and carbon isotope chemostratigraphy of Lower Jurassic carbonate deposits, Lusitanian Basin (Portugal): implications and limitations to the application in sequence stratigraphic studies. In: Ramkumar, M. (Ed.), Chemostratography. Concepts, Techniques, and Applications. Elsevier, pp. 341-371. doi.org/10.1016/B978-0-12-419968-2.00013-3.

SILVA, R.L., CARLISLE, C.M. and WACH, G. (2017). A new TOC, rock-eval, and carbon isotope record of Lower Jurassic source rocks from the Slyne Basin, offshore Ireland. *Marine and Petroleum Geology* 86: 499-511. doi.org/10.1016/j.marpetgeo.2017.06.004.

SLATER, S.M., TWITCHETT, R.J., DANISE, S., and VAJDA, V. (2019). Substantial vegetation response to Early Jurassic global warming with impacts on oceanic anoxia. *Nature Geoscience* 12: 462-467. doi.org/10.1038/s41561-019-0349-z.

SOARES, A.F., ROCHA, R.B., ELMI, S., HENRIQUES, M.H., MOUTERDE, R., ALMERAS, Y., RUGET, C., MARQUES, J., DUARTE, L.V., CARAPITO, M.C. and KULLBERG, J. (1993). Le sous-bassin nord-lusitanien (Portugal) du Trias au Jurassique moyen: histoire d'un "rift avorté". *CComptes Rendus de l'Académie des Sciences* 317: 1659-1666.

STORM, M.S., HESSELBO, S.P., JENKYNS, H.C., RUHL, M., ULLMANN, C.V., XU, W., LENG, M.J., RIDING, J.B. and GORBANENKO, O. (2020). Orbital pacing and secular evolution of the Early Jurassic carbon cycle. *Proceedings of the National Academy of Sciences* 1-9. doi.org/10.1073/pnas.1912094117.

STYAN, W.B. and BUSTIN, R.M. (1983). Sedimentology of Fraser River delta peat deposits: a modern analogue for some deltaic coals. *International Journal of Coal Geology* 3: 101-143. doi.org/10.1016/0166-5162(83)90006-X.

SUAN, G., MATTIOLI, E., PITTET, B. and LECUYER, C. (2008a). Evidence for major environmental perturbation prior to and during the Toarcian (Early Jurassic) oceanic anoxic event from the Lusitanian Basin, Portugal. *Paleoceanography* 23: PA1201. doi.org/10.1029/2007PA001459.

SUAN, G., PITTET, B., BOUR, I., MATTIOLI, E., DUARTE, L.V. and MAILLIOT, S. (2008b). Duration of the early Toarcian carbon isotope excursion deduced from spectral analysis:

consequence for its possible causes. *Earth and Planetary Science Letters* 267: 666-679. doi:10.1016/j.epsl.2007.12.017.

SUAN, G., MATTIOLI, E., PITTET, B., LECUYER, C., SUCHERAS-MARX, B., DUARTE, L.V., PHILIPPE, M., REGGIANI, L. and MARTINEAU, F. (2010). Secular environmental precursors to Early Toarcian (Jurassic) extreme climate changes. *Earth and Planetary Science Letters* 290: 448-458. doi.org/10.1016/j.epsl.2009.12.047.

SUAN, G., NIKITENKO, B.L., ROGOV, M.A., BAUDIN, F., SPANGENBERG, J.E., KNYAZEV, V.G., GLINSKIKH, L.A., GORYACHEVA, A.A., ADATTE, T., RIDING, J.B., FÖLLMI, K.B., PITTET, B., MATTIOLI, E. and LÉCUYER, C. (2011). Polar record of Early Jurassic massive carbon injection. *Earth and Planetary Science Letters* 312: 102-113. doi.org/10.1016/j.epsl.2011.09.050.

SUAN, G., VAN DE SCHOOTBRUGGE, B., ADATTE, T., FIEBIG, J. and OSCHMANN, W. (2015). Calibrating the magnitude of the Toarcian carbon cycle perturbation. *Paleoceanography* 30: 495-509. doi.org/10.1002/2014PA002758.

SUAN, G., SCHÖLLHORN, I., SCHLÖGL, J., SEGIT, T., MATTIOLI, E., LÉCUYER, C. and FOUREL, F. (2018). Euxinic conditions and high sulfur burial near the European shelf margin (Pieniny Klippen Belt, Slovakia) during the Toarcian oceanic anoxic event. *Global and Planetary Change*: 170, 246-259. doi.org/10.1016/j.gloplacha.2018.09.003.

SUÁREZ-VEGA, L.C. (1974). Estratigrafía del Jurásico en Asturias. *Cuadernos de Geología Ibérica* 3: 1-369.

SVENSEN, H., PLANKE, S., CHEVALLIER, L., MALTHE-SORENSSEN, A., CORFU, F. and JAMTVEIT, B. (2007). Hydrothermal venting of greenhouse gases triggering Early Jurassic global warming. *Earth and Planetary Science Letters* 290: 448-458. doi.org/10.1016/j.epsl.2007.02.013.

THEM II, T.R., GILL, B.C., CARUTHERS, A.H., GRÖCKE, D.R., TULSKY, E.T., MARTINDALE, R.C., POULTON, T.P. and SMITH, P.L. (2017). High-resolution carbon isotope records of the Toarcian Oceanic Anoxic Event (Early Jurassic) from North America and implications for the global drivers of the Toarcian carbon cycle. *Earth and Planetary Science Letters* 459: 118-126. doi.org/10.1016/j.epsl.2016.11.021.

THIERRY, J. and BARRIER, E. (2000). Middle Toarcian. In: Dercourt, J., Gaetani, M.A. (Eds.), Atlas Peri-Tethys. Palaeogeographical Maps CCGM/CGMW, Paris.

THIBAULT, N., RUHL, M., ULLMANN, C.V., KORTE, C., KEMP, D.B., GRÖCKE, D.R. and HESSELBO, S.P. (2018). The wider context of the Lower Jurassic Toarcian oceanic anoxic event in Yorkshire coastal outcrops, UK. *Proceedings of the Geologists' Association* 129: 372-391. doi.org/10.1016/j.pgeola.2017.10.007.

TREMOLADA, F., VAN DE SCHOOTBRUGGE, B. and ERBA, E. (2005). Early Jurassic schizosphaerellid crisis in Cantabria, Spain: Implications for calcification rates and phytoplankton evolution across the Toarcian oceanic anoxic event: *Paleoceanography* 20: PA2011. doi.org/10.1029/2004PA001120.

TYSON, R.V. and PEARSON, T.H. (1991). Modern and ancient continental shelf anoxia: na overview. *Geological Society, London, Special Publications* 58: 1-24. doi.org/10.1144/GSL.SP.1991.058.01.01.

TYSON, R.V. (1995). Sedimentary Organic Matter: Organic Facies and Palynofacies. Chapman & Hall, London, 632 pp..

UNITED STATES ENVIRONMENT PROTECTION AGENCY (2002). Methods for the Determination of Total Organic Carbon (TOC) in Solids and Sediments, Ecological Risk Assessment Support Center. NCEA-C-1282. Office of Research and Development, Las Vegas.

VAKHRAMEYEV, V.A. (1982). Classopollis pollen as an indicator of Jurassic and Cretaceous climates. *International Geology Review* 24-10: 1190-1196. doi.org/10.1080/00206818209451058.

VALENZUELA, M. (1988). *Estratigrafía, sedimentología y paleogeografia del Jurásico de Asturias*. Ph.D. Thesis. Departamento de Geología Universidad de Oviedo.

VAN BREUGEL, Y., BASS, M., SCHOUTEN, S., MATTIOLI, E. and SINNINGHE DAMSTÉ, J.S. (2006). Isorenieratane record in black shales from the Paris Basin, France: constraints on recycling of respired CO_2 as a mechanism for negative carbon isotope shifts during the Toarcian oceanic anoxic event. *Paleoceanography* 21: PA4220. doi.org/ 10.1029/2006PA001305.

VAN DE SCHOOTBRUGGE, B., MCARTHUR, J.M., BAILEY, T.R., ROSENTHAL, Y., WRIGHT, J.D. and MILLER, K.G. (2005). Toarcian oceanic anoxic event: An assessment of global causes using belemnite C isotope records. *Paleoceanography* 20, PA3008. doi.org/10.1029/2004PA001102.

VAN DE SCHOOTBRUGGE, B., BACHAN, A., SUAN, G., RICHOZ, S. and PAYNE, J.L. (2013). Microbes, mud, and methane: cause and consequence of recurrent Early Jurassic anoxia following the end-Triassic mass-extinction. *Palaeontology* 56: 685-709. doi.org/10.1111/pala.12034.

VAN DE SCHOOTBRUGGE, B., HOUBEN, A.P., ERCAN, F.Z., VERREUSSEL, R., KERSTHOLT, S., JANSSEN, N.M., NIKITENKO, B. and SUAN, G. (2019). Enhanced Arctic-Tethys connectivity ended the Toarcian Oceanic Anoxic Event in NW Europe. *Geological Magazine* 1-19. doi.org/10.1017/S0016756819001262.

VERA, J.A. (2004). Zonas Externas Béticas. In: J.A. Vera (Ed.), Geología de España. Geological Society of Spain-Instituto Geológico y Minero de España, pp. 354-389.

WARME, J.E. (1988). Middle Jurassic history and the Bajocian reef tracts. In: Warme, J.E., Crevello, P.D., Hazlet, B.A., Atmane, F., Benbouziane, M. (Eds.), Evolution of the Jurassic High Atlas Rift, Morocco: Transtention, Structural and Eustatic Controls on Carbonate Facies, Tectonic Inversion. AAPG Mediteranean Basins Conference, Field Trip 9, pp. XI/1–XI/19.

WIGNALL, P.B., NEWTON, R.J. and LITTLE, C.T. (2005). The timing of paleoenvironmental change and cause-and-effect relationships during the Early Jurassic mass extinction in Europe. *American Journal of Science* 305: 1014-1032.

WILMSEN, M. and NEUWEILER, F. (2008). Biosedimentology of the Early Jurassic post-extinction carbonate depositional system, central High Atlas rift basin, Morocco. *Sedimentology* 55: 773-807. doi.org/10.1111/j.1365-3091.2007.00921.x.

WILSON, R.L., HISCOTT, R.N., WILLIS, M.G. and GRADSTEIN, F.M. (1989). The Lusitanian Basin of west Central Portugal: mesozoic and tertiary tectonic, stratigraphic, and subsidence history. In: Tankard, A.J., Balkwill, H. (Eds.), Extensional Tectonics and Stratigraphy of the North Atlantic Margins. AAPG Memoir 46, pp. 341-361.

WRIGHT, V.P. (1992). A revised classification of limestones. *Sedimentary Geology* 76: 177-185. doi.org/10.1016/0037-0738(92)90082-3.

WRIGHT, V.P. and WILSON, R.L. (1984). A carbonate submarine-fan sequence from the Jurassic of Portugal. *Journal of Sedimentary Research* 54: 394-412. doi.org/10.1306/212F8427-2B24-11D7-8648000102C1865D.

XU, W., RUHL, M., JENKYNS, H.C., HESSELBO, S.P., RIDING, J.B., SELBY, D., NAAFS, B.A., WEIJERS, J.H., PANCOST, R.D., TEGELAAR, E.W. and IDIZ, E.F. (2017). Carbon sequestration in an expanded lake system during the Toarcian Oceanic Anoxic Event. *Nature Geoscience* 10: 129-134. doi.org/10.1038/ngeo2871.

XU, W., RUHL, M., JENKYNS, H.C., LENG, M.J., HUGGETT, J.M., MINISINI, D., ULLMANN, C.V., RIDING, J.B., WEIJERS, J.W.H., STORM, M.S., PERCIVAL, L.M.E., TOSCA, N.J., IDIZ, E.F., TEGELAAR, E.W. and HESSELBO, S.P. (2018). Evolution of the Toarcian (Early Jurassic) carbon cycle and global climatic controls on local sedimentary processes (Cardigan Bay Basin, UK). *Earth and Planetary Science Letters* 484: 396-411. doi.org/10.1016/j.epsl.2017.12.037.

ZONNEVELD, K.F., VERSTEEGH, G.M., KASTEN, S., EGLINTON, T.I., EMEIS, K.-C., HUGUET, C., KOCH, B.P., DE LANGE, G.J., DE LEEUW, J.W., MIDDELBURG, J.J., MOLLENHAUER, G., PRAHL, F.G., RETHEMEYER, J. and WAKEHAM, S.G. (2010). Selective preservation of organic matter in marine environments; processes and impact on the sedimentar record. *Biogeosciences* 7: 483-511. doi.org/10.5194/bg-7-483-2010.